Fabio BRANTSCHEN

Influence of bond and anchorage conditions of the shear reinforcement on the punching strength of RC slabs

Thèse N° 7315

École
Polytechnique
Fédérale
de Lausanne

2016

ÉCOLE POLYTECHNIQUE
FÉDÉRALE DE LAUSANNE

Influence of bond and anchorage conditions of the shear reinforcement on the punching strength of RC slabs

THÈSE No 7315 (2016)

PRÉSENTÉE LE 03 OCTOBRE 2016

À LA FACULTÉ DE L'ENVIRONNEMENT NATUREL, ARCHITECTURAL ET CONSTRUIT
LABORATOIRE DE CONSTRUCTION EN BÉTON
PROGRAMME DOCTORAL EN GÉNIE CIVIL ET ENVIRONNEMENT

ÉCOLE POLYTECHNIQUE FÉDÉRALE DE LAUSANNE

POUR L'OBTENTION DU GRADE DE DOCTEUR ÈS SCIENCES

PAR

Fabio BRANTSCHEN

acceptée sur proposition du jury :

Prof. I. Smith, président du jury
Prof. A. Muttoni, directeur de thèse
Prof. K. Beyer, rapporteuse
Prof. G. Plizzari, rapporteur
Dr. J. Sagaseta, rapporteur

ÉCOLE POLYTECHNIQUE
FÉDÉRALE DE LAUSANNE

Suisse
2016

À la mémoire de mon grand-père, le docteur Pierre Barbezat

Foreword

The thesis of Fabio Brantschen deals with the behaviour of slab-column connections with transverse reinforcement and, particularly, the influence of bond, anchorage and cracking on the punching shear strength. The punching shear resistance of reinforced concrete slabs has been one of the main research topics at the Structural Concrete Laboratory of EPFL over the last decade. This topic is very relevant for practice as, in many cases, the punching shear strength governs the design of slab-column connections of flat slabs (required slab thickness and column size). A mechanical model (called the "Critical Shear Crack Theory", CSCT) has been developed, validated by extensive experimental research and generalized to many cases during the last 15 years. This model was recently adopted by some codes of practice (Model Code 2010 of the International Federation for Structural Concrete and the Swiss Code for concrete structures SIA 262:2013) and is currently having a large impact on engineering practice.

Within this context, the work of Fabio Brantschen is a relevant addition to the work performed in the last years, as punching shear reinforcement is increasingly used to enhance the shear resistance (and thus to reduce the required slab thickness). In addition, this reinforcement enables also enhancing the deformation capacity and thus reducing the sensitivity to imposed deformations, the risk of progressive collapse and the influence of seismic actions. For these reasons, this reinforcement technique is increasingly gaining popularity in Europe and North America. Also, steel manufacturers are proposing tailored solutions in order enhance the mechanical efficiency and reinforcement ease of placing (reducing labour costs).

Lausanne, October 2016

Prof. Dr Aurelio Muttoni

"Se qualcuno ama un fiore, di cui esiste un solo esemplare in milioni e milioni di stelle,
questo basta a farlo felice quando le guarda. E lui si dice: «il mio fiore è la in qualche luogo…»."

Il Piccolo Principe, Antoine de Saint-Exupéry (1900-1944)

"Quand l'homme abandonne à son geste la mission que son esprit renie, il ne l'abjure pas,
il la passe à son servant, comme il passe la vie à son corps dans le sommeil."

Sodome et Gomorrhe, Jean Giraudoux (1882-1944)

"Sag morgens mir ein gutes Wort bevor du gehst vom Hause fort.
Es kann so viel am Tag gescheh'n, wer weiss, ob wir uns wiedersehn.
Sag lieb ein Wort zur guten Nacht, wer weiss, ob man noch früh erwacht.
Das Leben ist so schnell vorbei, und dann ist es nicht einerlei,
was du zuletzt zu mir gesagt, was du zuletzt mich hast gefragt.
Drum lass ein gutes Wort das letzte sein,
bedenk, das letzte könnt's für immer sein!"

Unbekannt, gefunden und abgeschrieben von einer Holztafel

"Весь мир разделен для меня на две половины: одна - она и там все счастье, надежда, свет;
другая половина - все, где её нет, там все уныние..."

War and Peace, Leo Tolstoy (1852-1910)

Acknowledgements

My research work for the past five years at the Structural Concrete Laboratory (IBETON) of the Swiss Federal Institute of Technology in Lausanne (EPFL) could not have been materialized in this thesis without numerous scientific and human contributions.

I am sincerely grateful to my supervisor, Prof. Aurelio Muttoni, for whom I have great admiration and respect. He offered me the opportunity to accomplish something really meaningful for me. Together with Dr. Miguel Fernández Ruiz, always available and involved, they provided me support, advice and inspiration during all these years which undoubtedly left an important imprint on the present document.

The jury members of my thesis are sincerely thanked for their engagement, valuable comments and interesting discussion, namely, Prof. Katrin Beyer, Prof. Giovanni Plizzari and Dr. Juan Sagaseta. Their respective interest in my work gave me a lot of satisfaction. Also, the important remarks and interventions of the president of the jury Prof. Ian Smith during the private defence were really appreciated and relevant for improving the thesis quality.

An important part of my research was dedicated to experimental investigations, and therefore I want to express all my gratitude to the technical staff involved in my laboratory work. Gilles, Gérald, Sylvain and François are thanked for their knowledge of the testing machine, measurements systems and related processes, as well as their willingness to keep an open mind to my ideas. The industrial skills of Armin, Fred, Serge and Patrice associated with their creativity allowed me to find solutions to any of my problems in an optimal time. Several students contributed significantly in this work by helping me in different test campaigns, always with a strong dedication and curiosity: Antoine, Jean, Lestio, Yassine, Cyril and Joël. They are thanked for all the moments we shared –good and less good– on the construction sites, on the road, in the laboratory or even outside EPFL.

Along these years, I had the chance to share my office with very smart and interesting people. Each of them had clearly and impact on myself and the present thesis. In particular, I would like to thank Galina, Francesco, António, Mathieu, Duarte and Jesper for the daily discussions about reinforced concrete (but fortunately not only). I also had the great pleasure to assist some local and foreign students in their final projects, with whom I exchanged and learnt a lot through their interrogations: Cyril, Denis, Rinaldo, Francesco, Andrea, Claudio, Hugo, Joël, Quentin, Darko, Roberto, Ivan and Luca. These people will always mean something special to me with respect to what we went through together. I am deeply touched by the confidence they have shown in me.

I am very thankful for the people that got involved in proofreading my thesis by providing me useful and thorough feedback on the theoretical developments, the readability of the figures and the quality of the language. I notably think to Duarte, João, Raffaele, Jesper, Filip, Bastian, Desmond and Deirdre. Also, many thanks to Richard, Jean-Pascal, Stefano, Ioannis, Mikhail and Olga regarding their help in translating the abstract into the languages of importance to me. I would like to express my gratitude to Dr. Olivier Burdet for the interesting talks we had related to every aspect of my work, sometimes for hours, it was very enriching. But also to Yvonne, who is simply so much more than just a secretary for me, making our everyday life simpler and more enjoyable. Her assistance in all the administrative matters of this research, as well as her thoughtful words in some difficult situations, have been really appreciated.

Throughout the last ten years of my life, spent here at EPFL, I had the opportunity to meet and interact with a lot of very talented and great-hearted engineers that helped me at different levels of my curriculum: Blaise, Gilbert, Pascal, Marc-André, Thomas, Alexander, Philippe, Marie-Rose, Romain, Didier, Carlos, Talayeh, Hadi, Stefan, Dimitrios, Luis, Stefano, Thibault, Dan, Georgia, Pia, Michael, Raphaël, Sarah, Alessandro, Ovidiu, Jaime, Maria, Carlos, Simone, Ioanna, Binbin, Francisco, Marco, Maléna, Manuel, Damjan, Antigoni, Hayami, Patrick, Richard, Ivan, Luca, Jürgen, Ioannis, Raluca, Beatrice, Eva, Reza, Mikhail and Tassos. The presence of my friends external to EPFL as Tiago, Jérôme, Mike, Reda, Marine and both Miltos was also particularly appreciated. I owe a lot to these people, as each of them made some contributions to my thesis achievements in the technical and/or social aspects.

All my current colleagues (IBETON) are truly thanked for the time spent together. You gave me the opportunity and the desire to go beyond the mere professional relationship, becoming appreciated friends. The contact with the members of the Construction Composite Laboratory (CCLAB), as well as the Earthquake Engineering and Structural Dynamics Laboratory (EESD), was also really appreciated and constructive. I wish you all the best for your future!

My special thanks go to a very limited amount of person, very significant to me, who had a notable impact on my life and that supported me the best they could –often from far– in my daily duties and responsibilities: Stefano, Ioannis, Filip, Eva and Olga. They made this period unforgettable to me from a personal point of view and I hope to have them close to me for all my life.

Finally, I am extremely grateful to my parents, Riccardo and Claire, and to my brother Sandro, for their unconditional support of every kind during all these years of study. It would have been impossible to ask them anything more. The education I received from my family and my grandparents throughout my life make me become who I am and allowed me to achieve this important personal milestone. I will always be thankful to them.

Fabio

Abstract

Reinforced concrete flat slabs constitute one of the most common and efficient modern construction methods. The design of such structural system might be governed by a brittle failure in the vicinity of the slab-column connection associated to punching shear. Several accidents in the last decades motivated the development of solutions to enhance the overall structural response of the slab and to prevent a progressive collapse. The arrangement of transverse reinforcement in the critical zone increases both the strength and the deformation capacity of the slab-column connection. Various punching reinforcing systems have been developed in the past based on intuition and testing. Recent advances on the understanding of the punching phenomena lead nowadays to a better approach of the differences in efficiency and to develop new reinforcement products on a more rational basis.

One of the main parameters identified as governing for the performance of this specific reinforcement is the quality of its anchorage and bond, influencing the development of cracks in the shear-critical region. Such characteristic is generally defined through force-slip relationships and is strongly influenced by the local state of stress and strain. Although the activation of reinforcement often takes place within already cracked concrete for many structural members, the conventional approaches supporting code formulations are still almost exclusively based on tests performed on uncracked specimens. Anchorage of reinforcement bars in cracked concrete is relevant to the structural response of the aging reinforced concrete buildings as well as for the new construction. In the coming years, an increased emphasis should be placed on the study of the performance of reinforcing details in such severe conditions, with the aim to improve the knowledge of this rather underrated but critical problematic.

Several experimental works were thus conducted in the frame of this thesis to improve the current knowledge on the role of the anchorage of the transverse reinforcement in punching shear phenomenon. A programme of pull-out tests on actual detailing solutions was performed in cracked conditions similar to those developing in slabs at the vicinity of the columns. The results highlighted significant differences amongst the evaluated types of anchorages, confirming therefore the various levels of performance observed in punching tests. The activation of this specific reinforcement is investigated in this thesis through tests on full-scale slab specimens provided with extended measurements of the force (external load cells) and crack openings (full and partial thickness variation devices). The use of an innovative reinforcing setup allowed to track the concrete and steel contributions in the punching phenomenon, providing the experimental information required

to validate the main assumptions of the Critical Shear Crack Theory for the failure mode within the shear-reinforced area.

Observations on straight bars with in-plane cracking supported the development of analytical formulations to evaluate the reduction of performance –in terms of strength and stiffness– for various anchorage details by analogous considerations to the aggregate interlock approaches. The model is validated through a refined numerical method and the main test results available from literature. Such developments can be partially used within the frame of the Critical Shear Crack Theory, which calculates the contribution of the shear reinforcement in the punching strength –for the failure mode of interest– with a physical model of activation for the transverse elements. The latter contains a number of general assumptions –perfect bond and anchorage conditions, simplified crack kinematics– which can be improved and refined on the basis of the experimental results of the present research. Proposals are formulated to take into account in the existing model a more realistic activation of the transverse reinforcement in the slab during punching –by considering the degradation of the force transfer actions due to the presence of flexural cracks– and thus to improve the understanding and the predictions associated to this failure mode.

Keywords:

punching shear, interior slab-column connections, shear reinforcement, Critical Shear Crack Theory, activation model, failure kinematics, bond and anchorage performance, pull-out tests, cracked concrete, serviceability and ultimate limit states conditions, force-slip relationships

Résumé

Les planchers-dalles en béton armé sont un système de construction moderne des plus fréquemment utilisés et efficaces. Le dimensionnement de ce type de système structural peut être dicté par une rupture fragile à proximité de la connexion dalle-colonne associée au phénomène de poinçonnement. Durant les dernières décennies, plusieurs accidents ont motivé le développement de solutions pour améliorer le comportement global de la dalle ainsi que pour prévenir un effondrement progressif. La disposition d'armature transversale dans la zone critique permet d'augmenter à la fois la résistance et la capacité de déformation de la connexion dalle-colonne. Plusieurs systèmes de renforcement au poinçonnement ont été développés par le passé sur la base d'intuitions et d'essais. Les récentes avancées dans la compréhension du phénomène du poinçonnement ont conduit à une meilleure approche des différences d'efficacité et à développer de nouveaux produits de renforcement sur une base plus rationnelle.

Un des paramètres identifié comme déterminant pour la performance de ce type d'armature spécifique est sa qualité d'ancrage et d'adhérence qui influence le développement des fissures dans la zone critique. Cette caractéristique est généralement définie par des relations force-glissement et est considérablement influencée par l'état de contrainte et de déformation local. Malgré le fait que les détails d'armature soient souvent activés dans un béton en partie fissuré pour de nombreux éléments structuraux, les approches conventionnelles sur lesquelles sont fondées les formulations des normes sont encore presque systématiquement basées sur des essais réalisés avec des échantillons non-fissurés. L'ancrage de barres d'armature dans un béton fissuré est important pour la réponse structurale d'ouvrages existants en béton armé ainsi que pour les nouvelles constructions. Dans les années à venir, un plus grand intérêt devra être donné à l'étude au comportement de détails d'armature dans ces conditions sévères, dans le but d'améliorer les connaissances de cette importante problématique plutôt sous-estimée.

Plusieurs investigations expérimentales ont été menées dans le cadre de cette thèse pour améliorer les connaissances actuelles sur le rôle de l'ancrage de l'armature transversale dans le phénomène de poinçonnement. Un programme d'essais d'arrachement en milieu fissuré a été entrepris sur divers détails d'armature dans des conditions de fissuration similaires à celles qui se développent dans les dalles à proximité des colonnes. Les résultats ont mis en avant d'importantes différences entre les types d'ancrages évalués, confirmant les disparités en terme de performance observées dans les essais de poinçonnement. L'activation de cette armature particulière est étudiée dans cette thèse au travers d'essais sur dalles à échelle réelle avec des mesures détaillées de la force (capteur de force externe) et de l'ouverture des fissures (dispositifs de variation d'épaisseur totale et par-

tielle). Une configuration novatrice de l'armature transversale dans la dalle a permis de caractériser les contributions du béton et de l'acier au phénomène de poinçonnement, apportant des certitudes expérimentales nécessaires à la validation des principales hypothèses de la théorie de la fissure critique pour le mode de rupture dans la zone renforcée.

Les observations sur des barres droites avec une fissuration longitudinale ont donné lieu au développement d'expressions analytiques pour évaluer la réduction de performance –en termes de résistance et de rigidité– associée à divers types d'ancrage en se basant sur des considérations relatives à l'engrainement des granulats. Le modèle est validé par une méthode numérique approfondie et par les principaux essais disponibles dans la littérature. Ces développements peuvent être en partie repris dans le cadre de la théorie de la fissure critique, qui définit la contribution de l'armature transversale dans la résistance au poinçonnement –pour le mode de rupture étudié– par un modèle physique d'activation spécifique. La théorie comprend un certain nombre d'hypothèses –conditions d'adhérence et d'ancrage parfaites, cinématique de rupture simplifiée– qui peuvent être améliorées et raffinées sur la base des résultats expérimentaux présentés dans cette recherche. Des propositions sont formulées pour prendre en compte dans le modèle actuel une activation plus réaliste de l'armature transversale lors du poinçonnement de la dalle –en considérant la dégradation des transferts de forces associée à la présence de fissures flexionnelles– pour une meilleure compréhension et prédiction de ce mode de rupture.

Mots-clés:

poinçonnement, planchers-dalles en béton armé, connexion dalle-colonne intérieure, armature transversale, théorie de la fissure critique, modèle d'activation, cinématique de rupture, performance d'ancrage et d'adhérence, essais d'arrachement, béton fissuré, conditions aux états limites ultimes et de service, relations force-glissement

Kurzfassung

Die Verwendung von Stahlbetondecken stellt eine der häufigsten und effizientesten, modernen Baumethoden dar. Für die Dimensionierung solcher Bauteile kann ein mögliches sprödes Versagen an der Verbindung zwischen Decke und Stütze massgebend sein, das als Durchstanzen bezeichnet wird. Mehrere Unfälle in den letzten Jahrzehnten haben dazu beigetragen, neue Lösungsansätze zu erarbeiten, um das globale Tragverhalten solcher Decken zu verbessern und ein progressives Versagen zu verhindern. Der Einbau von Querbewehrung in der kritischen Zone ermöglicht gleichzeitig den Widerstand und das Verformungsvermögen des Verbindungsbereiches zwischen Decke und Stütze zu erhöhen. Basierend auf intuitiven Beobachtungen und Testkampagnen wurden bereits viele verschiedene Systeme von Durchstanzbewehrungen entwickelt. Jüngste Erkenntnisse zum Verständnis des Durchstanzphänomens führen zu besseren Ansätzen in der Beurteilung der Funktionsweise und Wirksamkeit solcher Systeme wie auch der Entwicklung neuer Produkte gestützt auf rationelleren Grundlagen.

Einer der wichtigsten Parameter für das Funktionieren solcher Bewehrungssysteme ist die Qualität der Verankerung sowie des Verbunds, welche die Rissentwicklung im querkraftkritischen Bereich beeinflussen. Ihre Eigenschaften werden normalerweise mit Kraft-Schlupf Beziehungen charakterisiert und hängen stark vom lokalen Spannungs- und Verformungszustand ab. Obwohl die Aktivierung der Bewehrung oft im bereits gerissenen Beton stattfindet, basieren Normen und konventionelle Berechnungsmethoden fast ausschliesslich auf Tests mit ungerissenen Prüfkörpern. Die Verankerung von Bewehrungsstäben in gerissenem Beton ist relevant für das Tragverhalten von bestehenden Stahlbetonbauwerken aber auch von neuen Konstruktionen. In den kommenden Jahren sollte der Wirkungsweise dieser Bewehrungsdetails unter erschwerten Bedingungen verstärkt Beachtung geschenkt werden, mit dem Ziel das Wissen über diese heute eher unterschätzte, aber kritische Problematik zu erweitern.

Im Rahmen dieser Doktorarbeit sind mehrere Versuchskampagnen durchgeführt worden, um das heutige Verständnis über die Bedeutung der Verankerung der Querbewehrung für das Phänomen des Durchstanzens zu verbessern. Ein Programm von Ausziehversuchen an gängigen Bewehrungsdetails wurde in gerissenem Stahlbeton, mit ähnlichen Bedingungen, wie sie auch in Decken beim Übergang zu den Stützen durch die Rissbildung anzutreffen sind, durchgeführt. Die Ergebnisse haben signifikante Unterschiede zwischen den verschiedenen analysierten Verankerungssystemen aufgezeigt und bestätigen damit die abweichenden Niveaus in der

Leistungsfähigkeit solcher Systeme, wie sie bei Durchstanzversuchen beobachtet werden. Die Aktivierung der Durchstanzbewehrung ist mit Tests an Deckenproben in Originalgrösse untersucht worden. Dabei wurden umfangreiche Messungen der Kraft (externe Lastsensoren) und der Rissbreiten (Apparaturen zur totalen und partiellen Dickenvariation) durchgeführt. Die Verwendung eines innovativen Bewehrungssystems hat es ermöglicht, die Beiträge des Betons und der Bewehrung beim Durchstanzvorgang einzeln nachzuvollziehen und damit benötigte experimentelle Grundlagen zu liefern, die der Validierung der Hauptaussagen der Theorie des kritischen Schubrisses für den Versagensmechanismus in der schubbewehrten Zone dienen.

Beobachtungen zum Verhalten gerader Bewehrungsstäbe mit Längsrissbildung haben zur Entwicklung von analytischen Funktionen für die Beurteilung der reduzierten Wirksamkeit –in Bezug auf Tragfähigkeit und Steifigkeit– verschiedener Verankerungssysteme gedient, basierend auf analogen Überlegungen für die Verzahnung der Gesteinskörner. Das entstandene Modell wurde mithilfe einer vertieften numerischen Analyse und dem Vergleich mit einer Reihe von zentralen Testergebnissen aus der Literatur verifiziert. Diese Ansätze können teilweise im Rahmen der Theorie des kritischen Schubrisses verwendet werden, welche es ermöglicht, den Beitrag der Schubbewehrung zum Durchstanzwiderstand –den studierten Versagensmechanismus– ausgehend von einem physikalischen Modell zur Aktivierung der Querkraftbewehrung zu ermitteln. Die Theorie beinhaltet mehrere allgemeine Annahmen –Vorhandensein eines perfekten Verbundes, einer perfekten Verankerung sowie einer bestimmten Risskinematik– welche durch die experimentellen Ergebnisse der vorliegenden Forschungsarbeit verbessert und verfeinert werden können. Es werden Vorschläge formuliert, um die Aktivierung der Querbewehrung beim Durchstanzvorgang im existierenden Modell auf realistischere Weise –durch die Berücksichtigung des abnehmenden Krafttransfers bei der Bildung von Biegerissen– darzustellen und somit die entsprechenden Versagensmechanismus genauer vorhersagen zu können.

Stichworte:

Durchstanzen, Verbindungen zu inneren Deckenstützen, Querbewehrung, Theorie des kritischen Schubrisses, Aktivierungsmodell, Versagenskinematik, Verbund und Verankerungsverhalten, Ausziehversuche, gerissener Beton, Grenzzustand der Gebrauchstauglichkeit, Grenzzustand der Widerstandsfähigkeit, Kraft-Schlupf Beziehung

Riassunto

Il solaio piano in calcestruzzo armato rappresenta uno dei metodi moderni di costruzione più efficaci e frequentemente utilizzati. Il dimensionamento di questo sistema strutturale può essere influenzato da una rottura fragile in prossimità della connessione solaio-colonna, causata dal fenomeno di punzonamento. Vari incidenti e collassi degli ultimi decenni sono all'origine di soluzioni sviluppate per migliorare il comportamento globale del solaio ed evitare il suo crollo progressivo. La posa di armature trasversali nella zona critica aumenta sia la resistenza che la capacità di deformazione della connessione solaio-colonna. Nel passato sono stati sviluppati diversi tipi di rinforzi al punzonamento sulla base d'intuizioni e di prove sperimentali. I recenti sviluppi nella conoscenza del fenomeno del punzonamento hanno permesso di proporre nuovi prodotti di rinforzo, fondati su basi più razionali ed efficaci.

Uno dei parametri determinanti per l'efficacia delle armature trasversali è legato alla qualità dell'aderenza e dell'ancoraggio che influenzano lo sviluppo delle fessure nella zona critica. Queste caratteristiche sono generalmente definite da relazioni forza-scivolamento e sono influenzate dallo stato locale tensionale e di deformazione. Malgrado il fatto che l'attivazione di tali armature si produca in un calcestruzzo parzialmente fessurato, le formulazioni normative sono tutt'oggi quasi sistematicamente basate su prove di laboratorio realizzate su campioni non fessurati. L'ancoraggio delle barre d'armatura nel calcestruzzo fessurato è importante sia per il comportamento strutturale d'opere esistenti in calcestruzzo armato che per nuove costruzioni. Nei prossimi anni, dovrà essere prestata più attenzione allo studio del comportamento dei dettagli d'armatura in queste difficili condizioni, con l'obbiettivo di migliorare le conoscenze di questa problematica attualmente piuttosto sottovalutata.

Diverse indagini sperimentali sono state condotte in questa ricerca con lo scopo di migliorare la comprensione del ruolo svolto dall'ancoraggio dell'armatura trasversale nel fenomeno del punzonamento. Sono state effettuate delle prove d'estrazione su matrice fessurata su vari dettagli d'armatura sottoposti a condizioni simili a quelle esistenti in casi reali nei solai in prossimità delle colonne. I risultati hanno mostrato differenze importanti di comportamento dei vari dettagli d'ancoraggio analizzati, confermando le differenze d'efficacia osservate nelle prove di punzonamento. In questa ricerca viene studiata l'attivazione delle armature trasversali attraverso prove su piastre eseguite a scala reale e con misure dettagliate della forza (mediante cellule di carico) e dell'apertura delle fessure (con dispositivi di misura della variazione dello spessore totale e parziale). Una configurazione innovativa dell'armatura trasversale della piastra ha permesso di definire i contributi del calcestruzzo e dell'acciaio nella resistenza al punzonamento, fornendo i

dati sperimentali necessari alla validazione delle ipotesi principali della teoria della fessura critica per l'analisi del modo di rottura a punzonamento nella zona rinforzata.

I riscontri sperimentali ottenuti sulle barre dritte in presenza di fessure longitudinali hanno permesso di sviluppare delle espressioni analitiche per valutare la riduzione d'efficacia, in termini di resistenza e rigidità, associata a vari tipi d'ancoraggio e basandosi su considerazioni relative all'ingranamento degli aggregati. Il modello è stato validato grazie all'utilizzo di un raffinato metodo numerico e basandosi sui risultati di altre prove esistenti descritte nella letteratura. Queste procedure possono essere parzialmente utilizzate nell'ambito della teoria della fessura critica, la quale, per il tipo di rottura analizzato, definisce il contributo dell'armatura trasversale sulla resistenza al punzonamento con un modello specifico d'attivazione. Questa teoria si basa su alcune ipotesi – condizioni d'aderenza e d'ancoraggio perfette e cinematica di rottura semplificata – che possono essere migliorate e raffinate sulla base dei risultati sperimentali ottenuti con questa ricerca. Sono dunque proposte delle soluzioni per considerare, nel modello attuale, una modalità più realistica d'attivazione dell'armatura trasversale al momento del punzonamento della piastra – valutando la riduzione della capacità di trasmissione delle forze associata alla presenza delle fessure flessionali– allo scopo di permettere una migliore comprensione e predizione di questo meccanismo di rottura.

Parole-chiave:

punzonamento, solaio piano in calcestruzzo armato, connessione solaio-colonna interna, armatura trasversale, teoria della fessura critica, modello d'attivazione, cinematica di rottura, prestazioni d'ancoraggio e d'aderenza, prove d'estrazione, calcestruzzo fessurato, stato limite ultimo e di servizio, relazione forza-scivolamento relativo

Σύνοψη

Οι πλάκες χωρίς δοκούς από οπλισμένο σκυρόδεμα αποτελούν μια από τις πλέον διαδεδομένες και αποτελεσματικές σύγχρονες μεθόδους κατασκευής. Ο σχεδιασμός αυτού του δομικού συστήματος μπορεί να καθορίζεται από ψαθυρές αστοχίες κοντά στις συνδέσεις πλάκας-υποστυλώματος λόγω διάτρησης. Ορισμένα ατυχημάτα κατά τη διάρκεια των τελευταίων δεκαετιών αποτέλεσαν κίνητρο για την ανάπτυξη μεθόδων βελτίωσης της απόκρισης της πλάκας και αποφυγής προοδευτικής κατάρρευσης. Η διάταξη εγκάρσιου οπλισμού εντός της κρίσιμης περιοχής κοντά στα υποστυλώματα αυξάνει τόσο την αντοχή όσο και την ικανότητα παραμόρφωσης της σύνδεσης πλάκας-υποστυλώματος. Διάφορα συστήματα οπλισμού διάτρησης έχουν αναπτυχθεί στο παρελθόν βασιζόμενα στη διαίσθηση και σε πειράματα. Πρόσφατες εξελίξεις όσον αφορά τα φαινόμενα που σχετίζονται με τη διάτρηση οδηγούν σε καλύτερη κατανόηση των διαφορών σε αποτελεσματικότητα και στην ανάπτυξη νέων προϊόντων οπλισμού σε μια πιο συνεπή βάση.

Μία από τις βασικές παραμέτρους που επηρεάζουν καθοριστικά την επίδοση του συγκεκριμένου οπλισμού σχετίζεται με την αγκύρωση και τα χαρακτηριστικά συνάφειας που επηρεάζουν την ανάπτυξη ρωγμών στην κρίσιμη σε διάτμηση περιοχή. Το χαρακτηριστικό αυτό ορίζεται γενικώς μέσω σχέσεων δύναμης-ολίσθησης και επηρεάζεται σε μεγάλο βαθμό από την τοπική εντατική και παραμορφωσιακή κατάσταση. Παρότι η ενεργοποίηση του οπλισμού λαμβάνει συχνά χώρα υπό συνθήκες ήδη ρηγματωμένου σκυροδέματος για πολλά δομικά μέλη, οι συμβατικές προσεγγίσεις που αποτελούν βάση για τους κανονισμούς βασίζονται ακόμη σχεδόν αποκλειστικά σε πειράματα επί μη ρηγματωμένων δοκιμίων. Ενδελεχείς μελέτες πάνω στο θέμα αυτό δεν είναι τόσο πολλές όσο πιθανώς απαιτεί το πρόβλημα.

Στο πλαίσιο της παρούσας διατριβής, πραγματοποιήθηκαν αρκετές πειραματικές εργασίες με στόχο τη βελτίωση της υπάρχουσας τεχνογνωσίας σχετικά με το ρόλο της αγκύρωσης του εγκάρσιου οπλισμού στο φαινόμενο της διάτρησης. Μια σειρά πειραμάτων εξόλκευσης σε πραγματικές κατασκευαστικές διαμορφώσεις πραγματοποιήθηκε υπό συνθήκες ρηγμάτωσης παρόμοιες με αυτές που εμφανίζονται σε πλάκες κοντά στο υποστύλωμα. Τα αποτελέσματα έδειξαν σημανικές διαφορές ανάμεσα στους τύπους αγκύρωσης που εξετάστηκαν, επιβεβαιώνοντας το διαφορετικό επίπεδο απόδοσης που έχει παρατηρηθεί σε πειράματα διάτρησης. Η ενεργοποίηση των στοιχείων αυτών ερευνήθηκε στην παρούσα διατριβή μέσω πειραμάτων δοκιμίων πλάκας σε πλήρη κλίμακα, στα οποία μετρήθηκε η δύναμη (εξωτερικά

ηλεκτρονικά δυναμόμετρα) και το άνοιγμα της ρωγμής (πλήρης και μερική μέτρηση της αύξησης του πάχους της πλάκας). Η χρήση μιας πρωτότυπης πειραματικής διάταξης για τον οπλισμό επέτρεψε τον υπολογισμό της συνεισφοράς του σκυροδέματος και του οπλισμού στο φαινόμενο της διάτρησης, παρέχοντας πειραματικά δεδομένα για την επιβεβαίωση των βασικών υποθέσεων της Θεωρίας Κρίσιμης Διατμητικής Ρωγμής για αστοχία εντός της οπλισμένης σε διάτμηση περιοχής.

Παρατηρήσεις επί ευθύγραμμων ράβδων οπλισμού με εντός επιπέδου ρηγμάτωση οδήγησαν στην ανάπτυξη αναλυτικών σχέσεων για τον υπολογισμό της μείωσης της απόδοσης –όσον αφορά την αντοχή και τη δυσκαμψία– για διάφορους τύπους αγκύρωσης, κατ' αναλογία με μεθόδους υπολογισμού της αλληλεμπλοκής αδρανών. Η απόδοση του προσομοιώματος επιβεβαιώθηκε μέσω σύγκρισης με μια εξελιγμένη αριθμητική μέθοδο και αποτελέσματα πειραμάτων από τη βιβλιογραφία. Η προσέγγιση αυτή μπορεί να χρησιμοποιηθεί μερικώς στο πλαίσιο της Θεωρίας Κρίσιμης Διατμητικής Ρωγμής, η οποία υπολογίζει τη συνεισφορά του οπλισμού διάτμησης στην αντοχή διάτρησης –για τον τρόπο αστοχίας που εξετάζεται– βασιζόμενη σε ένα φυσικό προσομοίωμα ενεργοποίησης των εγκάρσιων στοιχείων. Η θεωρία αυτή περιέχει ορισμένες γενικές υποθέσεις –πλήρης συνάφεια, τέλειες συνθήκες αγκύρωσης και έναν απλοποιητικό κινηματικό μηχανισμό της ρωγμής– οι οποίες μπορούν να βελτιωθούν με βάση τα πειραματικά αποτελέσματα της παρούσας έρευνας. Αναπτύσσονται προτάσεις βελτίωσης του υπάρχοντος προσομοιώματος, έτσι ώστε να ληφθεί υπόψιν μια πιο ρεαλιστική ενεργοποίηση του εγκάρσιου οπλισμού της πλάκας μέσω απομείωσης της συνεισφοράς των μηχανισμών μεταφοράς φορτίου εξ αιτίας της παρουσίας καμπτικών ρωγμών.

Λέξεις-κλειδιά:

διάτρηση, εσωτερικές συνδέσεις πλάκας-υποστυλώματος, εγκάρσιος οπλισμός, Θεωρία Κρίσιμης Διατμητικής Ρωγμής, προσομοίωμα ενεργοποίησης, κινηματικός μηχανισμός αστοχίας, επίδοση συνάφειας και αγκύρωσης, πειράματα εξόλκευσης, ρηγματωμένο σκυρόδεμα, οριακή κατάσταση λειτουργικότητας και αστοχίας, σχέσεις δύναμης-ολίσθησης

Аннотация

Железобетонные конструкции - один из наиболее распространенных и эффективных методов современного строительства. Конструкция таких систем может сопровождаться трещинообразованием в результате критического напряжения плит у опорных колонн, лишающим конструкцию необходимых эксплуатационных качеств. Несколько несчастных случаев, произошедших в последние десятилетия, привели к разработке инженерных решений, позволяющих предотвратить возможные обрушения путем повышения прочности и трещиностойкости железобетонных плит. Поперечная арматура, помещенная в плиты в критической зоне у опорных колонн, увеличивает прочность и упругость соединения. Различные системы сопротивления динамическим нагрузкам ранее разрабатывались интуитивно, опытным путем. Последние достижения в исследованиях деформирования железобетонных конструкций ведут к лучшему пониманию эффективности различных методов повышения прочности и более последовательной разработке подходов к созданию новых видов арматуры.

Один из основных параметров, определяющих эффективность конкретной арматуры, связан с ее характеристиками по анкеровке стежня и сцеплению металла с бетоном, влияющими на трещинообразование в критических зонах. Такой параметр, как правило, определяется соотношением силы воздействия и степени сдвига и существенно зависит от локального уровня напряжения и деформаций. Хотя эффективность арматуры часто проявляется в конструкциях, уже имеющих трещины во многих элементах системы, все традиционные подходы до сих пор, почти без исключения, были основаны на результатах испытаний, выполненных на образцах без трещин. Фундаментальных исследований по этой теме пока меньше, чем требуется.

Поэтому в данной работе было проведено несколько экспериментов для расширения базы имеющихся знаний о степени эффективности использования поперечной арматуры для повышения прочности конструкций. Была реализована программа испытаний (пул-аут тестов) на основе существующих методов в условиях наличия трещин, максимально приближенных по характеристикам к появляющимся в бетоне вблизи опорных колонн. Результаты выделили значительные различия между исследуемыми видами крепления, подтвердив тем самым также различные уровни трещиностойкости. В приведенном исследовании протестировано использование арматуры с различной анкеровкой для полномасштабных образцов плит с использованием расширенных методов измерения силы воздействия (внешние датчики нагрузки) и степени раскрытия трещин (датчики

полного и частичного изменения толщины). Использование инновационной арматуры позволило отследить взаимодействие и эффективность бетона и стали в случае динамических нагрузок, и получить экспериментальную базу, необходимую для проверки основных предположений теории трещиностойкости с увеличением нагрузки на балку до предельного разрушающего значения в зоне поперечной арматуры.

На основе исследования стержней с прямой анкеровкой в плоскостях, имеющих трещины, были сформулированы аналитические выводы, сопровождаемые результатами соответствующих механических испытаний, позволяющими оценить снижение эффективности различных деталей анкеровки с точки зрения прочности и жесткости. Обоснование модели произведено с помощью усовершенствованного числового метода и основных результатов тестов, доступных в литературе. Такие наработки могут быть частично использованы в рамках теории трещиностойкости, которая рассчитывает эффективность использования поперечной арматуры в повышении прочности конструкций для рассматриваемого типа разрушения на основе физической модели. Последняя, как правило, содержит ряд общих допущений – идеальные условия сцепления бетона с металлом и фиксации арматуры и упрощенная кинематика трещин, которые могут быть улучшены и уточнены на основе экспериментальных доказательств из данного исследования. Рекомендации сформулированы таким образом, чтобы учесть в представленной модели более реалистичное воздействие поперечной арматуры на бетонные конструкции при деформации, принимая во внимание снижение возможности переноса силы воздействия в связи с наличием трещин в местах критического напряжения.

Ключевые слова:

Деформация, внутреннее напряжение бетонных плит у опорных колонн, поперечная арматура, теория трещиностойкости, модель определения степени воздействия, кинематика разрушения, эффективность анкеровки стежня и сцепления металла с бетоном, пул-аут тест, треснувший бетон, эксплуатационные свойства и определение критических условий, соотношение силы воздействия и степени сдвига

Table of contents

Notation

Latin upper case:

A_b	area of a bar
A_c	reduced contact area (cracked conditions)
A_{c0}	initial contact area (uncracked conditions)
A_h	area of the head (for headed bars details)
A_R	projected area of a single rib on the cross-section
$A_{sw,i}$	cross-sectional area of transverse reinforcement elements placed at perimeter i
E_c	modulus of elasticity of concrete
E_s	modulus of elasticity of steel
E_{sw}	modulus of elasticity of the transverse reinforcement
F	force acting on a bar or anchorage
F_0	force at which the anchorage start to slip (tri-linear law, modified activation model)
F_{strut}	force in the first concrete strut
F_u	ultimate force of a bar or anchorage (tri-linear law, modified activation model)
F_y	yielding force of a bar or anchorage
K	anchorage stiffness in cracked conditions (tri-linear law, modified activation model)
K_0	anchorage stiffness in uncracked conditions (tri-linear law, modified activation model)
V	applied concentrated load, shear force
V_{flex}	applied concentrated load associated to flexural capacity of the slab
V_R	punching strength
$V_{R,c}$	concrete contribution to punching strength
$V_{R,c0}$	concrete contribution to punching strength (failure load of reference slab)
$V_{R,c,exp.}$	experimental concrete contribution to punching strength ($V_R - V_{R,s1} - V_{R,s2} - V_{R,s3}$)
$V_{R,crush}$	punching strength, failure due to crushing of first concrete strut in CSCT
$V_{R,in}$	punching strength, failure within the shear-reinforced area in CSCT
$V_{R,ref}$	punching strength of a reference slab

$V_{R,s}$ transverse reinforcement contribution to punching strength

$V_{R,sy}$ maximum transverse reinforcement contribution to punching strength (yielding)

Q_{max} maximal hydraulic pressure in the limitating valve (nominal value from producer)

Latin lower case:

a_1, a_2, a_3 experimental parameters

b_0 perimeter of the critical section at $d/2$ from the column face (edges rounded)

$b_{0,ACI}$ perimeter of the critical section at $d/2$ from the column face (edges not rounded)

$b_{0,EC}$ perimeter of the critical section at $2d$ from the column face (edges rounded)

c concrete cover, side length of a square column or compressive depth (cracked section)

d effective depth (distance from the tension reinforcement to the extreme compressed fiber, considering a mean value of the two main reinforcement directions)

d' effective depth (distance from the compression reinforcement to the extreme compressed fiber, considering a mean value of the two main reinforcement directions)

d_b bar diameter

d_g maximum diameter of the aggregate

d_{g0} reference aggregate size (d_{g0} = 16mm)

d_h head diameter

d_v reduced effective depth for a slab

f_b maximum bond strength (cracked conditions)

f_{b0} maximum bond strength (uncracked conditions)

f_c average compressive strength of concrete (measured on cylinders)

$f_{c,eff}$ effective compressive strength of concrete

f_{ct} average tensile strength of concrete (measured on cylinders)

f_R bond index (relative rib area)

f_{rel} relative frequency of crack observation (for different widths)

f_t ultimate strength of flexural reinforcement

f_{tw} ultimate strength of transverse reinforcement

f_y yield strength of flexural reinforcement (for hot-rolled bars)

$f_{y,0.2}$ yield strength of flexural reinforcement (for cold-rolled bars)

f_{yw} yield strength of transverse reinforcement

h	slab thickness
h_i	vertical distance between the tip of the critical crack and the point of intersection with the shear reinforcement (at row i) in the activation model
h_R	equivalent rib height
$h_{R,max}$	maximum rib height
$h_R(\theta)$	rib profile along the periphery of the bar
$h_w(\theta)$	crack profile along the periphery of the bar
k	size effect factor in EC2
k_{dg}	coefficient related to the aggregate size in MC2010
k_{max}	factor that limits the maximum increase of shear strength for slabs with transverse reinforcement in EC2 (amended in 2014)
k_{sys}	coefficient describing the efficiency of a shear reinforcement system in MC2010
$l_{a,i}$	distance between the point where a transverse element is intercepted by the critical shear crack and its closest anchorage
$l_{a,s}$	distance between the point where a transverse element is intercepted by the critical shear crack and its anchorage found most far from that point
l_b	development length of a bar or an anchorage
$l_{b,i}$	bond development length between the point where a transverse element is intercepted by the critical shear crack and its lower anchorage (for a given σ_{sw})
$l_{b,s}$	bond development length between the point where a transverse element is intercepted by the critical shear crack and its upper anchorage (for a given σ_{sw})
l_w	length of the straight portion of the transverse reinforcement element
m_R	moment capacity per unit width
m_S	acting bending moment per unit width due to the applied load
m_r	radial bending moment per unit width
m_t	tangential bending moment per unit width
n_l	number of lugs
n_r	number of perimeter of transverse reinforcement
n_t	number of transverse elements per reinforcement row
r	radius of the mandrel (for bend bars details), distance from the center of the column
r_0	radius of the critical shear crack at the level of tensile reinforcement

r_c	column radius (taken as half of the column side length c in the case of square columns)
r_i	distance from the center of the column to a point i
r_q	distance between the center of the column and the point of application of the load
r_s	distance between the center of the column and the line of moment contraflexure
s	effective distance between reinforcement bars of the flexural reinforcement
s_0	distance between the face of the column and the first transverse reinforcement element
s_1	spacing between the first and second elements of the transverse reinforcement
s_r	spacing between consecutive transverse elements in the same reinforcement row (for elements of the second row or further)
s_t	spacing between elements of the same row of transverse reinforcement
s_R	mean rib spacing
t	geometrical dimension of an element or time
v	nominal shear stress at the control perimeter
v_R	nominal shear strength at a control perimeter
$v_{R,c}$	nominal shear strength at a control perimeter for slabs without shear reinforcement
$v_{R,c,s}$	nominal shear strength at a control perimeter for slabs with shear reinforcement
w	crack opening
w_i	vertical displacement (deflection) of a point i on the slab (for computation of Δw)
$w_{b,i}$	relative displacement parallel to the transverse reinforcement element (at row i)
$w_{flex.}$	crack opening associated to flexural solicitations (variable width)
$w_{li,1}$	maximum crack opening (Regime A)
$w_{li,2}$	maximum crack opening (Regime B)
w_r	radial crack opening of the at the surface of the slab
$w_{r,m}$	average opening of the radial crack (between tip of the crack and at slab surface)
x_{i-j}	distance between two points i and j on the slab (for computation of Δw)

Greek upper case:

Δd	partial thickness variation
$\Delta\delta$	slip associated to the pull-out descending branch (between peak and residual strength)
$\Delta\delta_p$	relative shift of the peak bond strength (cracked conditions)
$\Delta\delta_{p,max}$	maximum relative shift of the peak bond strength (cracked conditions)

$\Delta\varepsilon_{sw}$ strain in the transverse reinforcement (per unit length)

ΔF additional force in the transverse reinforcement elements (post-failure phase)

Δh full thickness variation (slab expansion)

$\Delta\theta$ change in the orientation of the bar according to crack (compared to initial disposition)

$\Delta\sigma_{sw}$ stress in the transverse reinforcement (per unit length)

ΔV additional load in the slab (post-failure phase)

Δw shear deformations at the column face (computed from deflections w_i and x_{i-j})

Δx unit length

$\Delta\varphi$ angle of a slab sector

Greek lower case:

α angle of the critical shear crack with respect to slab plane, or angle of the experimental failure crack observed in tests

α_H angle of the head (according to bar axis)

α_R rib flank inclination (perpendicular to rib orientation, according to bar axis)

β_i angle of the transverse reinforcement element with respect to slab plane (at row i)

β_R rib inclination (according to bar axis)

γ_1 experimental parameter

δ relative displacement between steel and concrete (slip)

$\delta_{b,i}$ relative displacement perpendicular to the transverse reinforcement element (at row i)

δ_i slip associated to the bottom anchorage (modified activation model)

δ_p slip at peak bond strength (cracked conditions)

δ_{p0} slip at peak bond strength (uncracked conditions)

δ_i slip associated to the top anchorage (modified activation model)

δ_u slip at ultimate force

$\varepsilon_{c,r}$ concrete surface strain in the radial direction of the slab

$\varepsilon_{c,t}$ concrete surface strain in the tangential direction of the slab

ε_{sw} strain in the transverse reinforcement

η_c strength contribution factor for concrete (punching failure within)

η_s strength contribution factor for transverse reinforcement (punching failure within)

θ	integration parameter (polar angle from center of the bar)
κ	critical shear crack opening factor in CSCT
κ_f	coefficient of proportionality
λ	crushing strength parameter in CSCT
ρ	flexural reinforcement ratio
ρ'	flexural reinforcement ratio (compressive)
ρ_w	shear reinforcement ratio
σ'	stress in the transverse element associated to the activation of both anchorages
σ_0	stress in the transverse element (associated to F_0)
σ_u	maximum stress in the transverse element (associated to F_0)
$\sigma_{b,i}$	stress in the transverse element from bond (prior to the activation of the anchorages)
σ_c	bearing stress on the concrete
σ_s	stress in steel elements
$\sigma_{sp,i}$	stress in the transverse element (at row i) associated to prestressing
$\sigma_{sw,i}$	stress in the transverse element (at row i)
τ	effective bond stress
τ_b	average bond stress (cracked conditions)
$\tau_{b,0}$	average bond stress (uncracked conditions)
χ_r	curvature of the slab in radial direction
χ_t	curvature of the slab in tangential direction
ψ	slab rotation
ψ_R	slab rotation at failure
$\psi_{R,ref}$	slab rotation at failure of a reference slab

Abbreviations

ACI 318-14	American Concrete Institute Building Code (refers to [ACI14])
CSCT	Critical Shear Crack Theory (refers to [Mut08a, Fer09, Fer10a])
COV	Coefficient of variation
EC 2004	Eurocode 2 (refers to [CEN04])
MC 2010	fib Model Code 2010 (refers to [FIB13])
SIA 2003	Swiss code 262 (refers to [SIA03])
SIA 2013	Swiss code 262 (refers to [SIA13])

Chapter 1 Introduction

Reinforced concrete still remains, in 2016, the most universal construction material. The structural interest of combining steel and concrete is beyond doubt, as long as the transfer of forces can be achieved adequately to consider the contribution of both components. Nonetheless, the latter has not always been a main concern for engineers, and many designs of early applications of this material may still be found in which the interaction between the steel and the surrounding concrete seems to have been entirely neglected.

In the beginning of the 20th century, experimental evidences [Sco10, Bac11a, Bac11b, Abr13] highlighted that detailing of the reinforcement might be of capital importance in the development of efficient structures. This problematic can be particularly well illustrated by the statements of Mörsch [Mör08] on plain bars, who recognized as one of the first the critical role of the anchorage in reinforced concrete in order to complete the transfer of force accomplished by bond mechanisms:

> *"The ends of reinforcing rods should have always be made with a hook so that sole dependence is not placed on friction or adhesion. […] By bending the end into a half circle […] the principle of rope friction is employed and a greater resistance is produced on the inner side of the bend, since the hook will be pressed hard against the concrete. […] These hooks possess the further merit of not depending to any great extent upon the character of the concrete or the care given to the work."*

In the same period, some manufacturers and constructors developed a structural concept specific to reinforced concrete in order to improve the efficient use of the material and the construction methods. Simple columns progressively replaced the combination of beams and frame systems –originally inspired from steel and timber structures– to support slab elements commonly defined as *flat slab*. The success of this new typology of construction resulted in several approaches regarding the arrangement of the flexural reinforcement –generally experimentally-based [Con13, Edd14, Tay16, Smu18]– as no design guidelines were yet available. The original opinion on this subject is very well represented by the thoughts of Eddy and Turner [Edd14]:

> *"The superiority of flat slab floor supported directly on columns, over other forms of construction when looked at from the standpoint of lower cost, better lighting, greater neatness of appearance, and increased safety and rapidity of construction, […] in this type of construction of great interest."*

As slab-column connections were quickly recognized as the critical part of this structural system, specific solutions –mainly related to a local enlargement of the column– were developed to reduce the spans and increase the part of load transferred directly [Edd14, Mai26]. The effectiveness and simplicity associated with this construction method significantly contributed to its wide application in practice, and numerous projects were proposed by engineers and architects (Figure 1.1*(a)*).

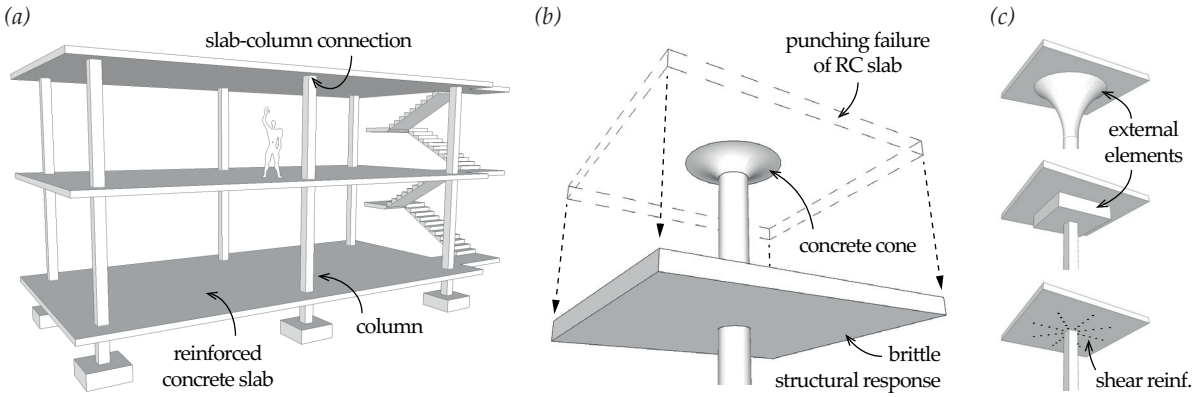

Figure 1.1 Reinforced concrete flat slabs: *(a)* project «Dom-Ino» by *Le Corbusier* in 1914 for mass production of housing; *(b)* typical failure mode of the slab-column connection; *(c)* solutions developed to limit the risk of collapse (from top to bottom: hyperbolic concrete drop panel, column capital or disposition of shear reinforcement in the vicinity of the column)

As a consequence, several accidents related to these structures were reported during the century – but also more recently [Woo01, Mut05]– characterized by the brittle detachment of a concrete cone in the vicinity of the slab and the column, the so-called *punching failure* (Figure 1.1*(b)*). The knowledge acquired in the analysis of such cases from experiments or real situations contributed to a better phenomenological understanding of punching shear mechanisms [Mut91]. The additional difficulties associated with the construction of external elements at the soffit of the slab (drop panels or column capitals) led nowadays to commonly dispose transverse reinforcement within the slab in the shear-critical region in order to limit the risk of collapse (Figure 1.1*(c)*). Significant amount of steel-based reinforcing systems were progressively developed and introduced to improve the response of the slab both in terms of strength and deformation capacity, complexifying however the potential failure modes with respect to the reference specimen (Figure 1.2).

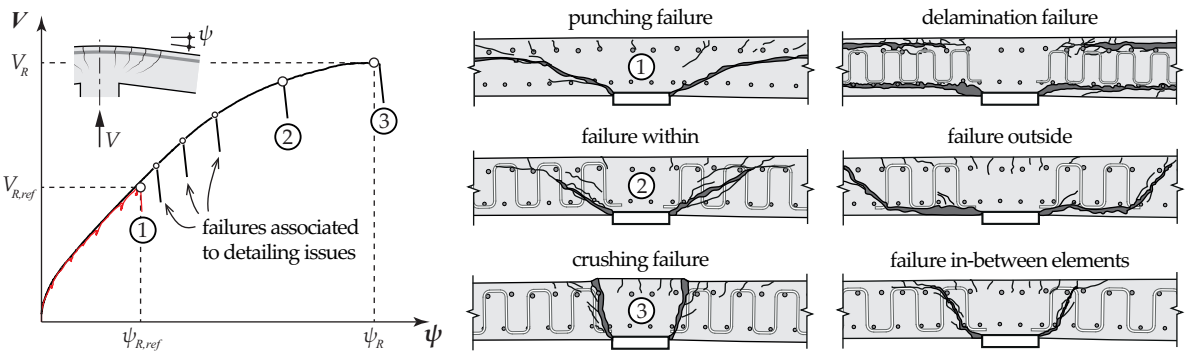

Figure 1.2 Potential punching failure modes and related load-rotation responses (V-ψ) for slabs without (red curve) and with shear reinforcement (black curves)

Although significant research was carried out since the middle of the 20th century on the latter topic, the difficulty in developing a general design model can be related to the important disparities of performance amongst the existing types of transverse reinforcement [Ein16a]. The question of what constitutes an efficient shear reinforcement system is one about which there has always been a diversity of opinion. Criteria related to production, material optimization, ease of disposition and structural performance, among others, were recently cited as characterizing the success of a given product in practice [Beu02]. In the context of the punching of reinforced concrete slabs, the development of the force transfer mechanisms –associated to bond and anchorage of the transverse elements– is affected by various conditions within the specimen. Although the confinement at the soffit of the slab in the vicinity of the column might be in this sense favorable, the presence of cracks on the tensile part rather tends to deteriorate the force transfer mechanisms of these systems.

The adequate disposition of shear reinforcement around the column aims at providing an additional transverse stiffness to the slab in this critical location in order to control the internal cracking, yet with variable performance amongst existing systems (Figure 1.3). The activation of the transverse elements can be potentially limited by anchorage issues of the reinforcing details [Fer09]. Therefore, the related slip should ideally be kept to a minimum in order to avoid secondary failure modes. Since the end of the 20th century, the endless developments by industrials of new punching reinforcement solutions –particularly innovative– were motivated by the desire to depict the role of bond and anchorage in this specific phenomenon.

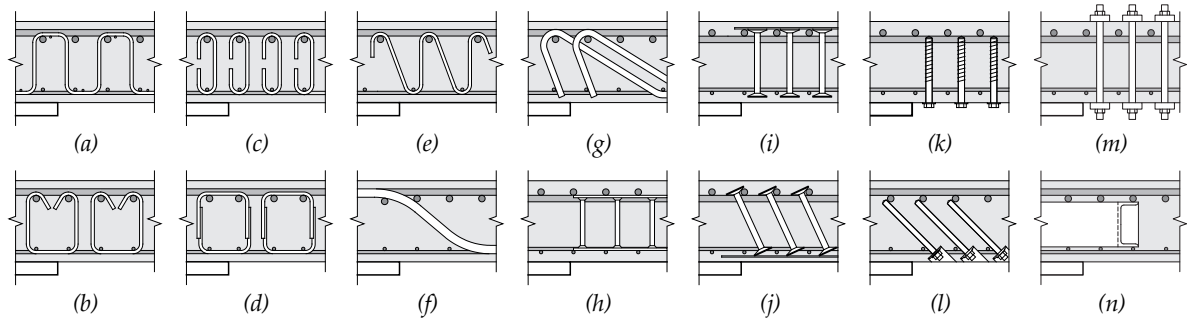

Figure 1.3 Common shear reinforcement solutions against punching of RC flat slabs: (*a-e*) bend bar details (continuous stirrups, single or double legged elements, individual links); (*f-g*) bent-up bars; (*h-j*) headed bars (single or double headed bars, ladder type); (*k-m*) post-installed elements (screws or threaded bars); and (*n*) shearhead made of steel profiles

The highlighted issues can be tackled by investigating the performance of reinforcing details –representative of the one used in shear reinforcement systems– in conditions similar to the ones which develop during punching, notably in the presence of cracks. However, such studies were relatively rare due to the substantial complexity associated to these experiments with respect to standardized tests (performed usually in uncracked concrete specimens). Also, the considerable amount of additional parameters involved in slabs including transverse reinforcement significantly complicates the potential modes of failure. Although such systems have been considered for decades, their activation is still under investigation nowadays, and is of major importance in the better comprehension of the punching phenomenon with shear reinforcement.

1.1 Research significance

This thesis intends therefore not to focus solely on the punching of flat slabs with shear reinforcement, but also on the force transfer mechanisms between steel and concrete in severe conditions, in order to specify the role of bond and anchorages of the transverse elements in the phenomenon.

The activation of reinforcing details in cracks is a rather underrated topic as, in many structural members, the aforementioned mechanisms are developed within already cracked concrete. This is particularly relevant for the transverse elements disposed in the vicinity of the slab-column connection which might be subjected to severe cracking conditions (Figure 1.4). Remarkably, few investigations [Reh79, Reg80b, Idd99] were conducted on the influence of cracks on the bond and anchorage performance. Most of the design codes still do not explicitly consider the problematic of the detailing of the transverse reinforcement in such conditions, although experimental evidences confirm its role on the structural response of reinforced concrete beams [Reh78a, Reh78b, Bac11a, Bac11b, Sal13, Kup72, Scr82, Bos84, Mir88, Reg04, Iso08, Var11, Alb11, Yan12, Wan12] and slabs [Els56, Lan76, Reg80a, Dil81, Voe81, Mok85, Gha92, Mar97, Oli00, Reg00, FIB01, Beu02, Eli06, Fer09, Fer10, Iná12, Lip12].

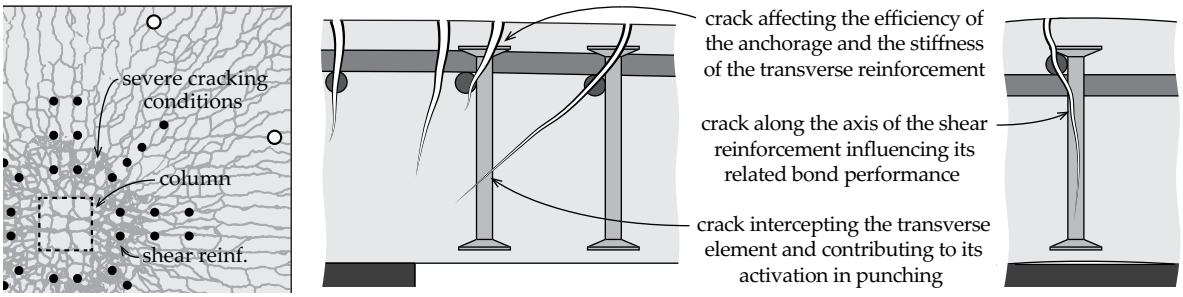

Figure 1.4 Cracks in punching phenomenon: typical surface crack pattern of a slab specimen reinforced with transverse elements (at failure) and related saw-cuts in the main directions

Based on a work initiated in the 1990's [Mut91], the Critical Shear Crack Theory (CSCT) was developed for beams [Mut08b], and slabs both without [Mut08a] and with shear reinforcement [Fer09]. It is the fundament of several one-way and two-way current shear provisions [SIA13, FIB13]. This physically-based approach regarding the transfer of shear forces in concrete –notably through aggregate interlock mechanisms– was validated in the last decade for various conditions for slabs both without [Gua09, Gui10, Sag11, May12, Clé14, Mic14, Sag14, Ein15, Dra16] and with shear reinforcement [Fer10a, Lip12b, Far14]. Regarding the failure mode of interest the present research –failure within the shear-reinforced area– both steel and concrete are involved in the phenomenon as the crack propagates through several rows of transverse elements. The activation model considered in the CSCT [Fer09] allows to estimate the contribution of the shear reinforcement (assuming perfect bond and anchorage conditions) to be added to the one related to the concrete (defined similarly for slabs without and with shear reinforcement [Mut08a]). These simplifications are not yet systematically supported by experimental results from literature. In this sense, the validation of the main assumptions of the CSCT and the consideration of more realistic bond and anchorage conditions in the activation of the shear reinforcement motivated the present research.

1.2 Objectives

The better understanding of the influence of bond and anchorage conditions on the activation of the transverse elements in reinforced concrete slabs during punching requires the consideration of several aspects. It appears to be necessary to cover to the following steps in order to contribute to the questions associated with this topic:

- Review the force transfer mechanisms in uncracked concrete for the main types of anchorages used for the transverse reinforcement in slabs (straight, hooked, U-shaped and headed bars);
- Summarize the tests performed by other researchers on the behaviour of such reinforcing details in cracked concrete (serviceability and ultimate limit state crack widths);
- Suggest the parameters influencing the disparities observed in the available studies;
- Conduct a rigorous experimental campaign in order to provide the necessary results to characterize the influence of cracking on the bond and anchorage performance (pull-out test series);
- Develop formulations to consider the influence of cracks on the response of the tested details;
- Highlight the importance of the anchorage conditions of the transverse reinforcement in the punching phenomenon and the diversity of products available;
- Detail the related experimental observations from literature for the specific failure mode within the shear-reinforced area;
- Investigate the activation of the transverse reinforcement during punching in full-scale slab specimens and the associated failure kinematics (punching test series);
- Discuss the assumptions of the CSCT from the main results and experimental evidences of the performed tests in order to point out its potential limitations;
- Propose some improvements for the determination of the transverse reinforcement contribution in the punching phenomenon (extension of the activation model) to consider more realistic bond and anchorage responses (on the basis of the experimental work performed).

1.3 Scope of the research

The study of the activation of the transverse elements in punching requires a certain limitation of the framework, as both central topics –the bond and anchorage performance, and the punching of slabs with shear reinforcement– could each be investigated separately in a specific work.

The present research aims at combining them appropriately through the consideration of detailing solutions representative of the types of shear reinforcement commonly used nowadays against punching. In this sense, systems as bent-up bars, bend bars with additional welded bars (composing most of the tested elements in [Reh79]) and the particular case of shearheads will not be treated. The review of the literature available focuses therefore on specific details (Figure 1.5) such as straight, headed, hooked and U-shaped bars (with or without passing-through elements) corresponding respectively to individual links, stirrups and double-headed studs systems in slabs. Although most of the reinforcing details are generally made of deformed steel –provided with a surface profile– attention was also given to plain hooks as they can still be found in existing structures (potentially subjected to severe conditions such as cracking). Also, as bond has a fundamental preliminary role in the contribution of the transverse reinforcement to the punching strength –prior to the activation of the anchorage– straight bars are also considered in the investigation.

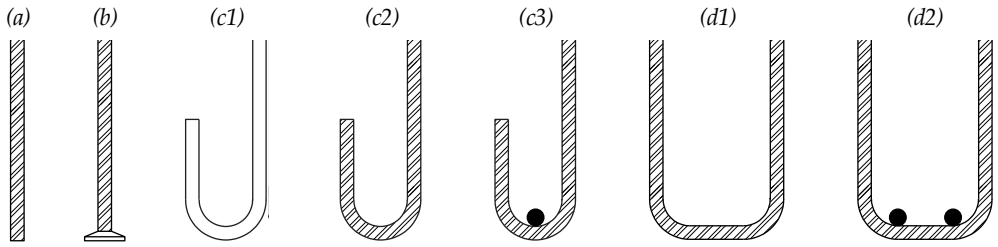

Figure 1.5 Types of reinforcement detailing solutions considered in the present research:
(a) straight bars; *(b)* headed bars; *(c)* bend bar details; and *(d)* U-shaped bars

The extensive pull-out campaign performed in this research aimed at characterizing bond and anchorage behaviour in conditions as close as possible to the ones that might occur throughout the service life of a reinforced concrete structure. A large range of crack openings was therefore considered to highlight the disparities of performance amongst the evaluated details and to justify the differences observed in slabs with regard to the activation of the transverse reinforcement.

Punching tests on full-scale specimens aimed at investigating the redistribution of forces at failure between the steel and concrete as well as the kinematics of the crack activating the transverse elements. A low amount of transverse reinforcement –mainly composed of post-installed elements, to limit interaction with bond and anchorage issues – was disposed in the critical zone.

In both experimental investigations, the material properties and test conditions were thoroughly defined in order to provide relevant observations and highlight analogies amongst the performed tests and other series of tests from previous research. To contextualize, the type of steel considered for the anchorage details evaluated in cracks is the same as the one that would generally be provided in Switzerland for a similar type of transverse reinforcement in slabs.

1.4 Organization

The thesis is organized around the two main directions of the research, namely the influence of cracks on bond and anchorage performance and the activation of the transverse elements in the punching of slabs for the failure mode within the shear-reinforced area.

Chapter 1 aims at introducing the issues that motivated the present investigation, it also depicts the organization of the document and the main objectives to be achieved.

Chapter 2 presents an overview of the force transfer mechanisms between steel and concrete –for straight, hooked, U-shaped and headed bars– in uncracked and cracked conditions. The few existing formulations from code provisions that account for the presence of cracks on the performance (straight bars only) are also highlighted and briefly discussed.

Chapter 3 details the extensive experimental campaign of pull-out tests conducted in flexural and transverse cracks (variable and constant opening on the height of the specimen). The results and observations arising from the latter are the bases for the development of analytical formulations to consider the influence of cracks on the performance of bond and anchorage force transfer mechanisms. The model is validated with tests from literature and a general numerical approach is proposed in order to extend it to more particular cases that can be found in practice.

Chapter 4 describes the phenomenon of punching according to the CSCT for slabs with and without transverse reinforcement. The main types of system available to improve the behaviour of slabs are briefly detailed in order to highlight the disparities amongst them in terms of use and performance. The different cracks potentially developing during punching are depicted in order to understand their respective roles on the activation of the transverse elements. Experimental observations gathered from specific investigations in literature –presenting a failure within the shear-reinforced area– highlight evidences on the activation of the transverse elements. Finally, the main code provisions are also compared in order to discuss the different approaches amongst them regarding the consideration of concrete and steel contributions on the punching strength.

Chapter 5 investigates the activation of the transverse reinforcement through innovative punching tests performed on full-scale slab specimens. The extensive and detailed measurements provide experimental evidences used to discuss the main assumptions of the CSCT regarding the punching failure within the shear-reinforced area. On that basis, and together with the main results related to bond and anchorage mechanisms in cracks (chapter 3), theoretical proposals are developed in order to improve the existing activation model considered for the aforementioned failure mode. Finally, suggestions are made regarding the further steps required for a complete implementation of the proposed extended model.

Chapter 6 concludes with the results achieved and the main contributions. It also provides an outlook for future research on the topics covered in the present research.

1.5 Personal contributions

Within this research, the following personal contributions were achieved and aimed at improving the knowledge on the role of bond and anchorage conditions in the activation of the transverse reinforcement in the punching of reinforced concrete flat slabs:

- Collect and consistently present the main experimental results associated to the force transfer mechanism of actual reinforcing details in uncracked and cracked concrete;
- Gather and highlight information on the activation of the transverse reinforcement from the investigations that presented a punching failure mode within the shear-reinforced area;
- Design and prepare specific test setups in order to perform the pull-out of anchorages in presence of in-plane flexural or transverse cracks;
- Elaboration of an innovative punching test series involving transverse reinforcement elements with a passive or active state, and monitored with particular measurement systems;
- Extensive experimental campaigns on beam (pull-out tests) and slab (punching tests) reinforced concrete specimens, with a thorough analysis and treatment of the test data;
- Development of a physically-based model –analogous to aggregate interlock approaches– to consider the influence of cracks on the bond and anchorage performance;
- Validation of the model through comparisons with performed tests and the ones obtained from existing literature, as well as through a refined numerical approach developed partly for this purpose (but also to extend it to specific cases not accounted);
- Investigation of the redistribution of internal forces at failure and the crack kinematics for the failure mode of interest;
- Critical review and validation of the main assumptions of the CSCT, notably regarding the estimation of the contributions to the punching strength of both the transverse reinforcement and concrete, as well as the maximum capacity associated to this type of failure;
- Extension of the activation model in order to consider more realistic (non-perfect) bond and anchorage conditions of the transverse elements;
- Implementation of the extended model within the frame of the CSCT in order to perform a parametric analysis and to discuss the influence of cracks on the punching response of slabs.

Throughout the research presented here, the candidate was also involved in the evaluation and development of innovative types of transverse reinforcement specific to punching applications for several industries. Although the results cannot be transcribed herein on account of obvious confidential conflicts, the experience and observations accumulated contributed significantly to the critical point of view on the influence of bond and anchorage of the shear reinforcement in punching.

Chapter 2 State of the Art on Bond and Anchorage in Concrete

Bond is one of the most instrumental phenomena in structural concrete characterizing the transfer of forces between concrete and steel. It generally governs the behaviour of reinforced concrete elements both at serviceability limit state (cracking development) and at ultimate limit state (strength, strain localization and deformation capacity). Bond is activated in many parts of a structure through the contact surface between the steel bars and the surrounding concrete. Depending on the properties of the interface, the external actions and the boundary conditions [FIB00], the bond response may vary considerably within a structural element. This is particularly the case with punching of flat slabs with transverse reinforcement (Figure 2.1), where several cases – potentially quite severe– might arise regarding the internal transmission of forces.

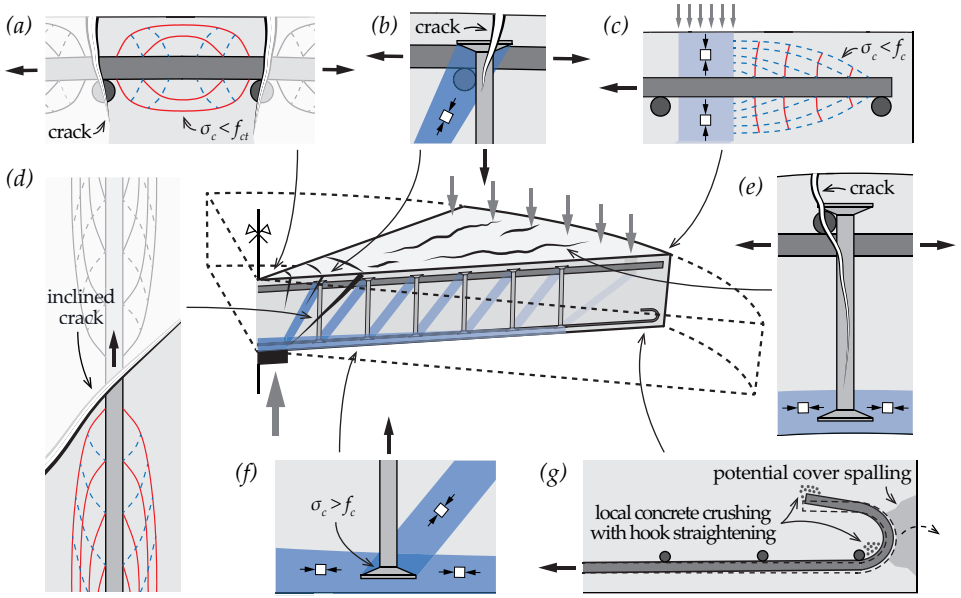

Figure 2.1 Local stress fields associated to internal forces transmission mechanisms between steel and concrete in the case of punching (dashed line for compression chord, and solid line for tensile chord, surface profile not represented for clarity purposes): *(a)* bond in flexural reinforcement; *(b)* anchorage of transverse reinforcement in tensile part of slab; *(c)* bond at extremity of the flexural reinforcement; *(d)* bond in transverse reinforcement; *(e)* crack affecting bond in flexural and transverse reinforcement; *(f)* anchorage of transverse reinforcement in compression part of slab; and *(g)* issues related to hooks anchorage

The concrete in direct proximity to the flexural reinforcement is subjected to local tensile stresses generated by bond (Figure 2.1*(a)*). Above the column, the formation of cracks is related to the local development of the material tensile strength required to achieve equilibrium. On the contrary, at the extremities of the flexural reinforcement (Figure 2.1*(c)*), the concrete remains typically subject-

ed to high compressive stresses due to the necessity to fully anchor the bar over a given length. Under some specific conditions such as a limitation of the available space, the use of reinforcement details with mechanical anchorage such as hooks (Figure 2.1*(g)*) or headed bars (for large diameter bars) is required to localize the transfer of forces and complete the activation. Potential issues related to local concrete crushing or spalling of the cover might therefore arise due to the straightening of the bend. The effective length of the transverse reinforcement used in punching –usually limited to less than the slab thickness for non-inclined elements– is generally not sufficient to guarantee solely and systematically the development of yield stresses in the bar. Additional anchorages at the extremities of the transverse elements are in this sense required –various detailing solutions were developed– to achieve a full activation and provide an adequate transverse stiffness against the formation and propagation of inclined cracks in the slab. In this sense, the performance of bond (Figure 2.1*(d)*) and of the mechanical anchorage (Figure 2.1*(b+f)*) mainly defines the steel contribution in the punching phenomenon. Although the presented force transfers are performed well in uncracked concrete, they might be significantly affected by the presence of cracks. This is notably the case for the flexural and transverse reinforcement (Figure 2.1*(e)*), as well as the anchorage of the latter in the tensile part of the slab (Figure 2.1*(b)*).

Several test setups and specimens (prisms or cylinders) were developed by researchers to experimentally reproduce the aforementioned conditions and to describe the related transfer of internal forces [FIB00], generally in terms of force-slip relationships. The slip (δ) usually denotes the relative displacement between the steel bar and the surrounding concrete. Together with the applied load (F), it characterizes the performance of the force transfer for a specific detailing solution. The procedures were then passably modified in order to minimise the effects of some specific aspects associated to the experiments –such as local confinement through the load introduction plate– leading to more complex investigations. Although these tests were initially developed mainly for straight bars, most of them were also adapted in order to study the behaviour of various anchorage types. Significant differences arise amongst common reinforcement solutions (Figure 2.2*(a)*), justifying a simplification of the detailing rules –notably a reduction of the development length (l_b)– when such systems are considered in comparison to straight bars (Figure 2.2*(b)*).

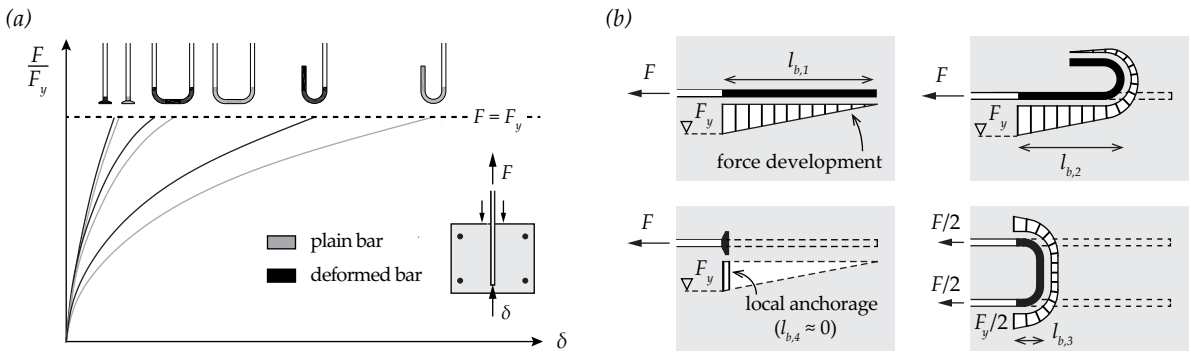

Figure 2.2 Activation of common reinforcing detail solutions in uncracked concrete (bond prevented on the straight part prior to anchorage): *(a)* qualitative force-slip relationships (partially adapted from the performed pull-out tests in the present research); and *(b)* qualitative differences in the force development ($l_{b,1} > l_{b,2} > l_{b,3} > l_{b,4} \approx 0$)

For instance, the required length for the full development of a straight bar can be significantly reduced by means of specific anchorage details. Yet, it is important to highlight that the disparities amongst the measured responses –especially for a given detail made of either plain or deformed bars– clearly indicate that more than one single force transfer mechanism is involved at the steel-to-concrete interface. Also, the dominant mechanism might vary considerably from one type of anchorage to another, as it will be affected differently by external conditions.

In this sense, in order to better capture the differences of performance amongst the main anchorage types composing the transverse reinforcement used in punching, the overview of the main force transfer mechanisms taking place in uncracked concrete focuses on straight, hooked and U-shaped bars as well as headed bar details (see Section 2.1). The problematic of cracking in reinforced concrete elements is then briefly presented with a qualitative discussion of the influences on the development of bond and anchorage under such conditions (see Section 2.2). The latter topic is then thoroughly documented through the available –yet relatively limited– experimental investigations found in literature for each of the aforementioned reinforcing solutions (see Section 2.3). Finally, the existing code provisions related to the effects of cracks on the force transfer action (bond phenomenon) will be presented to complete this literature review (see Section 2.4).

2.1 Force transfer mechanisms

Bond in reinforced concrete is a complex interaction of several force transfer mechanisms (Figure 2.3) taking progressively place at the interface between concrete and steel [FIB00]. Each reinforcing detail consists in a specific and unique combination of them [Eli06] leading to potential significant differences in the related performance.

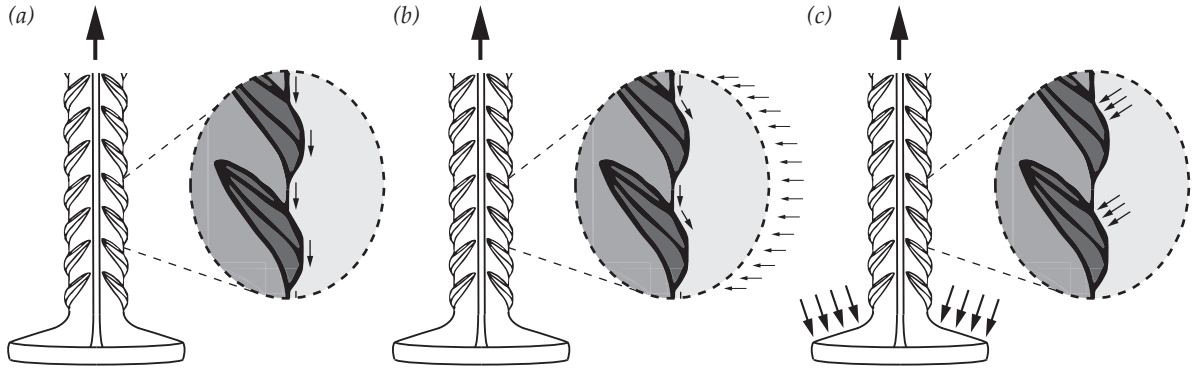

Figure 2.3 Force transfer mechanisms at the steel-to-concrete interface for a deformed headed bar; *(a)* chemical adhesion; *(b)* friction (with external pressure); and *(c)* mechanical action

Chemical adhesion (Figure 2.3*(a)*) develops at a micro level and only for relatively low values of slip. It is of major importance only in the case of plain straight bars, for which very limited surface roughness is provided. For details made of deformed bars, the related contribution is generally not significant with respect to the other force transfer mechanisms that can be activated. *Friction* (Figure 2.3*(b)*) is associated to the presence of a normal pressure (active or passive confinement) or during the unloading of the bar (due to Poisson's effect). It can be particularly important

in highly compressed zones, such as the soffit of the slab in the vicinity of the column during the punching phenomenon. For details made of plain bars, the shrinkage of the concrete around the element can already provide a certain contribution to the force transfer. *Mechanical action* (Figure 2.3*(c)*) is effective through the surface profile (ribs or indentations) and/or the anchorage (bend or head). Bearing of forces can only takes place once the adhesion has been entirely mobilized. In this sense, it is generally associated to larger values of slip and load in the bond response.

The transmission of forces between steel and concrete has been thoroughly investigated in the last decades [CEB82, CEB97, FIB00, FIB11, FIB14]. Experimental evidences have confirmed that the efficiency of the aforementioned mechanisms depends on a numerous amount of parameters:

- nature (static, dynamic or sustained), type (compression or tension), level (pre- or post-yield phase of the steel) and rate (slow, medium or fast) of loading
- casting orientation (in, perpendicular to or against the loading direction)
- concrete properties (tensile and compressive strength)
- local state of stress (uni- or multiaxial confinement/tensile)
- position (parallel or perpendicular), number (single or multiple cracks), type (constant or variable width) and opening (service or ultimate limit states) of the cracks
- material composing the reinforcing bar (steel, carbon or glass fibres)
- steel type (hot or cold formed for post-yielding phase) and bar surface (plain or deformed)
- geometrical properties of the surface profile and anchorage (inclination, bearing area)
- test setups (short or long pull-out tests, direction tension test, beam test, cantilever test)
- temperature (cryogenic, standard conditions, fire)

In the following, a distinction is done between straight bars (see Section 2.1.1), hooked and U-shaped bars (see Section 2.1.2) as well as headed bars (see Section 2.1.3) as major disparities arise among them regarding the force transfer mechanisms involved during activation. Also, the physical bases of the phenomena are developed and detailed through selected experimental works.

2.1.1 Straight bars

Much effort has been devoted to the characterization of bond properties in uncracked conditions for straight bars embedded in concrete [FIB00, FIB14]. In general, this has been performed with reference to specific test setups as standard (short) pull-out tests [RIL78], long pull-out tests or direct tension tests. The short pull-out test is aimed at determining the fundamental local bond-slip law characterizing bond (Figure 2.4*(a)*), and thus the development length (l_b) is kept low in order to get an almost constant slip (δ) along the bonded part of the bar (of diameter d_b). Indeed, under these conditions, the distribution of bond stresses τ can then reasonably be assumed constant over the contact length between the steel bar and the surrounding concrete. It is commonly assumed that the effects of all the force transfer mechanisms previously mentioned (*chemical adhesion*, *friction* and *mechanical action*) are idealized into one and unique uniform stress (τ_b) acting at the interface defined as Eq.(2.1). Typical relationships from such tests are qualitatively presented in Figure 2.4*(b)* for plain and deformed bars with significant differences in the structural responses.

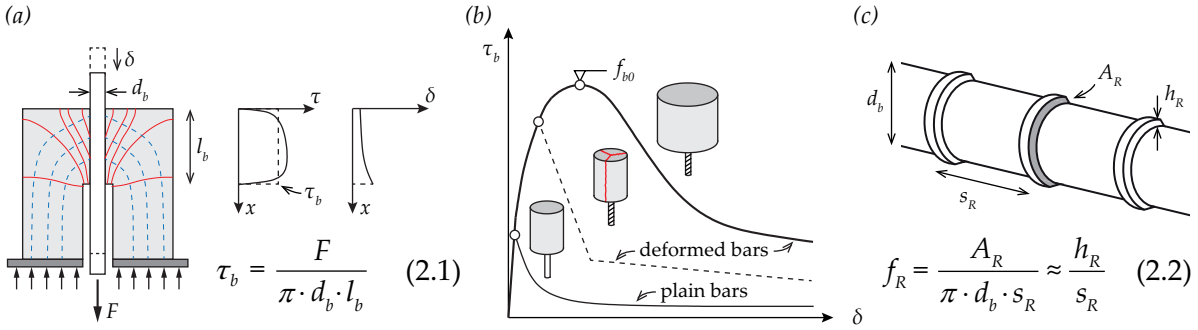

$$\tau_b = \frac{F}{\pi \cdot d_b \cdot l_b} \quad (2.1)$$

$$f_R = \frac{A_R}{\pi \cdot d_b \cdot s_R} \approx \frac{h_R}{s_R} \quad (2.2)$$

Figure 2.4 Characterization of bond properties for straight bars in uncracked concrete: *(a)* short pull-out test [RIL78] with principle stresses trajectories and formulation of the average bond stress; *(b)* typical bond-slip laws related to pull-out (solid lines) and splitting (dashed line) failures; and *(c)* definition of the bond index for deformed bars [FIB00]

Due to the surface properties of the interface, the force development of plain bars is mainly related to chemical adhesion, and therefore relatively limited. The fact that the deformed bars can additionally activate the mechanical action of the surface profile and friction mechanisms leads to significant higher maximum (f_{b0}) and residual bond strength. Yet, the presence of a surface profile (made of ribs or indentations, see Figure 2.7*(b)*) implies important modifications of the local state of stress in the vicinity of the bar in order to achieve the transmission of forces. In this sense, due to lack of sufficient concrete cover (dashed line in Figure 2.4*(b)*), a sudden limitation of the pull-out behaviour might potentially occur. Substantial disparities in terms of strength and stiffness were observed in the experimental work performed on single ribs of various geometry [Reh61]. The concept of the bond index (f_R) –originally named as relative rib area– was introduced by Rehm to characterize the influence of different type and arrangement of surface profiles, yet with several adjustments until the late 1960's [Reh69]. In its current and simplest form [FIB00], it is nowadays usually defined as Eq.(2.2), where A_R is the area of the projection of a single rib on the cross-section (Figure 2.4*(c)*). One may note that the bond index can be directly related to the ratio between an equivalent rib height (h_R) and the distance separating two consecutive ribs (s_R). More refined formulations are proposed by the European Committee for Standardization [ISO10], on which are based most of the current code provisions regarding the use of deformed bars for reinforcement in concrete structures. Large ribs ensure an adequate development of the aforementioned force transfer mechanisms at the interface, governing the correct activation of the steel and the related behaviour of the reinforced elements. However, for economic reasons, steel producers tend to provide small ribs to the bars leading to rather low values of bond index. To ensure sufficient bond strength, the Swiss code provisions for concrete constructions [SIA13, SIA15] –similarly to the European ones [CEN04, CEN05]– require minimum values for f_R –ranging from 0.035 to 0.056, function of the bar diameter– and exclude any structural use of plain steel even with end anchorage.

In this sense, it is interesting to mention how the manufacturers –partially in collaboration with researchers– have developed their technology since the beginning of the 20th century in order to experimentally define the most adequate surface profile for steel bar to be used as reinforcement in concrete structures. Several investigations specifically addressed this topic during the last century

[Abr11, Pos33, Cla46, Haj51, Sor79] and recognized parameters such as the angle, spacing, geometry and shape of the ribs or indentations as key factors in the bond phenomenon. The significant evolution of the bar surface profiles from plain steel –highlighted in Figure 2.5*(a)*– supports its role in the bond performance. Also, with the emergence of a large amount of bar section types (Figure 2.5*(b)*), notable differences arise in the workability of the reinforcement due to local changes in inertia (strong and weak axis of the bar). It thus became necessary to develop some recommendations for the steel producers regarding the allowable variation range of the aforementioned parameters [AST04, CEN05] in order to guarantee satisfactory steel activation for the engineers and bendability to the manufacturers. For instance, according to the European provisions [CEN05], it is required that the maximum rib height of the deformed bar ($h_{R,max}$) should be kept between $0.03 \cdot d_b$ and $0.15 \cdot d_b$, the rib spacing (s_R) between $0.4 \cdot d_b$ and $1.2 \cdot d_b$, the rib inclination related to bar axis (β_R) between 35° and 45°, and the rib flank inclination (α_R) larger than 45°.

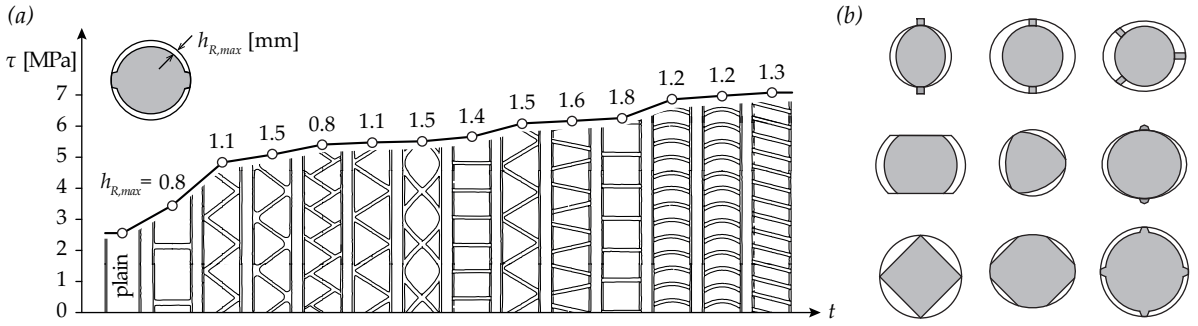

Figure 2.5 Surface profile of steel reinforcement bars: *(a)* influence on the maximum bond strength (f_c = 25 MPa and d_b = 22 mm, adapted from [Rošš50, Lin11]); and *(b)* variety of bar sections suitable for use in reinforced concrete constructions (according to [SIA13, SIA16])

The comprehension of the bond development is fundamentally related to the internal cracking phenomena. Long pull-out tests and direct tension tests were aimed for this purpose as, contrary to the short pull-out tests, the slip varies significantly along the bar. Goto [Got71] was the first to initially observe the formation of radial cracks from the ribs to the periphery of the tension ties specimen (Figure 2.6*(a)*) resulting from the development of bond. In fact, once the adhesion has been entirely mobilised, the forces are mainly transferred by mechanical action through interlock of the surface profile and the surrounding concrete with relatively low angle (approximatively 30° according to the bar axis). Radial internal cracks develop due to the associated circumferential tensile stresses and define concrete keys between the ribs. Transverse reinforcement or sufficient cover of the bar ($c/d_b > 1.5$) have to be provided in order to avoid the uncontrolled propagation of these cracks, potentially causing a sudden limitation of the bond strength and its associated slip (dashed line in Figure 2.4*(b)*). The latter phenomenon of splitting was analytically described by Tepfers [Tep73], whose model implied the existence of tensile stresses (tension rings) in the concrete specimen to satisfy the equilibrium and can describe accurately the related bond strength. When adequate dispositions are taken to control the development of these specific cracks, the pull-out of the bar (Figure 2.6*(b)*) takes place in several successive phases (solid line in Figure 2.4*(b)*). It is the failure mode of main interest in the present research regarding bond and anchorage phenomena.

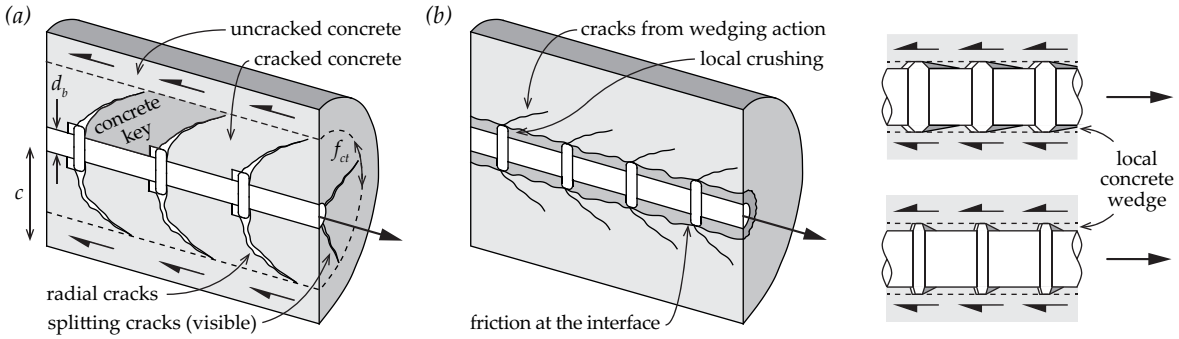

Figure 2.6 Bond phenomenon: *(a)* splitting failure mode and associated crack development [Got71]; and *(b)* pull-out failure mode and wedging action for different rib geometries and arrangements

For the pull-out failure of deformed bars, the increase of slip (with respect to the splitting failure) is related to local crushing at the face of the ribs or indentations and becomes significant with the formation of cracks at the extremities of the concrete keys. The propagation of these cracks defines the maximum bond strength (f_{b0}) leading to the pull-out of the bar through the concrete specimen. Wedging action resulting from the important crushed concrete takes place with a progressive smoothening of the interface (descending branch in Figure 2.4*(b)*) until the slip correspond approximately to the distance between the ribs. Then, due to the partial closure of the radial cracks, friction at the interface allows the development of residual bond stresses ($\sim 0.4 \cdot f_{b0}$) decreasing gradually with the available embedment length (plateau in Figure 2.4*(b)*). All the aforementioned phenomena were observed to be clearly dependant on the diameter of the bar considered with a maximum bond strength reduced by increasing the bar diameter (size effect).

Observations reported in [FIB00] from Cairns [Cai92] and Andreasen [And92] supported that different failures can occur at the interface between concrete and steel during the pull-out process depending on the properties of the surface profile. For bars with ribs of constant height, the development of the most probable failure mode seems to be related to a certain extent to parameters such as the inclination of the rib face (according to bar axis) or the distance between two consecutive ribs. For steep and close ribs, the failure mode corresponds mainly to a shear-off of the entire concrete in-between the ribs. However, for larger spacing of the ribs, crushing at the face might become dominant. Finally, for small inclination, the failure mode is generally governed by the slipping of the bar without significant mechanical contribution of the ribs. Several disparities arise in the determination of the length of the shear crack defining the concrete wedge: $2 \div 3 \cdot h_R$ [Tep73] and $6 \div 7 \cdot h_R$ [Reh61]. The fact that no significant differences in the maximum strength were observed despite the different types of failures previously described implies that other parameters – still not clearly defined– should be additionally considered in the definition of bond.

A thorough overview of the available literature on this phenomenon highlighted that significantly less attention was given by researchers to the influence on bond of parameters rather related to production. The lack of specific investigations and recommendations for deformed bars regarding the surface profile (made of ribs or indentations), the number of lugs (generally 2 per section, but

bars with 3 or 4 might also be found), the arrangement of the ribs (axisymmetric or asymmetric, constant or variable) and the presence of longitudinal ribs, led to an intense evolution of reinforcement products in the last decades (Figure 2.7*(a)*). It is evident that the revisions of the code provisions are in a way related to the latter developments. Nowadays, the height of the surface profile is generally optimized during the production processes –with the exception of some special types of reinforcement such as continuously threaded bars– and the arrangement of the ribs varies along the bar. The latter aspect is mainly required for the visual identification of the steel products [CEN05]. Thus, the reinforcement bars available on the market are relatively different from the ideal case presented in Figure 2.4*(c)*, and nowadays the tendency is to produce unique reinforcement solutions optimized for specific applications.

As a consequence, the phenomenon of bond might be much more complex, with a potential combination of several of the aforementioned failure modes on the same bar. Although the related performance might not be significantly affected by the considerable disparities amongst the available products under standard conditions, this is most likely not the case in presence of more specific and severe conditions (such as cracking). In this sense, the development of bars composed of four lugs (dotted line in Figure 2.7*(a)*) might be problematic as most of the investigations on bond phenomenon –on which are based the related code provisions and recommendations regarding bond– were performed on two-lugs bars (solid line in Figure 2.7*(a)*). The latter type of reinforcement might not represent anymore the majority on the construction market already in the next decade.

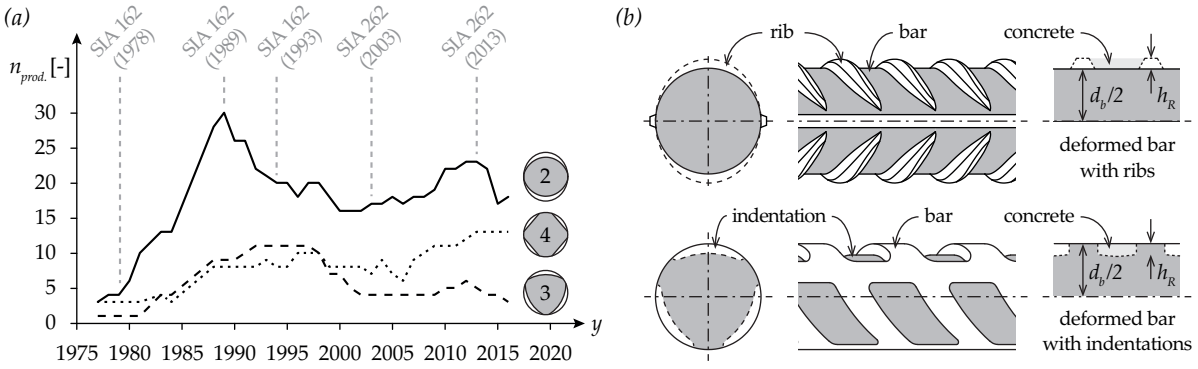

Figure 2.7 Steel reinforcement for reinforced concrete: *(a)* evolution of the available products in the Swiss market function of the number of lugs (according to [OFR15, SIA15, SIA16]); and *(b)* main types of deformed bars (surface profile with ribs or indentations)

The production processes necessary to create the surface profile on bars –additionally to the section (ribs) or within (indentations)– generally define two different types of deformed steel products (Figure 2.7*(b)*). A reduced volume of concrete is usually present between the indentations compared to the case with ribs for similar roughness properties of the bar. Also, the amount of steel between two consecutive indentations –constituting the profile of the bar– is normally larger than the ribs in the case of classical deformed bars made of two lugs. This difference of stiffness should in a way have a role in the development of the transfer of forces. Generally, the bars with three-lugs are most likely destined to progressively disappear by lack of interest, being an intermediate solution without notable advantages compared to the two aforementioned alternatives.

2.1.2 Hooked and U-shaped bars

The developments of bend bar details in concrete construction are closely related to those of straight bars (see Section 2.1.1). The origins of the latter go back to the late 19th century when a contractor observed a better behaviour –mainly through the cracking pattern– of reinforced concrete floors and roof elements when the steel bars used as reinforcements were profiled or provided with bent at their extremities [Hya78]. Another early structural application of plain bend bars was related to the use of spirals for the confinement of concrete columns [Con02], which inspired similar applied works [Bac05, Mör12]. Investigations on cube or beam elements, reported only at the beginning of the 20th century, supported the structural interest of bend details as end anchorages for plain bars [Bac07, Bac11a, Bac11b, Sal13, Abr13]. Besides the bar diameter, researchers mainly studied the influence of the bend angle and mandrel diameter, the disposition of a constructive transverse bar, the concrete cover and the presence of confinement. However, in most cases, the performance of the various types of details could not be completely evaluated due to issues related to slip measurement. The disparities of efficiency observed between the details could thus only be appreciated indirectly through the variation of the measured failure load, the deflections or the related crack pattern of the specimen (Figure 2.8). A better activation was associated to the increase of the bend angle, as the mechanical anchorage was progressively improved. The presence of the latter element therefore postponed the initiation of the slip compared to straight bars, influencing the development of cracks in the reinforced concrete specimen.

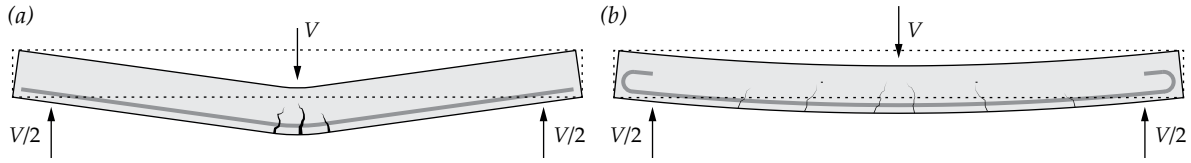

Figure 2.8 Influence of the detailing of plain flexural reinforcement on the crack pattern and deflections (for a similar load level, adapted from [CEB98]): *(a)* no end anchorage, localization of the deformation in the loading zone; and *(b)* hooks, redistribution of the deformation

The tests performed by Bach and Graf [Bac11b] are of major interest, being amongst the first attempts to link the load –acting on the beam– to the slip of the anchorages of the plain flexural reinforcement (Figure 2.9*(a)*) to quantify their efficiencies. The reported curves allow an appreciation of the disparities of performance –in terms of strength and stiffness– for the tested types of bend bars anchorages (Figure 2.9*(b)*). The detail of a bar bent at 180° –commonly denominated as *hook*– presented a significantly better behaviour than that of a bar bent at 90° –commonly denominated as *90° bend*– with a more distributed cracking on the beam specimens. Based on the slip measurement and on experimental evidences –such as the deformed shape of the detail after testing– it was concluded that the mechanical action provided by the hook mainly resulted from an important stress localization on the inside of the bend (Figure 2.9*(a)*). Due to the absence of an adequate surface profile, once the adhesion has been entirely activated along the plain details, significant slip develops, leading to the straightening of the bent part of the reinforcing element. A further activation is then only possible with the development of contact forces at the extremity of the detail to-

gether with a local crushing of the concrete (Figure 2.1*(g)*). If the tensile forces induced by this phenomenon cannot be controlled through adequate cover or confinement, splitting of the anchorage zone takes place with significant damage on the concrete specimen (Figure 2.9*(c)*).

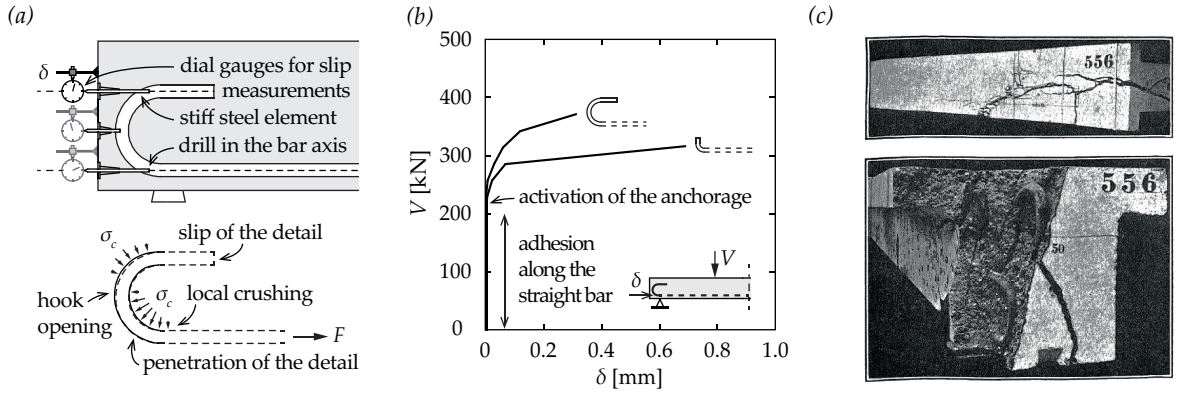

Figure 2.9 Experimental observations (adapted from [Bac11b]): *(a)* measurement device of the slip and assumed deformation kinematics of the hook; *(b)* load-slip relationships for different geometry of bend bar details; and *(c)* splitting failure in tested beam specimen

In this sense, Mylrea [Myl28] stated the main roles that should be fulfilled by an anchorage to be reliable for concrete construction: "*…an anchorage must be able to develop at least the yield stress of the bar (but preferably the ultimate strength) without damaging the concrete and with the minimum of slip to prevent secondary failure…*". Inspired by the previously mentioned investigations, the author carried out a thorough campaign of pull-out tests on plain hooks (extended in [Pos33]) to study in detail the behaviour of such details when splitting failures are avoided. The experimental orientation of this research was motivated by the fact that the related force transfer mechanisms were too complex in the specific case of hooks to be explicitly defined by the theory of elasticity. The use of an innovative measurement system of the slip (Figure 2.10*(a)*) associated with a continuous monitoring of the force, allowed the author to accurately evaluate the performance of the tested details for various confinement levels and bend radii. Several phases were highlighted in the behaviour of the hooks (d_b = 12.7 mm, $l_b = 22 \cdot d_b$, $f_c \approx 15$ MPa) and physical explanations were proposed to support these observations. Once the contribution of adhesion has been entirely consumed along the hook, the straightening of the bent part takes place with significant slip and even a potential decrease of the load (Figure 2.10*(b)*). When the pressure associated to the deformation of the detail becomes locally sufficient enough, a friction mechanism allows for the additional force development, although the hook already initiated to slip (confirmed later in [Fab05]). The latter phenomenon did not appear to depend on the bend radius as similar slopes were observed in the related behaviour curves for large values of slip (Figure 2.10*(b)*). The fact that the initial activation is more important for the details with the geometry the closest to a straight bar (top line in Figure 2.10*(c)*) might be related to the potential local loss of contact associated to specimens with important curvatures (bottom line in Figure 2.10*(c)*). Indeed, these tests confirm that, for a given embedment length and for limited values of slip, the most efficient way to transfer forces remains a straight bar regarding the peak strength (dashed line in Figure 2.10*(b)*). On the contrary, when important values of slip

are expected, the details with the smaller curvatures –smaller bend radii– should clearly be preferred as they provide an efficient mechanical anchorage with an interesting behaviour associated to a local friction during the straightening. In this sense, Mylrea's investigations also pointed out the beneficial effect of extending the hook with an additional straight part. Finally, the presence of an adequate confinement –modifying the failure mode from splitting to pull-out– is required in order to develop an important dissipation of energy during activation.

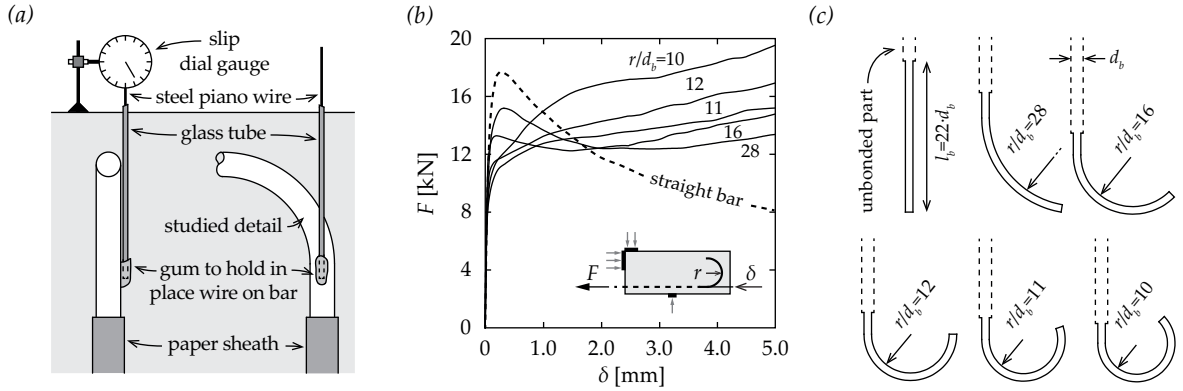

Figure 2.10 Experimental observations (adapted from [Myl28, Pos33]): *(a)* measurement device of the slip on the details; *(b)* influence of the bend radius for a given embedment length (selected average curves); and *(c)* geometry of the details considered in the study

With the development of deformed steel bars, it became necessary to evaluate the contribution of the surface profile to the performance of bend bar details. Fishburn [Fis47] observed a consequent increase in the load –with shearing and crushing of the concrete between the ribs– compared to plain details. For a similar geometry of the deformed details, the latter seemed to be related to the increase of the rib height, directly affecting the force transfer mechanisms by friction and mechanical action taking place in the inside of the bend. Also, the localization of the steel strains in the bar was observed to develop mainly at the straight part (before the beginning of the bend) rather than in the other parts of the details. For a given slip and embedment length, the deformed bars –regardless of the type of profile tested– were more activated than the plain bend bar details. Finally, the disposition of a constructive transversal bar in the bend did not provide a significant improvement of the behaviour, contrary to the case of plain details [Leo65, Reg80a].

The systematic experimental campaign performed by Leonhardt and Walther [Leo65] on plain bend details (d_b = 6.0 mm, $l_b = 25 \cdot d_b$, $f_c \approx 20$ MPa) is in this sense of major interest (Figure 2.11*(a)*). The tests clearly highlighted that the geometry of the detail is important only when the transversal bar is simply disposed in the bend (Figure 2.11*(b)*). The weld of the transversal bar strongly limits the activation and the influence of the rest of the detail, acting as a local mechanical anchorage providing a significant improvement of the behaviour. A certain dependence on the concrete strength was observed for plain hooks without welded transversal bars (Figure 2.11*(c)*) confirming that mechanisms related to concrete are involved in the deformation of the detail. Yet, the latter remarks are not directly applicable to deformed details as additional local mechanisms have to be considered associated to the presence of ribs or indentations on the surface of the bar.

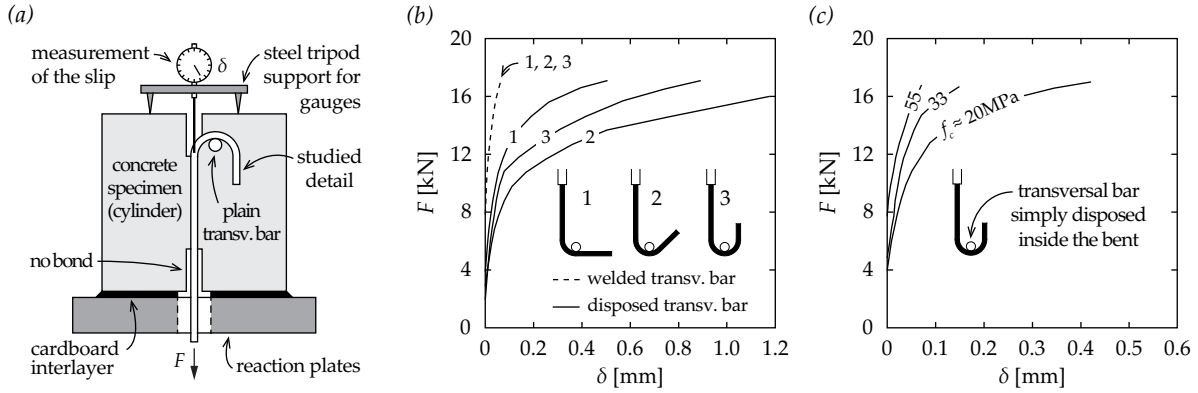

Figure 2.11 Experimental observations (adapted from [Leo65]): *(a)* test and measurement devices; *(b)* influence of a transversal bar in bent (simply disposed or welded) on the behaviour for different geometries of plain details; and *(c)* influence of the concrete strength on the behaviour of a hook with simply disposed transversal bar inside the bent

During the second half of the 20th century, a consequent amount of investigations was performed regarding the behaviour of hooks and bend anchorages made of deformed bars [Reh68, Min71, Jir72, Mar75, Pin77, Joh81, Sor86] in order to provide some design recommendations. The straightening of this type of detail –due to crushing of the concrete from the concentration of normal stresses on the inside of the bend– was generally confirmed by a partial loss of bond on the outside of the bend (Figure 2.12*(a)*). Also, Rehm's tests [Reh68] demonstrated that a bend bar detail –independently of its geometry– does not necessarily provide a better anchorage than a straight bar of the same length (confirmed later in [Kem68, Reh69, Min75]). The latter remarks support similar observations on plain details [Myl28, Pos33] partially presented in Figure 2.10*(b)*. Contrary to plain details, the contribution of the straight extension after the bend was not that effective in reducing the slip when deformed bars were used [Mar75] as most of the force transfer takes place in a very specific and limited zone –at the beginning of the bend on the loaded side– where friction is considerable. Minor and Jirsa [Min75] even claimed that 90° bends should clearly be preferred to hooks (partially confirmed later in [Shi08]). For similar conditions, although a bend provides generally slightly smaller activation than a hook, it is related to significantly smaller slips –almost half– as the crushing phenomenon is considerably reduced (Figure 2.12*(b-c)*).

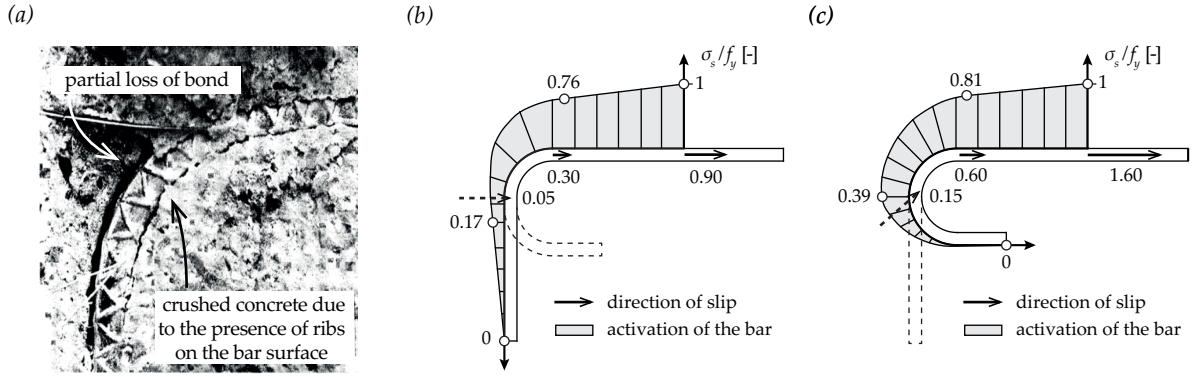

Figure 2.12 Experimental observations (adapted from [Jir72, Mac05]): *(a)* detailed view of the bend after pull-out test of a detail made of deformed steel; differences in the activation (σ_s/f_y) and the slip (in mm) for common reinforcing details as *(b)* 90° bend or *(c)* 180° hook (surface profile not presented on the bar for clarity purposes)

Regarding the deformation kinematics, the measurements of the slip –performed at the lowest point of the bend– clearly highlighted the main structural differences between these two types of details. As the hook is rather pulled towards the surface, the 90° bend rather follows the geometry of the detail during its straightening.

In very few cases, the observation of a concrete wedge directly under the bend of hooks anchorage –resulting from the local force transfer mechanisms (Figure 2.13*(a)*)– confirmed the previous remarks (see for instance [Bac11a]). The formation of this concrete element is associated to complex bearing phenomena inside the bend. Its position is strongly influenced by the deformation of the hook and the geometrical characteristics of the detail. Also, the performance of this type of anchorage is strongly related to the disposition of an adequate confinement or cover to control the lateral strains –potentially consequent– resulting from the penetration of this wedge into the surrounding concrete mass [Mar75, Pin77, Joh81, Sor86]. Limited investigations have been dedicated solely to this specific topic, despite its potential importance for such detailing solution. In this sense, the interesting tests performed by Stücki [Stü90] deserve to be mentioned for further developments on the understanding of the behaviour of bend bars (Figure 2.13*(b)*).

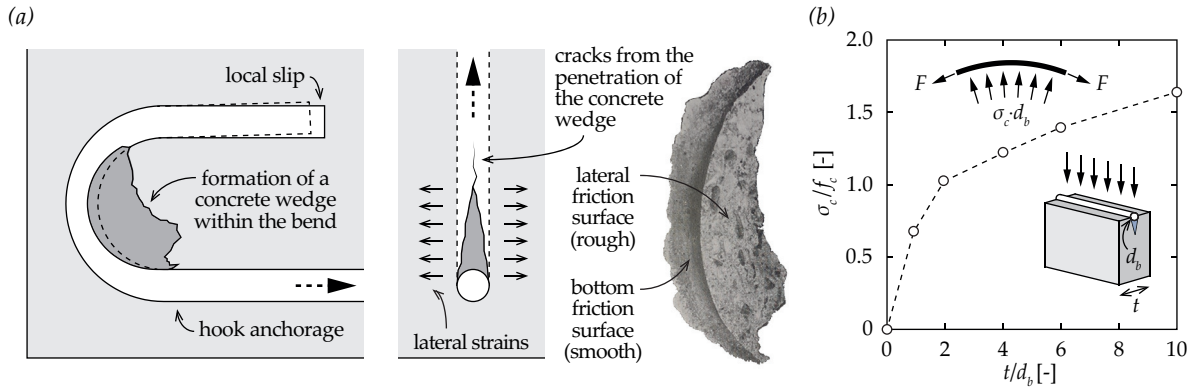

Figure 2.13 Experimental observations (adapted from [Bach11a, Mut97]): *(a)* concrete wedge typically formed inside the bend of hooks anchorage; and *(b)* influence of the lateral concrete cover on the maximum applied stress prior to the splitting of the unreinforced test specimen

The performance of details made of deformed bars is, similarly to the straight bars, affected by the properties of concrete in the vicinity of the anchorage. Although bond develops over the entire embedded length of the bar, the local formation of a concrete wedge supports the fact that additional force transfer mechanisms –such as friction– take place in this specific position. It justified the fact that hooks and bends are relatively sensitive to the casting direction of the specimen [Reh69]. The disparities in behaviour which were observed (Figure 2.14*(a)*) confirm that the critical part of such details is localized on the inside of the bend (rather on the side of the loaded extremity). Therefore, the performance of top anchorages in reinforced concrete structures with respect to the casting direction –as it is the case for the transverse reinforcement elements in punching– is potentially even reduced compared to bottom anchorages in uncracked conditions (Figure 2.14*(b)*). Also, the disposition of a transversal bar in the bend –with direct contact– allows the activation of 10 ÷ 30% more force for the same slip [Mül68], yet usually difficult to guarantee on site.

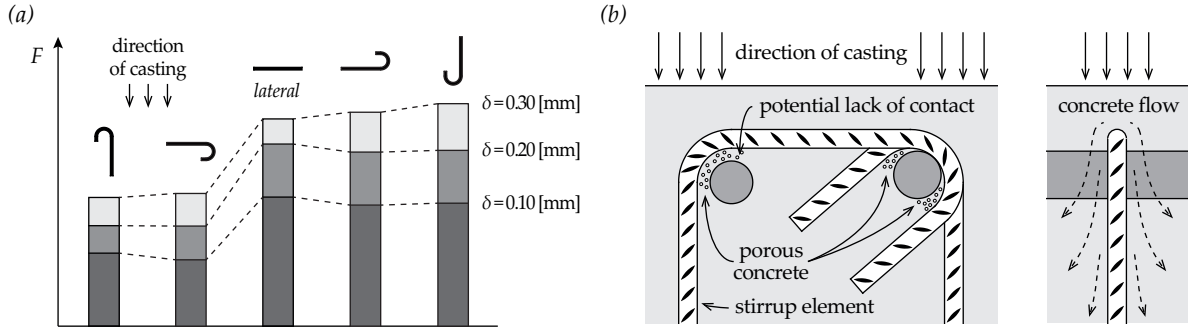

Figure 2.14 Experimental observations (adapted from [Reh69, Par75]): *(a)* influence of hook position during casting of concrete on the activation (at given values of slip); and *(b)* potential phenomena affecting the performance of the top anchorages of transverse reinforcement

In practice, according to Minor and Jirsa [Min75], the curvature of such details should be as large as possible in order to maintain the stiffness of the anchorage as close as possible to the one of a straight bar (Figure 2.10*(b)*) to limit the associated stress concentrations in the bend. However, this is in contradiction with the code provisions that requires only a minimal bend diameter for the mandrel (usually $4 \div 6 \cdot d_b$) to avoid steel fracture during the detailing process. These recommendations are often considered to be the commonly accepted solution by manufacturers to limit the excess of reinforcement in anchorage areas for hooks with large curvatures. Although the latter is probably not an issue in most cases, it might be of major importance for the behaviour of such type of detail under severe conditions such as cracking for which few studies exists. The pull-out campaigns performed in the 1980's by Rhem et al. [Reh79] and Regan [Reg80a] are in this sense of major interest, with the comparison of common anchorage types in cracked and uncracked conditions (see Section 2.3.2). The use of U-shaped bars appears to be the most efficient detailing solution as it avoids problems related to the straightening, potentially leading to spalling of the concrete cover and splitting. Although they are widely used in practice –notably in joints [Joe14]– the behaviour of such elements was not thoroughly investigated. Nowadays, research is still going on –mainly through numerical studies– to characterize the complex behaviour of bend bar details and U-shaped bars, notably regarding the evaluation of the individual contribution of the different force transfer mechanisms developing progressively during the related activation.

2.1.3 Headed bars

The concept of headed bars originated at the beginning of the 20th century and is associated to the development of systems providing an optimal activation to the reinforcement of concrete structures. Abrams [Abr13] considered the use of nuts and washers on plain bars –locally threaded only at their extremities– as a practical and efficient alternative to bend bar details for the anchorage of forces in concrete (Figure 2.15*(a)*). Contrary to the tests on hooks of the same series, the author could measure the slip in relation to the acting force and evaluate the differences of performance with respect to straight bars (Figure 2.15*(b)*). Although a splitting failure generally limited the maximum load (unreinforced concrete specimens), the results showed a very efficient behaviour despite the moderate size of the nut. The contribution of the washer –increasing the bearing area by

65% compared to the one related to the nut– is most probably not significant due to its limited thickness. The slight differences between both solutions –simple and double system– rather leads to disparities in the stiffness of the anchorage. In this case, it is interesting to observe that the activation of headed-like systems takes place in the continuity of the behaviour of the reference specimen (straight bar). More recent tests performed by Regan [Reg97] on similar details –but with fully threaded bars (Figure 2.15*(a)*)– highlighted the beneficial contribution of the straight part of the bar prior to the anchorage. The latter allows to notably delay the related activation with a significant improvement of the behaviour and a very limited slip at the loaded end (Figure 2.15*(c)*). Although this system might seem quite primitive in its aspect, it provides a pragmatic, very flexible, and rather underrated solution for the anchorage of forces in concrete.

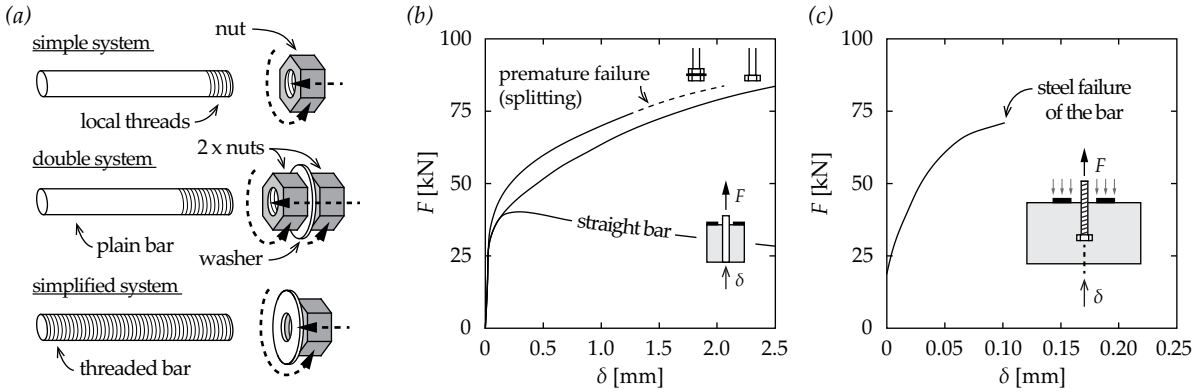

Figure 2.15 Experimental observations (adapted from [Abr13, Reg97]): *(a)* origins of headed bars systems; *(b)* first pull-out tests reported on headed-like anchorages (plain bar) compared with straight bar; and *(c)* pull-out test on headed-like anchorage (threaded bar)

Abrams's tests [Abr13] highlighted the fact that the activation of such details might also be function of the stiffness of the anchorage. This was confirmed by various researchers [Sho63, Reg80a, Fur93], with the potential risk of also developing larger bearing forces and premature failures. When an adequate confinement is provided to the concrete specimen, yielding of the steel can generally be achieved systematically with this type of reinforcing details. In the second half of the 20th century, the development of monolithic headed anchors with plain bars in the USA [Vie56, Gre61], mainly for composites applications –such as connections between concrete bridge's deck and steel profiles– confirmed the performance of this anchorage type for both tensile or shear solicitations. The thorough work performed by Rehm [Reh61] supported the fact that a unique rib (5 in Figure 2.16*(a)*) leads to a more efficient local transfer of forces between steel and concrete than with various small ones (1, 2, 3, 4 in Figure 2.16*(a)*). The latter confirmed the existence of several local mechanisms –potentially very different from one another in terms of performance– depending on the detailing. Amongst first reported tests on deformed headed bars [Sho63] confirmed that the use of a deformed bar considerably improves the behaviour of the anchorage by limiting the activation of the head (Figure 2.16*(b)*). The consideration of bent headed bars –also requiring an additional detailing phase– does not provide any improvement of the behaviour with respect to the straight one, being even slightly degraded. This is related to the development of a non-optimal bearing phenomenon under the head due to its position regarding the direction of solicitation.

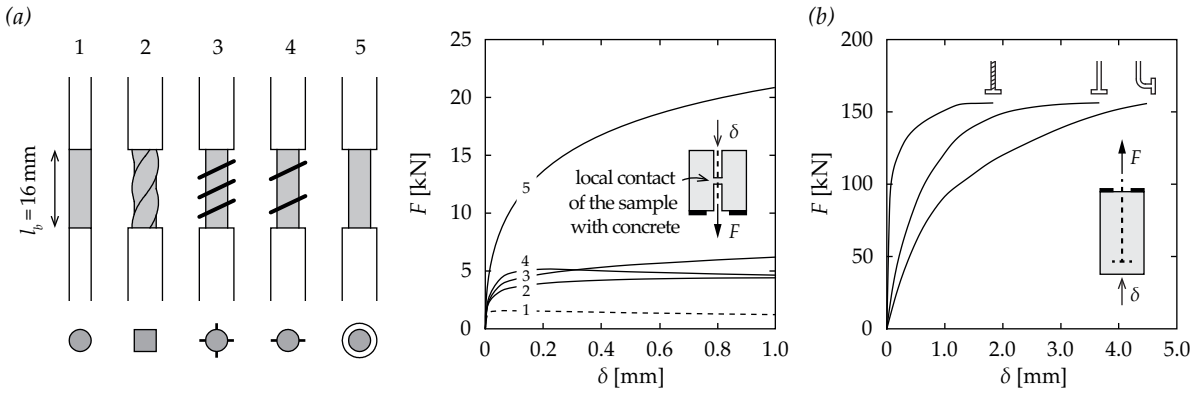

Figure 2.16 Experimental observations (adapted from [Reh61, Sho63]): *(a)* pull-out tests to evaluate the influence of the surface profile on the local force-slip behaviour; and *(b)* pull-out tests on various types of headed bars

The evolution from headed anchors to the actual form of headed bars (Figure 2.17*(a)*) initiated in the 1960's [Sho63, Sto74] through innovations in the fabrication process by some companies and the necessity of a few contractors to avoid congestion in specific zones of offshore and coastal reinforced concrete structures (Figure 2.17*(b-c)*). Most of the performed investigations relating to the general behaviour of such details are generally not accessible [NSW66, Drå86, Fyn86a, Fyn86b, Fyn86c, Ørj87] as they are the property of these companies. Only a limited part of this work was reported and usually focused on structural applications of headed anchorages to promote the use of this reinforcing solution [Ber91, Ber94]. Although few differences arise amongst the mentioned systems in standard conditions of use, some particularities mainly related to the fabrication process might potentially influence their behaviour in more specific and severe conditions.

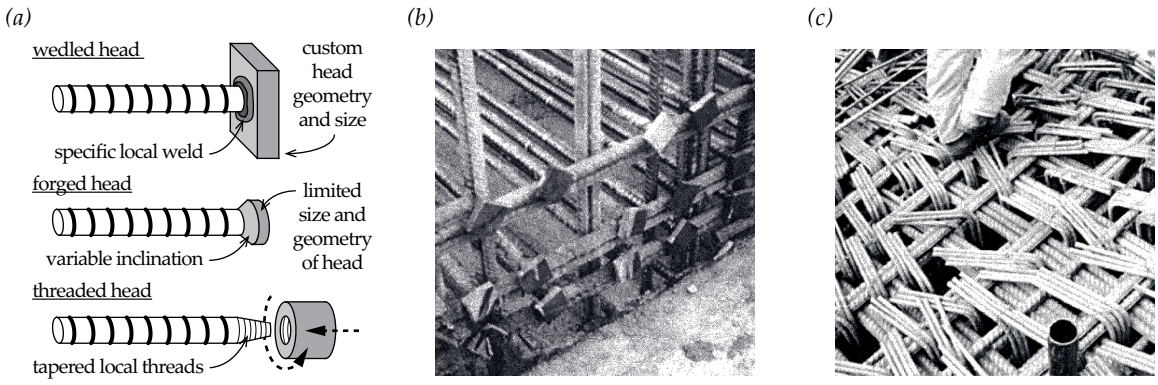

Figure 2.17 General observations (adapted from [Tho06, Ber91, Ber94]): *(a)* possible types of actual headed bars; *(b)* local anchorage solution in oil platform Gulafks C (80'000 headed bars used in the entire project); and *(c)* typical steel congestion at lower dome of an offshore platform associate to the use of conventional stirrups (with potential overlapping issues)

Details resulting from the disposition of a steel plate at the extremity of a deformed bar (welded system in Figure 2.17*(a)*) offer an important flexibility regarding the possible geometry, dimensions and thickness of the head. However, in the latter case, due to the production processes, the quality, depth and type of weld can potentially limit the performance of the anchorage.

Forged headed bars (forged system in Figure 2.17*(a)*) result from the intense heating of the extremity of the bar –generally through induction– directly followed by its arrangement in a specific device to form the head mechanically through the application of a normal force on the bar. The fabrication process determines the stiffness of the head through its diameter and thickness (generally not constant). The surface profile of the bar might thus still be partially present on the periphery of the head after production, with potential influences on its behaviour (see Section 3.2.4). This detail constitutes the most common solution nowadays available on the market for headed bars.

Finally, the installation of a steel element to the extremity of a deformed bar through a mechanical connection (threaded system in Figure 2.17*(a)*) is another solution to realise the anchorage in concrete. The fact that the force has to be transferred between the two pieces only through the threads –systematically presenting some fabrication tolerances– limits the stiffness of the anchorage compared to a monolithic version. In this sense, current details of this type are generally provided with tapered threads allowing for a significantly more efficient transmission of forces than the conventional threaded connections. Nevertheless, the costs related to this solution limit its application to very specific cases, where none of the aforementioned alternatives could be used easily.

The main companies that took part in these developments –generally through collaborations with research centres or universities– were *Nelson Stud Welding Company* [Mac73] in the USA (founded in 1939), *Metalock Industries* [Dyk88, Hol89, Tho90] in Norway (founded in 1979) that became *Headed Reinforcement Corporation* [Ger92, Bas96, Wri97, DeV99] in North America (early 1990's) and *DeCon* in North America (partnership between *DEHA* Germany and *Continental Studwelding* Canada, founded in 1989). Amongst these companies, the last one is of major interest in the frame of this research as it is based on the extensive works on double-headed bars for transverse reinforcement against punching by professors A. Ghali and W. H. Dilger at the University of Calgary [And77, And79, Voe80, Voe81, Dil81, Mok82, Mok85]. Their initial motivation was to find an alternative to replace closed stirrups known to be unsatisfactory under these specific conditions and difficult to dispose around the column in the critical zone of the slab-column connections.

The experimental results obtained in this period had a great impact on the community and confirmed the performance of this type of reinforcing detail in order to activate significant forces with very limited slip (Figure 2.18*(a)*). These investigations have contributed considerably to the applications of headed bars in reinforced concrete construction since the 1990's (see for instance [Gha05]). Some tragic events associated to the fast development and use of such anchorages in practice –for instance the Sleipner Platform accident in 1991 [Jak94]– required additional specific studies (notably regarding possible combined failure modes). Parameters such as the geometry, inclination and thickness of the head and the related bearing area were all recognized as key factors affecting the performance of this system when adequate confinement is provided (an exhaustive state of the art can be found in [Tho02]). In this sense, as previously mentioned, the type of headed bars (welded, forged or threaded) is of importance as these parameters are partially related to the fabrication processes.

Furche's work [Fur93] on headed-like anchorages (Figure 2.18*(b)*) allowed to evaluate the influence of the inclination of the head (α_H) on the slip at ultimate force (δ_u). The tested specimens even highlighted the presence of a concrete wedge –more or less well defined– directly under the head resulting from the development of a complex state of stress (Figure 2.18*(c)*).

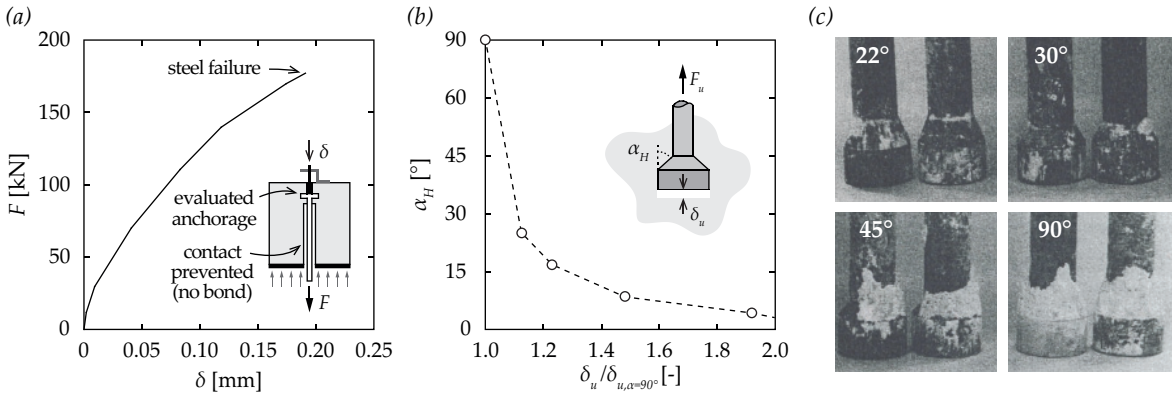

Figure 2.18 Experimental observations (adapted from [Dyk88, Fur93]): *(a)* typical load-slip relationship obtained from a standardized pull-out test [RIL78] of an actual headed bar detail (d_b = 20 mm) in high strength concrete ($f_c \approx$ 50 MPa); *(b)* influence of head inclination on the slip at ultimate force (base of comparison: perpendicular head with α_H = 90°); and *(c)* tested anchorage specimens after pull-out (α_H = 22°, 30°, 45°, 90°)

The efficient force transfer performed through the combination of bond phenomena on the straight part of the bar –notably when deformed steel products are considered– and above all the mechanical action of the head provides an optimal anchorage compared to other reinforcing solutions. Significant radial forces are generally induced around the head together with the formation of a concrete wedge from the bearing area (similarly to hooked bars, see Figure 2.13*(a)*). For conventional details –head diameter corresponding to three times the bar diameter– the stresses directly under the head might reach several times the concrete compressive strength associated to the development of a complex local bearing phenomenon.

Similar research on rigid plates of limited deserves to be mentioned here [Haw67a, Haw67b, Niy73, Niy74, Niy75, Wil79, Lie87] as evident similarities arise with headed bars (Figure 2.19*(a)*). The latter phenomenon appears to be of major importance in the characterization of the performance of such types of anchorage, as highlighted in the present section. In fact, if adequate constructive dispositions are taken –minimum lateral cover or transverse reinforcement– brittle failure modes related to splitting forces can be avoided (Figure 2.19*(b)*) and yielding of the bar is usually achieved for this type of detail. However, it must be noted that the slip associated to this activation is strongly related to the penetration of the concrete wedge which forms under the head. This phenomenon is therefore highly dependent on the geometrical and surface properties of the anchorage, as well as the surrounding conditions (type of loading, cracked or uncracked concrete, level of confinement, surface of the bar). Such a concrete element under the head has never been clearly observed in literature on this type of anchorage detailing solution. This might be linked to the fact

that test conditions were potentially not severe enough to allow its complete formation and to initiate the related penetration in the concrete specimen to be properly formed and visible.

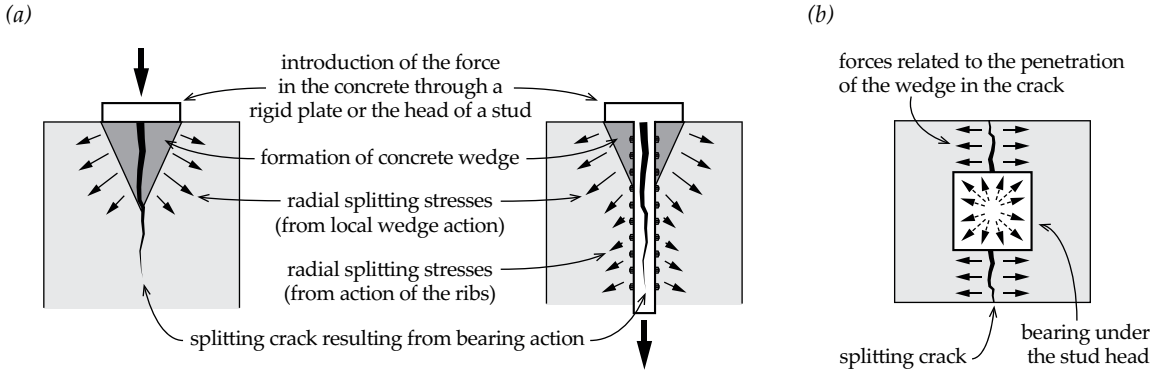

Figure 2.19 General observations (adapted from [Tho02]): *(a)* similarities between bearing of forces under a rigid plate and a headed bar with the formation of a concrete wedge; and *(b)* related splitting mechanism due to the penetration of the wedge in the concrete specimen

Most of the investigations performed since the development of this type of anchorage mainly focused on the failure modes associated to a lower limit of the load capacity –such as concrete-cone breakout (Figure 2.20*(a)*), lateral blow-up (Figure 2.20*(b)*) or splitting (Figure 2.20*(c)*)– for which the related knowledge is important (an exhaustive literature review can be found in [Eli06]). As they can generally be simply avoided through the disposition of an adequate constructive reinforcement, the mentioned failure modes are not further investigated in the present research.

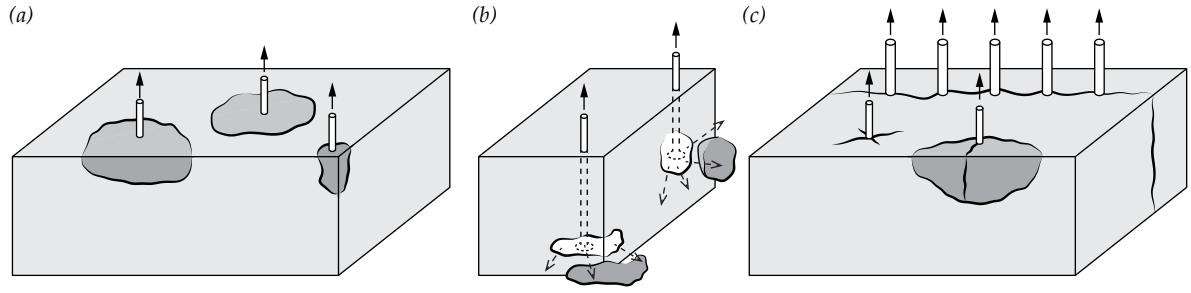

Figure 2.20 Main possible failure modes associated with tension loading of reinforcing details such as headed bars in concrete elements (adapted from [Eli06]): *(a)* concrete-cone breakout; *(b)* lateral blow-up; and *(c)* splitting

Therefore, when the state-of-the-art rules are correctly respected, the behaviour of headed bars is often characterized by a steel failure corresponding to the upper limit of the load capacity. For the latter, almost no specific studies have been dedicated (or were simply not published). This topic is however of major interest in order to provide consistent comparisons of performance with other details, notably regarding the differences in term of slip at ultimate load defining the stiffness of the anchorage. The fact that, in general, there is still ongoing research regarding the development of a general method to accurately evaluate the capacity and slip of headed bars reflects the complexity of the phenomena which take place during the transmission of forces between steel and concrete.

2.2 Cracking in structural elements

Cracks are inherent to reinforced concrete structures and develop when tensile stresses locally reach the material strength. They can result either from external action (overload) or from restraint of deformations (shrinkage, environment variations, support settlements). The relatively low tensile strength of concrete requires the disposition of a minimal reinforcement in order to limit the propagation of the cracks and the related risk of collapse of the concrete members. As former code provisions generally define the maximum width of these cracks (Figure 2.21*(a)*), current ones rather tend to prefer the limitation of the stresses in the reinforcement due to the uncertainties associated to the random nature of cracking in concrete. Indeed, this phenomenon is particularly complex to estimate and predict in structural elements due to the large number of parameters involved. Despite its importance, few studies have been dedicated to the latter topic [Eli89]. Although it is possible to distinguish regions of a structure that might stay uncracked during its service life, it seems reasonable to assume that elements such as reinforcement bars or anchorages have higher probability to be situated in cracks [Eli86, Lot87, May88, Ber88, Hsu89, Ben89]. In fact, it has been observed that cracks tend to develop in these specific positions as high tensile stresses are present resulting from the activation of several force transfer mechanisms between concrete and steel. Investigations performed by Elighausen and Bozenhardt [Eli89] highlighted that the crack openings generally do not exceed 0.4 mm under quasi-permanent loads –associated to the durability of the structure– and 0.6 mm under maximum permissible service loads, potentially affecting bond and anchorage performance to a considerable extent (Figure 2.21*(b)*).

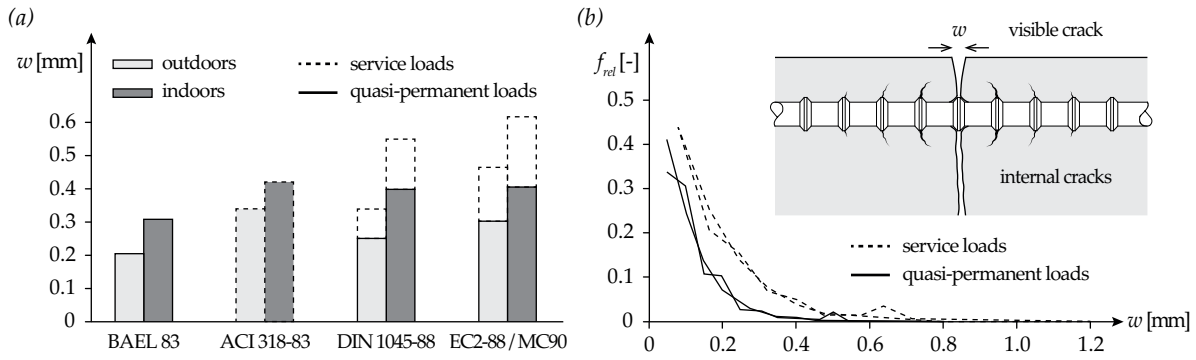

Figure 2.21 Cracks in reinforced concrete structures (adapted from [Eli92] according to [Eli89]): *(a)* admissible crack widths according to recommendations and codes of practice; and *(b)* relative frequency of the crack widths observed under permanent and service loads

The development of these cracks –constant or variable over the thickness of the element– can either be controlled by steel deformations or not (as for splitting failures). The first corresponds to cases such as the flexural reinforcement in slabs (Figure 2.22*(a)*), joints of precast elements with overlapping reinforcement (Figure 2.22*(b)*), suspension reinforcements or fasteners (Figure 2.22*(c)*), retaining walls (Figure 2.22*(d)*) or the anchorage of the web reinforcement in flanged sections members (Figure 2.22*(e)*). It is also the case of the punching reinforcement of two-way slabs [Ein16a], where intersecting cracks might even be present due to the fact that the bending moment acts in two main directions (Figure 2.1). This situation might be particularly critical regarding the activation of the

transverse reinforcement. The second corresponds to cases such as delamination cracks at the level of the flexural reinforcement of arch-shaped members [Fer10c] or members without transverse reinforcement (Figure 2.22*(f)*), and as it has been observed in slabs due to environmental situations [Aou13], where the development of these specific cracks can potentially lead to a premature failure.

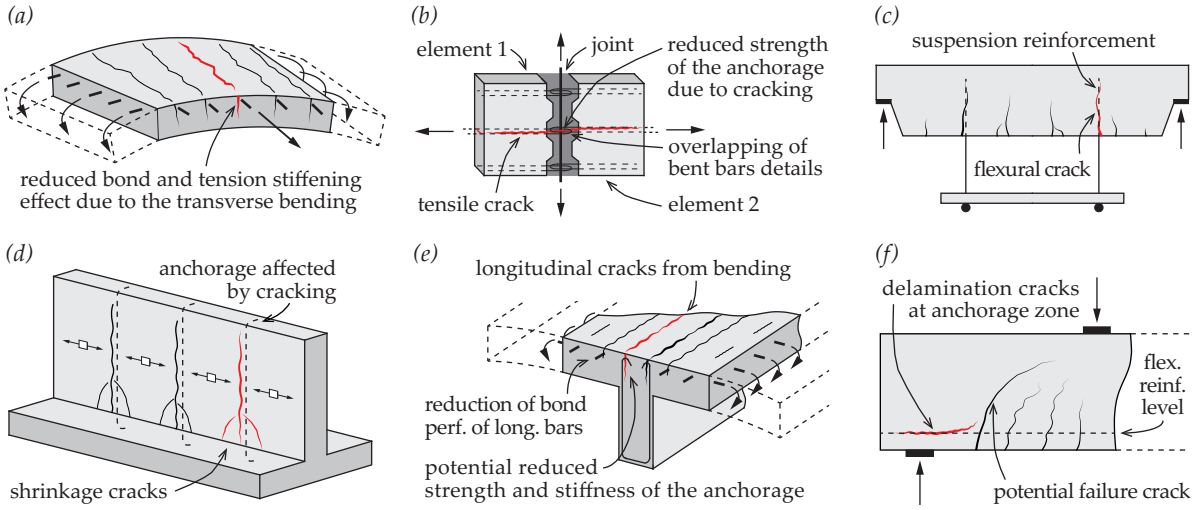

Figure 2.22 Practical cases in which cracks might develop in the plane of the reinforcement in structural concrete members: *(a)* flexural reinforcement in slabs [Daw12]; *(b)* joints of precast elements [Joe15]; *(c)* suspended loads or fasteners [Lot87]; *(d)* retaining walls; *(e)* T-section beam [Reh78a, Reh78b]; and *(f)* beams without shear reinforcement [Fer15]

It can be noted that, contrary to splitting failures in classical bond tests –as described by Tepfers [Tep73]– for cases where the width of the cracks w remains controlled, cracking at the plane of a deformed bar –limiting or even cancelling the tension ring [Hil83]– does not necessarily imply a bond failure (Figure 2.23*(a)*). Yet, the contact surface between the reinforcing bar and the concrete –through the ribs– is thus reduced (Figure 2.23*(b)*) and the performance of the force transfer is consequently diminished both in terms of strength and stiffness. Similarly, for deformed hooked and U-shaped details, the presence of cracks directly affects the bond development, therefore giving more importance to the anchorage provided by the bend of the bar. The influence of cracking on headed anchorage should be relatively limited due to the predominance of the mechanical action of the head and the large bearing area available. Reduction of the stiffness is also expected –much smaller than for straight or bend bars– and with no limitation of the ultimate strength.

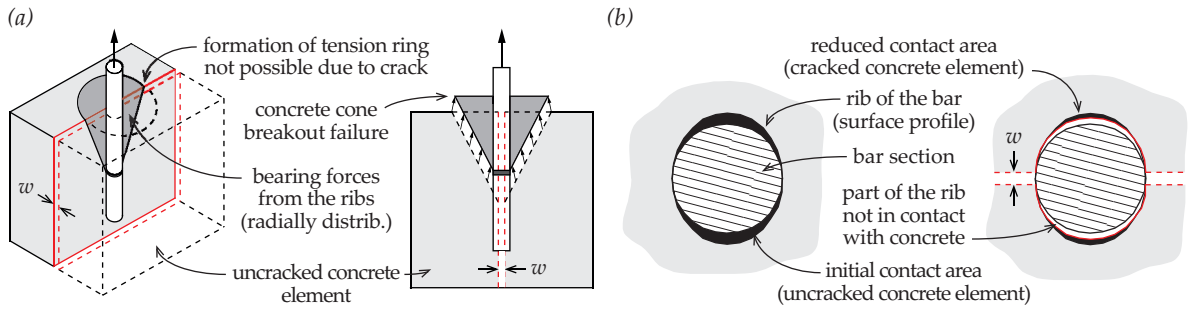

Figure 2.23 Transfer of forces in cracked concrete: *(a)* typical conical failure from limit analysis [Nie11]; and *(b)* local influence of the presence of a crack in the vicinity of a straight bar

2.3 Performance of reinforcing details in cracked concrete

Although it is evident that bond and anchorage mechanisms might be activated in many structural members within already cracked concrete, intensive investigations on the topic of anchorage strength have been performed since the 1970's but mainly on post-installed and bonded fasteners (see for instance [CEB97, FIB11]). The aim was to provide guidelines for the design of such reinforcing details both for uncracked and cracked conditions, usually considering only service crack widths. A direct use of these approaches and methods to embedded reinforcement such as the ones of interest in the frame of this research –straight, hooked, U-shaped or headed bars– is not straightforward [FIB00, FIB14]. Despite the fact that several studies are available –mainly for straight bars– the effect of cracks on the performance of the mentioned cast-in anchorages is still not well understood and is generally still neglected in the design procedures. The available literature associated to the study of the force transfer mechanisms in cracked concrete will be covered in the following, with a distinction between straight bars (see Section 2.3.1), bend bar details (see Section 2.3.2) and headed bars (see Section 2.3.3). The results have been thoroughly and systematically adapted to the SI unit system so as to simplify further comparisons and related developments.

2.3.1 Straight bars

Since the 1980's, specific test setups –with active or passive confinement during the pulling-out process– have been developed to experimentally investigate the influence of in-plane cracks on bond strength and stiffness of straight bars [Gam81, Gam85, Gam90, Gam93, Idd99, Sim07, Lin11, Mah12]. Based on these test results, several formulations were proposed by researchers to determine the reduced bond strength (f_b) as a function of the crack width (w) with respect to the reference strength (f_{b0}) in uncracked conditions. An increase of the slip associated to the peak strength was also generally observed with the presence of a crack, and significant changes arise in the several phases of the behaviour (dashed lines in Figure 2.24) compared to uncracked conditions (solid line in Figure 2.24).

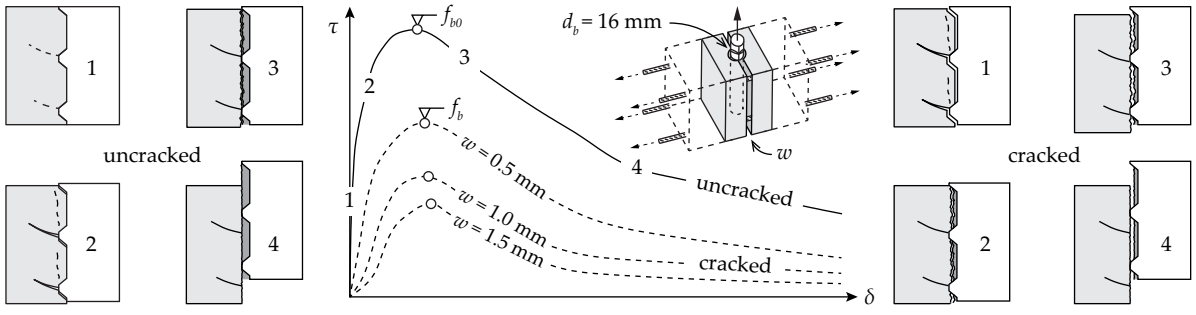

Figure 2.24 Typical results from pull-out tests of straight bars in concrete (adapted from [Idd99]): force-slip relationships of specimens 1 (BA11-BA16) and 2 (BA21-BA26)

In most of the investigations, the cracking of the concrete specimen is usually performed prior to the pull-out test. Therefore, a gap is formed between the ribs of the bar and the surrounding concrete, usually zeroed through an initial pre-loading. The behaviour reported by researchers gener-

ally considers the phases once this contact has been settled again. Prior to peak strength, the reduced contact area tends to limit the development of radial cracks (1 in Figure 2.24) compared to the case without cracks, until a premature failure of the extremity of the concrete cantilevers takes place (2 in Figure 2.24). The latter phenomena generally result in a significantly smaller stiffness than for the reference case in theses initial phases. The contraction of the concrete in the direct vicinity of the bar –associated to the partial closure of the mentioned radial cracks– then controls a friction mechanism up to the development of the maximum force defining the bond strength. With the increase of the relative displacement between the bar and the surrounding concrete, a progressive smoothening of the interface initiates the post-peak phase (3 in Figure 2.24). The related stiffness is not strongly affected by the presence of a crack, independently of its opening. Once the slip corresponds approximately to the distance between two consecutive ribs, the entire contact surface contributed to the force transfer and only a residual strength can be further provided (4 in Figure 2.24). The latter is reduced proportionally with the embedment length available until the bar is entirely pulled-out of the concrete specimen. In Idda's tests [Idd99], the disparities in the surface profile –not similar on both sides of the bar– highlighted the fact that the post-peak phases might potentially be influenced by the arrangement, disposition and type of surface profile. Indeed, in other similar tests from literature, the residual phase normally presents a progressive decrease of the load until the pull-out of the bar from the concrete specimen is completed.

In the following, the different proposals are briefly presented and discussed, where the original notation has been reworked for purposes of consistency and comparison. The test setups are also detailed due to the variety of solutions developed by researchers to study bond phenomenon in cracks. The test series without reference pull-outs (in uncracked concrete) have not been considered as the decrease of bond performance (f_b/f_{b0}) could not be calculated in a consistent manner.

A number of short pull-out tests conducted on concrete blocks with preformed cracks under active confinement by Gambarova et al. [Gam81, Gam85] on bars of 18 mm diameter ($f_R \approx 0.060$) led to the development of the first empirical formulations to consider the effect of in-plane cracks on the bond performance [Giu85, Gam89].

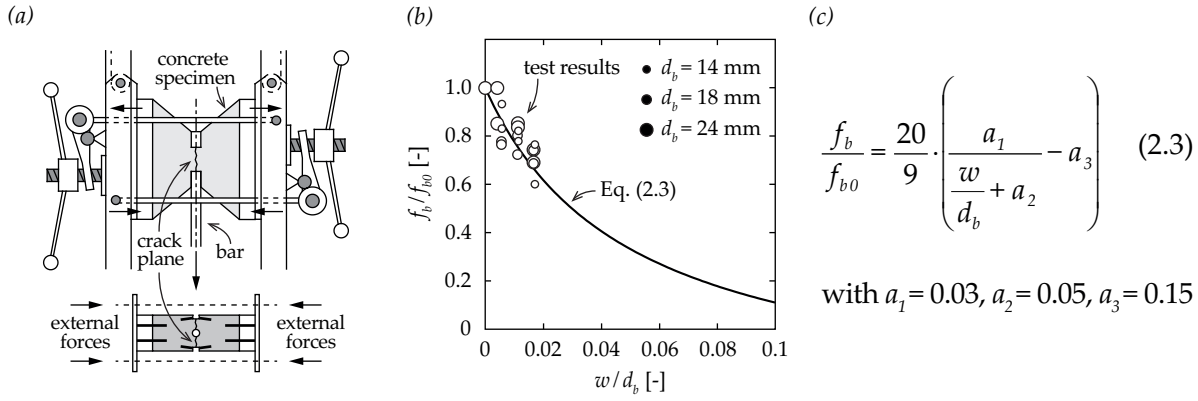

Figure 2.25 Bond phenomenon in cracked concrete (adapted from [Gam81, Gam85, Gam89, Gam90, Gam93, Gam97]): *(a)* test setup; *(b)* test results with proposed model; and *(c)* related formulation

Gambarova and Rosati [Gam97] presented a generalization of their initial proposal [Gam89] as additional similar tests in cracked concrete were performed by the authors on large (d_b = 24 mm, $f_R \approx 0.068$) and small (d_b = 14 mm, $f_R \approx 0.069$) bars [Gam90, Gam93]. The test setup developed for the investigations (Figure 2.25*(a)*) allowed to maintain the width of the crack constant along the bar during the pull-out process. The reduction of bond performance was derived as Eq.(2.3) where $a_1 = 0.03$, $a_2 = 0.05$, $a_3 = 0.15$ providing accurate predictions (Figure 2.25*(b)*). No limitations range of this empirically-calibrated formulation was clearly defined by the authors, but it should be noted that it was validated on the basis of tests performed in a normal strength concrete and a short bonded length ($l_b/d_b \approx 3.0$) for a maximum normalized crack opening (w/d_b) close to 0.020.

Based on the earliest test by Gambarova et al. [Gam81, Gam85], the equation proposed by Giuriani and Plizzari [Giu85] –in the frame of a more general work on bond phenomenon after splitting of the surrounding concrete [Giu91, Giu98] (Figure 2.26*(a)*)– is simply linearly dependent on the normalized crack opening (Figure 2.26*(b)*). Although the value for the experimental coefficient proposed by the authors (γ_1 = 42 for the mentioned tests) strongly limits the practical application of the formulation (crack width up to 0.1 mm, d_b = 18 mm), the expression defined as Eq.(2.4) has the merit of being relatively simple and pragmatic.

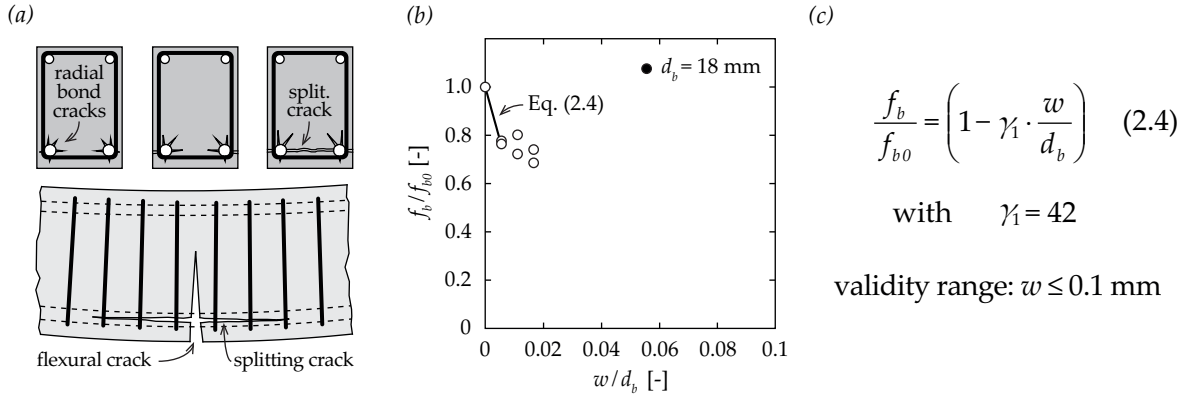

Figure 2.26 Bond phenomenon in cracked concrete (adapted from [Giu85, Giu91, Giu98]): *(a)* research interest of the performed investigations; *(b)* test results with proposed model; and *(c)* related formulation

Idda [Idd99] performed a large experimental programme of relatively short pull-out tests in cracked reinforced concrete ties, varying parameters such as the bonded length (l_b/d_b = 3.5 ÷ 12.5), the bar diameters (6, 10, 20, 28 but mainly 16 mm) and the type of concrete (normal and high-strength). Even though the longitudinal reinforcement of the test specimen was locally unbonded in order to minimize the passive confinement during the pull-out of the bar (Figure 2.27*(a)*), a variation of the crack width could not be totally avoided. The exponential expression proposed by the author –function of the ratio between the crack width and the maximum height of the rib– was empirically calibrated through a dimensional analysis thanks to the significant amount of tests conducted (Figure 2.27*(b)*). Assuming $h_{R,\max} \approx (4/3) \cdot \overline{f_R} \cdot d_b$ with $\overline{f_R}$ = 0.056, the effect of cracks on the ultimate bond strength can thus be derived from the original formulation as Eq.(2.5). Despite

the fundamentally different approach followed by Idda compared to Gambarova's work, it is interesting to highlight that a similar trend can be observed in both expressions. The significant scatter between the predictions of the model and the test results is justified by the fact that no measurements of the effective surface properties were performed by the author. Although the values reported were simply taken as granted from the ones required by the national code provisions [DIN84], the wide range of parameters considered in this study confirms that the decrease of bond performance might be significant for small values of normalized crack openings. Based on Idda's experiment [Idd99], additional finite element analyses were conducted by Purainer [Pur05] to evaluate the importance of several parameters. Finally, a linear correction term –also function of the crack width and maximum rib height– was adopted and supported the negligible effect of the crack spacing and concrete strength on the bond performance. Considering as previously $h_{R,\max} \approx (4/3) \cdot \overline{f_R} \cdot d_b$ with $\overline{f_R}$ = 0.056 and $\overline{d_b} = 20$ mm, it yields to Eq.(2.6). Logically, the trend of this expression follows Idda's but the influence of the crack is slightly reduced due to the linear term considered. The range of application of the proposed formulation is however strictly limited to that of the additional numerical investigations performed by the author (crack openings from 0.05 to 0.5 mm, and bars diameters 8, 14 and 25 mm).

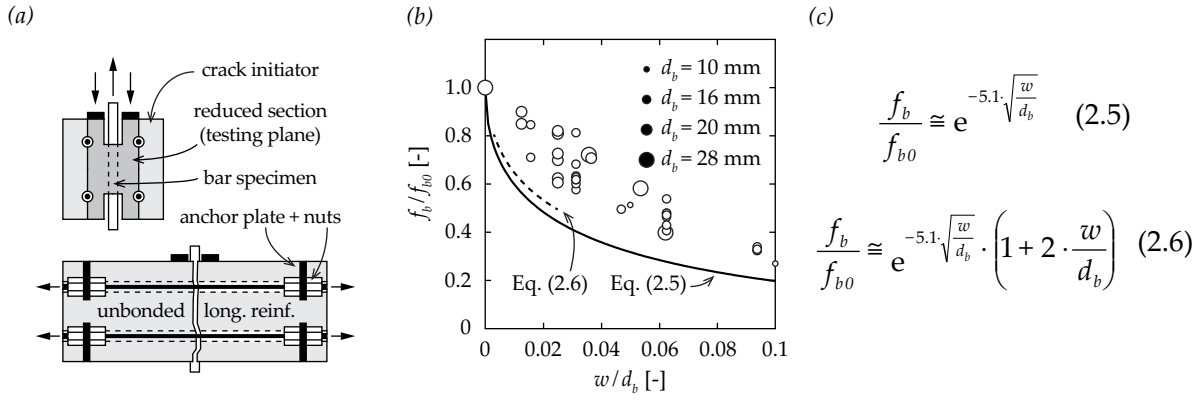

Figure 2.27 Bond phenomenon in cracked concrete (adapted from [Idd99, Pur05]): *(a)* test setup; *(b)* test results with proposed models; and *(c)* related formulations

The pull-out tests in cracked concrete performed by Simons [Sim07] in large reinforced concrete blocks (Figure 2.28*(a)*) on short embedded straight bars (l_b/d_b = 5 ÷ 8) –in the frame of a more general study on the bond performance of various resins for post-installed systems under cyclic solicitations– lead to the derivation of Eq.(2.7). This simple linear regression was obtained considering a maximum crack width of 0.4 mm (value at which the pull-out tests have been performed in the most severe cases) and $\overline{d_b} = 20$ mm as a reasonable average of the tested diameters (12, 20 and 32 mm, with respectively $f_R \approx$ 0.091, 0.082 and 0.075). The influence of cracks on the maximum bond strength (Figure 2.28*(b)*) is observed to be a good transition between previous formulation proposals (Eq.(2.3) to (2.6)). The significant scatter observed for small values of normalized crack opening might be related to the difficulties associated to the measurements, formation and control of limited cracks with the presented system, and of the surface profile of the bars.

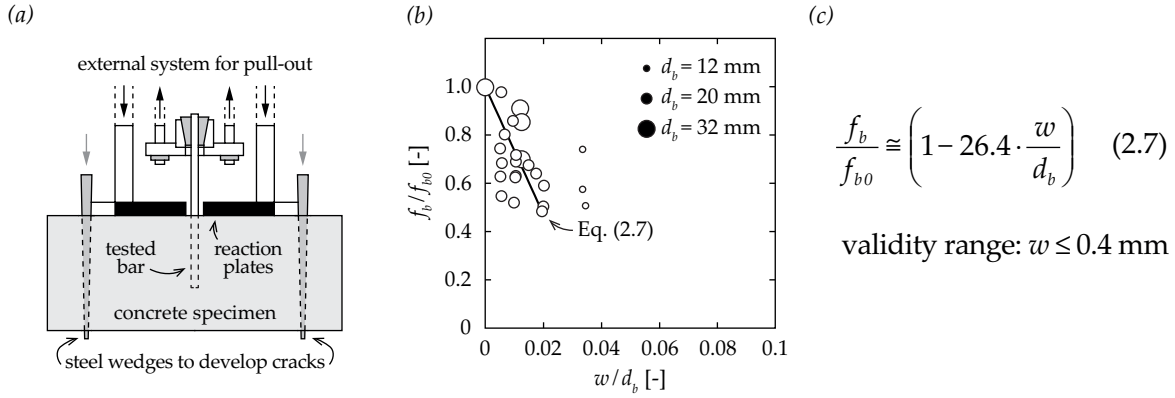

Figure 2.28 Bond phenomenon in cracked concrete (adapted from [Sim07]): *(a)* test setup; *(b)* test results with proposed model; and *(c)* related formulation

The study of bond fatigue in reinforced concrete under transverse tension led Lindorf [Lin11] to conduct some monotonic pull-out tests in cracks of interest in the present research. The test setup was composed of two perpendicular and independent frames (Figure 2.29*(a)*) aiming respectively at the development of cracks in the concrete specimen (horizontal direction) and then to process to the pull-out of the bar (vertical direction). Without really providing a formulation to estimate the decrease of the bond strength due to the presence of cracks, the author still confirms the trends observed by previous experimental series (Figure 2.29*(b)*). Also, the use of only 16 mm diameter bars ($f_R \approx 0.09$) associated to a well-defined test procedure provided results with very limited scatter in comparison to other similar works.

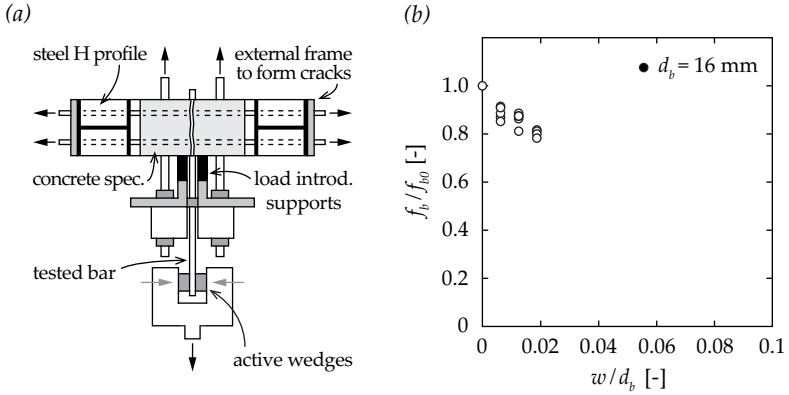

Figure 2.29 Bond phenomenon in cracked concrete (adapted from [Lin11]): *(a)* test setup; and *(b)* test results

More recently, some short pull-out tests ($l_b/d_b = 5$) on embedded bars of diameter 16 mm ($f_R \approx 0.07$) in cracks were performed by Mahrenholtz [Mah12] on reinforced-concrete ties (Figure 2.30*(a)*). Based on the conducted tests, and the aforementioned ones from literature [Gam81, Gam85, Gam90, Gam93, Idd99, Sim07, Lin11], a linear equation (Eq.(2.8)) was formulated for cracks smaller than the rib height ($w < h_R$) with good correlation (Figure 2.30*(b)*). The author justified this approach by the necessity of simplifying proposals advanced in available literature, so as to provide a pragmatic and accurate method for the evaluation of bond performance in cracks by practitioners.

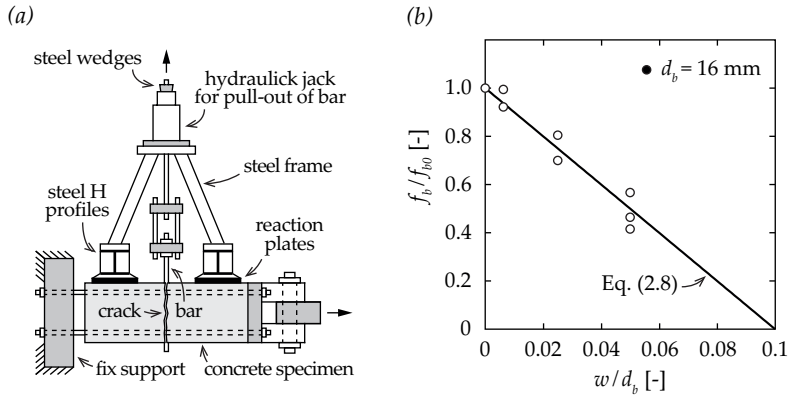

$$\frac{f_b}{f_{b0}} = \left(1 - 10 \cdot \frac{w}{d_b}\right) \quad (2.8)$$

Figure 2.30 Bond phenomenon in cracked concrete (adapted from [Mah12]): *(a)* test setup; *(b)* test results with proposed model; and *(c)* related formulation

Although there is a clear trend of decreasing the efficiency of the force transfer between steel and concrete in presence of cracks, a significant scatter arose amongst the proposed equations. This can be justified by the fact that the existing formulations mainly have an empirical background, thus depending mostly on the performed tests and calibration range. These disparities might result from the consideration of several bar types over three decades and a custom test setup for each of the investigations. In this context, the development of a mechanical-based model to characterize the bond performance of straight bars in cracked concrete is of first interest in order to make the practitioners aware of this important issue.

2.3.2 Hooked and U-shaped bars

In the late 1970's, Rehm et al. [Reh79] performed a large experimental campaign of pull-out tests on reinforced concrete tie specimens (Figure 2.31*(a-b)*) to study the behaviour of different bend bar details in cracks made of the same type deformed bar (d_b = 11 mm, $f_R \approx 0.072$). For bends, transverse welded bars were used in various positions to improve the response. In order to characterize only the performance of the anchorage, bond on straight part of the anchorages was carefully eliminated through the disposition of plastic tubes slightly larger than the bar diameter. Reference tests in uncracked conditions were also performed to evaluate the changes in the behaviour, both in terms of stiffness and ultimate strength. The crack opening was selected to be representative of service cracks, and thus limited to a maximum width of 0.3 mm. Although significant differences were observed in the performance of the tested details (Figure 2.31*(c)*), steel failure could generally be systematically achieved. The U-shaped bars (1 in Figure 2.31*(c)*) presented the most efficient behaviour, with a slip at ultimate load not even doubled in cracks compared to uncracked conditions with a load twice larger than the other tested elements. The activation of the dowel action on the transverse welded bar significantly decreased the slip and the related deformation of the 90° bend, therefore providing a suitable behaviour of the latter in cracked concrete (2 in Figure 2.31*(c)*). The only exception is for the 90° bend bars without transverse bar (3 in Figure 2.31*(c)*), where the limited cover finally led to the spalling of the concrete cover, yet at a load close to the one associated to yielding of the reinforcing bar.

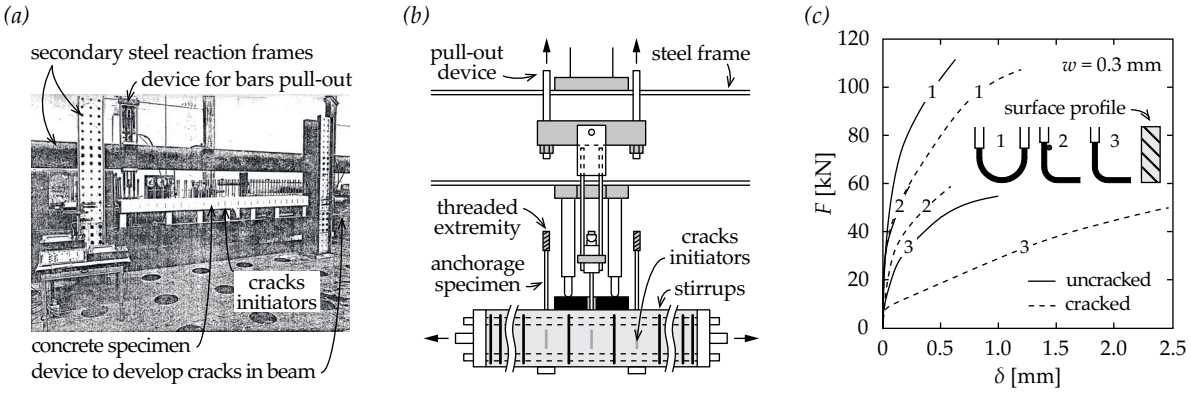

Figure 2.31 Bend bar details in cracked concrete (adapted from [Reh79]): *(a)* general view of the test setup; *(b)* detailed view of the test setup; and *(c)* force-slip relationships for various details (solid lines: uncracked concrete, dashed lines: cracked concrete)

In the frame of a study on the activation of transverse reinforcement such as stirrups or individual links in the punching phenomenon, Regan [Reg80a] performed several pull-out tests in beam specimens (Figure 2.32*(a)*) on 90° bends and hooks in small flexural cracks (up to 0.20 mm). Parameters such as bar diameter (6, 8 and 10 mm) and type (plain or deformed), bend diameter ($4 \div 10 \cdot d_b$) or surface profile ($f_R \approx 0$, 0.05, 0.095 and 0.13) were investigated. Significant differences were highlighted in the anchorage performance in cracked concrete among the mentioned details (Figure 2.32*(b-c)*), even though the crack widths were very limited. For the details made of plain bars, the degradation of the behaviour was more dramatic for bends than for hooks, for which the yield strength could not even be activated. The contribution of the chemical adhesion in the force transfer was strongly limited by the presence of a crack, and led to a premature straightening of the details with significant changes in the stiffness of the anchorage. On the contrary, for the details made of deformed bars, a partial activation of bond was still possible in cracks through the mechanical action of the ribs (see Section 2.3.1) and the initial stiffness could be kept reasonable.

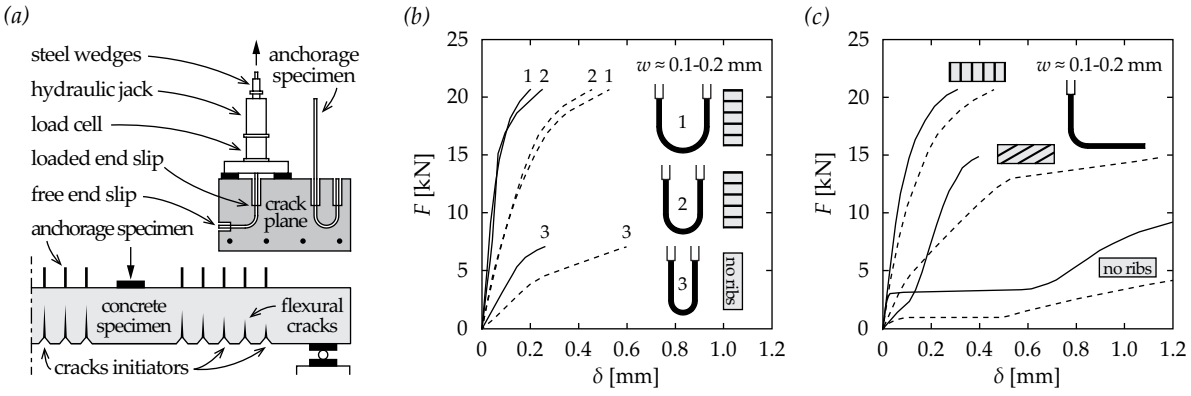

Figure 2.32 Bend bar details in cracked concrete (adapted from [Reg80a]): *(a)* test setup; *(b)* force-slip relationships for various hooks; and *(c)* force-slip relationships of 90° bends with different surface profile (solid lines: uncracked concrete, dashed lines: cracked concrete)

In general, between the different types of deformed steel used, and for a similar type of detail, the bars presenting the most efficient surface profile –associated to the largest value of bond index– were the least influenced by the presence of cracks. These differences in performance might be

related to the bearing and crushing phenomena on the inside of the bend. The variability observed in the behaviour of plain details and the low strength generally associated to this type of steel ($f_y \approx 250 \div 350$ MPa) confirms the necessity to avoid their use in any practical applications to the detriment of deformed bars.

During the same period, Regan [Reg80b] performed some additional pull-out tests on various deformed bend details ($d_b = 12$ mm) in large flexural cracks (up to 1.00 mm). The configuration of the test and the preparation of the anchorage specimens (Figure 2.33*(a)*) were relatively similar to the previous investigation [Reg80a]. Although the stiffness of the behaviour was significantly reduced, both details –the 90° bend (with the presence of a transverse bar at the bend) and the hook– were able to provide an anchorage for the activation of the entire load capacity (Figure 2.33*(b-c)*). The rather unexpected response of the details in such large cracks might be related to several factors. The important bonded length before the beginning of the bend ($l_b \approx 8 \cdot d_b$) contributes in a certain way to the force transfer and limits the activation of the anchorage itself. Also, the rib profile of the tested bars (*Swedish Kam steel Ks60*) was much more pronounced than standard steel bars used (*BSt500*) with a ratio between the related bond indices of almost 2. Also, the use of a transverse bar at the inside of the 90° bend finally led to a limitation of the differences between the details –both in cracked and uncracked conditions– as it contributed significantly to the improvement of the behaviour. In order to better characterize the anchorage performance of the bend, such additional reinforcing elements should preferably not be considered.

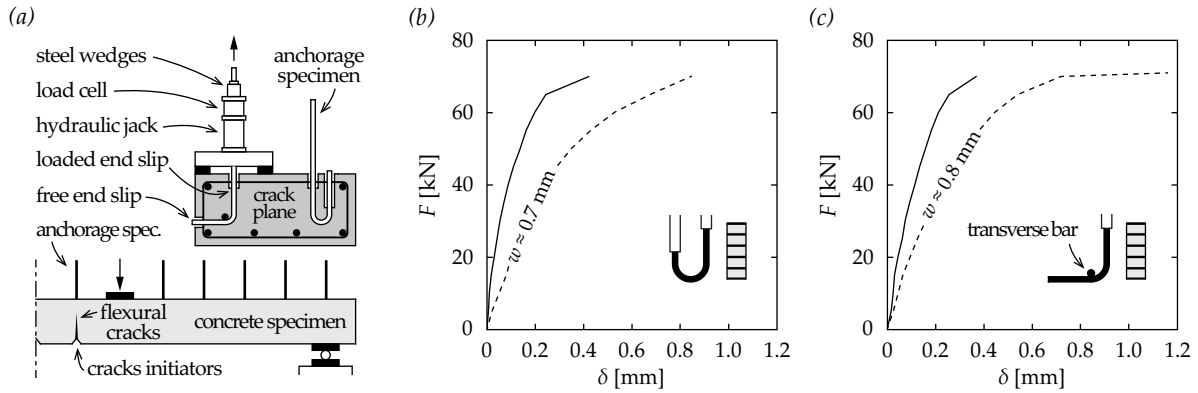

Figure 2.33 Bend bar details in cracked concrete (adapted from [Reg80b]): *(a)* test setup; *(b)* force-slip relationships of a hook; and *(c)* force-slip relationships of a 90° bend with transverse bar (solid lines: uncracked concrete, dashed lines: cracked concrete)

Although several experimental campaigns were conducted to investigate the anchorages made of bend bars in cracks, the results were generally insufficient for the development of any formulation regarding bond-slip characteristics (such as presented for straight bars). Furthermore, the extensive research performed on details with welded transverse bars is not representative of their uses in practice, rather related only to a contact (in the best case assured by a constructive steel tight) with significant differences in the behaviour. Additional investigations related to actual bend bar details in various range of cracks widths are in this sense necessary to thoroughly define the performance of such commonly used reinforcing solutions.

2.3.3 Headed bars

The previously mentioned pull-out test series of Regan [Reg80b] also included several types of headed bars (plain and deformed) with different head sizes (d_h = 2.5 ÷ 3·d_b) and bar diameters (12 and 16 mm). Uncertainties exist regarding the exact geometry of the head –notably its inclination– as only sketches of the reinforcing system were reported by the author. Although the cracks were relatively important, all the details provided an adequate anchorage with full activation of the steel bars (Figure 2.34*(a-c)*). However, the values of the crack widths were unfortunately not adequately selected and controlled in order to allow a direct comparison between the tested details. It is interesting to note that significant differences arise in the behaviour –mostly in cracked concrete– where the geometry of the head and the surface properties of the bar play an important role. Also, the results support that the contribution of the straight part of the bar prior to the head (l_b = 10·d_b) in the force transfer is not negligible, even in presence of large cracks. For instance, this is confirmed by the fact that similar values of slip were measured at ultimate load for the specimens made of plain (Figure 2.34*(a)*) or deformed (Figure 2.34*(b)*) bars, although larger cracks were measured in the latter. Thus, in the frame of a future investigation on the performance of headed bars, considerations should be made –similarly to the hooked bars– to limit the influence of bond in this specific zone to characterize only the one associated to the anchorage evaluated.

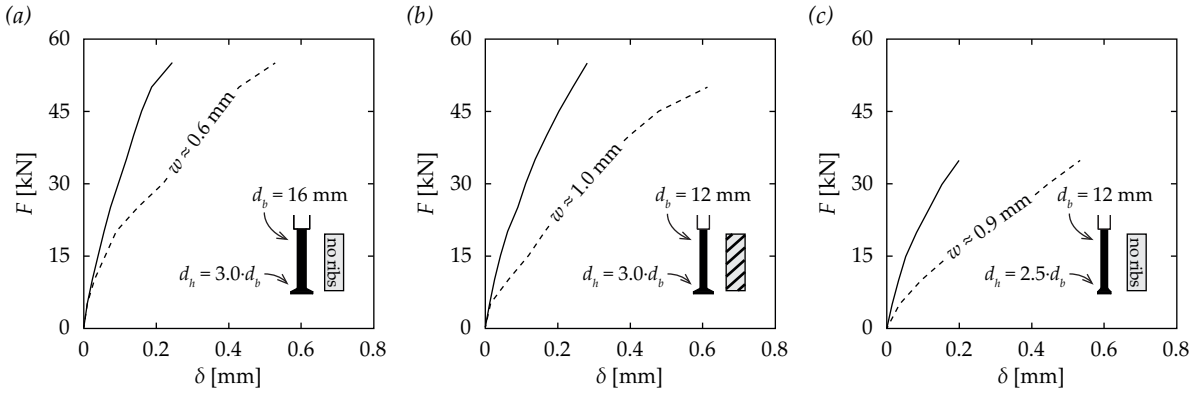

Figure 2.34 Headed bar details in cracked concrete (adapted from [Reg80b]): *(a-c)* force-slip relationships of various headed bars (solid lines: uncracked concrete, dashed lines: cracked concrete)

The series of investigations performed on plain anchors in cracks in Stuttgart in the 1980's –often not published [Kob85, Fur86, May88] and partially reported in several theses from the early 1990's [Leh90, Lot92, Fur93]– are mentioned but not further developed because they are rather related to the concrete-cone breakout failure mode. However, the latter tests are particularly interesting regarding the study of the formation and penetration of the concrete wedge forming under the head. Although several formulations were proposed to consider the effect of cracks on the load capacity for this type of anchorages, only the developments related to the evaluation of the slip in such conditions are relevant to be presented in the current research [Fur93]. The author differentiates several successive phases for the activation of steel anchors in cracked concrete. In the case of a theoretical unidirectional element in a single crack, the increase of the slip is mainly associated to

the presence of a gap resulting from the crack (1 in Figure 2.35*(a)*), then in a more moderate way, to the local crushing of the concrete (2 in Figure 2.35*(a)*) and finally to the penetration of the detail into the crack (3 in Figure 2.35*(a)*). The actual detailing of this type of anchorages –angle of the head α_H = 60 ÷ 80° and bearing area $A_h \approx 9 \cdot A_b$– gives significantly less importance to the last two phases described, and can reasonably be neglected. For such reinforcing details, the increase of slip in cracked concrete (compared to uncracked concrete conditions) is thus expected to be mostly related to the geometrical properties of the head (defining the gap). In this sense, to limit the reduction of stiffness associated to cracks, its inclination should be the most perpendicular to the bar. However, this is not really compatible with the way of producing most of these elements nowadays (see Section 2.1.3). The analytical investigations related to the presence of one single crack or two intersecting cracks at an axisymmetric anchorage highlighted the potential influences on the slip and the activation (Figure 2.35*(b)*). The proposed expressions –linearly function of the crack opening– were derived by equilibrium conditions depending on the geometry of the details. For comparison purposes, the simplified case of unidirectional anchorage is also presented. In the axisymmetric case with a single crack, the activation initiated without any significant slip (compared to the two other cases). This is related to the fact that, in the latter case, the detail can still develop a contact in the direction perpendicular to the crack opening. Although these formulations might be of major interest in the characterization of the performance of headed bars in cracks, they were never properly validated experimentally, and only qualitative recommendations were provided.

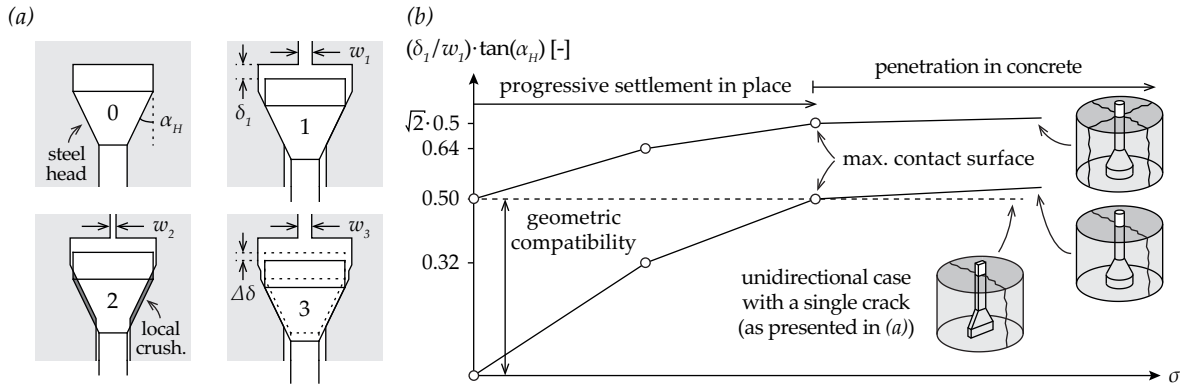

Figure 2.35 Headed bar details in cracked concrete (adapted from [Fur93]): *(a)* mechanisms of slip (for the theoretical unidirectional case); and *(b)* qualitative relationships between the initial slip and the pressure in the loaded area (corresponding to the activation of the bar)

Tests from literature have indicated that it is reasonable not to consider any reduction of the maximum strength for conventional headed bars in presence of cracks. Yet, there is an evident lack of experimental evidences allowing to properly define the associated slip for a large range of crack widths. For this type of anchorage, the reduction of stiffness associated to cracks is a main issue directly affecting its activation and the structural behaviour of the reinforced structures. In this sense, additional tests should be performed with the objectives of characterizing only the performance of the anchorage of actual headed bars –without considering the straight part prior to the head– to facilitate further developments and interpretations on this topic.

2.4 Main code provisions

Although it has clearly been confirmed that the presence of cracks passably influences the force transfer, design codes do not generally provide explicit recommendations to account for this phenomenon. It is usually suggested to arrange adequate transverse reinforcement in areas where tensile stresses might develop in the concrete cover. However, in some cases, this might not be always straightforward to accomplish in practice. Also, for rehabilitation purposes, it would be of major interest to be able to evaluate the residual capacity of an anchorage or a bar in such severe conditions. For these reasons, in the following, the few analytical expressions available from code provisions to account for the reduction of the bond strength on straight bars in in-plane cracks are presented (Figure 2.36). It has to be highlighted that no reductions are explicitly considered by the codes for anchorages such as headed or bend bar details in similar conditions (cracked concrete).

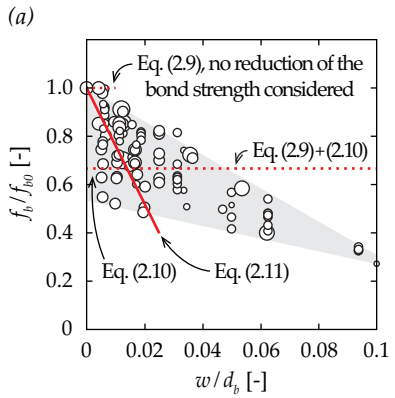

(b)

$$\frac{f_b}{f_{b0}} = \frac{2}{3} \quad (2.9)$$

validity range: $w \geq 0.2$ mm

$$\frac{f_b}{f_{b0}} \leq \frac{2}{3} \quad (2.10)$$

$$\frac{f_b}{f_{b0}} \cong 1 - 24 \cdot \frac{w}{d_b} \quad (2.11)$$

Figure 2.36 Bond phenomenon in cracked concrete: *(a)* current code provisions compared with test results from literature (empty dots); and *(b)* related formulations

The German national codes [DIN01] consider a constant reduction of 1/3 of the assumed mean bond strength for crack widths larger than 0.2 mm, leading to Eq.(2.9). Therefore, this formulation can potentially be not conservative for crack openings smaller than 0.2 mm ($w/d_b < 0.01$, mean bar diameter of 20 mm considered for the comparison), as all the presented expressions and test results confirmed a non-neglectable decrease of the bond performance already for this range of cracks.

A similar approach was followed by the Italian national codes [NTC08] with Eq.(2.10). However, the reduction of bond strength –at least the same value proposed by the German codes [DIN01]– is considered when the bar is located in areas where tensile stresses might develop. The expression is thus closer to the experimental evidences on the discussed crack range ($w \leq 0.2$ mm), but it still does not capture the phenomenon well (notably for large values of normalized crack opening).

Recently, Model Code 2010 [FIB13], in §6.1.1.3.3, allows the evaluation of the reduction of the bond strength in presence of a longitudinal crack along the bar axis, reformulated for consistency as Eq.(2.11). The crack opening is limited to a maximum value of 0.5 mm ($w/d_b < 0.025$, mean bar diameter of 20 mm considered for the comparison). This expression is linearly function of the crack opening and seems the most adequate –yet rather conservative– amongst the presented ones to provide recommendations on the bond degradation for serviceability limit state.

2.5 Synthesis

Since the beginning of the 20th century, the transfer of forces between steel and concrete has been recognized as an important issue for reinforced concrete structures. Several local mechanisms of variable efficiency have been identified together with the development of solutions to improve the activation of the reinforcement, as the latter was observed to be potentially insufficient in specific situations. Also, for a given detail, the transmission of forces is relatively complex as the contributions of the related mechanisms is unique and might vary considerably with the load level. The investigations conducted on straight, bend and headed bars therefore highlighted significant disparities in the behaviour amongst the details (see Section 2.1). The additional anchorage provided by the surface profile or by a specific geometry at the extremity of the bar induces important concentration of forces potentially limiting the load capacity. Splitting or concrete-cone breakout failure modes can occur if adequate constructive dispositions –such as minimum transverse reinforcement or sufficient cover– are not provided in the concrete specimen. Cracks are inherent to concrete members and have multiple origins. They generally reflect a transmission or redistribution of internal forces to satisfy equilibrium conditions. The localization of the cracks tends to be related to the position of the reinforcement bars or anchorages (see Section 2.2) as the development of bond phenomena locally activates the limited tensile strength available in the cement paste. Experimental works performed in the last decades confirmed that the aforementioned force transfer mechanisms are particularly sensitive to the presence of cracks even of limited width (see Section 2.3). Only a limited amount of design codes provide some recommendations for the evaluation of the latter phenomenon (see Section 2.4), although a reduction of the related structural performance of the reinforced concrete element was experimentally observed in several cases on beams and slabs. The main conclusions and interesting points that arise regarding the performance of straight, bend and headed reinforcing details in concrete are the following:

- The use of plain bars in modern structures should be avoided. Otherwise, an extremity anchorage should be systematically considered –rather a head than any type of bend– in order to achieve a certain activation even in presence of cracks;
- Deformed straight bars provide an additional mechanical effect through the surface profile (ribs or indentations). Nowadays, a large variety of steel types exists with differences in terms of strength, deformation capacity and bar diameter;
- The identification amongst these products is generally done visually through the adaptation of the layout of the surface profile according to some international standards. Although the arrangement of the ribs or indentations do not seem to affect the related performance in uncracked concrete, the latter statement is less evident in cracks;
- Bond strength and stiffness are affected non-linearly by the presence of cracks and empirically-based formulations were developed to quantify the related decrease of performance. Significant disparities exist amongst them, mainly associated to the different test setups and specimens or also steel products (variety of surface profile types);

- Bend bar details made of deformed steel assure, through their geometry, an additional mechanical anchorage complementary to the one provided by the surface profile for the force transfer. Thus, similarities exist between the performance of such anchorages and straight bars;
- Hooks and bends presented significant differences in the behaviour in presence of cracks. In few cases, the development of brittle failure modes –as spalling of the concrete cover– was observed due to the straightening of the detail associated to an important slip;
- The limited tests available on U-shaped bars in cracks however highlighted the performance of this type of detailing solution, mainly associated to its improved geometry that prevent any important slip of the bar but rather a crushing of the concrete directly inside the bend;
- Headed bars achieve the force transfer at the level of the head, where important bearing takes place on the concrete in this specific zone. The performance of this mechanical anchorage also requires the arrangement of adequate constructive dispositions to prevent splitting failures;
- Headed bars in cracks –even of large widths– systematically developed full activation of the steel together with a limited reduction of stiffness. Compared to other reinforcing details in similar conditions, the behaviour of the latter was significantly better with very limited slip;
- Experimental evidences support that, in general, the more the transfer of force is performed locally by the reinforcing detail, the less sensitive is the anchorage to conditions such as cracks;
- The formation of a specific concrete wedge for each of the mentioned details reflects the position where most of the transfer of forces is performed: at the face of the ribs for straight bars, inside the bent for hooks and right under the head for headed bars;
- The penetration of the latter into the surrounding concrete is, under some conditions such as cracking, strongly simplified and might lead to large displacement with a limited activation.

Current main codes generally provide rather conservative recommendations regarding bond and anchorage that should lead to a safe design for new constructions in the next decades. However, in the case of the assessment of existing structures –built under a previous version of provisions– it is necessary to identify the main vulnerabilities from a structural point of view. In this sense, the investigations on bond focus nowadays mainly on time-related phenomena such as corrosion, freeze-thaw cycle or fire conditions. The aim is to develop methods to evaluate as closely as possible to reality the influence of these severe conditions on the ultimate strength of a bar or anchorage. The present research is therefore a contribution of major interest on the activation of different actual detailing solutions in cracks of various openings (serviceability and ultimate limit states). A potential direction for the characterization of the anchorage performance would be related to the detailed study of the phenomenon of penetration of the concrete wedge forming locally for each of the mentioned details. Several references were in this sense specifically mentioned and partially described in the present section in order to gather the necessary bases for such further related developments.

Chapter 3 Experimental and Theoretical Investigations on the Performance of Anchorages in Cracked Concrete

Most classical investigations on bond and anchorage properties in reinforced concrete have been performed on the basis of pull-out tests, where a reinforcement bar is pulled-out from an uncracked cylinder, prism or cube (see Section 2.1). In presence of adequate constructive dispositions –preventing the premature failure of the concrete specimen– the behaviour is generally stiff enough to achieve a full activation of the steel bar. Contrary to these standardized tests, the transfer of forces is often developed within already cracked concrete in many structural members, with significant changes in the behaviour (see Section 2.3). The latter is particularly relevant for the reinforcement in beams and slabs, both for the flexural and transverse elements (see Section 2.2). Few empirically-based formulations have been proposed to quantify the effect of cracks on the response of reinforcing details –mainly for straight bars and related to the ultimate strength– with an important scatter regarding the tests available from literature. Generally, the code provisions rather formulate recommendations to prevent cracking in these specific zones than expressions to account for the latter phenomenon (see Section 2.4), even though experimental evidences exist.

The present chapter aims to contribute on the performance of actual anchorage types in cracked concrete through a combination of experimental, analytical and numerical investigations. The detailed description of the test campaign (see Section 3.1) allows a better understanding of the complexity and potential issues related to the topic of interest. A total of 110 monotonic pull-out tests were performed –from which 27 as reference in uncracked concrete– on details such as straight, hooked, U-shaped and headed bars. The tests were thoroughly conducted for crack openings ranging from 0.2 to 2.0 mm (generally constant width on the thickness) in order to cover conditions both at serviceability and ultimate limit states. For some details, tests in flexural cracks (variable width on the thickness) were additionally performed to highlight potential disparities. This experimental work considerably improved the related state of the art and confirmed a significant influence of in-plane cracking, with a decrease of bond and anchorage performance for increasing crack openings (see Section 3.2). The force-slip relationship –characterizing the performance of a reinforcing detail– is also analytically investigated and compared to test results with accurate predictions (see Section 3.3). Finally, a refined numerical approach is developed to validate the proposed model and to depict the influence of the orientation of the crack on the bond strength of various types of straight bars (see Section 3.4).

3.1 Experimental campaign of pull-out tests

The main objective of this investigation is related to the performance of anchorage details in cracked concrete similar to those used as transverse reinforcement for punching. The diameter of the bars was limited to 10 and 14 mm in order to serve as a good representation of the uses of practice in reinforced concrete flat slabs. The test campaign was divided into two series of pull-outs depending on the type of cracks. It was originally inspired by the reference work conducted by Rehm in the late 1970's [Reh79], to which several modifications and improvements were brought.

The first series was performed in flexural cracks (see Section 3.1.2) to be the closest to practical situations taking place in structural elements (Figure 2.21). Three types of anchorage –intentionally chosen to be fundamentally different– were selected in order to define the potential variation range of the performance. Also, this series validated several important points regarding the fabrication and preparation of the reinforcing details or of the concrete specimens but also the measurement and testing devices (see Section 3.1.1). It took place in the laboratory of the Civil Engineering Institute (IIC) of École Polytechnique Fédérale de Lausanne (EPFL) from December 2013 to June 2014.

The second series was performed in transverse cracks (see Section 3.1.3) due to the complexity of the test procedure highlighted in the first series regarding the development of flexural cracks. A significantly larger amount and variety of details was investigated under different configurations in the laboratory of the IIC of EPFL from July 2014 to April 2015.

3.1.1 Material properties, measurement devices and test procedures

In order to perform a thorough and accurate study on the performance of bond and anchorages in cracked concrete, a specific attention was dedicated to the preparation of the reinforcing details on the basis of the related limitations highlighted in similar previous works (see Section 2.3). In this sense, it appeared essential to be involved in the earliest phases of production of these elements. The latter allowed the observation and the control of the detailing processes necessary to transform simple steel bars or rods into specific anchorage elements for reinforced concrete structures.

During the realisation of the straight, hooked and U-shaped details –all made from the same steel product (Figure 3.1*(a)*)– the main issue was related to the orientation of the indentations composing the surface profile of the rods. In order to affect as much as possible the performance of the related force transfer mechanisms, the details were arranged with the indentations disposed parallel to the position of the crack. Despite the fact that more than the double of the amount of details strictly necessary was produced –to select only the most adequate ones– a certain torsion of the rod around the axis could yet not be totally avoided. The latter phenomenon appeared more significant for the small diameter due to the reduced torsional inertia. The use of last-generation bending machines –automatized with servocommand (Figure 3.1*(b-c)*)– ensured the accurate definition of the geometry for the evaluated anchorages. For each different type of detail or bar diameter, additional manual phases were required to change the steel mandrel –defining the inside diameter of the bend– and for the reprogrammation of the detailing steps.

Figure 3.1 Production of straight and bend bar details: *(a)* steel manufacturer *Pfefferlé SA* (Sion, Switzerland); *(b)* machine with servocommand used for the bending process of the steel rods (*Twinmaster 12S*); and *(c)* steel mandrels for rod straightening prior to detailing

The production of headed bars requires fundamentally different resources than for bend bar details. This is particularly the case when the process used to generate the head is not related to welds or threads (see Section 2.1.3). The details considered in the present research –standard forged studs– result from the heating of the bar extremity (Figure 3.2*(a)*) directly followed by the materialization of the head through a well-defined mechanical process (Figure 3.2*(b)*). This type of anchorage might also present some local disparities regarding the head inclination or centering, although the production process is automatized. The experimental work performed confirms that the latter aspects are of importance for the performance of the studs under some specific and severe conditions (see Section 3.2.4). Also, although the bars used for the headed bars were made of deformed steel, the part of the straight bar in the vicinity of the head generally presents almost no surface profile due to the local heating associated to the production processes (Figure 3.2*(c)*).

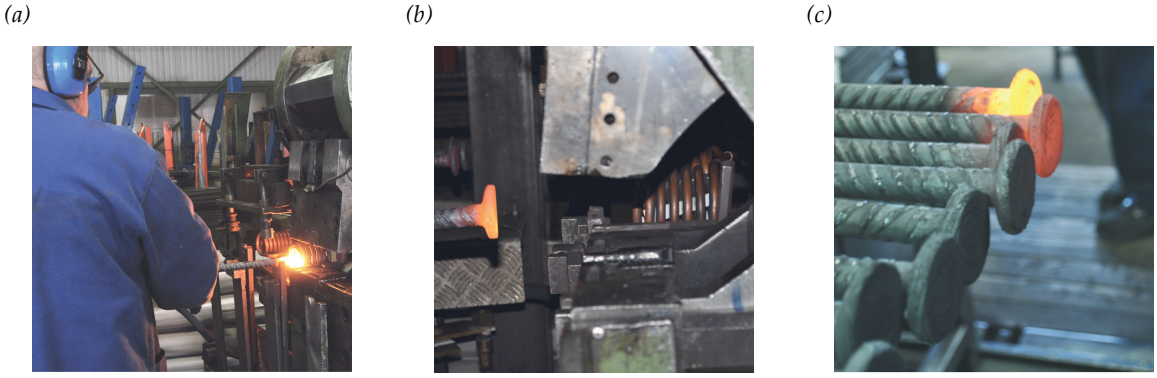

Figure 3.2 Production of forged headed bars (courtesy of *Ancotech SA*): *(a)* heating of the extremity of the straight bar (generally through induction process); *(b)* mechanical materialization of the head; and *(c)* progressive cooling of the reinforcing elements after detailing

Once produced, each detail required a specific preparation –prior to the casting of the concrete specimens– in order to be able to accurately measure the slip during the pull-out test. This notably included the drilling of a 2 mm diameter hole in the axis of the bar (Figure 3.3*(a)*)–with approximately one-diameter depth– and the disposition of a PVC tube –slightly larger than the bar and the surface profile ($d_{b,int}$ = 13 mm / $d_{b,ext}$ = 16 mm for d_b = 10 mm and $d_{b,int}$ = 17 mm / $d_{b,ext}$ = 20 mm for

d_b = 14 mm)– on the part of the detail not of interest in the present investigation. The latter were generally arranged at a distance of one diameter from the anchorage (Figure 3.3*(b)*), defined as the enlarging of the bar for headed bars or the beginning of the bend for hooked and U-shaped bars. A steel rod of 2 mm diameter was disposed temporarily in the drilled hole to allow an accurate installation of the details in the formwork. The latter was substituted after casting by a stiff piano wire of diameter 1.5 mm fixed at the extremity of the drilled hole with cyanoacrylate glue through a syringe (concrete specimens turned momently upside-down during drying). The diameter of the piano wire was selected to be stiff enough and to limit the contact with the surrounding concrete, therefore minimizing the disturbances associated to a potential friction. A steel piece –detailed in Figure 3.10*(a)*– connected the piano wire and the inductive sensor (LVDT from HBM), providing an extensive and accurate measurement of the slip during the pull-out test (up to 30 mm).

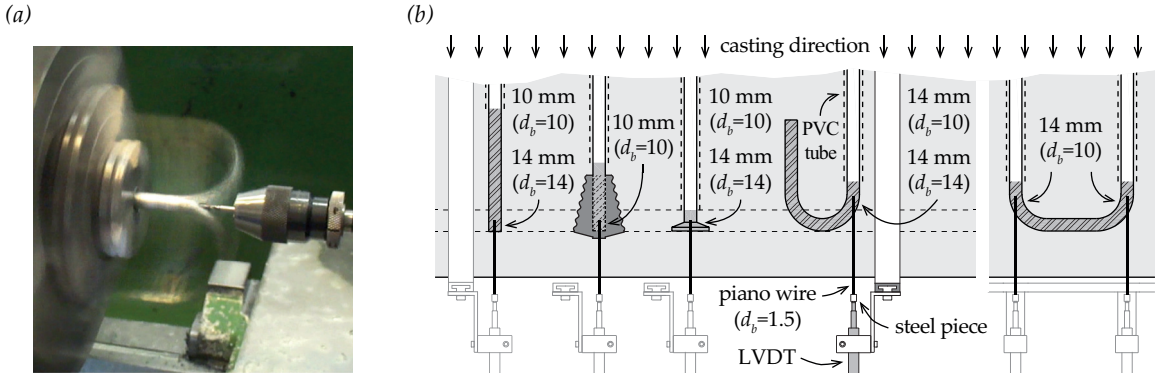

Figure 3.3 Preparation of the details for the measurement of the slip: *(a-b)* definition of the related measuring points by a systematic drill in the axis of the bar (depth in [mm]) and precise disposition of PVC tubes to locally prevent the contact between the bar and the concrete

The production of concrete specimens for both test series took place in similar conditions in the precast company *Proz Frères SA* (Riddes, Switzerland). The requirements regarding cracking at specific positions of the elements motivated the development of a specific formwork in EPFL, used for all the mentioned investigations (Figure 3.4*(a)*). The effective dimensions of the concrete specimens (300 × 250 × 3000 mm) allowed the disposition of 11 transverse details in each of them for the pull-out tests. Steel plates acting as crack initiators were arranged in the formwork reducing the effective section locally by 20% to guarantee the localization of the cracks at these exact locations. The concrete specimens were reinforced in the longitudinal direction by means of four high-strength cold-formed steel bars (nominal yield strength $f_{y,0.2}$ equal to 670 MPa) in order to avoid the presence of a plateau and being able to cover intermediate values of crack opening. Also, no transverse reinforcement was disposed so as not to influence the development of the force transfer during the pull-out test. For all specimens, *Genetti SA* (Riddes, Switzerland) provided a concrete of normal strength (ranging between 27.5 MPa and 36.2 MPa, tested on 320 x 160 mm cylinders) with a maximum aggregate size of 16 mm. The concrete was poured from the top, specimen by specimen, prior to the activation of the vibrating table for a few minutes (Figure 3.4*(b)*). For the main test series, the pull-out was performed with a direct contact on the concrete specimen thus the local disparities of the surface were carefully rectified with a very thin layer of plaster (Figure 3.4*(c)*).

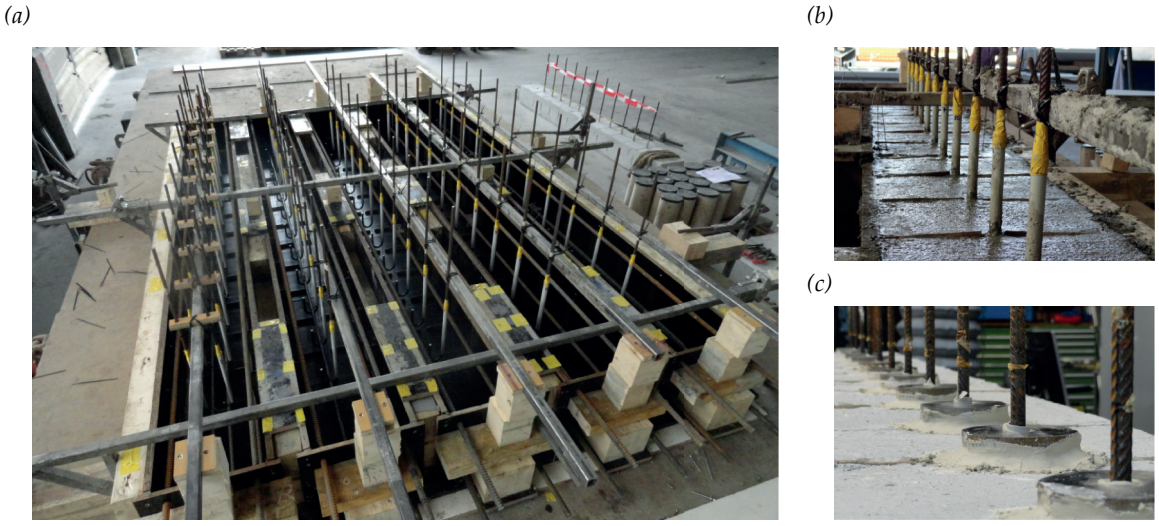

Figure 3.4 Production of the concrete specimens: *(a)* formwork with disposition of the anchorage details and steel inserts (bottom and laterals); *(b)* casting of the specimen and disposition of the steel top inserts; and *(c)* preparation of specimens prior to pull-out test with installation of load introduction steel plates with plaster to adjust the surface asperities

The test procedure followed was similar in both series so as to be consistent for further interpretations and comparisons. Once the concrete specimens were thoroughly prepared with the measurement points for the monitoring of the crack opening, they were carefully arranged in the test setup (different for each series). Then, between one and three control bars –generally two– were pulled out before the development of the cracks at the location of the tested details in order to have a reference behaviour in uncracked concrete. The latter point is essential to characterize the sensitivity of an anchorage to the presence of cracks. To that aim, a hollow hydraulic jack combined with a hollow load cell was used in most of the cases. A specific description of the testing device and support conditions considered in the test series can be found in the related section of this chapter. The concrete specimens were then progressively loaded and the crack widths tracked by using continuous (displacement gauges) or discrete (deformeter) displacement measurement systems. At the defined crack widths, the loading of the concrete specimen was stopped and kept constant as the bars were pulled out at a rate of approximatively 1.5 kN/sec. The response of the details in terms of force-slip was recorded at a frequency of 2 Hz to capture the potential sudden changes.

The main properties of the reinforcement composing the details evaluated are summarized in Table 3.1, for which the notations considered in Chapter 2 have been used. The surface parameters and sections of the bars or rods (Figures 3.5 - 3.9) were defined through Digital Image Correlation (DIC) measurement system on some representative samples. The reported yield strength –$f_{y,0.2}$ for cold-rolled steel, and f_y for hot-rolled steel– were obtained from standardized tensile tests on straight bars. It must be noted that the effective values for the tested details might be reduced due to the fabrication process during detailing. This was confirmed in the experimental work, notably for headed bars where a reduction of 20% was observed. The plain hooks were from the same production as the deformed ones, but the surface profile was manually removed with the use of a milling machine and sand paper to strongly limit the development of bond.

Figure 3.5 Detail of the reinforcement (d_b = 10 mm) used for the plain hooks (*SB16*)

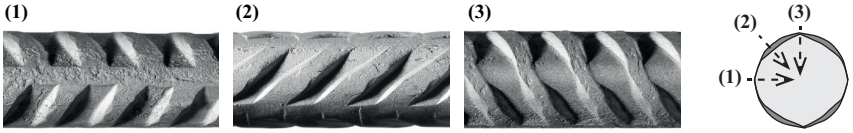

Figure 3.6 Details of the reinforcement (d_b = 10 mm) used for the straight (*SB6*, *SB7*), hooked (*SB2*, *SB11*, *SB13*, *SB14*) and U-shaped (*SB10*, *SB15*) bars made of deformed steel

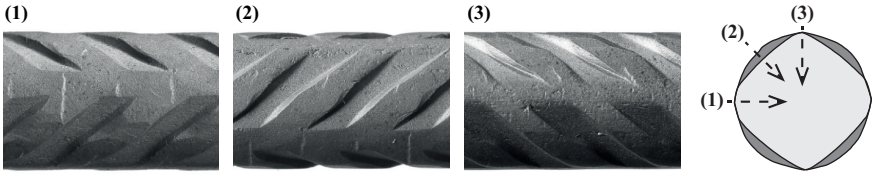

Figure 3.7 Details of the reinforcement (d_b = 14 mm) used for the deformed hooks (*SB12*)

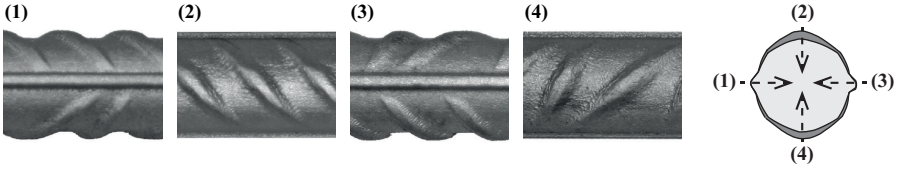

Figure 3.8 Details of the reinforcement (d_b = 10 mm) used for the headed bars (*SB3*, *SB9*)

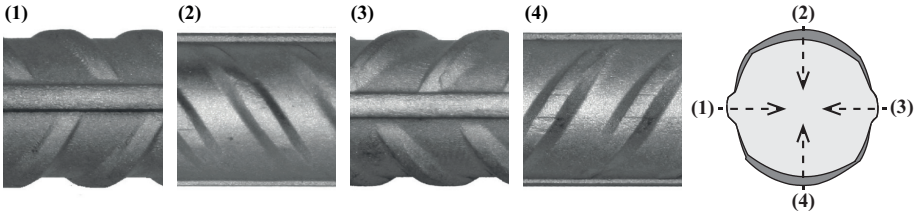

Figure 3.9 Details of the reinforcement (d_b = 14 mm) used for the headed bars (*SB8*)

Table 3.1 Main material and surface parameters of the tested reinforcing details

Detailing	d_b / d_h [mm]	Steel grade and type	f_y, $f_{y,0.2}$ / f_t [MPa]	s_R (1) [mm]	f_R (2) [-]	$h_{R,max}$ / h_R [mm]	α_R (3) / α_H (3) [°]	β_R (4) [°]
hooked	10	*Topar-R, B500B cold rolled, de-coiled rods*	552 / 602	-	-	-	-	-
straight, hooked and U-shaped	10	*Topar-R, B500B cold rolled, de-coiled rods*	552 / 602	6.40	0.050	0.65 / 0.32	35	44
straight and hooked	14	*Topar-R, B500B cold rolled, de-coiled rods*	572 / 630	9.10	0.056	1.08 / 0.51	44	41
headed	10 / 30	*BST 500, B500B hot rolled, bars*	706 / 736	6.60	0.058	0.90 / 0.38	35 / 73	52 / 44
headed	14 / 42	*BST 500, B500B hot rolled, bars*	655 / 734	8.40	0.058	0.99 / 0.49	49 / 73	57

(1) distance between two consecutive ribs or indentations determined as the number of gaps on the measured length ($l_b = 10 \cdot d_b$)

(2) defined as described in [ISO10], in agreement with minimal recommended values for conform reinforcing steel [SIA13, SIA16]

(3) transverse rib flank inclination / angle of the head according to bar axis, and (4) rib orientation according to bar axis

3.1.2 Tests in variable width cracks

The objectives of this test series were to reproduce in the most realistic manner the conditions developing in the vicinity of the anchorage of the transverse reinforcement used in the phenomenon of punching (Figure 2.1) and to validate the device for the measurement of the slip (Figure 3.10*(d)*), essential for the characterization of the behaviour of the tested reinforcing solutions. The test setup therefore aims at performing the pull-out of a detail in a flexural crack (Figure 2.1*(b)*) or in a zone of active confinement (Figure 2.1*(f)*) with indirect support at 45° representing the activation through a strut (Figure 3.10*(c)*). The dimensions of the concrete «beam» specimens –3000 x 300 x 250 mm– were defined to correspond to bands of the slabs usually considered in the investigations on punching at EPFL (3000 x 3000 x 250 mm). Also, the longitudinal reinforcement was defined to be comparable with the amount of steel frequently disposed in these slabs (ρ=1.5%).

The test setup consisted in a rigid frame composed of two lateral stiff steel box profiles, a prestressed tie of coupled *Dywidag* bars and the concrete specimen (Figure 3.10*(a)*). The system was loaded through the tie placed on top, introducing locally a bending moment and a normal force in the concrete specimen (the eccentricity of the tie to the centre of gravity of the beam was around 1350 mm). The installation of confinement systems in the load introduction areas was necessary to prevent concrete crushing (Figure 3.10*(b)*), notably after 2 tested specimens (out of 5) were seriously damaged. The force in the tie was adapted in order to control the crack width at the level of the bottom longitudinal reinforcement, also corresponding also to the position of the anchorage. Even though the solution of a 4-points bending –often used in similar works from literature [Reg80a, Reg80b]– was initially considered, the aforementioned one was finally preferred to optimize the number of pull-out tests to be performed (11 per specimen). It also prevented the use of stirrups or similar transverse reinforcement in the concrete specimen –required for the transfer of shear forces resulting from bending– that might interfere with the activation of the anchorages during the test.

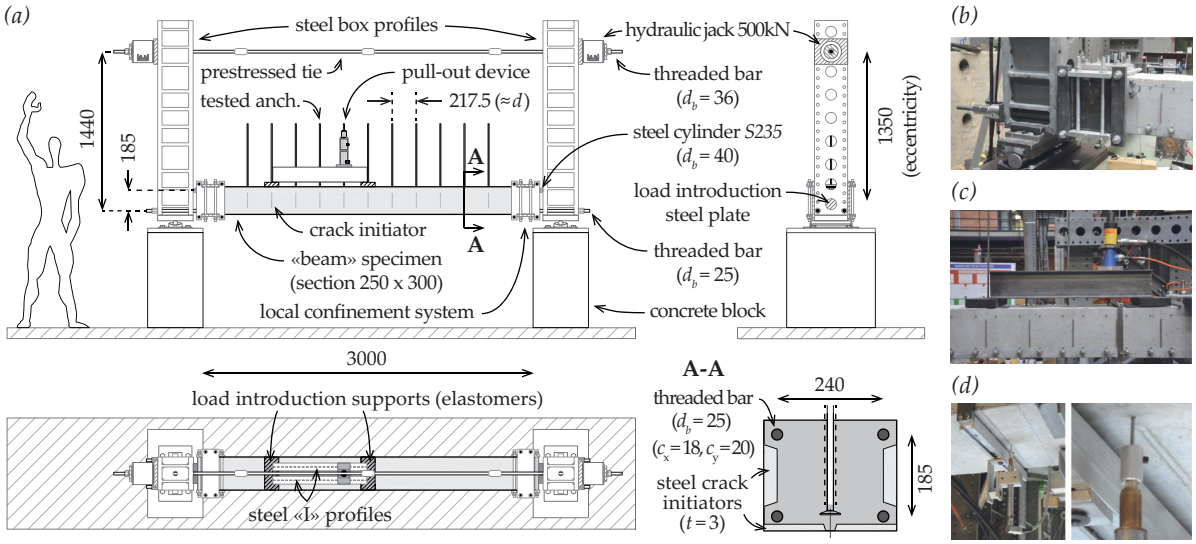

Figure 3.10 Test setup for the anchorages tested in flexural cracks (concrete specimen under bending solicitation): *(a)* detailed plans and description (dimensions in [mm]); *(b)* local confinement system; *(c)* pull-out device; and *(d)* measurement details of the slip

A total of 21 reinforcing details of various types (Figure 3.11*(a)*) –including 5 reference ones– were finally pulled-out from three concrete specimens (see Section 3.1.1 for the description of the test procedure) according to the arrangement presented in Figure 3.11*(b)*). In this test series, the width of the cracks ranged from 0.2 to 1.4 mm.

- Specimen *SB1*, presenting anchorages by means of conical profiled blocks made of Ultra-High Performance Fibre-Reinforced Concrete (UHPFRC) acting similarly to headed bars [WIP10];
- Specimen *SB2*, presenting anchorages by means of hooked bars with the cracking plane perpendicular to the evaluated details;
- Specimen *SB3*, presenting anchorages by means of headed bars (steel studs).

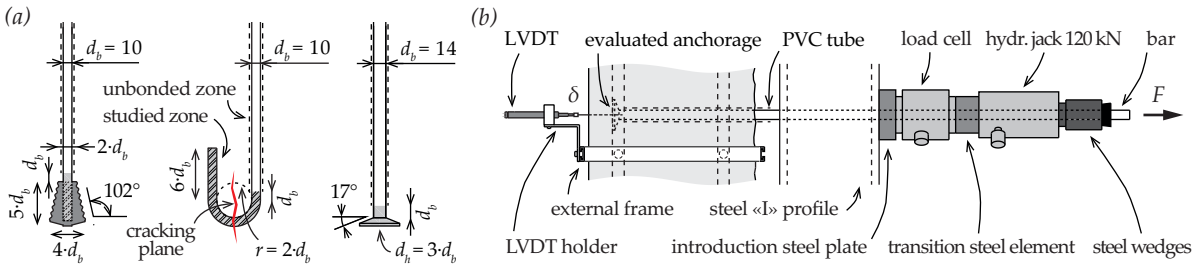

Figure 3.11 Pull-out tests in flexural cracks: *(a)* details of the geometrical properties for the anchorages considered in the experimental program (dimensions in [mm]); and *(b)* detailed testing and measurement devices

Although the tests provided the expected results –with an accurate definition of the force-slip relationship of the evaluated anchorages (see Section 3.2)– they also highlighted the necessity to considerably simplify the development of the cracks in the concrete. Similar difficulties were also recognized in the literature. Only a partial systematic comparison between the different types of details for a given crack opening could be performed. The installation of the entire test setup for each specimen was also, in this sense, very demanding timewise and deserved some improvements.

3.1.3 Tests in constant width cracks

Taking advantage of the preparation of the details and the measurement devices –completely satisfactory in the previous test series– the main objective was to investigate the response of actual anchorages detailing solutions in cracked concrete in a more pragmatic and systematic manner. Pull-out tests in transverse cracks aimed to address the latter, by also providing a lower bound of the performance of the details compared to similar tests in flexural cracks.

The use of an independent testing machine –*Schenck-Trebel 10 MN* (Figure 3.12*(a)*)– allowed an optimal regulation of the crack development by displacement control with an external inductive sensor. The target values of crack openings were thoroughly defined as 0.2, 0.5, 1.0 and 2.0 mm in order to cover situations representative of both serviceability and ultimate limit states. The concrete «tie» specimens were fabricated in similar conditions and within the same formworks as the previous test series, symmetrically reinforced with four bars of 18 mm diameter. Again, no transverse reinforcement was arranged in the concrete specimens, with the exception of the evaluated

anchorage elements, so as not to interfere with the force transfer developing during test. The pull-out device was similar to that previously used –detailed in Figure 3.11*(b)*– at the difference that it was directly supported by a circular plate (outer diameter 80 mm and inner diameter 20 mm) on the surface, as in Figure 3.4*(c)*. The original testing device (Figure 3.12*(b-c)*) was simply doubled for the tests on U-shaped bars (Figure 3.12*(d-e)*).

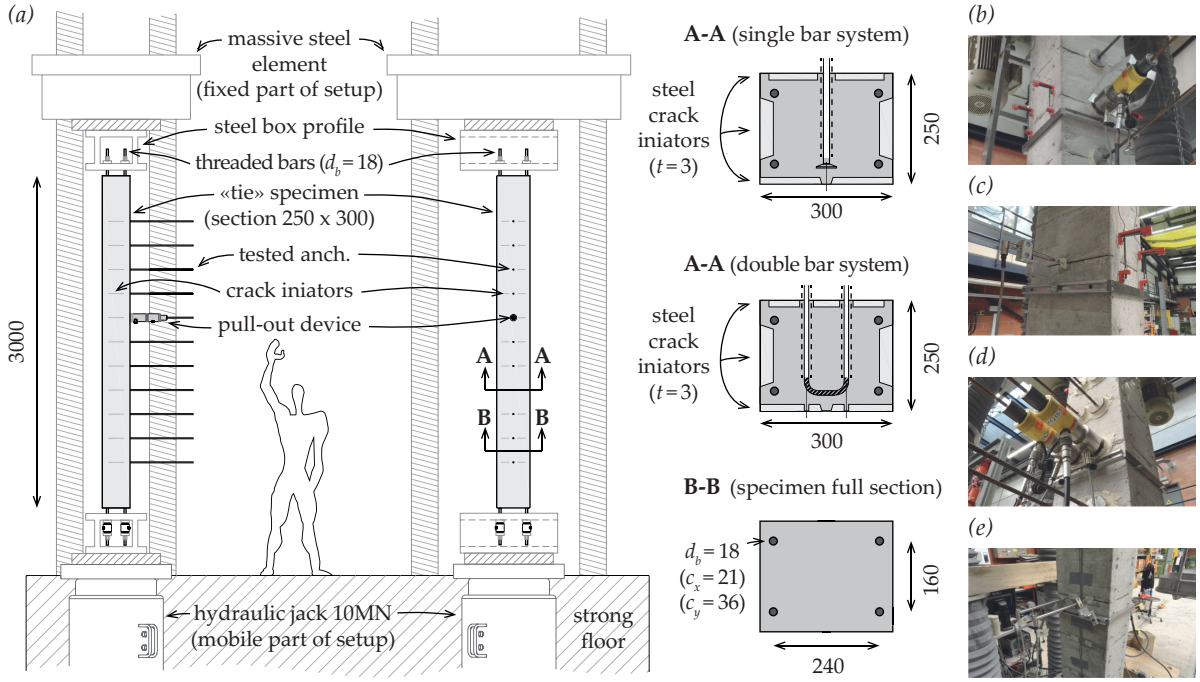

Figure 3.12 Test setup for the anchorages tested in transverse cracks (concrete specimen under tensile solicitation): *(a)* detailed plans and description (dimensions in [mm]); test and measurement devices for *(b-c)* simple system and *(d-e)* double system (U-shaped bars only)

A total of 89 details of various types (Figure 3.13) –including 22 reference ones– were finally pulled-out from eleven concrete specimens with crack widths ranging from 0.2 to 2.0 mm (see Section 3.1.1 for the description of the test procedure). Size effect was also evaluated for all the tested details by the systematic consideration of two different diameters for each type of steel product used (10 and 14 mm). After the pull-out, specific saw-cuts were thoroughly performed through the cracked planes of the concrete specimens in order to get a representative overview of the tested details for further interpretations (see Section 3.2).

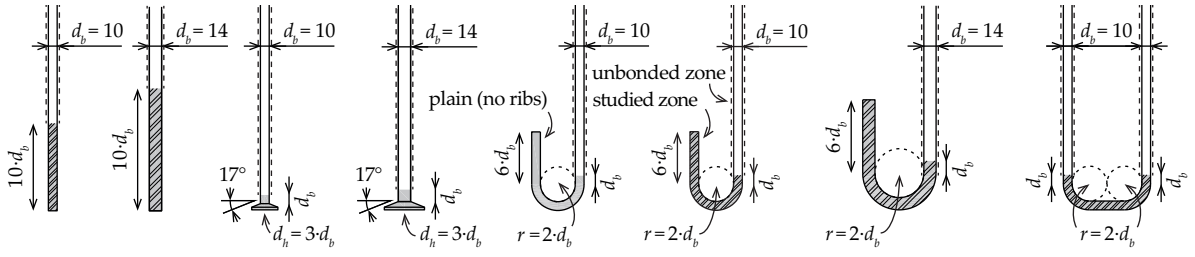

Figure 3.13 Pull-out tests in transverse cracks: details of the geometrical properties for the anchorages considered in the experimental program (dimensions in [mm])

- Specimens *SB6* and *SB7*, presenting straight bars with embedment length of $10 \cdot d_b$;
- Specimens *SB8* and *SB9*, presenting anchorages by means of headed bars (similar to *SB3*);
- Specimen *SB16*, presenting anchorages by means of plain hooked bars with the cracking plane parallel to the detail;
- Specimens *SB11* and *SB12*, presenting anchorages by means of hooked bars with the cracking plane parallel to the detail;
- Specimen *SB13*, presenting anchorages by means of hooked bars with the cracking plane perpendicular to the detail (similar to *SB2*);
- Specimen *SB14*, presenting anchorages by means of hooked bars with the cracking plane parallel to the detail with passing-through reinforcement (d_b=14 mm);
- Specimens *SB10* and *SB15*, presenting anchorages by means of U-shaped bars, respectively without and with passing-through reinforcement (d_b=14 mm).

The phase of installation of the concrete specimens in the test setup was considerably simplified and could be performed in several steps by only one person, simultaneously controlling the displacement of the crane and the testing machine (Figure 3.14). Although the testing phase was more challenging than in the previous series –the vertical position of the concrete specimen required to perform the pull-out of the transverse elements in the horizontal direction–the entire details could still be tested in one day. The results obtained were very consistent between them and highlighted interesting facts (Section 3.2). As continuous monitoring could not be set up for each tested anchorage, a considerable amount of work was necessary prior to the latter phases in order to prepare the concrete specimens. Notably, regarding the installation and the determination of the reference points for the measurement of the crack opening. It allowed a thorough comparison of the performance of various reinforcing details in cracked concrete, thus contributing greatly to the existing state of the art on the topic (rather limited, see Section 2.3).

Figure 3.14 Installation steps of the concrete specimen in the test setup prior the crack development and pull-out of the details in the transverse direction

3.2 Main results and observations

The performed tests confirmed the tendency observed in the literature. The performance of actual anchorages is in most cases considerably reduced by the presence of cracks. It also confirmed the significance of the present research highlighting significant differences in the activation amongst the evaluated reinforcing details.

This section aims at presenting the response of the details of both test series as a function of the load-slip curves for several values of crack openings (transverse or flexural). In the following figures, the grey area represents the envelope of the pull-out tests performed for a given crack opening, and the black curve the associated mean. The scatter between the tests performed under similar conditions was relatively limited and reflects the attention dedicated to the preparation of the details. When only one pull-out test could be performed for a given crack opening, the corresponding curve is indicated in the legend with an asterisk «*». The axis scale of the figures was chosen in order to facilitate the comparison between similar types of details and to discuss the observed phenomena in the best manner. No normalization with the strength of concrete was applied in the presented results as the concrete strength did not vary significantly amongst the concrete specimens (for a given test series). A complete summary of the main properties and test results – ultimate force and related slip for each of the performed pull-out– can be found in [Bra16].

3.2.1 Straight bars

The behaviour of straight bars (specimens *SB6* and *SB7*) was noticeably influenced by the presence of transverse cracks (Figure 3.15). It is interesting to note that, in presence of such conditions, the load-slip curve was governed by two regimes prior to reaching the maximum bond strength (empty dots in Figure 3.15). The former corresponded to a rather stiff behaviour –bond stresses were activated almost without noticeable slips at the free end– followed by a second regime with a less stiff response. After the maximum bond strength was reached, the load-slip behaviour presented a softening behaviour, with decreasing bond strength for increasing values of the slip. It is interesting to note that, independently of the crack opening, the development of a residual strength – associated to friction mechanism– was observed for a slip approximately corresponding to the spacing between two consecutive indentations (s_R = 6.4 mm for *SB6* and 9.1 mm for *SB7*) in uncracked concrete, and even for smaller values of slip in presence or cracks.

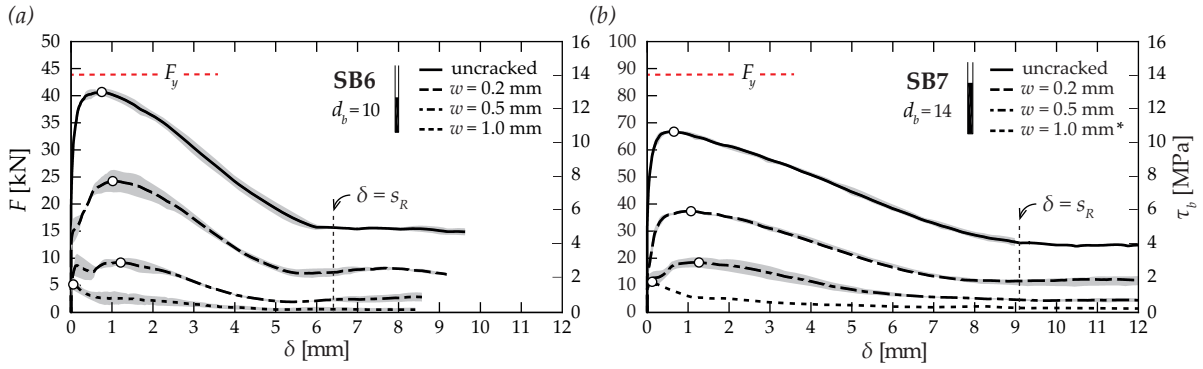

Figure 3.15 Force-slip relationships of straight bars in transverse cracks: *(a) SB6*; and *(b) SB7*

In all cases, the maximum bond strength significantly decreased, even for relatively low values of the crack opening that can be expected under serviceability conditions (w = 0.2 mm). With respect to the slip associated to the maximum bond strength, it was observed to increase for decreasing bond strength except for very large crack openings (of about 1 mm) where the maximum strength was reached for very low slip levels (first regime governing). The embedment length of $10{\cdot}d_b$ was not sufficient to activate the entire capacity of the bar –yield stresses– even in uncracked concrete. This is related to the surface roughness of the bar –characterized through the bond index f_R– close to the lower permissible bound to develop adequate bond properties [SIA13]. A size effect was also highlighted –differences of 20% in the maximum bond strength without presence of cracks– confirming that local mechanisms of force transfer are more efficient for smaller diameters.

3.2.2 Hooked bars

The asymmetry of hook details required the evaluation of the performance in cracks under different configurations to capture the potential variation range of the related behaviour (Figure 3.16).

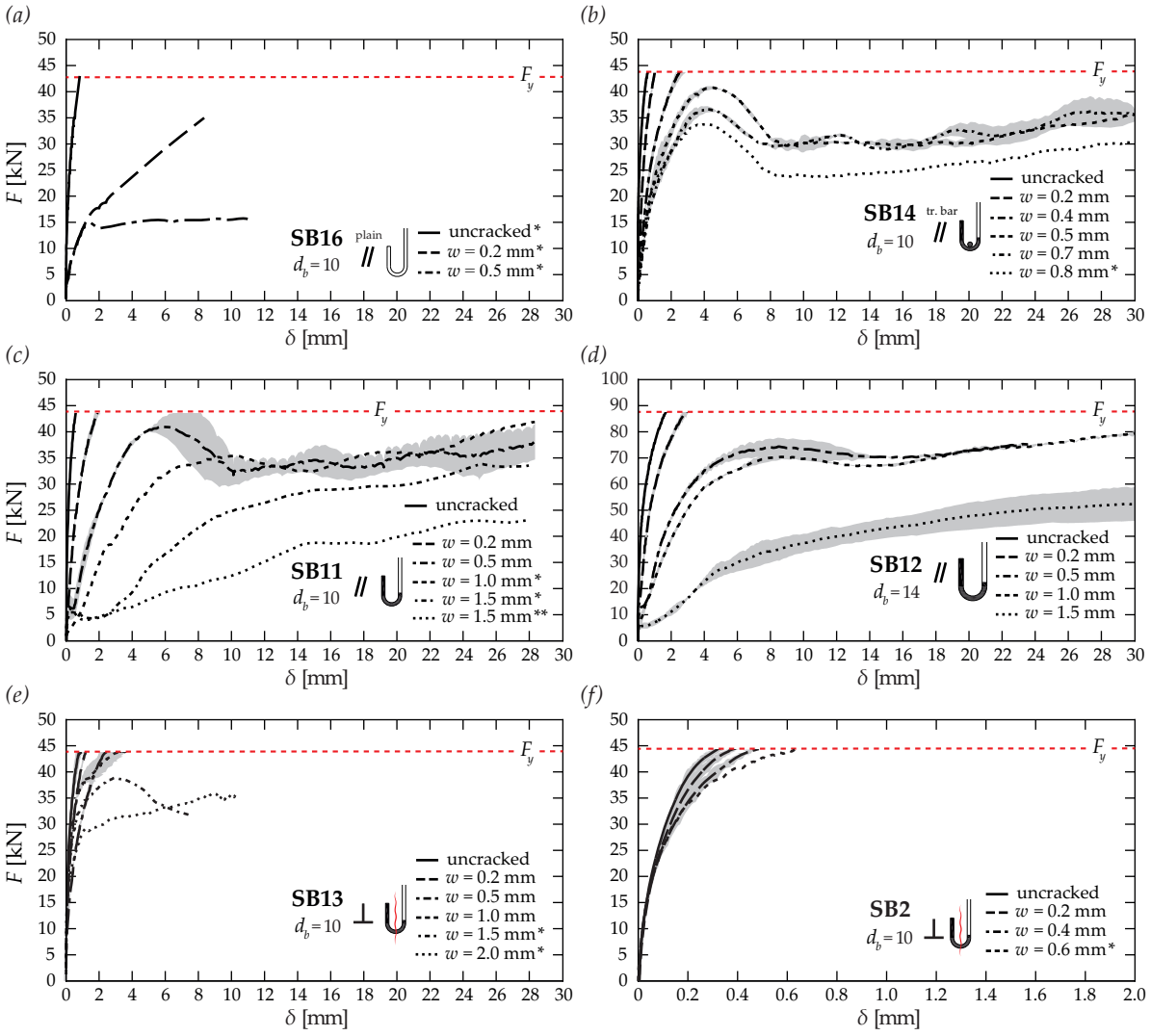

Figure 3.16 Force-slip relationships of hooks in transverse and flexural cracks:
(a) SB16; *(b) SB14*; *(c) SB11*; *(d) SB12*; *(e) SB13*; and *(f) SB2* (flex. crack)

The influence of transverse cracks was dramatic for hooks made of plain bars disposed parallel to the cracking plane (Figure 3.16*(a)*). A notable reduction of the strength and stiffness was observed, even for very low values of the crack opening (lower than or equal to 0.5 mm). Full activation of the bar –achieved for uncracked conditions– could no longer be developed in presence of cracks. A straightening of the detail with very limited local crushing resulting from the absence of surface profile on the bar was confirmed in the performed saw-cuts (Figure 3.17).

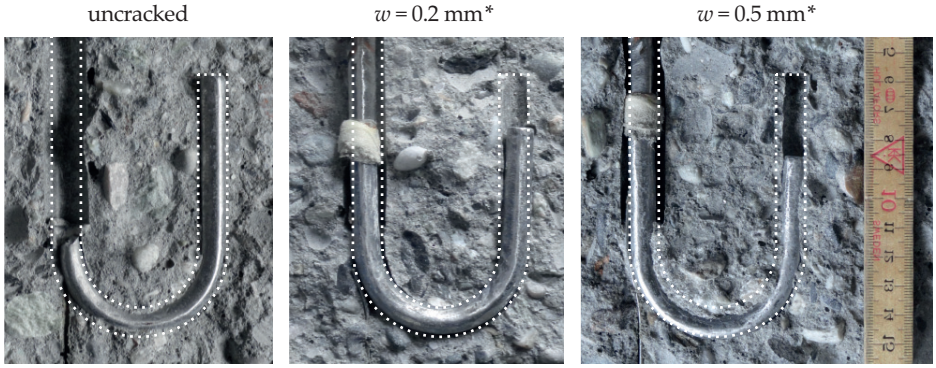

Figure 3.17 Saw-cuts performed after test in specimens *SB16* with plain hooks disposed parallel to cracks (dashed line for initial position and geometry of the detail)

Deformed hooks in a similar configuration behaved considerably better than plain details due to the contribution of the surface profile to the force transfer. Significant reductions in the strength and stiffness were yet confirmed (Figure 3.16*(c-d)*), resulting from the progressive straightening with local crushing and penetration of the detail through the cracking plane (Figure 3.18).

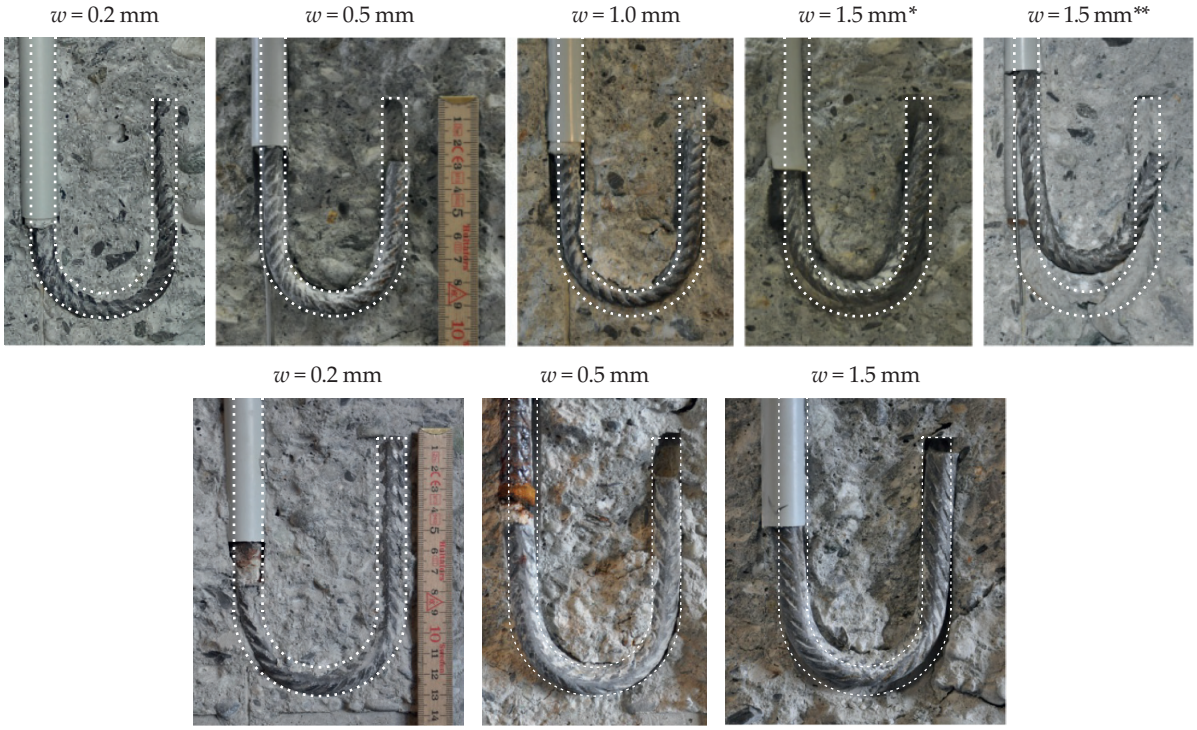

Figure 3.18 Saw-cuts performed after test in specimens *SB11* (up, d_b=10 mm) and *SB12* (down, d_b=14 mm) with deformed hooks disposed parallel to cracks (dashed line for initial position and geometry of the detail)

Full activation of the details was only possible for very low values of the transverse crack openings, but could not be achieved once the cracks were larger than 0.5 mm. It is interesting to highlight the similarities between the sudden decrease of the load in the behaviour of the hooks ($w = 0.5$ mm in Figure 3.16*(c)*) and that observed for straight bars (Figure 3.15*(a)*), both presenting $\Delta\delta \approx 5$ mm. The peak observed in the response of the hooks might thus be related to the maximum contribution of the bond phenomenon along the embedded part of the detail. A combination of residual friction, local crushing and mechanical anchorage then leads to a degradation of the behaviour characterized by an important slip but still a capacity to carry the applied load. As observed for straight bars, the peak is progressively softened with increasing crack opening until the development of the previously described residual post-peak phase. Also, the formation of a concrete wedge inside the bend could be observed in several cases (Figure 3.19) –similarly to previous observations from literature [Bac11a]– confirming the complex interaction of mechanisms that takes place for the force transfer (Figure 2.13). The penetration of the latter concrete element governs the behaviour of such detailing solution for large values of slip –independently of the crack opening– as similar slopes of the post-peak phase are observed for all the performed pull-out tests.

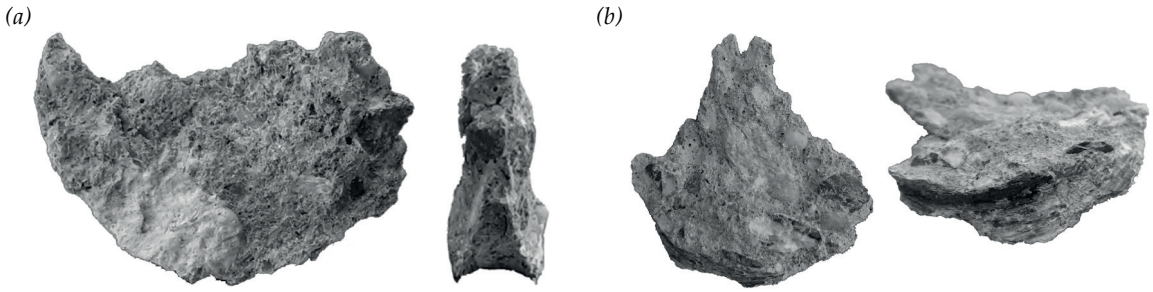

Figure 3.19 Concrete wedges observed at the inside of the bend for hook details after pull-out: *(a)* d_b =10 mm (*SB11*), for w = 1.0 mm; and *(b)* d_b =14 mm (*SB12*), for w = 0.5 mm

A deformed hook with a longitudinal bar passing through the bend is a common detail in structural concrete. The presence of this constructive bar strongly limits the reduction in the initial stiffness (Figure 3.16*(b)*) compared to details without the latter element in similar conditions (Figure 3.16*(c)*) by preventing the penetration into the crack (Figure 3.20). The bars could be fully activated for low crack openings, but this was again not possible above values larger than 0.5 mm.

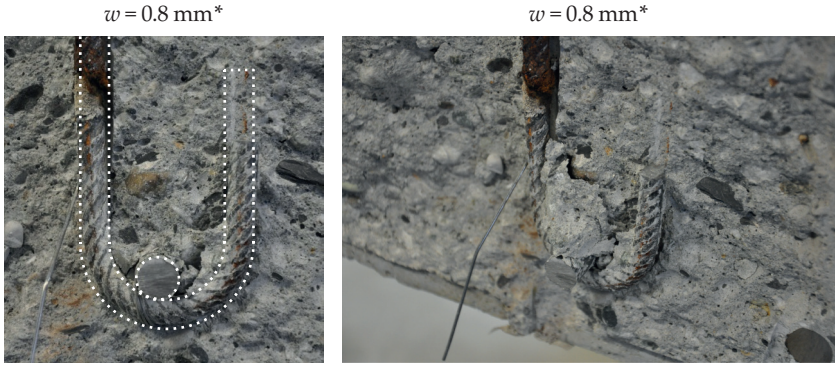

Figure 3.20 Saw-cut performed after test in specimen *SB14* with deformed hooks disposed parallel to cracks with long. bar (dashed line for initial position and geometry of the detail)

Finally, deformed hooks disposed perpendicularly to the cracking plane exhibited a rather different –and less affected– behaviour than similar details in parallel cracks (Figure 3.16*(e)*). This observation is coherent as most of the anchorage is located in uncracked concrete (Figure 3.21). For very large crack openings, the bars could still not be fully activated and quite important losses of stiffness were measured. Although these tests were interrupted prematurely, the development of peak and post-peak phases also reflects the potential presence of a concrete wedge.

Figure 3.21 Saw-cut performed after test in specimen *SB13* with deformed hooks disposed perpendicularly to cracks (dashed line for initial position and geometry of the detail)

In presence of moderate flexural cracks (up to 0.6 mm), deformed hooks in the same configuration exhibited a progressive deterioration of the behaviour for increased crack opening, yet the full development of the bars was systematically achieved (Figure 3.16*(f)*). The test results between both test series are consistent and highlighted that the performance of such details –potentially of others– is reduced more strongly in a transverse crack than in a flexural one (for a given width). The latter might be justified by the fact that, in a flexural crack, the penetration into the crack is progressively restrained due to the reduction of the opening on the height of the specimen.

3.2.3 U-shaped bars

The behaviour of U-shaped bars parallel to the crack plane (Figure 3.22) was significantly better than any other bend detail in the same configuration. Although the activation required the double of force compared to a hook, the improved geometry ensured a systematic full development of the bar with consequent slip only for very large values of crack openings ($w \geq 1.5$ mm).

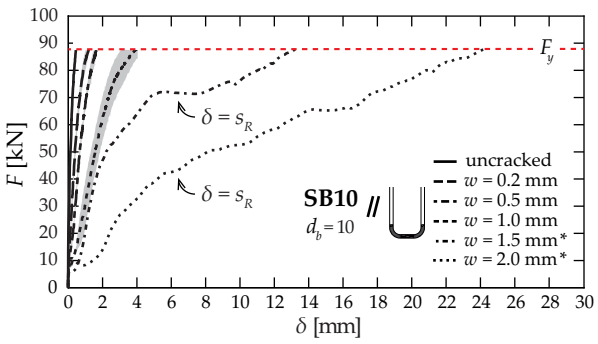

Figure 3.22 Force-slip relationships of U-shaped bars in transverse cracks (spec. *SB10*)

The performance of this type of anchorage is justified by the fact that it does not necessarily rely on bond mechanisms for the force transfer, thus being significantly less sensitive to cracking phenomena compared to other details such as hooks. In fact, a progressive crushing of the concrete within the bend is also clearly observed through the performed saw-cuts (Figure 3.23), with a progressive change in the geometry of the detail. The apparent whitening of the concrete in this specific zone reflects the important dissipation of energy related to the force transfer and the formation of a concrete wedge. It resulted in reductions of the stiffness, yet remained lower for the same level of transverse crack opening compared to any other types of bend bars tested. It is also interesting to note that the progressive degradation of the behaviour for large values of crack opening (w = 1.5 and 2.0 mm in Figure 3.22) is characterized in the force-slip relationships by a constant slope –similarly to the post-peak phase of hooks (Figure 3.16)– initiating at a value of slip corresponding to the distance between the surface profile (s_R = 6.4 mm for the tested bars). Therefore, the sudden increase of the slip measured would be associated to an important penetration of the detail resulting from the development of residual bond stresses at the beginning of the bend.

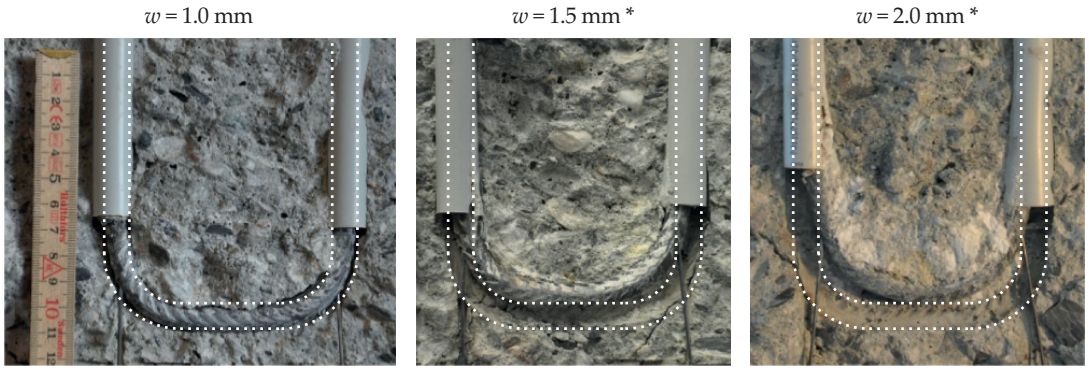

Figure 3.23 Saw-cuts performed after test in specimen *SB10* with deformed U-shaped bars disposed parallel to cracks (dashed line for initial position and geometry of the detail)

The concrete specimen *SB15* composed of U-shaped bars with two passing-through reinforcements was damaged during manipulation. Therefore, only pull-out tests in uncracked concrete could be performed on the intact part of the tie, showing consistent results with specimen *SB10*.

3.2.4 Headed bars

The performance of headed bars was significantly better than any other detail considered in the experimental program (Figure 3.24 and 3.26). Full activation was achieved in all the tested anchorages regardless of the type and opening of the crack, yet a progressive reduction of the stiffness could not be avoided. Flexural cracks were generally less severe than transverse cracks for the details, confirming similar observations on hooked bars. Also, as bond phenomenon is not involved in the force transfer, a better reliability regarding the behaviour in cracks is provided. Thus, test results confirmed the very limited variability of the performance of headed bars in cracks up to 1.0 mm compared to any other tested details. For very large crack widths, a sudden modification was observed in the behaviour –generally associated to a thud sound– and it even became difficult to develop yield strength in the bar (w=2.0 mm in Figure 3.24).

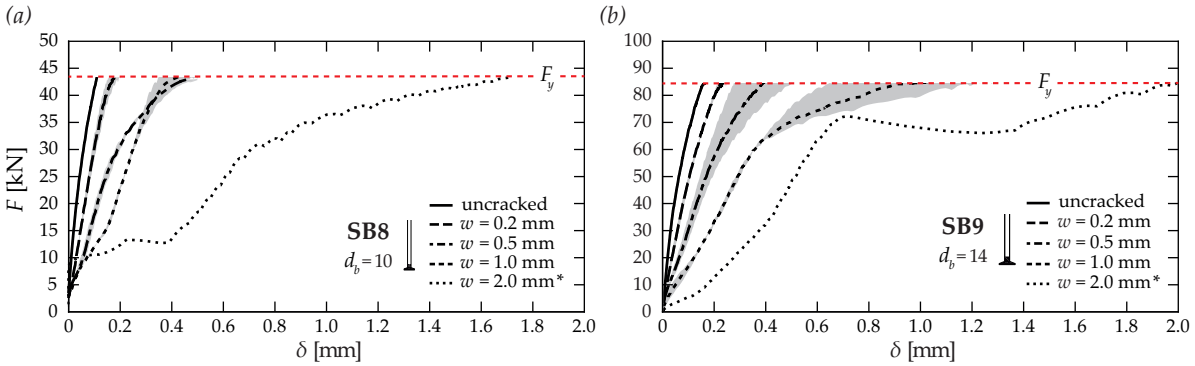

Figure 3.24 Force-slip relationships of headed bars in transverse cracks: *(a) SB8*; and *(b) SB9*

The large bearing area provided by the head usually tends to prevent any lack of anchorage as such observed in the tests. A possible explanation for the latter would be related to the sudden settlement in place due to local imperfections at the periphery of the head resulting from the production process (Figure 3.2*(c)*). In fact, detailed observations confirm the presence of ribs in this specific zone similar to the ones on the straight part of the bar. This is in agreement with the measurement of the surface properties of the bars which these details are made of ($h_{R,max}$ = 0.90 and 0.99 mm, respectively for d_b = 10 and 14 mm in specimens *SB8* and *SB9*). Thus, a crack opening of 2 mm –twice the maximum height of the ribs– is potentially sufficient to develop a local phenomenon such as that observed in the vicinity of the head. The formation of a crack at the periphery observed in the saw-cut (Figure 3.25*(a)*) might then simply be related to the shock associated to this settlement in place of the anchorage during loading.

Figure 3.25 Observations from the saw-cut performed after test in specimen *SB9* with headed bars for w = 2.0 mm: *(a)* crack development at the extremity of the head; *(b)* concrete wedge observed directly under the head; and *(c)* conical failure surface (inclination ≈ 15°)

The performed saw-cuts on the tested specimens for large values of crack openings confirmed the existence of a conical concrete wedge directly under the head (Figure 3.25*(b)*), still intact due to local confinement. It is interesting to note that similar observations were previously made for bend bar details (Figure 3.19). Once formed, the penetration of this wedge into the crack potentially controls the behaviour of this detail for large values slip. In this sense, a whitening of the concrete was observed at the interface between the concrete wedge and the surrounding concrete resulting from a relative displacement between both parts (Figure 3.25*(c)*).

Pull-out tests in flexural cracks highlighted a progressive whitening of the concrete directly under the head (Figure 3.27), not observed in the tests in transverse cracks. The latter phenomenon became more important in presence of larger cracks. It might result from a local friction associated to the contraflexure taking place during the pull-out of the detail. No saw-cuts were performed.

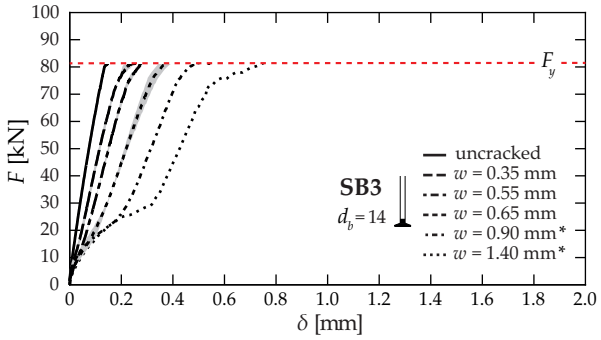

Figure 3.26 Force-slip relationships of headed bars in flexural cracks (spec. *SB3*)

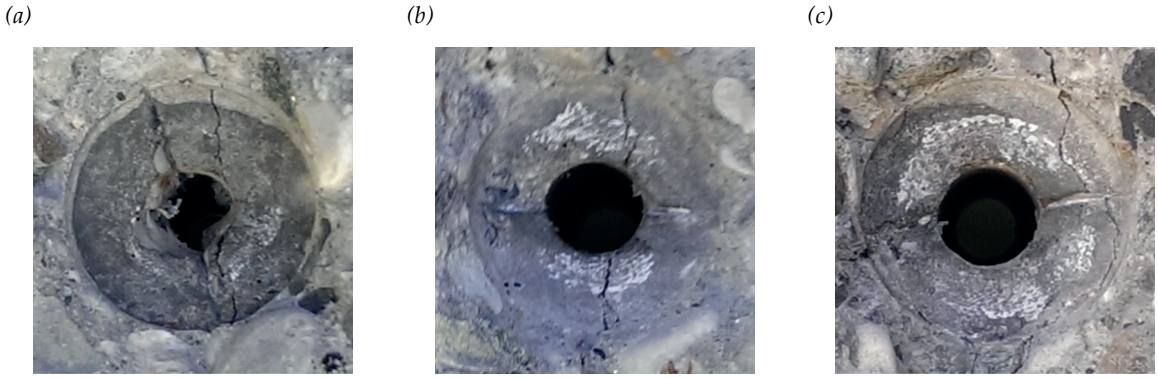

Figure 3.27 Progressive damage from friction observed on the surface directly under the head after test in specimen *SB3*: *(a)* uncracked; *(b)* w = 0.55 mm; and *(c)* w = 1.40 mm

3.2.5 Other system

Although the embedment length was very limited ($5 \cdot d_b$), the bond performance of UHPFRC ($\tau_b \approx 30$ Mpa) provided a full activation of the detail in uncracked concrete and in presence of small cracks (Figure 3.28). Under more severe conditions, the behaviour of this anchorage was not satisfactory and confirmed the interest of the present research. No saw-cuts were performed.

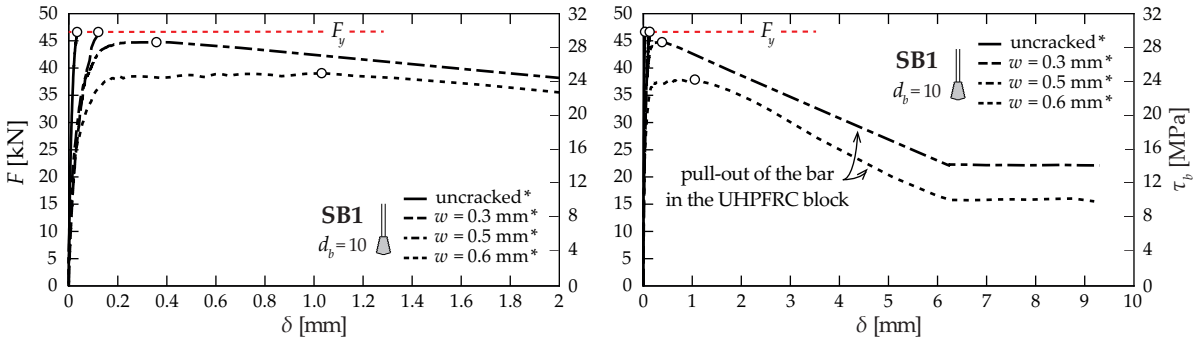

Figure 3.28 Force-slip relationships of headed-like anchorages made of UHPFRC blocks in flexural cracks (spec. *SB1*): zoom (slip 0 ÷ 2 mm) and full (slip 0 ÷ 10 mm) response

3.3 Behaviour of tested details under in-plane cracking

The experimental investigations have shown in a consistent manner that the presence of in-plane cracks –resulting from flexural or tensile solicitations– influences the performance of reinforcing details, with significant differences amongst them. Although the use of efficient anchorage systems –such as headed bars– ensures the development of the yield strength regardless of the crack width, the stiffness is systematically reduced. The latter might be an issue for specific applications where the amount of reinforcement details is strongly limited by external conditions but where the activation should nevertheless be optimal. This is for instance the case for the slabs with transverse reinforcement –as highlighted in the present research– where a lack of activation of these elements in the vicinity of the column can potentially lead to a premature punching failure.

In the following, the performance of bond and anchorage in cracks is investigated by means of a simplified analytical approach –originally presented in [Bra16]– whose results will be compared to those of the experimental program (see Section 3.2) as well as other tests available from literature (see Section 2.3). In this sense, the present section reproduces the main developments and results obtained in the mentioned publication as a basis of discussion for the numerical method (see Section 3.4). The analytical approach focuses on the evaluation of the reduction of strength and stiffness in the response of straight bars in transverse cracks (see Section 3.3.1). The formulations and conclusions are extended to other cases, as it will be briefly discussed for headed bar details in similar conditions (see Section 3.3.2).

Regarding bend bar details –hooked and U-shaped bars– the complex interaction of bond, friction and mechanical anchorage (provided by the bend) did not allow a direct application of the model. Interesting analogies were highlighted with straight bars and additional investigations are required to differentiate the contribution of the several force transfer mechanisms involved.

3.3.1 Bond

Strength in cracked concrete

Whenever splitting and concrete-cone breakout are not the governing failure modes, bond strength can be investigated as analogue to the contact stresses developed by aggregate interlock –as described by Walraven [Wal81]– with concrete crushing at the bar-to-concrete interface (Figure 3.29).

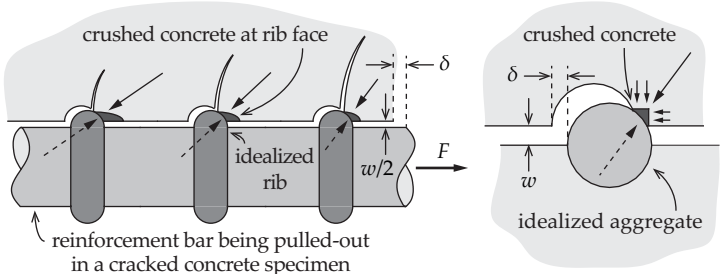

Figure 3.29 Analogy between the pull-out of a deformed bar in cracks and the aggregate interlock phenomenon (as described by Walraven [Wal81])

The contact stresses –typically characterized by a rigid-plastic material behaviour [Wal81]– act on the contact area between the ribs of the bar and the surrounding concrete. Considering uncracked conditions, and assuming a simplified geometry of the bar (circular section) and of the rib (constant height h_R –leading to the same projected area A_R as the actual reinforcement with a maximum rib height $h_{R,max}$)– the initial contact area (Figure 3.30) can be defined as Eq.(3.1).

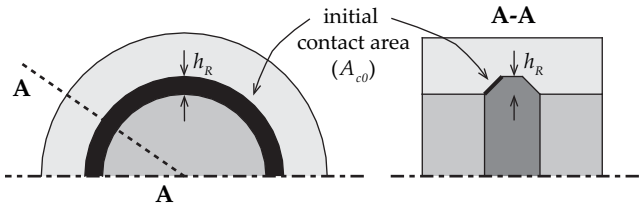

$$A_c = A_{c0} \cong \pi \cdot d_b \cdot h_R \qquad (3.1)$$

Figure 3.30 Initial contact area (black surface) between the rib (dark grey surface) of a bar (medium grey surface) and the surrounding concrete (light grey surface)

The formulation of the reduced contact area when an in-plane crack of low opening develops (Eq.(3.2)) is obtained by assuming $h_R << d_b$, and is only valid if $w < w_{li,1} = 2 \cdot h_R$ (Regime A in Figure 3.33*(a)*). The latter crack opening corresponds to the limit case for which the concrete surface becomes tangent to the rib at the extreme points parallel to cracking (Figure 3.31).

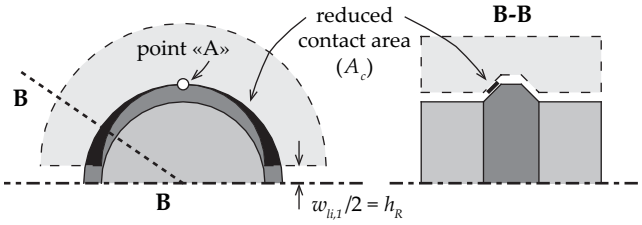

$$A_c \cong A_{c0} - d_b \cdot w = A_{c0} \cdot \left(1 - \frac{w}{\pi \cdot h_R}\right) \qquad (3.2)$$

Figure 3.31 Contact area (black surface) between the rib (dark grey surface) of a bar (medium grey surface) and the surrounding concrete (light grey surface) for low crack openings (limit case of Regime A with $0 \le w \le w_{li,1}$)

For larger crack openings (Regime B in Figure 3.33*(b)*), the reduction of the contact surface continues, yet at a lower rate. Eventually, for a given crack opening $w_{li,2}$ (Figure 3.32), no contact happens between the rib and the surrounding concrete ($A_c = 0$). By considering $h_R << d_b$ (i.e. $h_R^2 \rightarrow 0$) in Eq.(3.3), the limit crack opening for this phase results as Eq.(3.4).

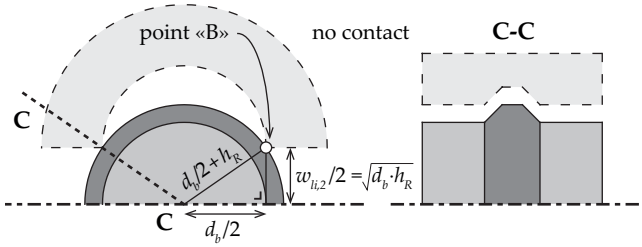

$$\left(\frac{d_b}{2} + h_R\right)^2 = \left(\frac{w_{li,2}}{2}\right)^2 + \left(\frac{d_b}{2}\right)^2 \qquad (3.3)$$

$$w_{li,2} \cong 2\sqrt{d_b \cdot h_R} \qquad (3.4)$$

Figure 3.32 Contact area (black surface) between the rib (dark grey surface) of a bar (medium grey surface) and the surrounding concrete (light grey surface) for large crack openings (limit case of Regime B with $w_{li,1} \le w \le w_{li,2}$)

The resulting expression is plotted in Figure 3.33*(a)* consisting of 2 regimes (linear and hyperbolic). It can be noted that it follows correctly the trend of some of the formulations proposed in the literature and fitted on the basis of test results (see Section 2.3.1), yet the presented approach is derived mechanically. In fact, for small values of w/h_R –and assuming $h_R \propto d_b$– the expression is linear similarly to the development from Giuriani and Plizzari [Giu85], Simons [Sim07] and Mahrenholtz [Mah12]. For larger values of w/h_R (proportional to w/d_b), the expression is hyperbolic similarly to what was formulated by Gambarova et al. [Gam89, Gam97] (that also was shown to have a similar trend to the exponential proposal of Idda [Idd99]).

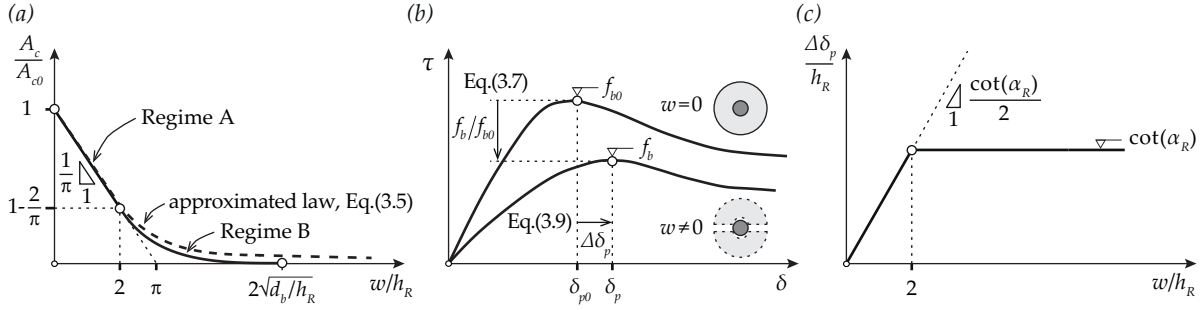

Figure 3.33 Bond phenomenon under transverse in-plane cracking: *(a)* contact area law: two regimes (solid line) and approximation (dashed line); *(b)* bond-slip relationships; and *(c)* shift of the peak for maximum bond strength

For practical calculation of the maximum bond strength, the following assumptions are made:

- The contact area law (solid line in Figure 3.33*(a)*, defined by two functions) is approximated by a single curve (dashed line) formulated as Eq.(3.5). This is performed by assuming that $h_R \ll d_b$ leading to an asymptote at the horizontal axis ($d_b/h_R \rightarrow \infty$), and by respecting at $w/h_R = 0$ both the value of the curve ($A_c = A_{c0}$) and its slope (equal to $-1/\pi$) according to Eq.(3.2).

$$\frac{A_c}{A_{c0}} = \frac{1}{1+\frac{1}{\pi}\cdot\frac{w}{h_R}} \qquad (3.5)$$

- The bond strength (Figure 3.33*(b)*) is assumed proportional to the contact area amongst the rib and the concrete ($f_b \propto A_c/A_{c0}$). For full contact ($A_c = A_{c0}$), the bond strength is assumed equal to that of a specimen without in-plane cracking (f_{b0}), yielding to Eq.(3.6).

$$\frac{f_b}{f_{b0}} = \frac{1}{1+\frac{1}{\pi}\cdot\frac{w}{h_R}} \qquad (3.6)$$

- The equivalent height of the rib (h_R) is estimated proportional to the bond index according to Eq.(2.2) as $h_R = f_R \cdot s_R$. If the distance amongst ribs (s_R) is also assumed proportional to the bar diameter (d_b), then $h_R \propto f_R \cdot d_b$ and the bond strength can be defined as Eq.(3.7).

$$\frac{f_b}{f_{b0}} = \frac{1}{1 + \frac{\kappa_f}{f_R} \cdot \frac{w}{d_b}} \qquad (3.7)$$

$$\text{with} \quad \kappa_f \approx 0.75 \cdot n_l \qquad (3.8)$$

Where κ_f is the coefficient of proportionality –assumed for the development of the simplified model– that depends upon the actual geometry of the ribs (rib profile, inclination and orientation of the rib as well as lug width and spacing among others). For practical purposes, it has been observed that relating κ_f to the number of lugs per rib (n_l) –through Eq.(3.8)– provides a fine estimate of the test results. This is shown in Figure 3.34, where the available tests from literature and the ones performed in the present experimental campaign are compared to the proposed formulation.

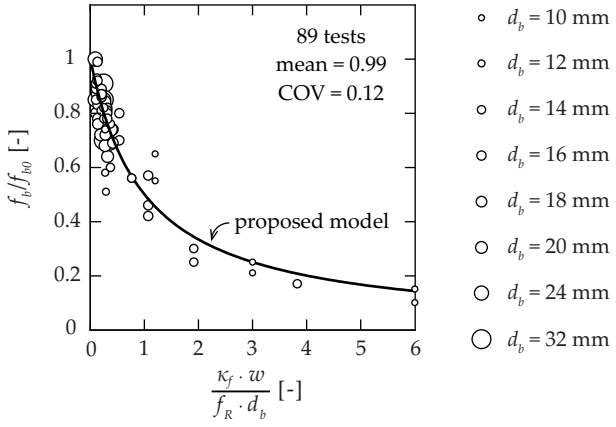

Figure 3.34 Comparisons between the predictions of the bond model (solid line) and the test results (empty dots) from conducted experimental program and literature [Gam81, Gam85, Gam90, Gam93, Sim07, Lin11, Mah12] on straight bars in cracked concrete

It has to be noted that the experiments of Idda [Idd99] –detailed in Section 2.3.1– are not included in the previous comparison as the effective values of the rib geometry of the bars were not reported (only nominal values according to codes in use at that time [DIN84] were provided). Yet, the individual comparisons presented for some of the mentioned test series in Figure 3.35 confirm that the proposed formulation still captures well the reduction of performance for the latter case.

In general, a fine agreement is observed, with the trend of strength reductions being suitably reproduced by the proposed model (solid line in Figure 3.35). A value of $\kappa_f = 3$ was considered for the tests conducted in the experimental program presented within this thesis (specimens *SB6* and *SB7*) as the de-coiled rods used were composed of four lugs ($n_l = 4$). A value of $\kappa_f = 1.5$ (half of the previous one) was generally adopted for the tests found in literature due to the rib arrangement with two lugs (ordinary deformed reinforcing bars, $n_l = 2$), except for specimen *ME12* of Simons [Sim07] (threaded bars consisting of only one continuous lug, $n_l = 1$ thus $\kappa_f = 0.75$). The comparison illustrates well the difference of bond performance between the types of bars considered (1-lug, 2-lugs or 4-lugs), being not all similarly affected by the presence of in-plane cracks.

It can be highlighted that the expression given by Model Code 2010 [FIB13] (dashed line in Figure 3.35) –valid up to a crack opening of 0.5 mm, equivalent to a decrease of the bond strength of 60% with respect to uncracked conditions– tends to provide rather conservative predictions of the test results (except for the 4-lugs indented rods). The proposed model allows for a good estimation of the phenomenon throughout the range of crack openings (not only service crack widths).

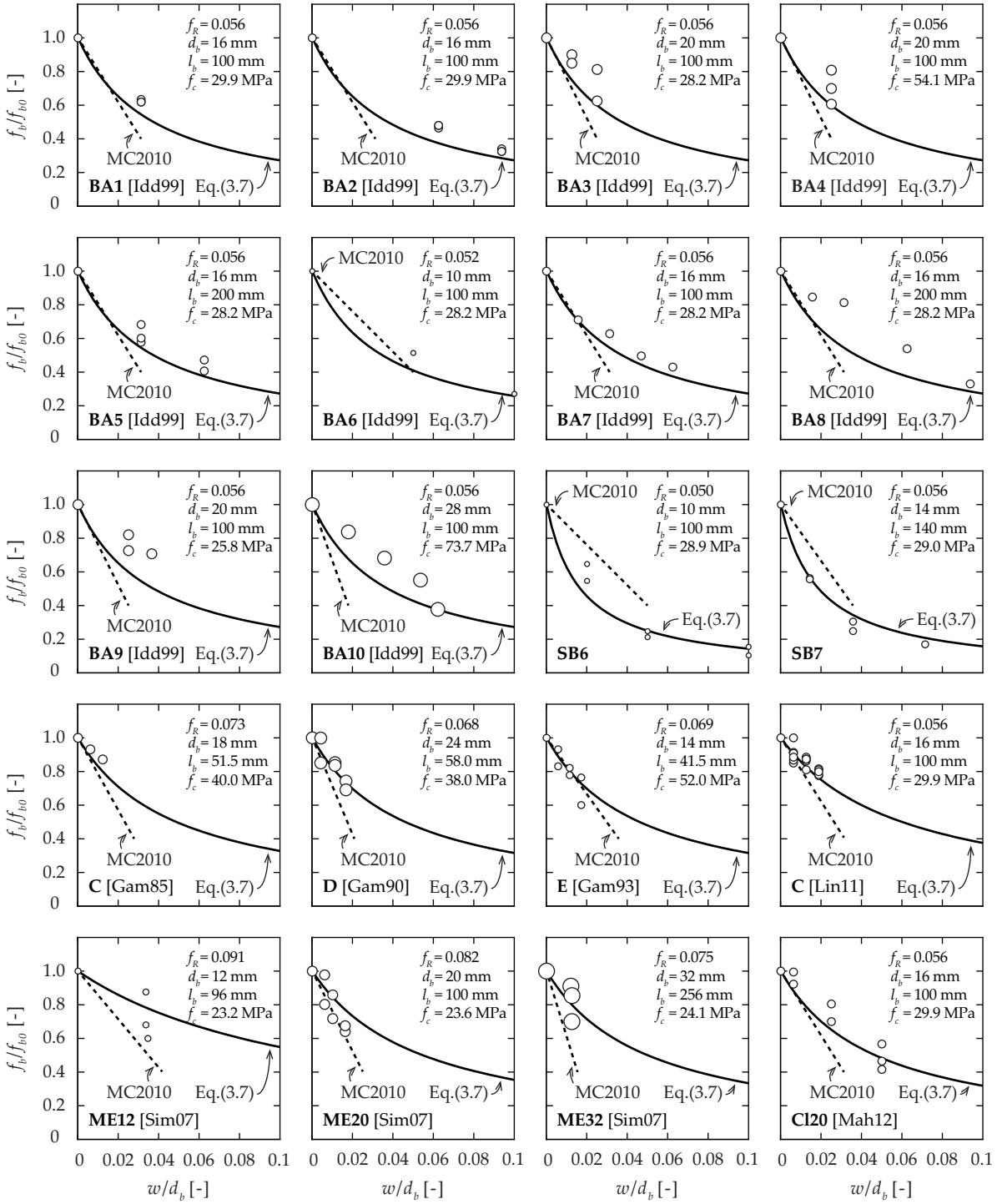

Figure 3.35 Comparisons between the predictions of the bond model (solid line) and MC2010 [FIB13] (dashed line) for the main test series on straight bars in cracked concrete from literature and from the present research for normalized crack openings

Even though a consistent agreement of the expression was confirmed for the wide range of parameters investigated (Figure 3.36), further work is suggested for a more comprehensive determination of the value of the coefficient κ_f (or a generalization of the bond index f_R) to better characterize the role of the surface profile of the reinforcement bars in the phenomenon. In this sense, additional investigations should be carried out regarding the effective rib geometry or specific related parameters (such as h_R/s_R) influencing certainly the bond performance in presence of cracks.

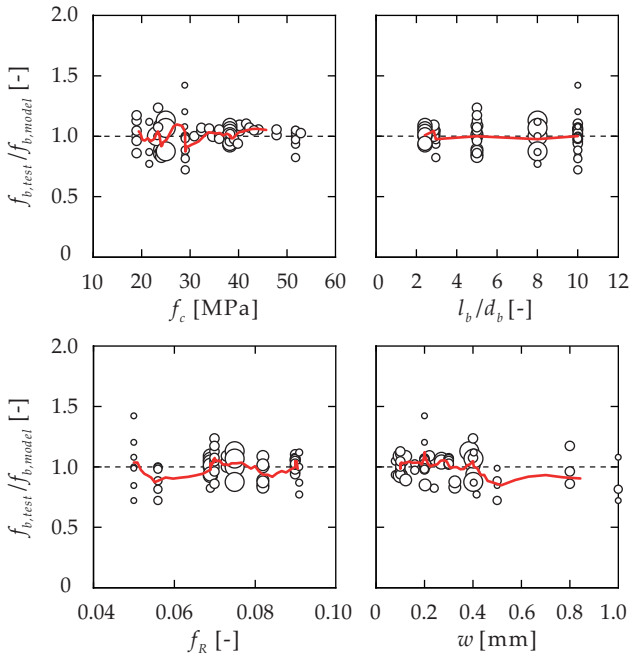

Figure 3.36 Predictions of the test results (empty dots) from conducted experimental program and literature on straight bars in cracked concrete with respect to the bond model (moving average in red) function of the concrete compressive strength (f_c, on 160 x 320 mm cylinders), the embedded length (l_b/d_b), the bond index (f_R) and the crack opening (w)

Stiffness in cracked concrete

Other than the bond strength, the complete bond-slip curve can additionally be calculated by accounting for the gap between the rib and the concrete (Figure 3.37). Although an integration of the individual contribution of each differential contact area is possible, the analytical or numerical treatment becomes rather cumbersome and lacks of practical interest. However, the point at which maximum bond strength is attained (δ_p in Figure 3.33*(b)*) can be easily determined. This can be performed by referring for Regime A of Figure 3.33*(a)* ($w < 2 \cdot h_R$) to the last point where the contact occurs (point "A" in Figure 3.31) as Eq.(3.9) depending on the rib geometry.

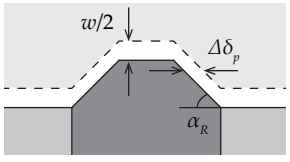

$$\Delta\delta_p = \frac{w}{2} \cdot \cot\alpha_R \qquad (3.9)$$

Figure 3.37 Gap resulting from crack and associated relative shift of the peak bond strength (for openings smaller than $2 \cdot h_R$, Regime A)

The maximum is thus reached at $w = 2 \cdot h_R$ (Figure 3.38). For larger crack openings, this shift ($\Delta\delta_p$) is however constant, as the outermost point of contact is always located at the outer perimeter of the rib (corresponding to point "B" in Figure 3.32) and corresponds to Eq.(3.10). The shift on the slip leading to the maximum bond strength is thus composed of two linear parts (Figure 3.33*(c)*).

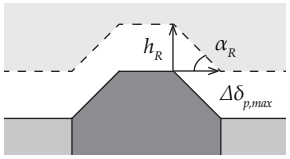

$$\Delta\delta_{p,max} = h_R \cdot \cot\alpha_R \qquad (3.10)$$

Figure 3.38 Maximum gap resulting from crack and associated relative shift of the peak bond strength (for openings equal or larger than $2 \cdot h_R$, Regime B)

It should be noted that for relatively large crack openings, this value might be quite sensitive to the local undulations (meso-roughness) of the crack [Fer15]. This is in fact observed for specimens *SB6* and *SB7* (Figure 3.15) where failure occurs in a premature manner for the largest crack openings (w = 1.0 mm). The formula is thus not considered applicable in those cases ($w > 2 \cdot h_R$). The proposed expressions are plotted in Figure 3.39 with respect to the test results of the performed pull-out campaign, showing again nice agreement. In this comparison, a value $\cot\alpha_R = 2$ has been used to account for the fact that the ribs were not perpendicular to the bar axis (and thus $\cot\alpha_R$ has to be lower than the measured one, reported in Table 3.1, considered perpendicularly to the lug axis).

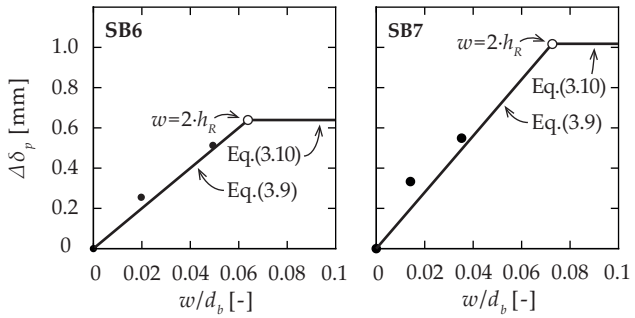

Figure 3.39 Shift of the slip at peak bond strength: comparisons between the predictions of the bond model (solid line) and the mean test results (full dots) for normalized crack openings

3.3.2 Mechanical anchorage

For headed bars, the contact surface in presence of a crack was almost the same as for uncracked concrete due to the large bearing are available. Thus no reductions on the total strength of the bar were observed, but led to a shift of the slip where it was attained.

The previous approach considered for bond can be adapted for the latter case. Due to the production process of the detail (forged headed bars), it should be noted that the angle varies through the head from 0 to α_H (angle on the straight part of the head according to bar axis). The inclination of the head is therefore rarely constant. Therefore, from the real situation (Figure 3.40*(a)*), some simplifications of the geometry were required (Figure 3.40*(b)*) in order to be able to formulate the shift

of the slip at full activation ($\Delta\delta_p$) for headed bars as Eq.(3.11). Similar considerations were also followed by Furche for headed anchors in cracks [Fur93].

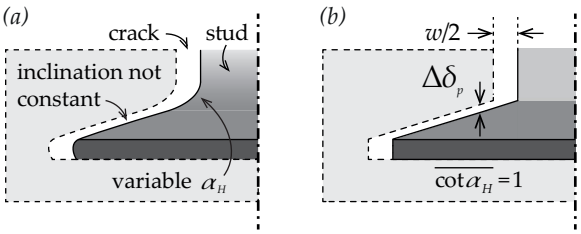

$$\Delta\delta_p = \frac{w}{2}\cdot\overline{\cot\alpha_H} \approx \frac{w}{2} \qquad (3.11)$$

Figure 3.40 Headed bars: *(a)* realistic representation of the local geometry of forged details (as the ones used in the present investigation); and *(b)* simplified geometry considered for the definition of the shift of the slip at full activation in presence of cracks

A comparison of Eq.(3.11) to the tests performed in the experimental programme (specimens *SB8* and *SB9*) is presented in Figure 3.41 by using a constant value of $\overline{\cot\alpha_H}=1$ showing fine and consistent agreement. The local variations in the geometry –observed through performed laser scans– might be a factor that explains the increase of the scatter with increasing crack widths.

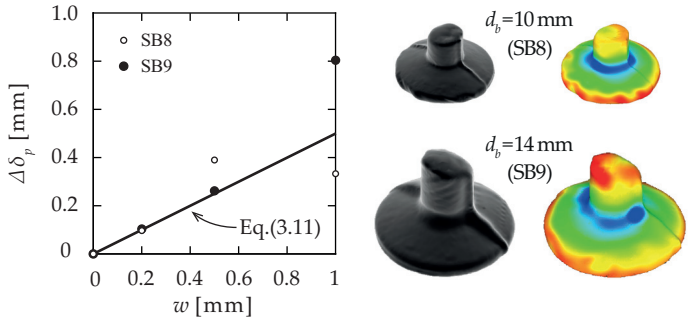

Figure 3.41 Headed bars in cracked concrete: shift of the head slip at maximum strength (solid line) compared with the mean test results (dots) of studs pulled-out in transverse cracks (specimens *SB8* and *SB9*), and laser scans of the tested details

Tests with crack openings larger than 2 mm were not considered as very different local behaviour was observed (see Figure 3.24*(b)* for instance). Indeed, the saw-cuts (Figure 3.25*(a)*) confirmed the presence of a local phenomenon –cracks starting from the edge of the head– that did not appear for smaller crack openings, justifying the exclusion of the mentioned tests in the comparison.

For hooks and U-shaped bars, there are regions of the anchorage that are not influenced by the opening of in-plane cracks (direct contact amongst the bar and the concrete after crack opening), whereas other regions follow a similar behaviour as for the development of straight bars (loss of contact after crack opening). Nevertheless, for the former regions, the presence of cracks also reduces the capacity of concrete to transfer stresses and its stiffness [Vec86], leading to a similar phenomenon as the one observed for the regions where development of the bar occurs by bond stresses. The experimental evidences highlighted in this section confirm this behaviour and the validity of the presented approach for other reinforcing details.

3.4 Numerical approach for circular bars

The development of a numerical-based approach for the evaluation of the bond performance in presence of constant width cracks aims at validating the proposed model and extending it to more general cases. Indeed, several situations might occur in practice, potentially quite different from the few idealised ones that have been evaluated by researchers in the last decades (see Section 2.3.1). For instance, the type of bars used is not systematically composed of 2 lugs, and the position of the crack according to the ribs not limited to the most critical possible configuration.

In a preliminary phase, it was necessary to thoroughly characterize the surface profile of the bar tested in the present research. The bars were disposed in a fix drilling machine –similar to that used in the preparation of the reinforcing details for the experimental campaign– to be centred on their axes. A green light was used to minimize the noise associated to the ambient light in the room, therefore improving the quality of the measurements. Specific acquisition procedure performed with DIC –in four steps on the bar periphery, every 90°– allowed to define the surface profile in terms of polar coordinates (Figure 3.42). It was observed that a sinusoidal approximation of the latter could reasonably be assumed. Due to the normalization, the integral of the surface profile on the periphery of the bar corresponds to the related projected area A_R (similar for all the bars).

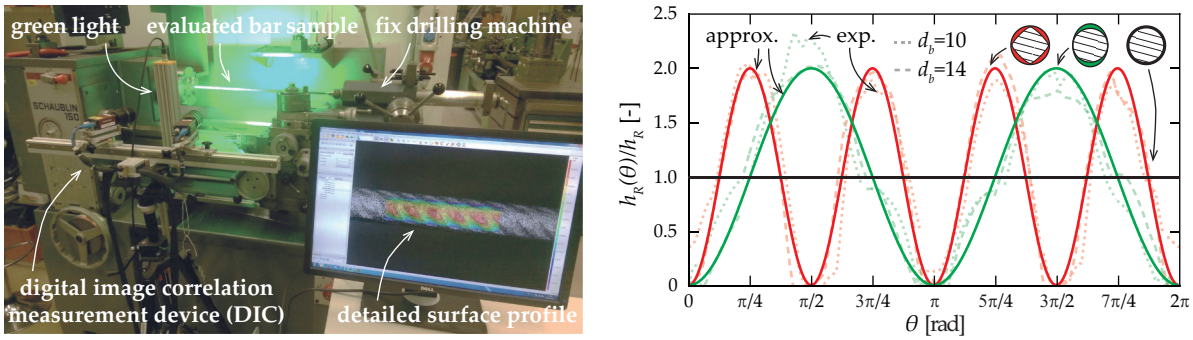

Figure 3.42 Digital image correlation (DIC) measurement device used to define the main geometrical properties of the surface profile for the tested reinforcement and normalized profile (dashed and dotted lines for experimental results, solid lines for approximations)

The developments are considerably simplified in the case of deformed bars with ribs than with indentations, as the section can reasonably be assumed circular (Figure 2.7*(b)*). For indented bars, the consideration of a more complex geometry for the effective section is necessary –triangular for 3-lugs bars or squared for 4-lugs bars– to evaluate correctly with the presented approach the decrease of bond strength in cracked concrete (case not directly presented hereafter).

In the following, a distinction is made amongst the steel products regarding the number of lugs composing the bars (1, 2, 3 or 4), as the latter was confirmed to have a certain influence on the bond performance in cracks (see Section 3.3.1). In a first approach, it is assumed that the crack opens symmetrically on both sides of the bar from its centre (as described in Figure 3.43). Another assumption of the model is related to the normalization of the rib profile ($h_{R,\max} \approx (4/3) \cdot f_R \cdot d_b$) and is derived from experimental observations (already considered in Section 2.3.1).

3.4.1 1-lug bars

This type of reinforcement is related to bars with a continuous and uniform thread providing an ideal profile of constant height around the section of the bar. As the latter steel product is not optimal from the production and cost points of view, it is generally only used in very specific conditions for which standard types of bars –composed of 2 or 4 lugs– cannot be properly used.

The perfect symmetry of the surface profile does not require the investigation of several configurations ($\Delta\theta$) with respect to the crack. Thus, the consideration of a unique study-case is representative for this type of reinforcement regarding bond performance in cracked concrete. The influence of cracking is relatively limited due to the uniform rib distribution around the bar (Figure 3.43). Even for large values of normalized crack openings, 1-lug bars still provide a significant contact area (A_c) compared to the initial one in uncracked concrete (A_{c0}) for the transfer of forces. It has to be noted that, locally, an entire loss of contact is observed –independently of the height and profile of the rib– which importance is only related to the crack opening ($2{\cdot}w/d_b$).

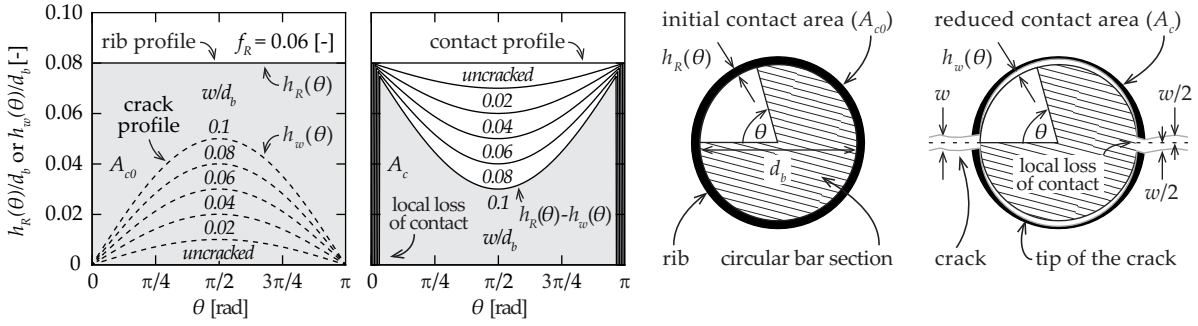

Figure 3.43 Normalized contact profile of 1-lug bars (f_R = 0.06) under various normalized crack and definition of the main parameters considered in the numerical approach

Under the assumptions considered in the numerical approach, 1-lug bars present no influence regarding its orientation to the crack (Figure 3.44). The use of more efficient surface profile –through the increase of the bond index (f_R)– considerably limits the reduction of the contact area compared to the initial situation, notably in the presence of large values of crack openings.

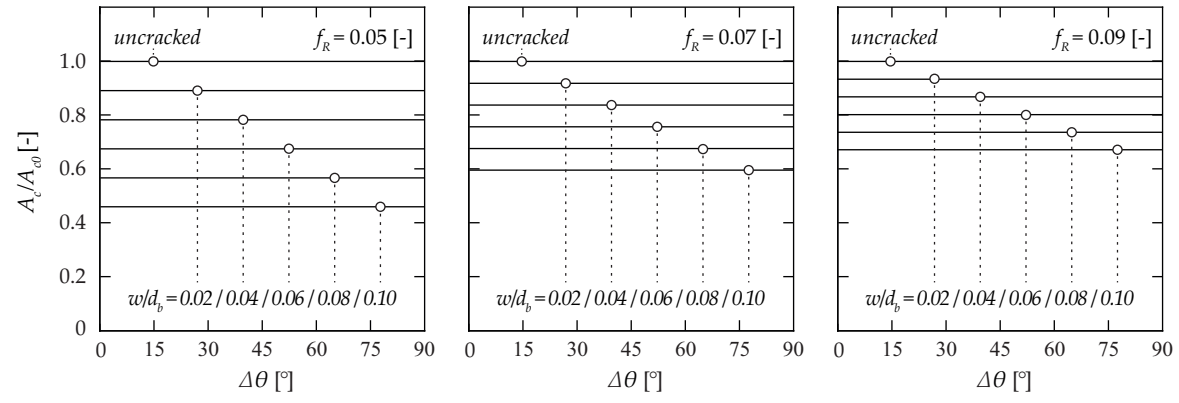

Figure 3.44 Influence of the orientation according to the crack of 1-lug bars on the reduction of the contact area for various values of bond index

3.4.2 2-lugs bars

This reinforcement represents most of the bars used in reinforced concrete construction, as confirmed by the consequent number of studies related to this steel product. The surface profile was optimized –compared to the 1-lug bars– and is variable on the section of the bar. The longitudinal ribs of such types of bars are not represented as they do not enter into account in the phenomenon.

The asymmetry of the surface profile leads to some disparities in the force transfer compared to the previous ideal case (1-lug bars). It is therefore necessary to consider the main positions of the bar according to the crack to estimate the potential variation range of the bond performance. The influence of cracking on the contact area is significant, with considerable differences between the main orientations of the bar according to the crack (Figure 3.45). The presence of the main ribs parallel to the crack ($\Delta\theta = 90°$) is much less favourable, as an important loss of contact takes place with increasing crack openings. The other disposition ($\Delta\theta = 0°$) is more efficient limiting the rib profile to the minimum where the influence of the crack is potentially the largest.

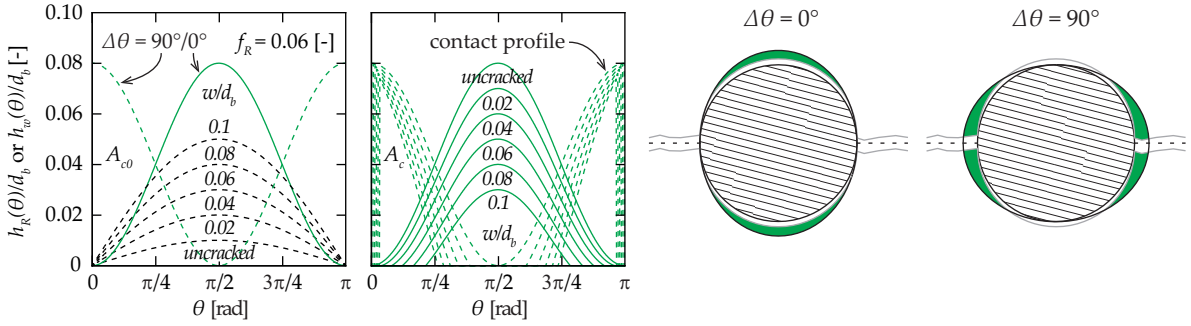

Figure 3.45 Normalized contact profile of 2-lugs bars ($f_R = 0.06$) under various normalized crack and for the investigated positions of the bar according to the crack ($\Delta\theta = 0°$ and 90°)

As expected, the performance of 2-lugs bars strongly depends on its disposition with respect to the crack (Figure 3.46), with differences of up to 30% in the reduction of the contact area (A_c/A_{c0}) for large crack widths and low values of f_R. This sensitivity is progressively attenuated with the use of bars with more pronounced surface profiles –large values of f_R– limiting the related disparities.

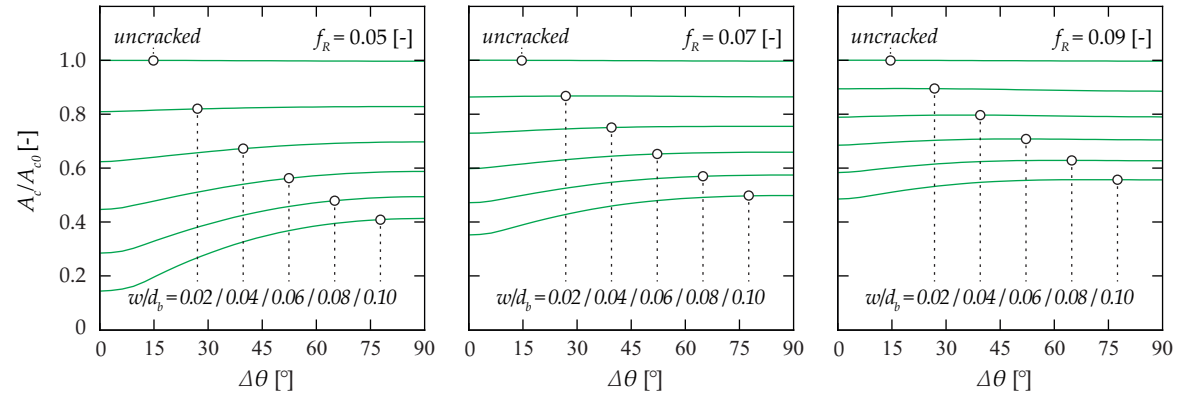

Figure 3.46 Influence of the orientation according to the crack of 2-lugs bars on the reduction of the contact area for various values of bond index

3.4.3 3-lugs bars

This type of reinforcement is generally related to deformed bars composed of indentations and is usually associated to specific applications (such as high strength steel). However, in the following, only its alternative composed of ribs can be considered by the numerical approach as previously stated. It therefore provides an upper bound of the performance of the latter in cracked concrete.

The asymmetry of the section also requires the consideration of the possible orientations of the bar according to the crack (Figure 3.47). From the previous study on 2-lugs bars, three main different positions arise in this sense: that with a rib parallel to the crack ($\Delta\theta$ = 30°), that directly opposed to the previous case ($\Delta\theta$ = 90°) and the intermediate one ($\Delta\theta$ = 0°) with a rib perpendicular to the cracking plane. Also, for this type of bar, the fact that the surface profile is composed of three ribs instead of two –for the same projected area (A_R)– tends to localize the contact area even more, being potentially more affected by the presence of a crack (notably for $\Delta\theta$ = 30°). For the other cases ($\Delta\theta$ = 0° and 90°), the more uniform distribution of profile is favourable compared to 2-lugs bars.

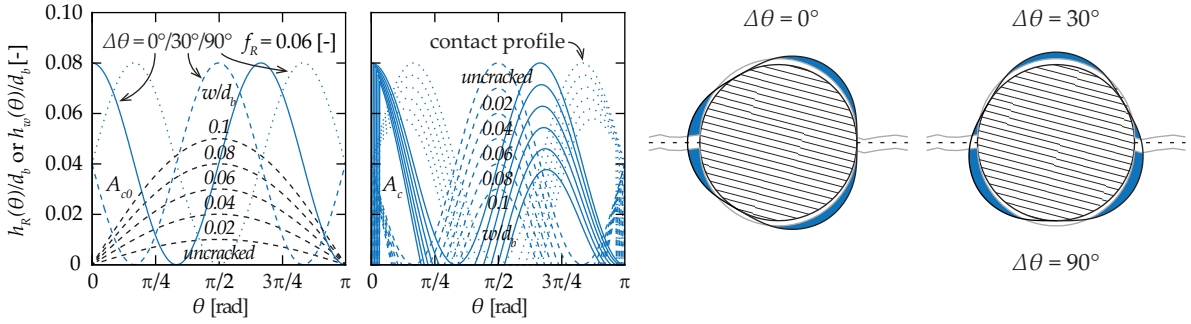

Figure 3.47 Normalized contact profile of 3-lugs bars (f_R = 0.06) under various normalized crack and for the investigated positions of the bar according to the crack ($\Delta\theta$ = 0°, 30° and 90°)

Although 3-lugs bars appear particularly sensitive to the disposition according to the crack (Figure 3.48), this is not exactly the case. Indeed, considering a mean response for the situation presented in Figure 3.47 ($\Delta\theta$ = 30° and 90°), the performance is equivalent to that of 2-lugs bars. Yet, the results are representative of the case if the crack opens non-symmetrically (see Section 3.4.5).

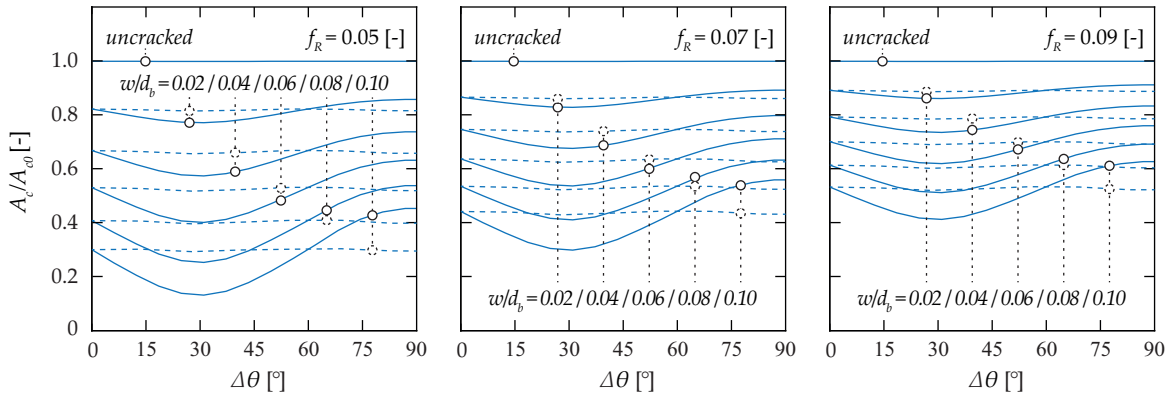

Figure 3.48 Influence of the orientation according to the crack of 3-lugs bars on the reduction of the contact area for various values of bond index (mean response in dashed lines)

3.4.4 4-lugs bars

This type of reinforcement is –similarly to 3-lugs bars– usually related to deformed bars with indentations, and is often associated to steel low-to-middle class of ductility. Also, it was observed to progressively take more and more importance on the construction market (Figure 2.7), although a very limited amount of investigations on bond have been dedicated to the latter steel product.

The asymmetry of the section defines two specific dispositions of the 4-lugs bars according to the crack to investigate: that for which a pair of ribs is being directly intercepted by the cracking plane ($\Delta\theta$ = 45°), and the other one ($\Delta\theta$ = 0°). The repartition of the projected area (A_R) into four ribs of equal importance leads to an even more pronounced localization of the contact than in the case of the 3-lugs bars (Figure 3.49). Therefore, a significant reduction in presence of cracks is to be expected –already for relatively small values of crack openings– as all the ribs are systematically considerably affected. Nonetheless, the distribution of the surface profile for 4-lugs bars is the most favourable of the types of bars investigated regarding the sensitivity to the position of the crack.

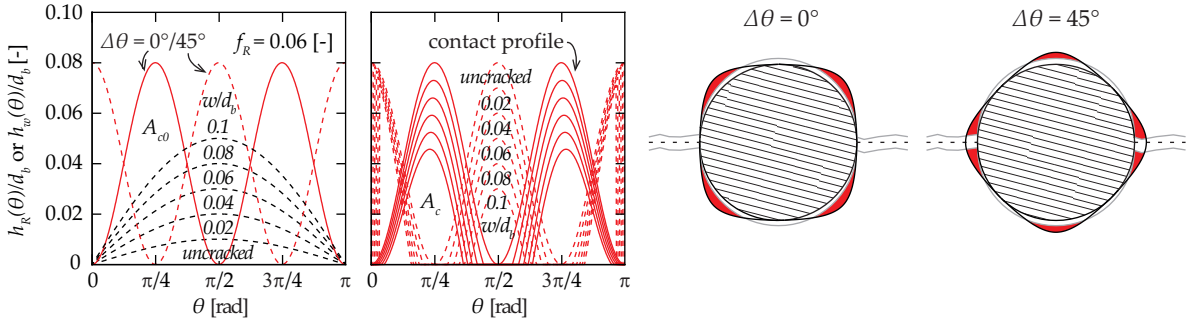

Figure 3.49 Normalized contact profile of 4-lugs bars (f_R = 0.06) under various normalized crack and for the investigated positions of the bar according to the crack ($\Delta\theta$ = 0° and 45°)

The variation of the contact area is very limited between the different configurations, and even though it is much more evident for other types of bars –notably 2-lugs bars– the existence of a less affected orientation is also confirmed ($\Delta\theta$ = 45°). Even for large values of f_R, the performance of 4-lugs bars in cracks is considerably affected by the presence of cracks, like no other types of bars.

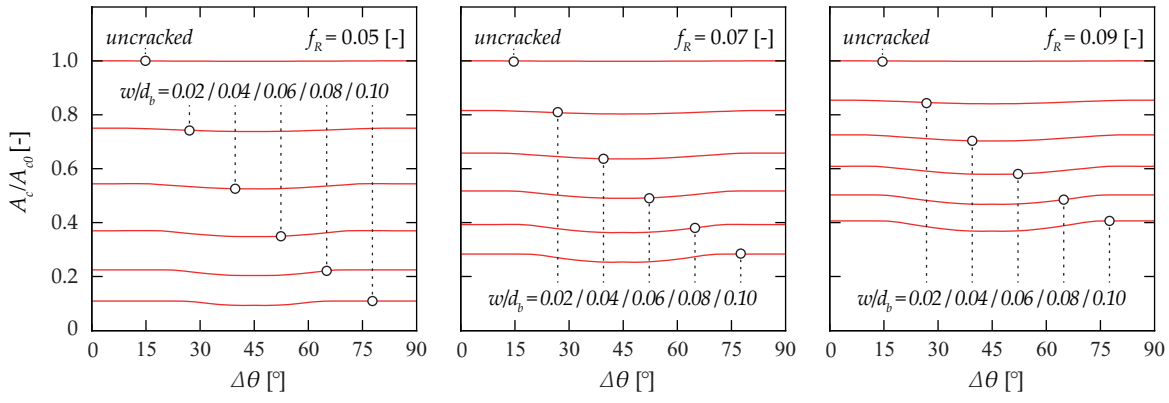

Figure 3.50 Influence of the orientation according to the crack of 4-lugs bars on the reduction of the contact area for various values of bond index

3.4.5 Comparisons and interpretations

The numerical approach highlighted the influence of the surface profile –characterized by the bond index f_R– and the orientation of the bar on the reduction of the contact area in presence of cracks of the main types of steel products available. The results are summarized in Figure 3.51 for bars composed of 1, 2 and 4 lugs considering that the crack opens symmetrically from the centre of the bar and therefore defining an upper bound of the bond performance in cracked concrete.

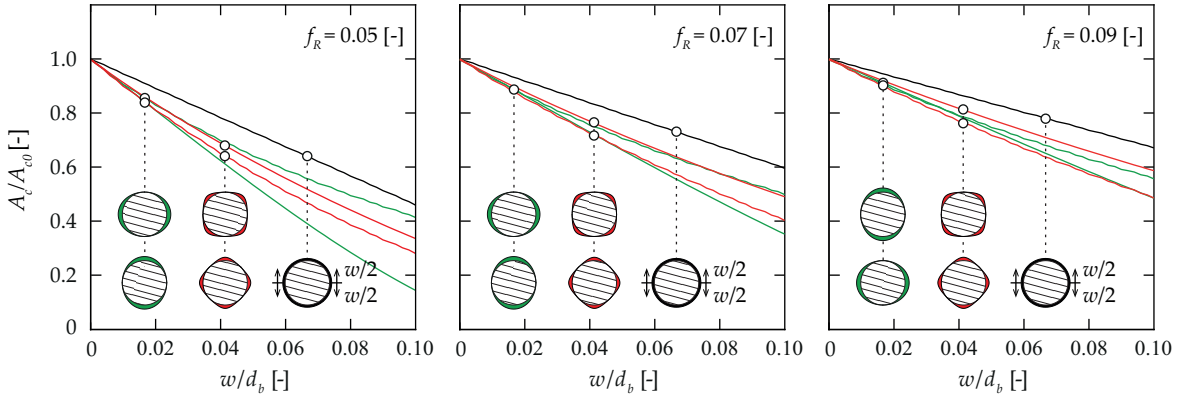

Figure 3.51 Influence of the crack opening on the reduction of the contact area for a reinforcement bar composed of 1, 2 or 4 lugs (upper bound, symmetric crack opening of $w/2$)

It can be observed that the reduction of the contact area tends to be more sensitive to the presence of cracks when the bars are provided with poor surface profile (low values of bond index). On the contrary, with larger values of bond index, the disparities amongst the different types of bars and various possible dispositions with respect to the cracking plane are generally attenuated. It is interesting to note that 1-lug bars systematically represent the type of bars that are the least affected by the presence of cracks, as 2 or 4-lugs bars are alternately the most affected (depending on the value of the bond index and the normalized crack opening).

Similar developments were done for an asymmetrical opening of the crack from the centre of the bar –solely on one side– therefore defining a lower bound of the bond performance (Figure 3.52).

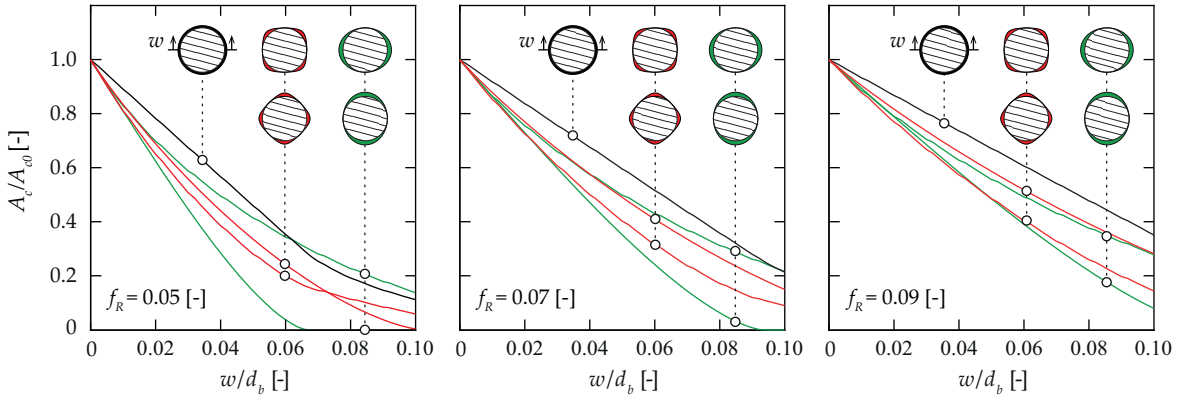

Figure 3.52 Influence of the crack opening on the reduction of the contact area for a reinforcement bar composed of 1, 2 or 4 lugs (lower bound, asymmetric crack opening of w)

Generally, the trends previously observed are confirmed and accentuated (more important non-linearity). In the case of 1-lug bars and for low values of bond index, it is interesting to highlight that the reduction of the contact area presents two distinct regimes as considered in the development of the analytical bond model (see Section 3.3.1, notably Figure 3.33*(a)*). The sudden modification observed in the curve –from linear to non-linear– is associated to a crack width corresponding to the maximum height of the rib, therefore markedly limiting the rate of reduction of the contact area for larger cracks.

Regarding 3-lugs bars, a simplification was made in order to correctly evaluate the reduction of the contact area with increasing cracking, notably to define the upper bound (Figure 3.53). For the latter case, the main issue is related to the fact that this type of bars presents specific orientations for which the influence of the crack is not equivalent on both sides (under a symmetric opening). Thus, it was necessary to consider a mean response for the approximation of the latter aspect (dashed line in Figure 3.48). As previously mentioned, due to the particular disposition of the ribs, the lower bound for this type of bar –associated to the opening of the crack only on one side– presents significant differences between the orientations (Figure 3.54). In comparison to the other bars investigated, the reduction of the contact area rather corresponds to an intermediate response.

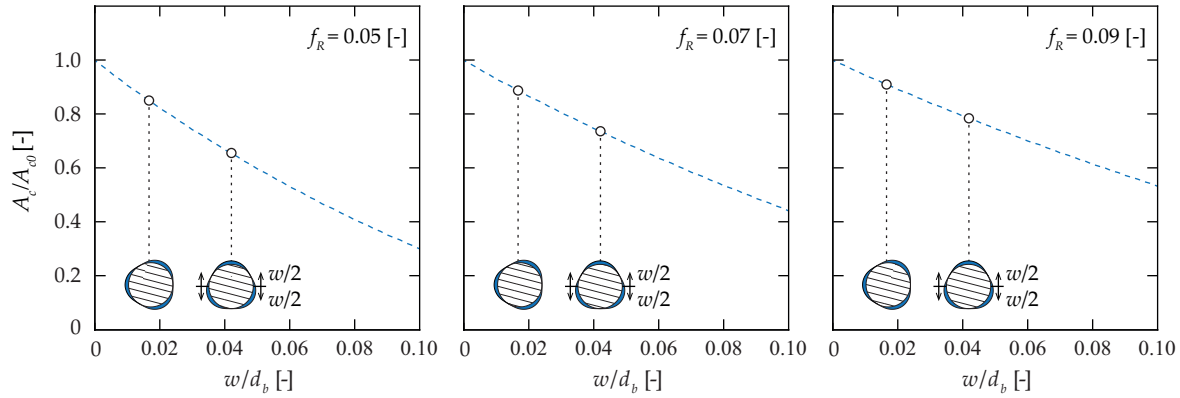

Figure 3.53 Influence of the crack opening on the reduction of the contact area for a reinforcement bar composed of 3 lugs (upper bound, symmetric crack opening of $w/2$, considering mean response as in Figure 3.49)

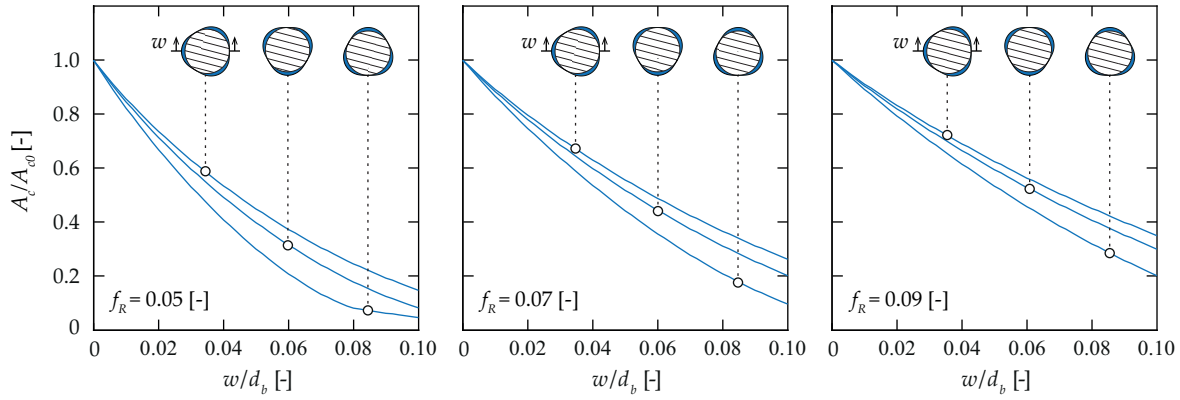

Figure 3.54 Influence of the crack opening on the reduction of the contact area for a reinforcement bar composed of 3 lugs (lower bound, asymmetric crack opening of w)

Considering that the decrease of the bond strength (f_b/f_{b0}) can be assumed as directly proportional to the decrease of the contact area (A_c/A_{c0}) between the ribs of the bar and the surrounded concrete –as stated in Section 3.3.1– it is possible to compare the predictions of the numerical approach (shaded area in Figure 3.55) with the test results from literature and the present research (dots in Figure 3.55). In order to also represent the proposed bond model (solid lines in Figure 3.55), it was necessary to assume a representative value of the bond index for the given data set –the average one ($\overline{f_R}$)– for each type of bars.

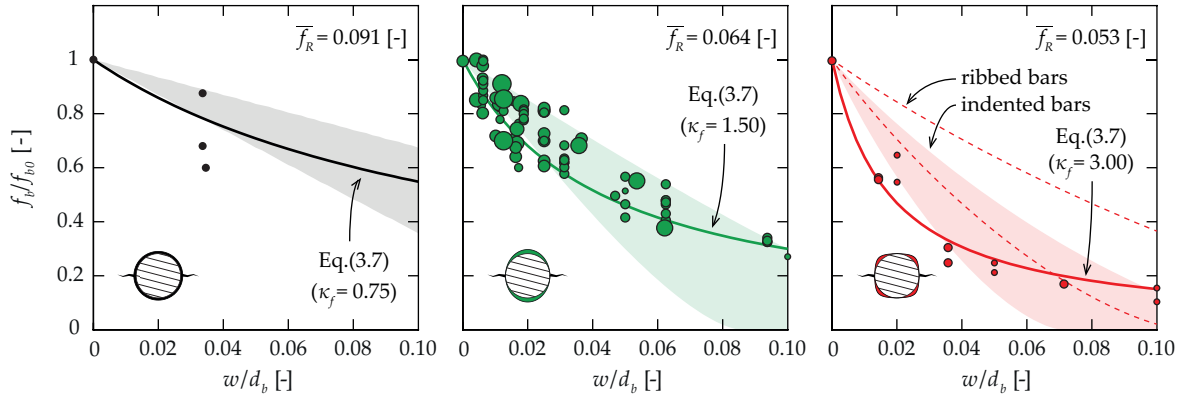

Figure 3.55 Comparison of the numerical approach –envelope of lower and upper bounds (shaded area)– and the bond model (solid lines) with the tests (dots) from the present research and from literature for the different types of bars (composed of 1, 2 or 4 lugs)

A consistent agreement with the experimental data is generally observed between both methods –numerical and analytical– for the various ranges of crack widths and test properties investigated. It is interesting to note that the proposed formulation –Eq.(3.7)– is almost systematically included in the envelope of the numerical approximation –shaded area defined by the lower and upper bound for a given bar orientation– confirming the pertinence of the approach. Also, the results indicate that the crack development might potentially be changing depending on the ratio w/d_b, being rather asymmetric for low values and progressively symmetric for larger values.

The limited amount of tests performed with 1-lug bars is not representative for the correct evaluation of the accuracy of the developed methods, contrarily to the series performed on 2-lugs bars. The bond model considers the coefficient κ_f to perform some local adjustments of the bond performance depending on the type of bars based on the available related tests from literature. For the 4-lugs bars, the assumption of the numerical approach regarding the geometry of the bar –perfectly circular– leads to unconservative predictions of the bond strength in presence of cracks (dashed lines in Figure 3.55). This can be improved by considering that the surface profile is made of indentations (through an adaptation of the section of the bar). Indeed, this directly affects the profile of the crack that becomes more severe in the latter case than as presented in Figure 3.49. Therefore, significant and fundamental differences arise between ribbed and indented bars in presence of cracks, and additional investigations are required in this specific topic to provide some specific and useful recommendations regarding their uses in practice.

3.5 Synthesis

The transfer of forces between a steel reinforcement and the surrounding concrete is performed at the interface, governed by the concrete strength and the bar surface properties (bond index, rib geometry and arrangement). The present chapter has aimed at understanding the latter phenomenon in presence of cracks, when the activation of the bar is not limited by the sudden splitting of the concrete specimen. The extensive pull-out test campaign (see Section 3.1) considerably improved the amount of available experimental data on the topic. The results confirmed the decrease of performance of bond and anchorages in presence of cracks (see Section 3.2) as observed in the literature review (see Section 2.3). The related developments (see Sections 3.3 and 3.4) tend to provide recommendations and formulations for the evaluation of the reduction of both strength and stiffness for a large range of cracks (not limited to service crack widths). From the performed work, the main conclusions and interesting points are the following:

- Bond behaviour is significantly influenced by in-plane cracks, even when the opening remains low and controlled;
- Experimental evidences from the pull-out campaign confirm that it may markedly differ from the response resulting from the classical and standardized pull-out tests, which are the basis of the bond-slip laws adopted in design;
- The performance depends on the anchorage detailing. Nevertheless, all the evaluated details consistently presented a reduction of the strength and/or stiffness in the force-slip curves;
- Straight deformed bars and plain hooks exhibited the greatest sensitivity to in-plane cracking;
- Deformed hooked bars generally underwent degradation of the behaviour –both on the stiffness and strength– due to cracking. The degree of the reduction is function of the disposition of the hook with respect to the crack and to the presence of a bar passing through the detail;
- Headed and deformed U-shaped bars exhibited the lowest sensitivity to the presence of cracks and were in most cases merely affected by a reduction of the stiffness (notably forged studs);
- Interesting similarities were highlighted between straight and hooked bars –made of similar deformed steel– regarding the contribution of bond to the behaviour;
- A concrete wedge was observed for hooks and heads anchorage in the saw-cuts after tests. The form and location of this element was related to the bearing area of the detail. Its penetration into the cracked concrete seems to govern the stiffness of the behaviour for large values of slip;
- The influence of in-plane cracking on bond behaviour can be reproduced analytically by considerations analogous to the aggregate interlock approaches. On that mechanical basis, simple formulas were derived allowing to calculate the reductions of the strength and of the stiffness for various details (straight and headed bars);

- The bond index f_R does not seem sufficient to properly characterize –in its current and well-known form– the influence of various rib geometry of the reinforcement bars on the bond strength in cracked conditions;
- In this sense, related parameters such as rib inclination/orientation/shape or lug width/spacing for different steel products should be further investigated in order to consistently describe bond properties in presence of cracks;
- The coefficient κ_f –correlated to the number of lugs– aims to adjust the bond index f_R in order to account for the differences in the distribution of the surface profile for the various types of bars investigated in the literature and in the present research. It might also benefit from additional studies related to a detailed definition of the rib geometry for different type of bars;
- The developed numerical approach also provides accurate predictions regarding the influence on the bond strength of straight bars for several orientations of the crack and steel products (1, 2, 3 or 4 lugs). It also confirms the pertinence of the formulation proposed in the bond model;
- The performed investigations tend to show that the performance of deformed bars with ribs or indentations is fundamentally different in presence of cracks (up to 20% smaller in the latter case). Additional related studies for this specific type of bars are strongly recommended.

A recent experimental work [Des15] highlighted well the actual issues and required improvements related to the study of bond performance in cracks. According to the authors, the orientation of the crack with respect to the rib pattern is of minor importance to the bond strength, contrarily to the presented numerical approach. This might highlight the fact that the local state of the concrete –at the position of the maximum rib height– could be of importance, and that the decrease of bond strength might therefore not only be related to the reduction of the contact area. This could also be related to the low values of normalized crack openings considered in these recent tests, for which a large scatter was observed in the literature. The simplicity of the test setup, associated to its innovative procedure to perform the cracks, need to be mentioned and are of major interest in the frame of a standardization of pull-out tests under such conditions. However, the lack of details in the description of the surface profile –only maximum rib height and angle according to bar axis are provided– strongly limits the related interpretations of the results and further developments by other researchers. In this sense, it is evident that an accurate definition of the main geometrical characteristics of the profile of the bar should be systematically performed with modern measurement systems (for instance DIC that showed satisfactory results in the present research).

Finally, it should be noted that additional efforts are needed in order to investigate the structural implications of bond decay in cracked concrete, and to formulate "tailored" bond stress-slip curves for other types of anchorage solutions such as hooked bars (commonly used in practice). The analogies observed with straight bars are in this sense of major interest. Also, tests on plain details could provide useful information regarding the differentiation of the force transfer mechanisms for such details (mechanical anchorage provided by the hook and bond along the bar).

Chapter 4 State of the Art on the Punching of Flat Slabs

Punching around the columns is characterized by brittle failures and occurs together with flexural deformations at the shear-critical zone of the slab (Figure 4.1*(b)*). This phenomenon can take place at various locations of a structure depending on the loading and boundary conditions (Figure 4.1*(a)*). It is generally recognized as governing for the design of slender reinforced concrete flat slabs since the 1960's and was therefore studied in consequence through extensive experimental and analytical works. However, recent tragic events [Mut05] tend to show that the phenomenon is still of actuality and deserves some additional investigations.

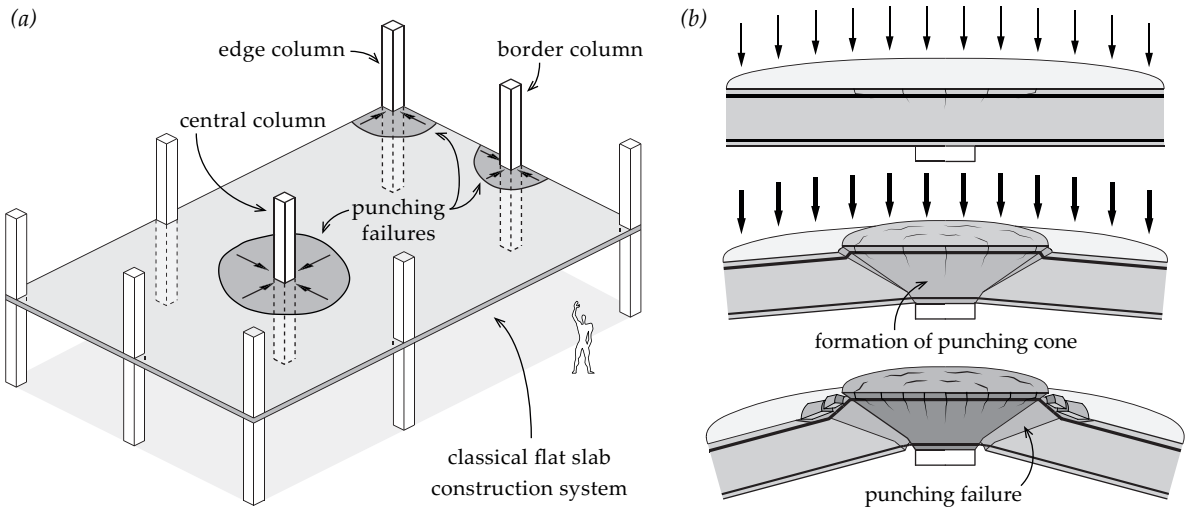

Figure 4.1 Punching phenomenon in reinforced concrete structures: *(a)* failure types in a typical flat slab; and *(b)* consecutive phases for axisymmetric solicitation (central column)

Various researchers were involved in the development of the first models to describe the punching behaviour of flat slabs [Kin60, Kin63, She89, Bro90a, Hal96, Mut08a, Ein16b, Bro16]. Amongst them, the physical-based approach proposed by Muttoni [Mut08a] –known as the Critical Shear Crack Theory (CSCT)– has a central role in the present research.

The main idea of the CSCT consists in reducing the effective compressive strength of a theoretical inclined strut supported at the column periphery ($f_{c,eff} < f_c$) depending on the cracking state (Figure 4.2*(b)*). The opening of the critical shear crack (w) is assumed to be proportional to the product of the slab rotation with the effective depth ($\psi \cdot d$). The critical crack is assumed to have an

inclination (α) of 45° with respect to the slab plane (Figure 4.2*(c)*). The nominal shear strength (v) at a control perimeter (b_0) located at distance $d/2$ from the column edge is thus a function of $\psi \cdot d$. In the compression strut, forces have to be transmitted through cracks. As the aggregate size (d_g) influences the coarseness of the crack, Muttoni [Mut08a] has proposed a failure criterion (Eq.(4.1)) that includes the latter parameter so as to consider its role in the carrying capacity of the strut. A simplified analytical model known as the *quadrilinear* –similar to the one proposed by Kinnunen and Nylander [Kin60]– may be used to define the relation between the rotation (ψ) of an isolated axisymmetric slab element and the applied load (V). The latter depends on parameters associated to the specimen geometry, the type of loading and the material properties. For more particular conditions, this relationship should rather be determined through specific (non-linear) numerical analysis. The failure is simply predicted to take place at the intersection of the load-rotation curve and the failure criterion (Figure 4.2*(a)*), defining both the related strength V_R and rotation ψ_R of the slab. Punching might also occur at a load level corresponding to the flexural capacity of the slab V_{flex} (estimated for instance through yield-line methods [Joh62]) and is generally associated to significant deformations (intersection of the failure criteria and the plateau of the load-rotation curve).

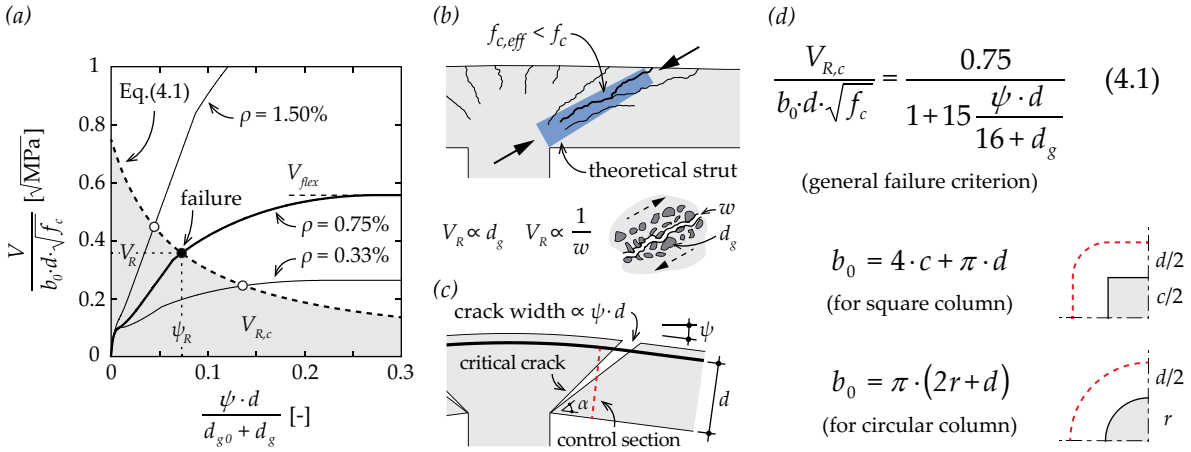

Figure 4.2 Bases of the CSCT: *(a)* load-rotation curves for similar slabs with different flexural reinforcement ratios ρ (solid lines) and the failure criterion (dashed line); *(b)* reduction of the concrete strength in the compression strut around the column; *(c)* nominal crack width and control perimeter for the shear strength; and *(d)* main related formulations [Mut08a]

In the cases where the carrying capacity of the slab is limited by punching ($V_R < V$), the structure needs to be adapted in order to fulfil the design requirements regarding the strength and deformation capacity. Classical solutions (Figure 4.3*(a-b)*) included the modification of the slab thickness (h) and/or the size of the support area (c) in order to increase the control section ($b_0 \cdot d$).

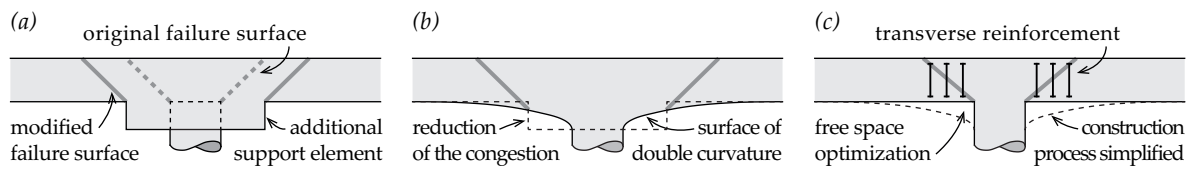

Figure 4.3 Possible modifications to improve the punching strength of a slab: *(a)* use of column capitals (in concrete or steel); *(b)* fabrication of concrete drop panels; and *(c)* disposition of transverse reinforcement in the vicinity of the column (shear-critical zone)

However, since the aforementioned methods are often not available due to practical, economical or architectural considerations, the disposition of transverse reinforcement in the shear-critical zone (Figure 4.3*(c)*) has been progressively established as a commonly used solution to allow the construction of slender flat slabs since the end of the 20th century. In the latter case, another material –usually steel– is involved to increase locally the transverse stiffness of the slab, leading to an improvement of the punching phenomenon. The use of such reinforcing systems influences the crack development within the slab, and the punching is therefore associated to several potential failure modes (Figure 1.2). Also, depending on the type, amount and disposition of the transverse reinforcement, its related contribution to the slab behaviour was observed to differ markedly.

It became therefore necessary to consider the beneficial effect of this additional reinforcement in the punching phenomenon in order to provide reliable guidelines and recommendations for designers. The existing theories were consequently adapted [Gom99a, Bro05, Fer09, Lip12a] and specific models were also developed on different bases [Men99, Bir04, Fer10c, Hoa16]. Most of these, however, are generally limited in their application to reinforcement with good anchorage properties. The common difficulty associated to all these punching models is mostly related to the evaluation of the contribution of both transverse steel and concrete. Although experimental evidences confirm the existence of disparities in terms of performance amongst the main systems, the previously mentioned approaches do not systematically consider the latter aspect.

In this sense, the extension of the CSCT [Fer09] is of major interest, notably its activation model specific to the transverse reinforcement. The latter allows to evaluate –through simple physical considerations on bond, anchorage and crack kinematics– the increase of force in these elements during the punching phenomenon with accurate predictions for various cases [Fer09, Fer10a]. However, several observations thoroughly gathered from literature tend to show that some of the related assumptions might not be conservative. The present work will therefore focus on the validation and the adaptation of the existing activation model regarding anchorage and bond issues.

In the following, an overview of the transverse reinforcement used for slabs against punching is presented (see Section 4.1) in order to understand the evolution of the most common types of systems found in practice. The current trends regarding the development of such specific reinforcement –based on recent patented products– are also presented so as to highlight the future direction of interest in this field. The different cracks observed during the punching phenomenon are then detailed (see Section 4.2), with a description of the associated failure modes and the related formulations according to CSCT (see Section 4.3). Selected experimental investigations from literature presenting failures within the shear-reinforced zone –associated to a failure crack intercepting one or several rows of transverse elements– are thoroughly depicted (see Section 4.4). The latter section aims at gathering specific information both on the failure crack kinematics and on the activation of the transverse reinforcement during punching. Finally, the main code provisions for punching are presented and briefly discussed (see Section 4.5) to highlight the disparities between the considered approaches.

4.1 Types of shear reinforcement

The main parameters defining the quality of the transverse reinforcement used in punching were highlighted by Beutel [Beu02] based on several investigations. Above all, the system should be able to develop the entire material properties –strength and ductility– through adequate bond and anchorage mechanisms (ideally within both the tension and compression zones of the slab). The material and production costs as well as the interaction with the flexural reinforcement were also cited as relevant factors influencing the choice of a punching reinforcement system in practice.

4.1.1 Bent-up bars

Similarly to what was developed for beams in the beginning of the 20th century (an extensive overview can be found in [Ric27]), the use of plain bent-up bars in slabs in the late 1930's by Graf [Gra38] –amongst the first reported punching tests with transverse elements– increased the related ultimate strength and deformation capacity. Other investigations performed on slender specimens with similar reinforcing systems (Figure 4.4) either with end anchorages [Ros59, Yit66, Mir10, Tas11] or without [Els56, And63, Fra64, Sun77, Pet79, Hal96, Mar97, Bro00, Mir10, Tas11, Ein16a] supported these observations for various arrangements (radial or orthogonal), amount and type of bars (generally deformed). It was concluded that the efficiency might be easily –and significantly– reduced by bond and anchorage limitations associated to a local crushing at the inside of the bend.

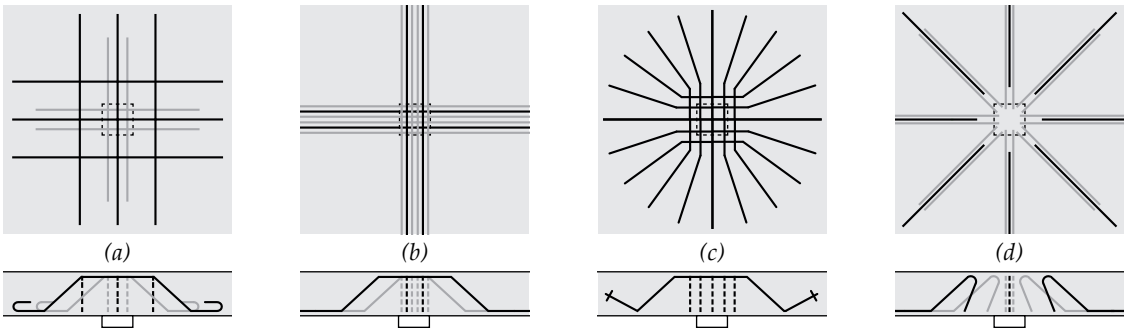

Figure 4.4 Detailing of bent-up bars as punching reinforcement: *(a)* with end anchorages (adapted from [Gra38]); *(b)* without end anchorages (adapted from [Els66]); and *(c-d)* alternative solutions (adapted from [And63, Ein16a])

Detailing was therefore recognized as a critical point for the performance of punching shear reinforcement. The bending process of the bars –limiting the use of large diameters– required the disposition of several elements in the vicinity of the column in order to provide noticeable improvement on the structural response. Although this congestion locally increases the flexural strength and guarantees the integrity of the slab, the related constructive difficulties led to a progressive loss of interest for bent-up bars as transverse reinforcement to the benefit of more efficient products.

4.1.2 Bend bar details

Taking advantage of the available bending technology, an alternative reinforcement system composed of small diameter bars was developed simultaneously with the limitations observed on bent-up bars in the middle of the 20th century. Considerable types of these elements –commonly

denominated as *stirrups*– were tested, such as continuous [Kee54, Els56, And63, Nyl72, Sei77, Pil82, Bro90b, Mar97, Pil97, Lad98, Lip12a, Ein16a], closed [Fra64, Wan69, Car70, Pra79, Pil82, Tol88, Gha92, Hug95, Oli00, Tim03, Fei07, Vol10], one-legged or individual links [Mar77, Reg80a, Nil83, Mül84, Lov90, Cha92, Yam92, Cha93, Hal99, Lee99, Oli00, Pis00, Tra01, Reg01, Beu03, Tim03, Heg07, Ein16a] yet with significant differences in the improvement of the slab strength and ductility. The evolution of the system (Figure 4.5) tends to highlight the intention to simplify its arrangement in the slab (radial, uniform, orthogonal), notably by limiting potential interactions with the flexural reinforcement. In this sense, in most of the actual applications, such a reinforcing system is generally delivered on site in preassembled units connected through welded constructive reinforcement (Figure 4.5*(d)*). Although the latter aspect was observed to improve the behaviour in presence of cracks [Reh79], the main issues associated to such reinforcing details were still related to the anchorage performance. The various solutions evaluated in the aforementioned investigations confirmed the importance of both top and bottom anchorages in the efficiency of the punching system. The use of plain bars –or of deformed bars in the case of thin slabs– considerably limits the development of bond that can generally not contribute sufficiently to the force transfer to complete the entire activation of the material strength. Also, the local crushing of the concrete on the inside the bend potentially limits the anchorage capacity –if not enclosing properly the flexural reinforcement– with the risk of delamination of the shear-reinforced core [Vol10].

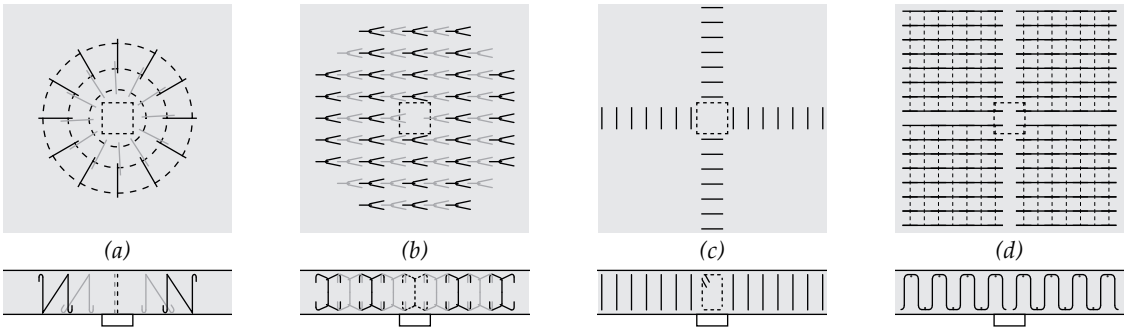

Figure 4.5 Detailing of stirrups as punching reinforcement: *(a)* continuous (similar to [Kee54]); *(b)* individual elements (similar to [Mar77]); *(c)* closed (similar to [Oli00]); and *(d)* actual solution (similar to [Lip12a])

4.1.3 Headed bars

Since the late 1970's, several reinforcing elements were developed on different bases than bent-up bars or stirrups. The aim was to propose a system that would provide efficient anchorage for thin slabs, a convenient disposition on the site and of low cost. Inspired by the shearhead proposed by Corley and Hawkins [Cor68, Haw74] –not further developed in the present research– that was found to be non-justifiable economically, Ghali and Walther [Lan76] (also evaluated later in [Reg85, Gom99b]) investigated the use of segments of standard steel I-profiles (Figure 4.6*(a)*) as an interesting alternative to the aforementioned solutions. The promising results initiated the optimization of this –way to massive– system [And77, Sei77, Sti80, And81], and led in the early 1980's to the first version of plain double headed bar as transverse reinforcement for punching

(Figure 4.6*(b)*) [Voe81]. Intensive investigations were conducted in order to determine the ideal proportion and geometry of the anchorage –notably related to the head– that would develop yielding stresses in the bar without an important concrete crushing. The actual version of this type of reinforcing system is commonly denominated as *studs* and is provided with a circular head (with a dimension of around three times the diameter of the bar). Several variations of the latter product were developed by researchers and manufacturers, such as single headed studs [Moh85, Reg85, Koc90, Mar97, Reg01, Ste07], double headed studs [Mar97, Gom00, Reg01, Beu03, Bro07, Bir08, Ett09, Riz11, Lip12a, Hei12, Fer14] or other alternatives [Mül84, Gom00, Reg01, Tra01, Mus04, Vaz09, Tra11, Ran15]. Although the anchorage is achieved at the head level –the related performance is almost independent of the bond properties along the straight part of the bar (compared to bent-up bars and stirrups)– these elements are nowadays generally made of deformed bars (see Section 2.1.3). Similarly to bend bar details, they are usually constructively connected together with small diameter bars or slender steel plates in order to simplify the installation. The latter aspect might be favourable for the related behaviour when disposed on the tensile part of the slab where significant crack openings may occur. The arrangement of the studs around the column depends on the local usage –orthogonal in the USA as Figure 4.6*(c)*, and radial in Europe as Figure 4.6*(d)*– but nowadays is generally concentrated in the main axes of the slab.

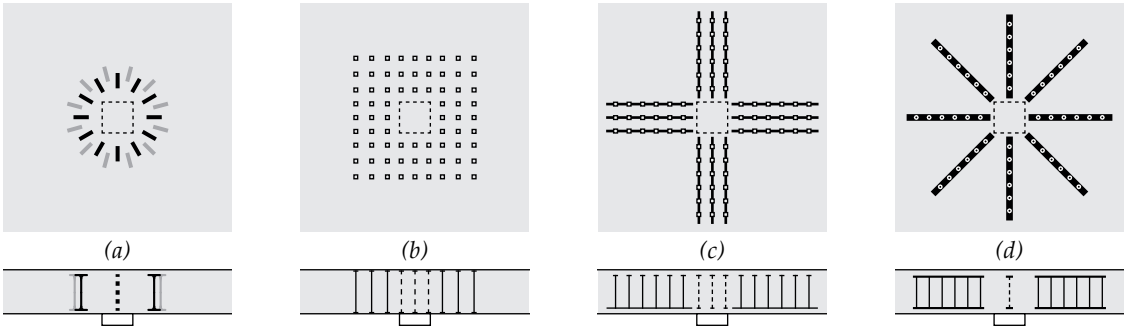

Figure 4.6 Detailing of studs as punching reinforcement: *(a)* segments of standard steel I-profile (similar to [Lan76]); *(b)* double headed bars (similar to [Voe81]); *(c)* single headed bars with rail (similar to [Mok85]); and *(d)* alternative solution (similar to [Tra01])

Limitations of the anchorage capacity for studs were only observed experimentally in very specific situations during the phenomenon of punching. In the latter cases, it might result in a concrete cone breakout or a delamination of the shear-reinforced core leading to a premature failure load (see Section 4.2). Thus, adequate cover –limited to the minimum possible– and disposition of the first element –with respect to the column face– are required to avoid the development of such unexpected failure modes. It is reasonable to claim that the main aspects potentially affecting the contribution of studs in punching are related more to its arrangement around the column –spacing and extension– than to its anchorage quality. The use of studs is therefore generally preferred by researchers for the tests with transverse reinforcement as it allows to focus mainly on the physical aspects of the punching phenomenon by limiting the interaction with potential anchorage issues associated to less performant reinforcing systems.

4.1.4 Innovative systems

Recent advances on the understanding of the failure mechanisms associated to punching (see Section 4.3) lead nowadays to better capture their differences in efficiency and to develop new products on a more consistent basis. The current trends in the development of transverse reinforcement against punching are orientated into two main directions: the use of high performance materials (Figure 4.7*(a)*) and the adaptation of the geometry of classical details such as stirrups (Figure 4.7*(b)*) or studs (Figure 4.7*(c)*). As a consequence, the transverse stiffness of the slab is locally increased, providing a better control of the development of out-of-plane cracks. In the first case, the knowledge on Ultra-High Performance Fibre-Reinforced Concrete (UHPFRC) or carbon fibres resulted in several patents [WIP10, WIP14], yet the cost of such materials –compared to steel– often limits their applications in practical situations. In the second case, the performance is improved through a modification of the geometry of classical systems [WIP11, WIP12, WIP15]. An inclination around 30 ÷ 60° is provided to the transverse elements –through one or several bents– so as to intersect the failure crack in the most perpendicular manner possible. Local crushing –associated to a force concentration at the bend– or delamination –associated to a consequent activation of the anchorage with limited constructive dispositions– might then govern the efficiency of these systems.

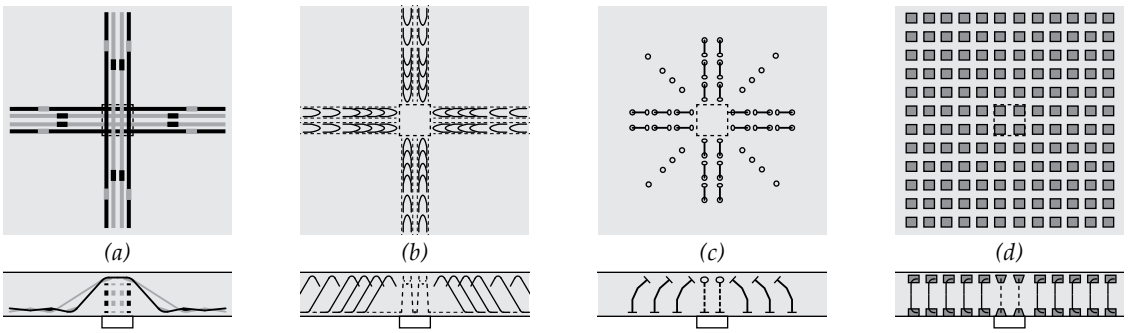

Figure 4.7 Current trends in the detailing of transverse reinforcement against punching: *(a)* coated carbon-fibres strips (adapted from [WIP14]); *(b)* inclined stirrups with improved anchorage in tensile part (adapted from [WIP12]); *(c)* bent studs (adapted from [WIP15]); and *(d)* individual links (90° bends) embedded in UHPFRC blocks [WIP10]

Also, the potential complexity related to the installation of such innovative types of transverse reinforcement on the construction site, limits their use only to specific cases where high performance systems are required. In this sense, out of convenience and by force habits, the more familiar products have a greater chance of being chosen, in practice, for most of the standard projects. Therefore, the association of high performance materials to common types of transverse reinforcement appears to be a promising direction for the development of efficient and practical systems. An interesting solution of this type was evaluated within the frame of this research [WIP10] providing a considerable improvement of the structural response of the reinforced slab (Figure 4.7*(d)*). The anchorage of the individual links composing the system was enhanced by enclosing the end hooks in blocks of UHPFRC. The density of the matrix of such material allowed the disposition of the system directly in contact with the formwork and to take advantage of its related bond performance in order to provide an optimal activation to the transverse reinforcement.

4.1.5 Influence of bond and anchorage conditions on punching performance

The intensive development and evaluation of transverse reinforcement during the second half of the 20th century provided experimental evidences supporting the fact that the detailing and the type of punching system have a significant influence on the structural response of the reinforced slabs [Els56, Lan76, Mar77, Reg80a, Dil81, Voe81, Mok85, Tol88, Gha92, Yam92, Mar97, Oli00, Pis00, Reg00, Beu03, Pil03, Roj07, Bir08, Vaz09, Fer09, Iná12, Lip12a, Sil12, Ein16a]. The arrangement of transverse elements in the vicinity of slab–column connection increases both the strength and the deformation capacity –compared to a reference slab– yet with variable efficiency. Punching tests performed at EPFL in the last decade on similar slabs ($\rho \approx 1.5\%$, $c = 260$ mm, $d \approx 210$ mm) highlighted clearly these disparities between different types of reinforcing systems (Figure 4.8).

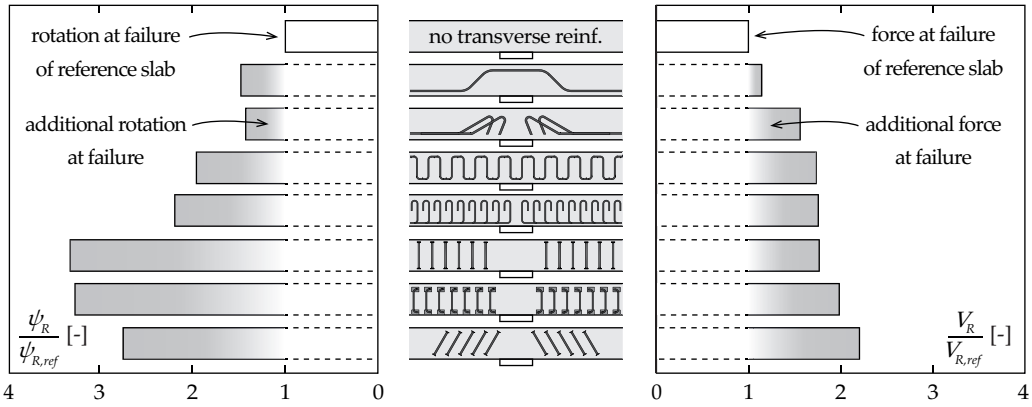

Figure 4.8 Contributions in terms of normalized rotation (left) and strength (right) at failure of several different punching reinforcing systems for punching tests on similar slabs in comparison to the reference slab without transverse reinforcement (adapted from [Ein16a])

The differences in the response of the slab are mainly attributed to the disparities in the anchorage performance under the specific conditions occurring during punching [Ein16a], and confirm the relevance of the present research. The relatively poor efficiency of bent-up bars –compared to any other actual reinforcing solution– justifies the lack of interest for the latter system in practice [Dil08], especially when improvements of both ductility and maximum strength are required. It is interesting to highlight that the deformation capacity of the slab –measured in terms of rotation– is in general not similarly sensitive to the type of the system used than the maximum strength. In fact, significant differences arise in the contributions to the punching behaviour between standard stirrups and studs –compared to the reference slab without transverse reinforcement– mostly related to the deformation capacity (increase of respectively 97% and 263%) rather than to the maximum strength (increase of respectively 73% and 94%). In general, the transverse reinforcement providing the largest strength is not systematically the one providing also the largest capacity of deformation. The latter points are strongly related to the activation of the transverse elements through the internal cracks, a complex phenomenon still under investigation. In order to contribute to the existing state of the art on the latter problematic, the development of cracks in the concrete during punching will be thoroughly investigated and reported in the following sections, as well as the role of the anchorage on the activation of the transverse reinforcement.

4.2 Cracking associated to punching phenomenon

As previously mentioned (see Section 2.1), the development of cracks is intrinsic to reinforced concrete elements. It reflects the transfer of forces between its two main components –the steel reinforcement and the surrounding concrete– and is necessary under certain reasonable limits –at serviceability limit state (SLS)– to guarantee adequate behaviour to the structure.

In the case of the punching, the complex interactions of forces lead –at ultimate limit state (ULS)– to the presence of several types of cracks (Figure 4.9), with disparities in their opening ranges. The internal cracking phenomenon affects the stiffness of the slab response and interacts with the transverse reinforcement by intercepting it. Most of the failure modes associated to punching with transverse reinforcement result from the sudden propagation of one of these specific cracks (see Section 4.3), or in some cases from the combination of some of them. Thus, in the frame of this research, it appeared important to detail the sequence of the crack development in the vicinity of the column during the progressive loading of a concentric and isolated slab specimen.

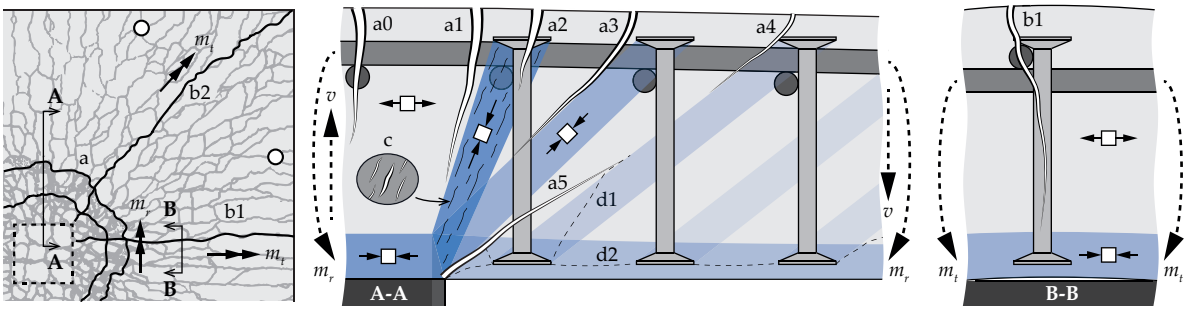

Figure 4.9 Schematic representations of the cracks potentially developing at ULS in punching of slabs with transverse reinforcement (strong direction): *(a)* cracks associated to tangential moments; *(b)* cracks associated to radial moments; *(c)* cracks in the concrete strut; and *(d)* cracks associated to a potential concrete-cone breakout or to delamination phenomenon

Cracks develop initially on the tensile part of the slab for low load level (10 ÷ 20% of the ultimate load) and are associated to tangential bending moments m_t, generally in the main directions (crack b1 in Figure 4.9) prior to the diagonals (crack b2 in Figure 4.9). Since the distance between these radial cracks was observed to be related to the spacing of the flexural reinforcement [Mar77], the associated crack pattern tends to correspond to the reinforcement layout in the main directions of the slab. Also, the use of transverse reinforcement might lead to the existence of some weaker plans in the slab, increasing therefore the potential risk of crack development in their vicinity. The latter aspect was highlighted in the extensive experimental punching test campaign conducted by Beutel [Beu03] for slabs reinforced with studs. The development of the radial cracks might be important –openings up to 2 mm before failure at the level of the flexural reinforcement– yet not critical regarding the punching failure. They might affect the bond performance on the straight part of the transverse reinforcement as well as the efficiency of the top anchorage (B-B in Figure 4.9), as both force transfer mechanisms were confirmed in the present research (see Section 2.3) to be very sensitive to the presence of cracks (even of limited widths).

The increase of the load (30 ÷ 60% of the ultimate load) leads to the formation of cracks around the column associated to radial bending moments m_r (cracks a0-a4 in Figure 4.9). These cracks are whose which development is associated to the punching failure of the slab. The yielding of the flexural reinforcement is progressively achieved at the column face and large openings are observed in the existing cracks (cracks a0 and a1 in Figure 4.9), resulting in the development of new tangential cracks extending gradually further away (cracks a2-a4 in Figure 4.9). The latter flexural-based cracks are of primordial importance in the present study because of their significant widths (up to 3 mm before failure, even more) but also for the high probability of their affecting the top anchorage of the transverse elements (position not directly related to the one of flexural reinforcement, as in the case of radial cracks). Observations on several saw-cuts indicate that the location of these cracks might be strongly influenced by the position of the top anchorage of the transverse reinforcement [Ein16a], independently of its type. At around half of the failure load, the crack pattern is normally completed –with moderate openings– as represented in the surface view of the slab in Figure 4.9. No significant differences were generally observed with the use of different types of transverse reinforcement [Sei80]. The propagation of the tangential cracks into the slab towards the column face is associated to a complex interaction of flexural and shear deformations, still under investigation by researchers (A-A in Figure 4.9). Thus, contrary to radial cracks, tangential cracks will not develop along the axis of the transverse elements, affecting thus mainly the performance of the top anchorage (crack a2 in Figure 4.9). Immediately before punching (90 ÷ 95% of the ultimate load), the deformations concentrated into the punching cone –through the formed cracks– localize into one failure crack (crack a5 in Figure 4.9) that propagates suddenly to achieve the ultimate load capacity of the slab [Pra79]. The latter phase might potentially be limited by some local anchorage issues, such as concrete-cone breakout (crack d1 in Figure 4.9) or delamination (crack d2 in Figure 4.9). Depending on the development of the failure crack, the contributions on the punching load of both concrete and steel might vary significantly. The following section aims to detail, classify and discuss the possible failures occurring in slabs with transverse reinforcement.

4.3 Failure modes of shear-reinforced slabs

The presence of transverse elements adequately disposed in the slab is always beneficial for the punching phenomena, but it also makes the transfer of forces more complex –compared to the case of slabs without such reinforcement– with multiple possible failure modes (Figure 4.10*(a)*). For systems with good anchorage performance –such as studs– significant differences arise amongst them regarding the deformation capacity at failure (dashed lines in Figure 4.10*(b)*). The development of a crack through the transverse reinforcement –failure within the shear-reinforced area– is highly beneficial for the ductility of the structure, avoiding the sudden and pronounced drop of the load associated to other punching failures (as in the crushing failure of the first strut). Although the ultimate load is potentially smaller –in the former case– the related behaviour at failure makes it considerably more interesting and safer for structural applications. Independently of the failure mode, the activation of the transverse reinforcement is generally performed through a complex combination of struts and cracks intersecting the elements (Figure 4.9), still under investigation.

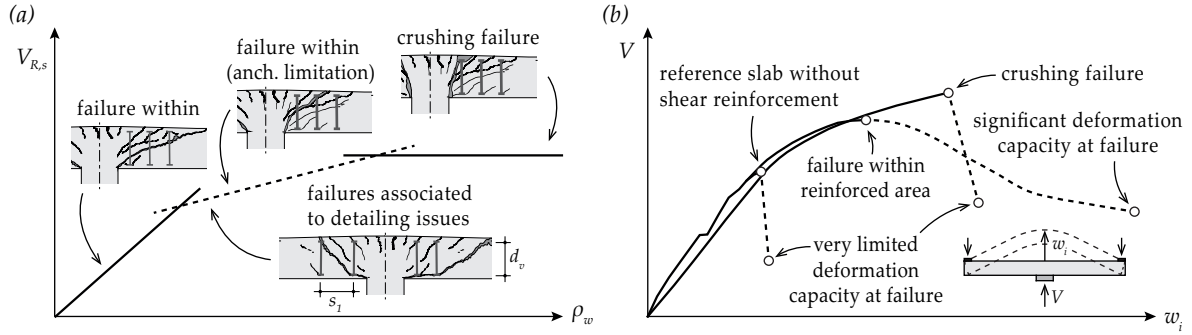

Figure 4.10 Punching failure modes of slabs with transverse reinforcement: *(a)* effective contribution of the transverse elements to the punching strength at failure for different amount; and *(b)* differences in the deformation capacity at failure (adapted from [Voe81])

Punching failures associated to the detailing of transverse reinforcement may result from a lack of rigour in the disposition of the elements and were resolved through experimental iterations. The most common are related to an insufficient number of rows of the transverse reinforcement (n_r) or to an excessive spacing between two consecutive elements (s_1), leading respectively to a failure outside the reinforced area or in-between the elements (Figure 4.10*(a)*). More rarely, an excessive spacing between two elements of the same row (s_t) –potentially the case when the transverse reinforcement is disposed cruciformly around the column– might also result in a particular failure mode [Ein16a]. The reduced effective depth (d_v) was recognized to be one of the key parameters characterizing the aforementioned phenomenon, as the theoretical strut is no longer supported on the column face but on the bottom anchorage of the last element of the transverse reinforcement.

If the arrangement of the transverse reinforcement is done according to the state-of-the-art, the critical failure mode mainly depends on the amount and the performance of the punching system (bond properties and anchorage detailing). Thus, the development of the failure crack through the reinforcement is controlled by a combination of these parameters and generally the inclination gets steeper by increasing the transversal stiffness (associated to the type and amount of system used). The failure mode might therefore change from a rather ductile one associated to steel failure (failure within in Figure 4.10*(a)*) to a more brittle one associated to concrete crushing (crushing failure in Figure 4.10*(a)*) with a not well-defined transition phase (dashed line in Figure 4.10*(a)*). This was confirmed by several experimental test series [Yam92, Gom99, Pis00, Vaz09] where the effective contribution of a given type of system was observed to be clearly not directly proportional to its amount (also partially reported in [Reg01]). The latter seems to be related to the development –under certain specific conditions (such as cracking)– of some anchorage limitations of the transverse reinforcement systems, similarly to what was observed for individual elements (see Section 2.3). This might lead to premature failures of the slab specimens with a reduction of the effective contribution of the transverse steel –yielding not achieved– in the punching phenomenon (failure with anchorage limitation in Figure 4.10*(a)*). Elstner and Hognestad [Els56] were among the first to claim that the local crushing of the concrete under the bends of the reinforcing details might potentially have contributed to the anchorage issues highlighted in their testing program. Possible interactions between the aforementioned failure modes can be also expected when

the slabs are reinforced with non-axisymmetric anchorage systems –such as individual links (Figure 4.5*(b)*)– as their performance might be different between the main axes (strong and weak reinforcement directions of the slab). If all the previously mentioned failure modes can be avoided through an adequate use of transverse reinforcement, the flexural capacity of the slab can be achieved (punching might still occur depending on the effective deformation capacity of the slab).

In the following, the punching failure modes for which bond and anchorage conditions of the transverse reinforcement have an important role are detailed physically and depicted according to the CSCT [Fer09]. This is the case for the crushing failure (see Section 4.3.1) and the failure within the shear-reinforced area (see Section 4.3.2). In the frame of this research, particular interest will be given to the latter one –generally associated to low amounts of shear reinforcement– as the related assumptions of the CSCT regarding the activation of transverse elements are not systematically supported by experimental evidences.

4.3.1 Crushing failure

This failure mode is associated to the limitation of the load-carrying capacity of the concrete strut between the first transverse reinforcing element and the column face (Figure 4.11*(b)*). The force in the strut (F_{strut}) depends on its angle, which in fact depends on the position of the top anchorage of the first row of transverse reinforcement. A larger distance between the first transverse element and the column face (s_0) leads to a lower inclination of the strut and therefore to a higher force in the strut. The effective strength of the strut ($f_{c,eff}$) depends on the cracking state, as already highlighted in Figure 4.2*(b)*). If the inclination is low, the strength can be reduced by flexural cracks propagating into the strut and if the inclination is too steep, the strength can also be reduced by the cracks due to tension in the transverse reinforcement. Thus, an optimal position exists for the first element, where the ratio between the strength and the force in the strut is the highest. In the latest recommendations of the *fib* Model Code 2010 (MC 2010) [FIB13], this distance ranges between $0.35 \cdot d_v$ and $0.75 \cdot d_v$ with slight differences in the values amongst the different code provisions.

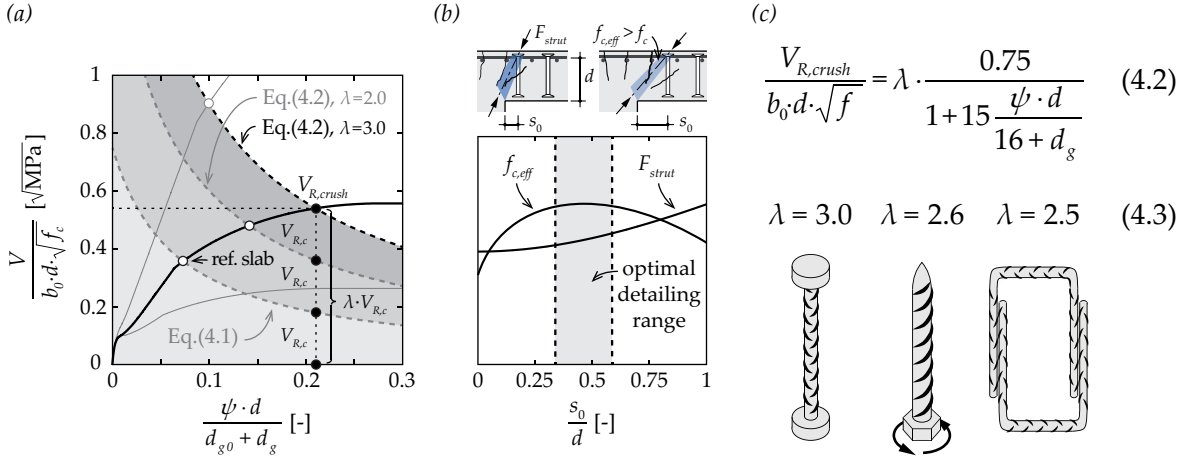

Figure 4.11 Crushing failure of the first strut according to the CSCT: *(a)* load-rotation curves; *(b)* qualitative curves for the determination of the optimal position of the first transverse reinforcement regarding to the column face; and *(c)* main related formulations [Fer09, Fer10a]

Considered as an upper bound of the punching strength for slabs with shear reinforcement, this failure mode is generally treated by most of current code provisions through semi-empirical approaches with good correlation. Considering that the disposition of the first transverse element in agreement with the recommendations, the punching strength ($V_{R,crush}$) is simply estimated – according to the CSCT [Fer09]– with Eq.(4.2) through the multiplication of the original failure criterion (for slabs without transverse reinforcement, see Eq.(4.1)) by a semi-empirical factor (λ) depending on the efficiency of the type of transverse reinforcement system considered. The representation in the normalized load-rotation of the failure criteria (Figure 4.11*(a)*) allows to appreciate the substantial contribution of the transverse reinforcement in terms of strength and deformation capacity compared to the reference case. Conservatively, the value of λ is set to 2.0, but higher ones can be considered – Eq.(4.3)– if experimental data demonstrates a better performance. This allows for an easy adaptation of the calculation model for various types of shear reinforcing systems [Fer10a, Ein16a] confirming the pertinence of the approach. The range of values generally considered for λ can be physically explained notably by the differences in the performance of the support of the concrete strut provided by the top anchorage of the first element of the transverse reinforcement. The additional slip of the anchorage –associated to less efficient reinforcement systems– leads to a reduction of the confinement of the concrete strut at the column face with increased lateral expansion (cracks c in Figure 4.9), limiting therefore its related carrying capacity.

4.3.2 Failure within the shear-reinforced area

This failure mode is related to the activation of transverse elements by a failure crack similar to the one that develops for slabs without transverse reinforcement (crack a4 in Figure 4.9). The phenomenon involves both steel ($V_{R,s}$) and concrete ($V_{R,c}$), making the definition of the related punching strength ($V_{R,in}$) less evident than for the other aforementioned failure modes. In this sense, the physical model proposed by Fernández Ruiz and Muttoni [Fer09] for the CSCT is of major interest (Figure 4.12), as it allows to estimate and sum up the individual contributions (Eq.(4.4)).

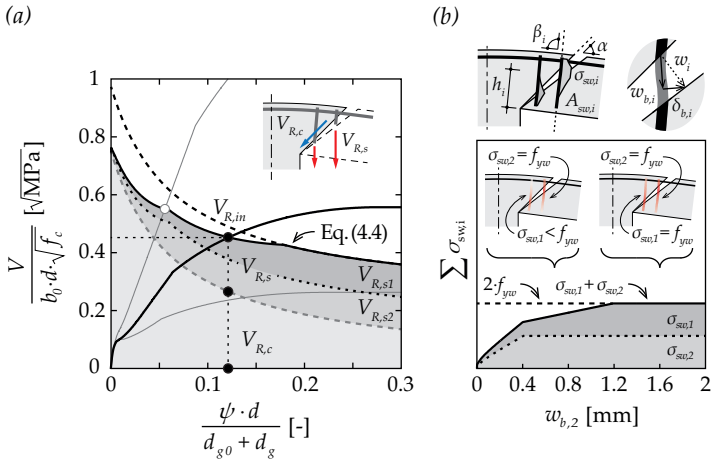

$$V_{R,in} = V_{R,c} + V_{R,s} \quad (4.4)$$

$$V_{R,c} = 0.75 \cdot \frac{b_0 \cdot d \cdot \sqrt{f_c}}{1 + 15\frac{\psi \cdot d}{16 + d_g}} \quad (4.5)$$

$$V_{R,s} = \sum_{i=1}^{n} \sigma_{sw,i} \cdot A_{sw,i} \cdot \sin(\beta_i) \quad (4.6)$$

$$w_{b,i} = \kappa \cdot \psi \cdot h_i \cdot \cos\left(\alpha + \beta_i - \frac{\pi}{2}\right) \quad (4.7)$$

$$\sigma_{sw,i} = f(w_{b,i}) \le f_{yw} \quad \text{Appendix A}$$

Figure 4.12 Failure within the shear-reinforced area according to the CSCT (n=2 elements intercepted by the critical crack): *(a)* load-rotation curves; *(b)* activation of the transverse reinforcement (h_1/h_2 = 2/3, the anchorages of the transverse elements were not represented only for clarity purposes); and *(c)* main related formulations [Fer09]

Both the concrete and steel contributions are obtained assuming the development of a critical crack –similar to the one considered for punching without transverse reinforcement (angle α of 45°, centre of rotation at the column face, opening proportional to $\psi \cdot d$)– through the transverse elements and localizing half of the deformations at failure ($\kappa = 0.5$). The concrete contribution ($V_{R,c}$) can thus be defined by the same failure criterion previously derived (Eq.(4.5)). The steel contribution ($V_{R,s}$) is defined in its general form as Eq.(4.6), where $A_{sw,i}$ is the sum of the cross-section area of all the transverse elements in the row i and β_i their inclination according to the plane of the slab. For each transverse element at row i –intersected by the crack at a given height (h_i) from tip of the crack (Figure 4.12*(b)*)– the component of the crack opening (w_i) activating the reinforcement ($w_{b,i}$) can be simply calculated as Eq.(4.7). Assuming perfect bond and anchorage conditions, and depending on the type of system considered (casted-in or post-installed reinforcing details) and type of steel product (plain or deformed bars), several formulations were derived by the authors to relate the crack opening to the stresses in the transverse elements [Fer09]. The complete analytical developments of the relations σ_{sw} - w_b can be found in Appendix A. In the following, this physical-based method will be denominated as the *activation model* and has a central role in the present thesis.

This model defines the increase of force in efficient shear reinforcing systems –such as deformed studs– through several consecutive phases depending on the state of deformation of the slab (through rotation ψ) and the position of the crack intersection with the transverse elements (discrete method). As the latter aspect might result in a certain sensibility, a smeared approach was also proposed and validated recently [Fer09, Lip12a]. In general, different activation cases arise during the development of the punching failure: bond only (first row element in Figure 4.12*(b)*), bond and bottom anchorage, bond and top anchorage (second row element in Figure 4.12*(b)*) or bond and both anchorages (top and bottom). The related failure criteria –Eq.(4.4)– is therefore a complex function (Figure 4.12*(a)*) that predicts a partial activation of the transverse reinforcement for small rotations (high flexural reinforcement ratios, prestressed slabs or footings), and usually controlled by the yielding of the transverse elements for large rotations (low flexural reinforcement ratios). In this sense, the punching within the shear-reinforced area is generally the governing failure mode for slabs with low to moderate amount of shear reinforcement.

The two main assumptions of the activation model –related to the kinematics of the crack activating the transverse reinforcement and to the perfect bond and anchorage conditions– might lead in some cases to non-conservative predictions. For the failure mode of interest, a more important activation of the furthest element of the transverse reinforcement intersected by the failure crack (in comparison to the closest one) was never systematically confirmed in experimental works (see Section 4.4). Also, the pull-out tests performed (see Section 3.2) as well as the literature review (see Section 2.3) confirmed that the force transfer mechanisms are considerably degraded in presence of cracks and significantly different in function of the reinforcement detailing. In this sense, although the theory provides good predictions, the fact that it could clearly benefit from additional developments in the consideration of realistic bond and anchorage conditions of the shear reinforcement motivated the extension of the activation model in the present research (see Section 5.5).

4.4 Activation of the transverse reinforcement

The present section aims at discussing the experimental observations of selected punching tests on slender slabs with transverse reinforcement found in literature that developed a failure within the shear-reinforced area. Measurements of steel strains (ε_{sw}) –converted into steel stress (σ_{sw})– and slab expansion (Δh) –related to internal crack development– were of main interest in studying the activation of the transverse reinforcement (σ_{sw}/f_{yw}). In order to investigate properly the phenomenon associated to the crack kinematics, only slabs presenting a failure crack intercepting at least the two closest rows of transverse elements were generally considered in the following. Also, the choice to select mainly slabs reinforced with stud-like elements was motivated by the fact that these systems tend to present significantly less anchorage issues (steel I-profiles excluded), thereby allowing focus on the related phenomenological aspects. Exceptions were generally made for some major studies of slabs reinforced with stirrups-like elements (bent-up bars excluded), so as to be also representative of the reinforcement types commonly used nowadays in practice.

The difficulty of interpretation often associated to punching tests with transverse reinforcement might be related to the various –and sometimes very specific– representations of the results by the authors. Thus, for consistency purposes, the original format of the test data –layout, units and axes of the figures– have been in most cases thoroughly reworked for the discussion (considered units are [kN] for forces or loads and [mm] for displacement). Also, when a reference test was performed within the same test series –on similar slabs but without transverse reinforcement– it was systematically indicated (with empty dots) as analogies were confirmed [Lip12a]. Although the original numeration of the measurements was simplified, the denomination of the specimens was kept identical to the original one for reference purposes. Regarding the transverse reinforcement, when the system used by the researchers was not common, a detailed sketch is generally provided in order to better appreciate the potentially related issues. A similar approach was done regarding the measurement devices used for the evaluation of specific parameters (slip of the anchorage for instance). In each of the following figures presenting test results, the failure crack is reported either with a solid line (according to performed saw-cuts) or with a dashed line (according to the statements of the authors or from personal observation of the available documents). Also, the transverse reinforcement and the measurements performed are represented as close as possible to their exact positions in order to simplify the related interpretation and discussion of the results.

Marti et al. [Mar77] tested a prototype of stirrups made of deformed bars (d_b = 8 mm, f_{yw} = 539 MPa, ρ_w = 0.35%) as transverse reinforcement for concrete slabs (Figure 4.13*(a)*) disposed uniformly around the column (circular). They were among the first to quantify the development of the failure crack during the test through specific measurements of the slab expansion (Figure 4.13*(b)*). The reinforcing system was effective in controlling the formation of internal cracks in the slab specimen *P3*. The latter phenomenon was observed to accelerate considerably at a load level similar to the one corresponding to the failure of the reference specimen *P2* without transverse reinforcement (Figure 4.13*(c)*). Although tangential cracks with openings of up to 2.5 mm were measured close to

failure on the tensile side of the slab –potentially affecting the performance of the reinforcing system– no anchorage limitations were reported. This is most probably related to the important bond length available and the presence of constructive welds at the extremities. The adequate activation of the transverse reinforcement led therefore to a relatively ductile failure mode –in comparison to the reference slab– with important vertical translations associated to the yielding of one or several transverse elements (similarly to Figure 4.10*(b)*). Prior to failure, the authors also observed a significant penetration of the slab at the column face –associated to shear deformations– reflecting the initiation and the propagation of the failure crack from this position.

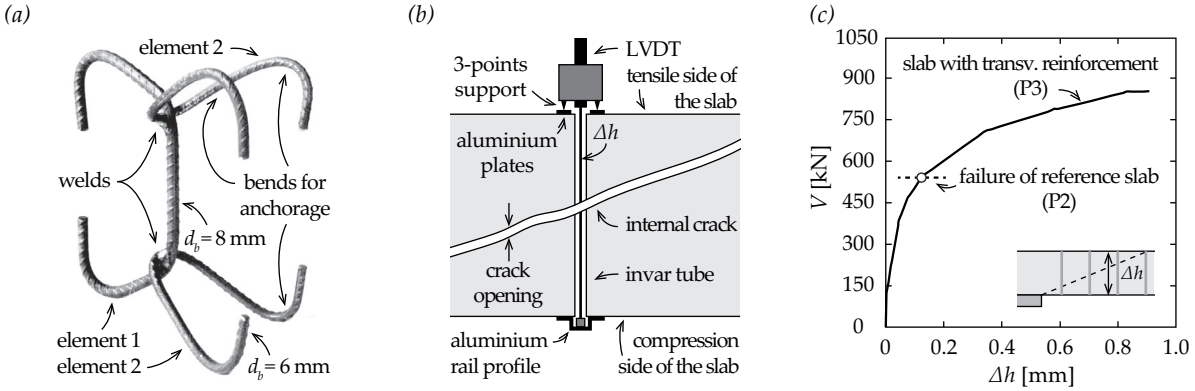

Figure 4.13 Experimental observations (adapted from [Mar77]): *(a)* detail of the transverse reinforcement; *(b)* slab expansion measurement device; and *(c)* average slab expansion

The punching tests conducted by Van der Voet [Voe80] (partially reported in [Voe81]) are amongst the first ones performed on slabs with plain double headed bars as transverse reinforcement (Figure 4.6*(b)*), arranged uniformly around the column (square). Delamination problems were considerably limited in this case as no cover was provided to the elements (both at the compression and tensile sides of the slab). In addition to the measurements of the force in the transverse reinforcement –through strain gauges– and the slab expansion, an attempt was made to evaluate (during tests) the slip of the head of the stud (in the compression side) in order to investigate more specifically potential interactions associated to the anchorage conditions (Figure 4.14*(a)*). The specimen *MV6* (d_b = 4.8 mm, f_{yw} = 325 MPa, ρ_w = 0.2%) is the only one of the test series that presented a failure within the shear-reinforced area, and has thus a central role in the following discussion. The activation of the transverse reinforcement was observed to be proportional to the proximity of the transverse elements to the column (Figure 4.14*(b)*), with a systematic development of yield stresses prior to failure. The first row of studs was therefore activated more than the second, and the second more than the third, in agreement with the measured crack sequence (solid lines in Figure 4.14*(c)*). Most of the activation of the transverse elements –at least 50%– was achieved after the load level of the failure of the reference specimen *MV1*. The latter might be related to the development of important shear deformations. Although the bearing surface of the head (A_h) at the extremities of the transverse reinforcement was designed by the author to avoid any crushing of the concrete –when the bar of section (A_b) would achieve its full capacity ($A_h/A_b > 25$, $\sigma_c/f_c \approx 0.6$)– the slip of the anchorage (δ) could not be totally avoided (dashed lines in Figure 4.14*(c)*), even in the

compression side of the slab. It is interesting to highlight –for the first row of transverse reinforcement– the similarities between the curves of the slab expansion and the slip of the head once the failure load of the reference slab was reached. This indicates that, under certain conditions, the lack of stiffness of the head might potentially contribute significantly to the development of a crack at the position of the transverse element. From other tests performed in the same test series, the importance of the slip appears to be related in a way to the shear reinforcement ratio, being larger for small amount of transverse elements. This can be justified by an increase of the effective activation of the studs –similar crack development but decreased transverse stiffness– and the associated crushing under the head. However, as the full activation of the transverse reinforcement could systematically be achieved prior to failure, the author concluded that the performance of its anchorage should not have such importance in the determination of the related punching strength (also previously claimed by Andrä [And77]). The latter remark could be justified for the elements used in these tests –as well as for others of this period ($A_h/A_b \approx 15$)– that were made of steel with relatively limited yield strength. The related issues could be markedly different with the actual version of such reinforcing systems, for which considerable progress has been made since then regarding the size of the head ($A_h/A_b \approx 9$) and the steel properties ($f_{yw} \geq 500$ MPa). Even though the presence of ribs along the straight part of the detail would nowadays lead to a reduction of solicitation at the anchorage level, high bearing stresses on the concrete (σ_c) would still develop under the head ($\sigma_c/f_c > 2.0$), with all the potential aforementioned problematics related.

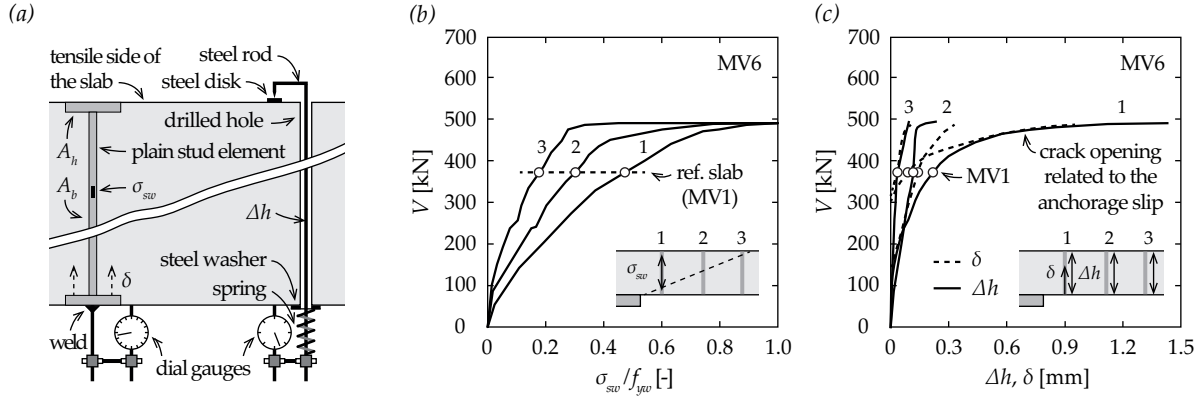

Figure 4.14 Experimental observations (adapted from [Voe80]): *(a)* measurement devices of the slab expansion and the slip of the head; *(b)* average activation of the transverse reinforcement; and *(c)* average slip of the head of the transverse reinforcement (dashed lines) and average slab expansion (solid lines)

Conscious of the issues associated to the detailing of the transverse reinforcement, Regan [Reg80a] performed punching tests on slabs reinforced with deformed individual links (d_b = 6.0 mm, f_{yw} = 740 MPa, ρ_w = 0.20% and d_b = 8.0 mm, f_{yw} = 510 MPa, ρ_w = 0.35%) combined with some pull-out tests (see Sections 2.1.2 and 2.3.2). In this sense, the aforementioned work is of particular interest as a similar approach was followed in the present research. In order to facilitate the disposition of the transverse reinforcement around the flexural bars, the elements were detailed to avoid being planar (Figure 4.15*(a)*). For the failure mode of interest, increasing the amount of transverse rein-

forcement –for a same uniform arrangement around the column (square)– delays the opening of the critical crack (Figure 4.15*(b)*), without any apparent modifications on the related kinematics. As the transverse stiffness is improved, the crack development –initiated at a load level close to the failure of the reference slab (specimen *1*)– is better controlled and its propagation less sudden. For both specimens *2* and *3*, the strain measurements of the transverse elements support the latter observation with a progressive and stable activation followed by a considerable development at the failure load of the reference specimen. The force in the first row of transverse reinforcement was generally more important than in the other ones at failure, as suggested by the slab extension profiles obtained during the tests. The fact that only a limited amount of details achieved their full capacity can be partially explained by the high yield strength of the steel used, notably in the case of specimen *2*. From the measurements performed, it can be therefore concluded that the failure of these specimens seems to be related more to the sudden development of a crack than to the yielding of the transverse reinforcement. In the last tested slab of the series –specimen *4* (d_b = 8.0 mm, f_{yw} = 510 MPa, ρ_w = 0.35%)– a redistribution of forces was even highlighted in the transverse reinforcement close to the column prior to failure (Figure 4.15*(c)*), most probably associated to some anchorage limitations. Also, notable differences were observed between the activation of the transverse elements in both the weak and strong directions of the slab –defined as in Figure 4.15*(a)*– the latter being generally less solicited by about half. This can be justified by the fact that the details were systematically hanged in the same direction (strong axis) leading to an asymmetry of the anchorage performance of the transverse reinforcement regarding punching phenomenon.

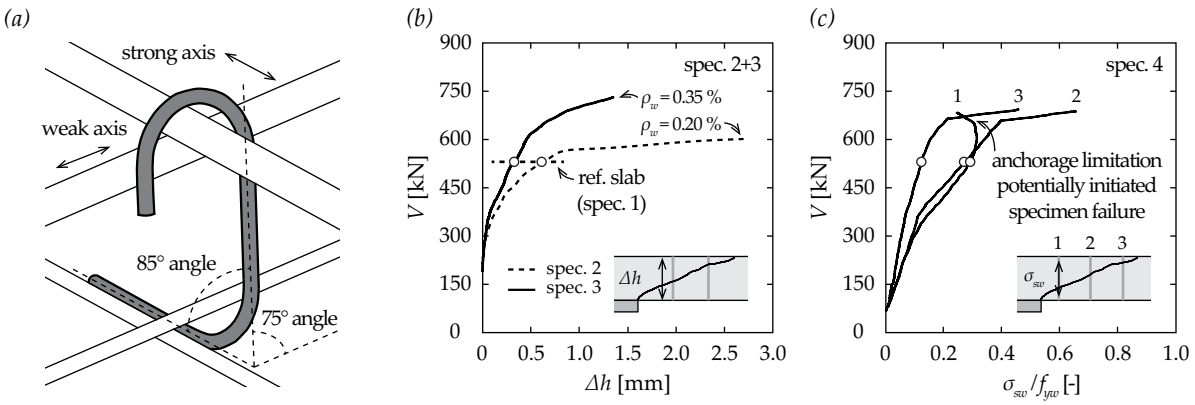

Figure 4.15 Experimental observations (adapted from [Reg80a]): *(a)* detail of the transverse reinforcement and definition of weak and strong reinforcement directions of a slab; *(b)* average slab expansion of slabs with similar layout of transverse reinforcement that presented similar failure mode; and *(c)* activation of the transverse reinforcement (strong axis)

In the continuity of the investigations performed by Van Der Voet [Voe80], the punching tests by Mokhtar [Mok82] (partially reported in [Mok85]) involved an enhanced headed bars reinforcement (d_b = 9.5 mm, f_{yw} = 278 MPa, ρ_w = 0.71%) disposed orthogonally around the column (square). Compared to the original version, the elements were produced with heads at the tensile side of more reasonable dimensions ($A_h/A_b \approx 10$), and with a steel rail at the compression side substituting the heads in order to facilitate the installation of the system. Also, most of the transverse elements

were provided with a cover –both at the compression and tensile side of the slab– to be more representative of the effective anchorage conditions that can be found in a practical application of the reinforcing system (compared to its former alternative [Voe80]). Similarly to previous observations, the development of a crack in the vicinity of the column –at a load close to the ultimate one of the reference slab *AB1* (Figure 4.16*(a)*)– contributes greatly in the activation of the first and second rows of transverse reinforcement up to failure (Figure 4.16*(b)*). Although the closest studs to the column are generally the most activated at failure –in agreement with the observed crack sequence– this appears not to be the case prior to the failure load of the reference slab for specimen *AB2*. The author claimed that this initial stronger activation of the second row –compared to the first one– might result from the interception of the transverse reinforcement element by a flexural-based crack at a distance d from the column face (resulting from tangential moments). The combined interpretation of the measurements related to the slip of the heads (Figure 4.16*(c)*) and of the activation of the transverse elements (Figure 4.16*(b)*) indicates in specimen *AB5* a relatively stiff behaviour of the anchorage up to a load corresponding to the failure of the reference slab. Then, the increase of force in the studs is accompanied by moderate to important slips up to failure, decreasing progressively the transverse stiffness provided by the studs. The latter facilitates considerably the development of cracks in the shear-critical region, potentially leading to the failure of the specimen (not observed in this case). Although values of slip larger than 1.0 mm were recorded prior to failure, this type of detail allowed –in comparison to less efficient systems [Reg80a]– a progressive and relatively constant development of stresses in the steel. The latter aspect is essential for the adequate use of transverse reinforcement in punching. Similar tests by Van der Voet [Voe80] highlighted interesting points regarding the role of the anchorage conditions in the punching phenomenon. Notably, comparing the activation of the transverse reinforcement in both cases (Figure 4.16*(b)* and Figure 4.14*(b)*), it appears that when cover is provided to the head of the stud (more realistic conditions) the anchorage performance and the related increase of force in the elements are affected. Also, the slip measured at the level of the head (Figure 4.16*(c)* and Figure 4.14*(c)*) exhibits some notable differences, being systematically more important if the anchorage is provided with a cover, although the activation is not even fully achieved.

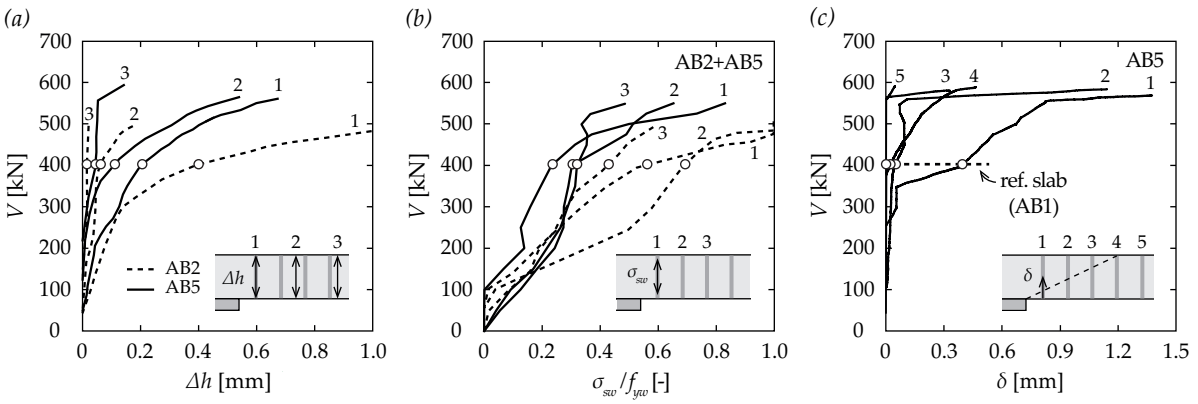

Figure 4.16 Experimental observations (adapted from [Mok82]): *(a)* average slab expansion; *(b)* average activation of the transverse reinforcement; and *(c)* slip of the head of the transverse reinforcement (strong axis)

The tests performed by Tolf [Tol88] on slabs reinforced with small amount of deformed closed stirrups (d_b = 5.0 mm, f_{yw} = 710 MPa, ρ_w = 0.28% and d_b = 10.0 mm, f_{yw} = 670 MPa, ρ_w = 0.21%) arranged radially around a circular column (Figure 4.17*(a)*) confirmed the anchorage issues associated to such a type of reinforcing system. It is now accepted that, in thin slabs especially, the activation by bond is generally not optimal due to the limited development length available for the respect of durability requirements (minimal concrete cover). The problematic is such for this type of transverse elements that the contribution to the punching strength –partially based on the transfer of forces by bond– might almost be null with respect to the reference slab. This was confirmed with specimens *S1.3s* and *S1.4s* (h = 120 mm, c = 125 mm), where no substantial increase of the load was reported although the failure crack intercepted all the transverse elements (Figure 4.17*(b)*). The author investigated the influence of the size effect on the activation of the transverse reinforcement through tests performed on slabs of double dimension. The specimens *S2.3s* and *S2.4s* (h = 240 mm, c = 250 mm) exhibited a more efficient use of the transverse elements (Figure 4.17*(c)*) for a relatively similar shear reinforcement ratio. In both cases, the first row was slightly more activated than the second one until some anchorage limitations –or other phenomena– led to the development of the failure crack, as already observed by Regan [Reg80a]. Also, in all the tests, yielding of the transverse steel could never be achieved, even at failure, due to inappropriate conditions for an adequate activation of the reinforcing elements.

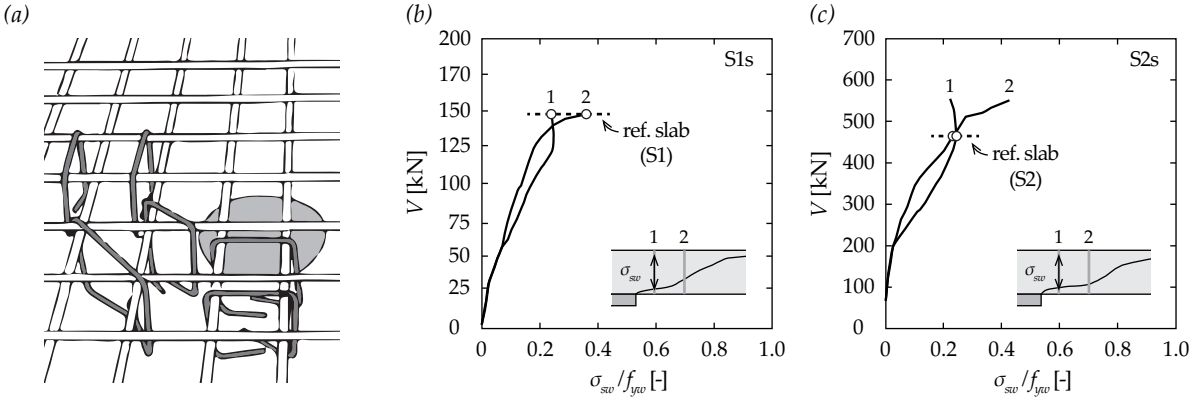

Figure 4.17 Experimental observations (adapted from [Tol88]): *(a)* type and arrangement of the transverse reinforcement (flexural reinforcement in compression side of the slab not represented for clarity purpose); *(b)* average activation of the transverse reinforcement (*S1.3s* and *S1.4s*); and *(c)* average activation of the transverse reinforcement (*S2.3s* and *S2.4s*)

Beutel [Beu03] conducted an extensive experimental campaign of punching tests (partially reported in [Beu02]) to study the role of detailing and anchorage performance of the transverse reinforcement (deformed stirrups and studs). The consequent amount of studs disposed radially around the column (ρ_w > 1.00%) –associated to the anchorage quality of this type of detail– resulted mostly in failures by crushing of the concrete strut (not of interest in the present research). The related tests (Z series) will thus not be further developed in the following. The several variations of stirrups –disposed uniformly around the column (square)– were generally all provided with constructive transverse bars of small diameter. This solution was considered by the author as it was reported to substitute well 90° bends or hooks –from an anchorage point of view [Reh79]– even

without enclosing the flexural reinforcement (usually required for such type of systems). Therefore, although the amount of reinforcement used in these tests was relatively small (0.39% < ρ_w < 1.03%), the failure was generally related to concrete crushing close to the column. As most of the specimens were also reloaded after failure, the interpretations of the saw-cuts and crack pattern on the top of the slab cannot be considered as representative of the situation at failure. However, the specimen *P4-III* (d_b = 8.0 mm, f_{yw} = 597 MPa, ρ_w = 0.40%) was the only one interrupted at failure, without any reloading (Figure 4.18*(a)*). A significant activation of the first three rows of transverse reinforcement was measured prior to failure (Figure 4.18*(b)*) and provided to this slab one of the most significant deformation capacities of the entire test series. The performance of the anchorage was stated several times by the author as a main issue for the punching of slabs with transverse reinforcement. This problematic can be well illustrated with specimen *P3-I* (d_b = 8.0 mm, f_{yw} = 597 MPa, ρ_w = 0.40%) in which a redistribution of forces –notably between rows 1 and 3– was highlighted (Figure 4.18*(c)*), similarly to previous experimental observations with analogous reinforcing details [Reg80a, Tol88]. According to Hegger and Beutel [Heg99], this might be related to a slip of the transverse elements –associated to the development of significant flexural cracks in the vicinity of the column– limiting thus the activation through bond and anchorage mechanisms.

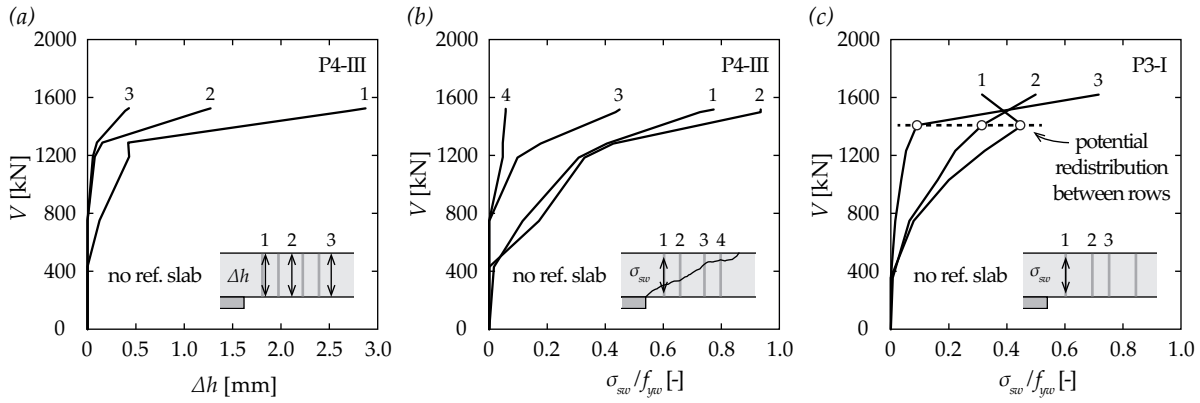

Figure 4.18 Experimental observations (adapted from [Beu03]): *(a)* average slab expansion; *(b)* average activation of the transverse reinforcement; and *(c)* average activation of the transverse reinforcement (with possible anchorage limitations)

The investigations by Birkle [Bir04] (partially reported in [Bir08]) were performed on slabs reinforced with plain studs (rail in the compression side) disposed radially or orthogonally around the column (square). This experimental work aimed at studying the performance of relatively low amounts of transverse reinforcement (0.23% < ρ_w < 0.66%). It is therefore of major interest in the present research providing accurate results and specific interpretations on the activation of the transverse elements by limiting considerably potential issues related to bond or anchorages. The use of studs systematically increased the load capacity of the reinforced slabs when compared to reference specimens, with no apparent influence of the layout of the transverse reinforcement. However, disparities arose regarding the ductility at failure of the various specimens (dashed lines in Figure 4.19*(a)*), as previously observed by Dilger and Ghali [Dil81]. In the case of specimen *3* (d_b = 9.5 mm, f_{yw} = 393 MPa, ρ_w = 0.43%) and specimen *12* (d_b = 12.7 mm, f_{yw} = 409 MPa, ρ_w = 0.23%), the development of the critical crack through several rows of the reinforcement (Figure 4.19*(d)*)

provided an appreciable capacity of deformation compared to the other specimens that presented a crushing of the concrete strut. This is confirmed by the fact that the activation of the transverse reinforcement for specimens *9* (d_b = 9.5 mm, f_{yw} = 393 MPa, ρ_w = 0.21%) and *12* (Figure 4.19*(b)*) was significantly larger than for any other failure modes, with a systematic achievement of the full capacity of one or several of the closest studs to the column. Similar observations were done regarding the slab expansion, with larger values reported closer to the column (Figure 4.19*(c)*), in agreement with the failure crack visible on the saw-cut (Figure 4.19*(d)*) and the previously highlighted activation sequence. The sudden development of the crack and activation prior to failure in specimen *12* (position 1 and 2) might be strongly associated to the shear deformations in this specific region. All the aforementioned observations are also generally supported by specimen *11* (d_b = 12.7 mm, f_{yw} = 460 MPa, ρ_w = 0.35%) which presented a failure within the reinforced area. Although anchorage limitations were not directly observed through measurements –as it was the case for other less efficient reinforcing systems– a saw-cut performed on specimen *12* confirmed some previous statements (Figure 4.19*(e)*). The presence of a crack along the axis of the stud –similarly to crack b1 in Figure 4.9– might have affected the bond performance of all the elements on the rail. Also, the activation of the transverse reinforcement might be significantly reduced if the failure crack does not intercept the transverse elements (right stud in Figure 4.19*(e)*) –similarly to crack d in Figure 4.9– compared to the expected situation (left stud in Figure 4.19*(e)*), intercepted at approximatively a quarter of its height. The important distance between the elements –associated to an orthogonal arrangement of the reinforcement– might partially explain these observations. It is however difficult to discuss further the influence of this aspect on the failure of the slab specimen.

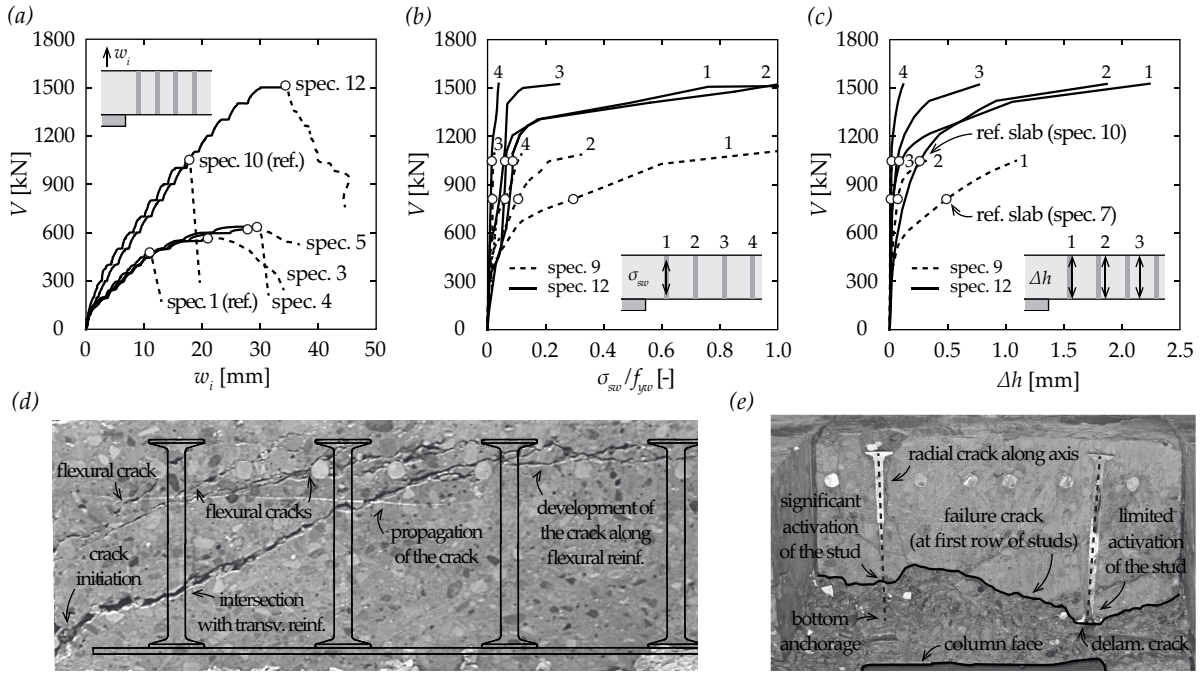

Figure 4.19 Experimental observations (adapted from [Bir04]): *(a)* centre deflections of selected slab specimens (post-failure phases in dashed lines); *(b)* average slab expansion for specimens that presented failure within the reinforced area; *(c)* average activation of the transverse reinforcement; *(d)* saw-cut of specimen *12* in the strong axis (picture from correspondence with the author); and *(e)* saw-cut of specimen *12* at the level of the first row of studs with failure surface in perspective (picture from correspondence with the author)

The experimental study conducted by Vaz [Vaz07] (partially reported in [Vaz09]) on slabs reinforced radially around the column (circular) with a low amount of plain stud-like elements (Figure 4.6*(d)*) is also of interest in the present work. Most of the tested specimens (d_b = 4.2 mm, f_{yw} = 708 MPa, ρ_w < 0.20%) presented a failure through the transverse reinforcement. In general, the development of yielding stresses was achieved in at least the first row of elements (Figure 4.20) as a result of the anchorage performance of the reinforcing system. The disparities in the activation at failure between the different rows of transverse reinforcement corroborate the propagation of the critical crack from the column face, similarly to aforementioned investigations [Voe80, Bir04]. Compared to most of the previous investigations, no significant differences arise regarding the sequence of activation amongst the rows up to the failure load of the reference specimen. The latter fact might be associated to a possible effect of group, related to the use of continuous welded steel plates for the bottom and top anchorages –ladder type reinforcement– instead of several individual elements [Voe80]. The limited stresses in the transverse reinforcement –prior to the development of the failure crack– are probably related to the limited stiffness of the system.

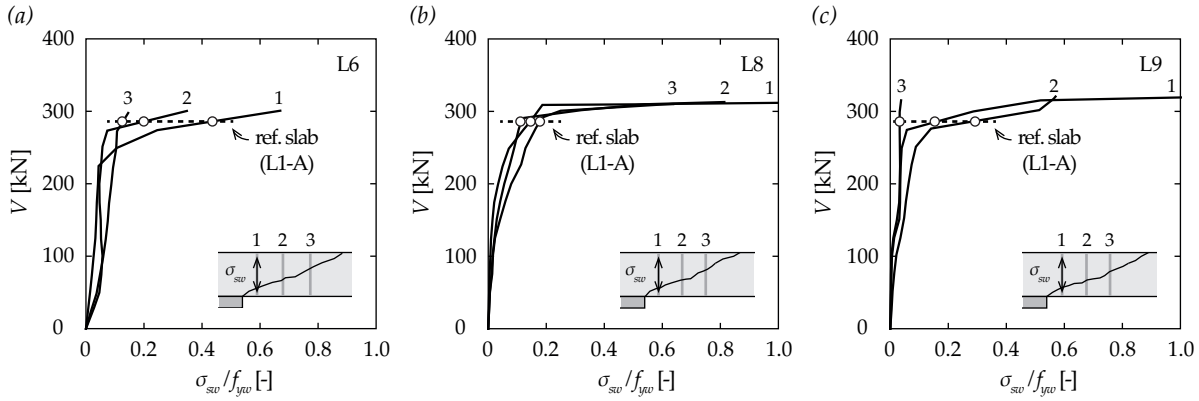

Figure 4.20 Experimental observations (adapted from [Vaz07]): average activation of the transverse reinforcement in the specimens *(a) L6*; *(b) L8*; and *(c) L9*

Recently, a test campaign was performed to specifically investigate the punching failure of slabs within the shear-reinforced area [Fer10c] (partially reported in [Fer14]), mainly performed with circular columns. This alternative to square columns is interesting in the study of the activation of the transverse reinforcement as it limits the localization phenomena associated to the presence of the edges. The authors selected double headed studs (rail in the tension side) made of deformed bars as transverse reinforcement, generally disposed radially around the column in a reasonable amount (0.25% < ρ_w < 0.47%). The choice of this specific reinforcing system was supported by previous similar experimental works that confirmed its systematic activation with limited anchorage issues. However, the important constant thickness of the head –simply welded to the bar– decreased the effective length of the transverse element by almost 10% compared to similar forged details. This problematic was confirmed with the development of several cracks associated to anchorages –notably in the compression part– potentially limiting the contribution of the transverse reinforcement. Also, a significant amount of steel plates were disposed on the tensile part of the slab –not in a uniform or systematic manner– in order to facilitate the installation of the elements.

The latter point is highly questionable regarding the phenomenological study of this specific failure mode as it directly affects the performance of the studs (top anchorage less sensitive to cracks). In the slabs that presented the failure mode of interest in the present research –such as specimen *LS02* (d_b = 10.0 mm, f_{yw} = 573 MPa, ρ_w = 0.47%)– the transverse elements in the vicinity of the column (square) were generally the most activated with the development of yield stresses prior to failure (Figure 4.21*(a)*). The first row appeared considerably less activated than the second one up to around 90% of the ultimate load, similarly to other observations (Figure 4.16*(b)*) from previous experimental works [Mok82]. This might be related to the formation of tangential cracks potentially intercepting and limiting the force development of the studs. The flexural-based kinematics associated to these specific cracks would tend to activate more the elements the further from the column face (crack less inclined) for a given deformation at the tip. Although the increase of force in the first row appears to be independent of the deformation state of the flexural reinforcement, it is interesting to note that this might not be the case for the second row (points A, B and C in Figure 4.21*(a)*). Regarding the activation of the transverse elements of the third and fourth rows, differences arise only at a load level close to the one associated to the failure of the reference specimen, and therefore most probably resulting from the development of a new crack.

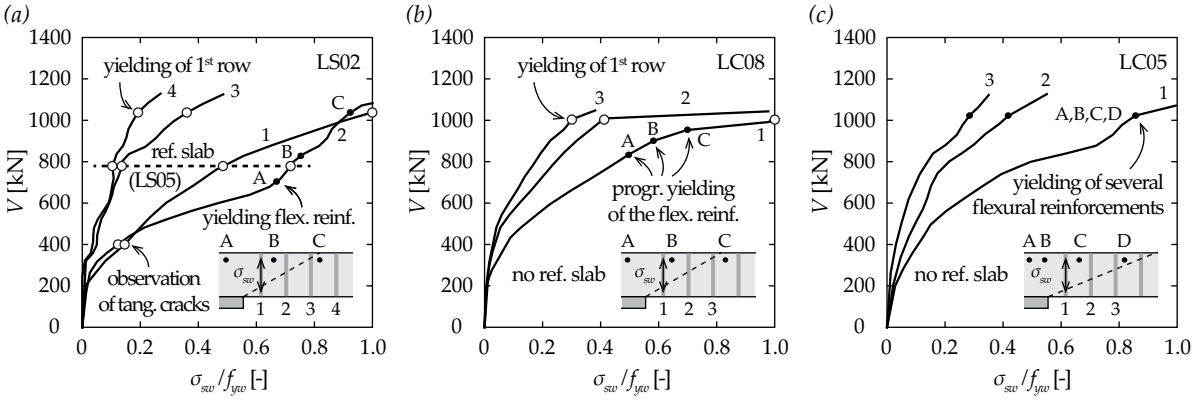

Figure 4.21 Experimental observations (adapted from [Fer10c]): average activation of the transverse reinforcement in the specimens *(a) LS02* (square column, $\rho \approx 1.5\%$); *(b) LC08* (circular column, $\rho \approx 1.6\%$); and *(c) LC05* (circular column, $\rho \approx 2.0\%$)

The comparison with similar slabs (to specimen *LS02*) but with a circular column –specimen *LC08* (d_b = 10.0 mm, f_{yw} = 573 MPa, ρ_w = 0.32%)– is interesting regarding the activation of the transverse reinforcement, since localization phenomena associated to the edges of the square column are avoided. Although in both cases the force development was very similar in the elements of the first and third rows, notable disparities arise in the second row of reinforcement (Figure 4.21*(b)*). With the circular column, the activation of the first row of reinforcement appears to be associated to the progressive yielding of the flexural bars (points A, B and C in Figure 4.21*(b)*). The sudden lack of transverse stiffness –once full capacity is achieved in the first row of transverse elements– leads to the uncontrolled development and propagation of the failure crack from the column to the periphery of the slab with a progressive activation of the following rows of transverse reinforcement. In specimen *LC05* (d_b = 10.0 mm, f_{yw} = 573 MPa, ρ_w = 0.25%) –also with circular column– the activation

of the different rows of reinforcement (Figure 4.21*(c)*) was relatively close to the one previously observed in specimen *LC08*. However, the use of an important amount of flexural reinforcement allowed to delay the yielding of the steel that takes place at a same load level in several positions (points A, B, C and D in Figure 4.21*(c)*). In this specific case, the failure does not result from the yielding of the transverse reinforcement, but the lack of information regarding the internal crack opening –although recognised as a key parameter of the activation of the transverse reinforcement– makes any further interpretations or developments quite complex.

Lips et al. [Lip12b] presented the main results of an experimental campaign on slabs with large amounts of transverse reinforcement –deformed stirrups and studs (rail in the tension side)– disposed around a square column [Lip12a]. This work confirmed that the use of such reinforcement –correctly arranged– enhances both the strength and deformation capacity compared to reference specimens by delaying the development of the critical crack. The slabs reinforced with low-to-moderate amount of deformed studs (radially disposed) –specimens *PL11* (d_b = 10.0 mm, f_{yw} = 592 MPa, ρ_w = 0.23%) and *PL12* (d_b = 10.0 mm, f_{yw} = 592 MPa, ρ_w = 0.47%)– are of major interest with the development of a failure crack intercepting several transverse elements. The measurements of slab expansion highlighted three different successive crack opening phases until the failure of the specimens (Figure 4.22*(a)*). The first one is mainly related to the development of flexural deformations (initial linear part) and takes place until the load corresponds to the failure of the reference slab which is associated to the formation of one (or several) new crack(s). The second one is a transition phase (not linear part) which most likely depends on the stiffness of the transverse system –amount of reinforcement and anchorage performance– controlling more or less efficiently the development of the recently formed cracks. This is supported by the fact that the specimen *PL11* is significantly more sensitive to the latter phenomenon than the specimen *PL12*, which is provided with twice the amount of transverse reinforcement than the latter. The third one is mostly related to shear deformations Δw (plateau) –computed on the basis of the vertical displacement measurements and assuming localization of them at the column face– and was observed to become significant only at a high load level close the ultimate one (Figure 4.22*(b)*). Independently of the shear reinforcement ratio, the slab expansion at failure was systematically larger closer to the column, as already previously observed. The present measurements indicate that the proportion resulting from shear deformations might be related to the quantity of transverse reinforcement. Indeed, the shear deformations represent only around 25% of the crack opening at failure for specimen *PL11* (ρ_w = 0.23%), but this value tends to 75% for specimen *PL12* (ρ_w = 0.47%). This suggests that for large transverse reinforcement ratio the shear deformations might be of primary importance for this specific failure mode. It is also interesting to observe the appreciable ductility post-failure provided by the interception of the failure crack with several rows of transverse elements (compared to the reference specimen *PV1*). The activation of the transverse reinforcement (Figure 4.22*(c)*) appears strongly related to the crack development and is consistent with the highlighted kinematics (Figure 4.22*(a-b)*), with the distinction of several phases. In general, it appears that most of the shear force is carried out by those elements closest to the column. Similarly, the

main differences between the tested specimens arise mainly after the load corresponding to the failure of the slab without transverse reinforcement. The force development in the studs of specimen *PL12* was then observed to be more important and progressive than in specimen *PL11*, as a larger transverse stiffness was provided. In this sense, most of the transverse reinforcement activation at failure of specimen *PL12* –around 80%– resulted from a kinematics not related to shear deformations. The fact that the elements of the first row of reinforcement carry less force than the ones of the second row might be associated to some anchorage limitations, as consequent crack openings were measured on the surface of the slab (up to 3 mm in this specific position). Due to the relatively limited stiffness associated to specimen *PL11*, only the sudden development of shear deformations prior to failure contributes greatly –around 50%– to the activation of the first and second rows of studs at ultimate load. Although the specimens were relatively similar in terms of disposition and amount of transverse reinforcement, the activation mechanisms appeared to be potentially relatively different, thus confirming the complexity associated to this failure mode.

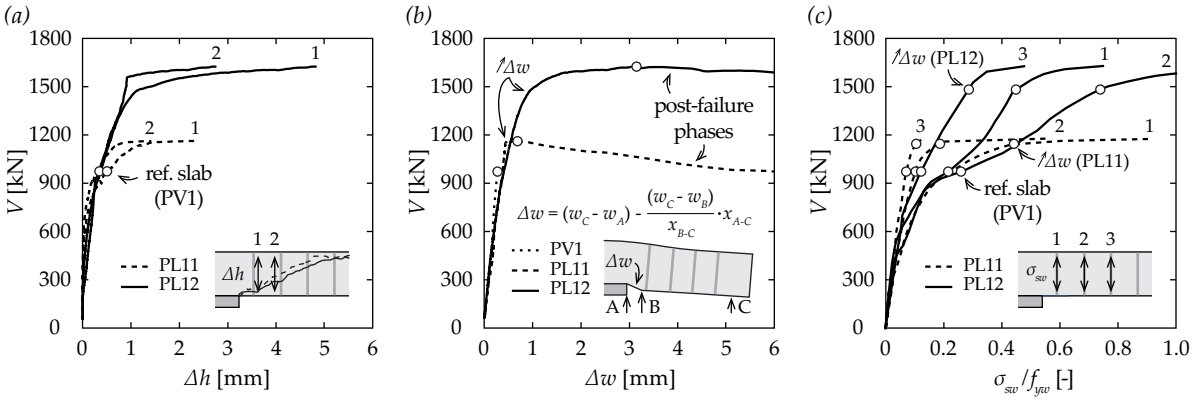

Figure 4.22 Experimental observations (adapted from [Lip12a]): *(a)* slab expansion (weak axis, up to failure load); *(b)* shear deformations (computed based on deflections measurements, weak axis); and *(c)* average activation of the transverse reinforcement (up to failure load)

The punching test *PB2* (d_b = 10.0 mm, f_{yw} = 590 MPa, ρ_w = 0.79%) performed at EPFL for the validation of a patented system of transverse reinforcement with UHPFRC blocks [WIP10] (partially reported in [Ein16a]) uniformly distributed around a square column (as in Figure 4.7*(d)*) confirms several of the problematics highlighted in the present chapter. To ensure the anchorage quality of the new reinforcing system, preliminary pull-out tests were conducted [Kun11]. Comparisons were done with respect to a similar detail –90° bends– embedded only in normal strength concrete (instead of UHPFRC). The use of such high performance material significantly improved the bond behaviour and the admissible bearing stresses under the bend, limiting considerably the risk of splitting of the concrete test specimen (160 x 160 x 100 mm cubes). Although the non-uniform distribution of the steel fibres in the anchorage block led to a certain variability of the slip at ultimate load, all the tested elements achieved yielding of the bar with considerable reduction of the slip compared to the classical solution (Figure 4.23*(a)*). These observations confirmed the potential interest of this new anchorage detailing. Nevertheless, as previously highlighted (see Chapter 2), the simplicity of the performed standardized tests [SIA89] might not be conservative regarding the performance of the system in its specific application conditions. In the case of punching, the sup-

port conditions of the anchorage of the transverse elements during the activation are more concentrated into an inclined strut than on a uniform horizontal surface [Reg80a, Reg00]. Also, a better behaviour than the one measured in the standardized pull-out tests is expected for the anchorage in the compression side of the slab due to the presence of a favourable state of stress (bond considerably improved by external confinement). The disposition of the transverse elements directly in contact with the bottom surface of the slab –reduced cover of the related steel ensured through the use of a dense concrete matrix– limits considerably the problems of delamination, that are shown to be a potential issue in punching with transverse reinforcement. Generally, the performance of the anchorage in the tensile side of the slab is the critical point of most of the transverse reinforcement systems, being affected by the presence of various flexural-based cracks (see Section 4.2). The strain measurements tend to support the latter remark with the observation of a clear distinction between the behaviour of both bottom and top anchorages (Figure 4.23*(b)*). The favourable conditions in the compression part of the slab led to a progressive, stable and efficient activation of the transverse reinforcement (dashed lines) up to the development of some anchorage limitations in the tensile part (solid lines).

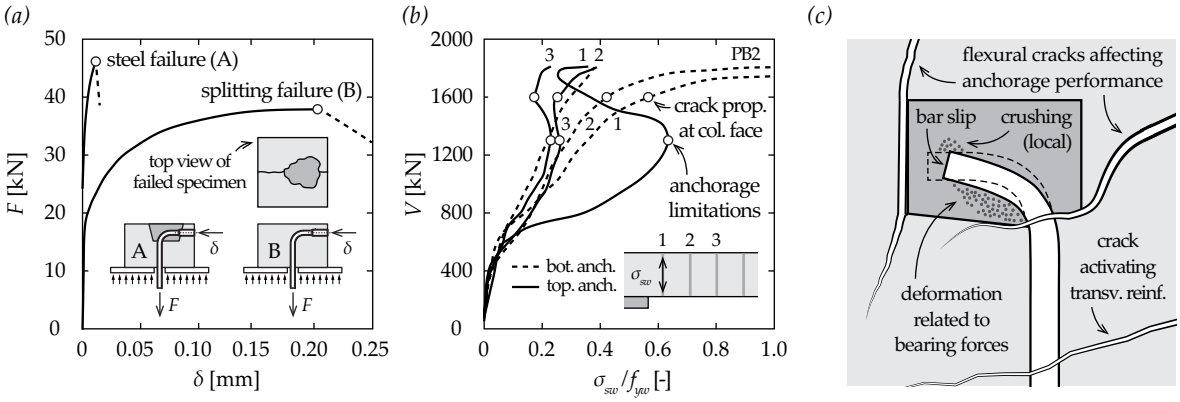

Figure 4.23 Experimental observations: *(a)* average force-slip relationships from pull-out tests of bend bar details in ultra-high fibre reinforced concrete block [Kun11]; *(b)* activation of the transverse reinforcement (weak axis); and *(c)* representation of the top anchorage of the first row of transverse element (as observed on the saw-cuts after the punching test)

The saw-cuts performed after the punching test in the main axes confirmed the latter thoughts. A straightening of the bar together with a partial failure of the UHFPRC block were observed (Figure 4.23*(c)*), resulting from a limited bond performance under these severe conditions. The additional slip associated to this phenomenon is likely to have contributed to the progressive decrease of the activation of the top anchorages leading to a redistribution of forces with the bottom ones. The gradual loss of transverse stiffness precipitate the development and propagation of the failure crack in the specimen. Although the system showed some limitations, it considerably improved the strength and deformation capacity of the reinforced slab compared to the reference specimen [Ein16a]. It has to be noted that if the top anchorages could have been fully activated, the slab would most likely have been able to achieve its flexural capacity. In this sense, this experimental work itself summarizes well the potential issues and possible interactions between the anchorage of the transverse reinforcement and the punching of flat slabs.

4.5 Main code provisions

The design of flat slabs against punching requires the definition of the adequate amount, disposition and type of transverse reinforcement providing the necessary load-carrying capacity to resist the solicitations, without developing any of the previously mentioned possible failure modes (see Section 4.3). The failure within the shear-reinforced area governs the amount of transverse reinforcement needed: the bar diameter (d_b) and the number of elements on a perimeter (n_t). The failure outside of the shear-reinforced area dictates its extension: the required number of perimeters (n_r). The failure of the first concrete strut –or crushing failure– defines the maximum achievable punching strength for each reinforcing system. The latter is therefore of interest when the applicability of a given type of transverse reinforcement has to be confirmed for a particular case.

In the following, the provisions of the main codes of practice [ACI14, CEN04, FIB13] are depicted regarding the punching phenomenon of symmetric interior slab-column connections reinforced with transverse elements. It is supposed that the transverse reinforcement is adequately disposed in the shear-critical area and detailed to be properly activated, without the development of any of the secondary failure modes (outside the shear-reinforced area or in-between transverse elements). For consistency and comparison purposes, the notation of the formulations –systematically in SI-units format– was reworked and all safety factors were taken equal to 1.0.

In all the considered code provisions, the punching resistance is verified by comparing a nominal shear stress (v) on a control section to the nominal shear strength of that section (v_R). The shear stress is defined as:

$$v = V/(b_0 \cdot d) \tag{4.8}$$

where V is the concentrated load acting on the slab, b_0 is the control perimeter (its definition varies between the codes) and d is the effective depth of the slab (mean value of the two main directions).

4.5.1 ACI 318-14 (2014)

In the American punching provisions [ACI14], the control perimeter ($b_{0,ACI}$) is located at a distance of $0.5 \cdot d$ from the column face. In the case of square or rectangular columns, the corners of the control perimeter are not rounded.

For square interior columns with $c < 4 \cdot d$ and normal strength concrete, the concrete contribution to the nominal shear strength is calculated as:

$$v_{R,c,ACI} = 0.33 \cdot f_c^{1/2} \tag{4.9}$$

where f_c is the concrete cylinder compressive strength in MPa.

The punching shear strength of slabs reinforced with transverse elements is:

$$v_{R,cs,ACI} = 0.5 \cdot v_{R,c,ACI} + \rho_{w,ACI} \cdot f_{yw} \leq 1.5 \cdot v_{R,c,ACI} \tag{4.10}$$

In the case of double-headed studs (also complying with stricter detailing rules):

$$v_{R,cs,ACI} = 0.75 \cdot v_{R,c,ACI} + \rho_{w,ACI} \cdot f_{yw} \leq 2 \cdot v_{R,c,ACI} \tag{4.11}$$

The shear reinforcement ratio ($\rho_{w,ACI}$) is defined as:

$$\rho_{w,ACI} = A_{sw} / \left(b_{0,ACI} \cdot s_r \right) \tag{4.12}$$

where A_{sw} is the total reinforcement area on one perimeter of transverse reinforcement units and s_r is radial spacing between the perimeters.

4.5.2 Eurocode 2 (2004)

According to the European punching provisions [CEN04], the concrete contribution to the nominal shear strength at a control perimeter ($b_{0,EC}$) –with edges rounded– located at a distance $2 \cdot d$ from the column face is:

$$v_{R,c,EC} = 0.18 \cdot k \cdot \left(100 \cdot \rho \right)^{1/3} \cdot f_c^{\,1/3} \geq 0.035 \cdot k^{3/2} \cdot f_c^{\,1/2} \tag{4.13}$$

where ρ is the flexural reinforcement ratio (geometric mean of two perpendicular directions, taken at most 2.0%, f_c is the concrete cylinder compressive strength in MPa and $k = \left(1 + \sqrt{200/d} \right) \leq 2$ is a size effect factor, with the effective depth d in mm.

The nominal shear strength of slabs with transverse reinforcement is (according to a recent amendment [CEN14]):

$$v_{R,cs,EC} = 0.75 \cdot v_{R,c,EC} + 1.5 \cdot \rho_{w,EC} \cdot f_{yw,ef} \cdot \sin\beta \leq k_{max} \cdot v_{R,c,EC} \tag{4.14}$$

where β is the angle between the transverse elements and the plane of the slab, the effective yield strength of the latter reinforcement is $f_{yw,ef} = 1.15 \cdot \left(250 + 0.25 \cdot d \right) \leq f_{yw}$ in MPa, with d in mm and account for the limited activation in thin slabs, k_{max} is a recent factor which is recommended to 1.5 but higher values may be considered if they are experimentally validated [CEN14], notably for closed stirrups or double headed studs.

The shear reinforcement ratio ($\rho_{w,EC}$) is defined as:

$$\rho_{w,EC} = A_{sw} / \left(b_{0,EC} \cdot s_r \right) \tag{4.15}$$

An additional verification has to be performed at the periphery of the loaded area [CEN10], where the shear stress has to be lower than:

$$v_{R,c,EC(0d)} \leq 0.24 \cdot \left(1 - \frac{f_c}{250} \right) \cdot f_c \tag{4.16}$$

4.5.3 *fib* Model Code 2010 (2013)

The punching provisions of MC 2010 [FIB13] are based on the CSCT [Mut08a]. Similarly, the control perimeter (b_0) is located at a distance $0.5 \cdot d$ from the column face and the corners have to be rounded for a square column.

The failure criterion of the CSCT (Figure 4.2) was validated with 99 tests from literature and calibrated to provide a mean value of the test capacities. Thus, for MC 2010, the original formulation –Eq.(4.1)– was modified to correspond to the characteristic value of the test results as:

$$v_{R,c,MC} = \frac{1}{1.5 + 0.9 \cdot \psi \cdot d \cdot k_{dg}} \cdot f_c^{1/2} \tag{4.17}$$

where, $k_{dg} = 2/\left(1 + d_g / d_{g0}\right) \geq 0.75$ with d_g the maximum aggregate size and d_{g0} a reference aggregate size (16 mm).

In axisymmetric cases, the relationship between the applied load (V) and the slab rotation (ψ) can be calculated by integrating the tangential moments between the centre of the column and the line of moment contraflexure [Mut08a]:

$$V = \frac{2\pi}{r_q - r_c} \cdot \left(m_r \cdot r_0 + \int_{r=r_0}^{r=r_s} m_{t,i}(\chi) dr \right) \tag{4.18}$$

where r_q is the distance between the centre of the column and the resultant of the load applied on a slab sector, the radius of the column r_c (taken as half of the column side length in the case of square columns) and r_s is the distance between the centre of the column and the line of moment contraflexure (taken as half of side length in the case of square specimens).

The quadrilinear model –from which the latter formulation derives– makes a distinction between the inner and outer parts of the slab with respect to an inclined crack (Figure 4.24). The inner core is assumed to have constant curvatures and moments in both radial and tangential directions. The outer part –where a segment is usually considered for the equilibrium– is assumed to undergo rigid body in the radial direction. Therefore, the slab deforms accordingly to a conical shape.

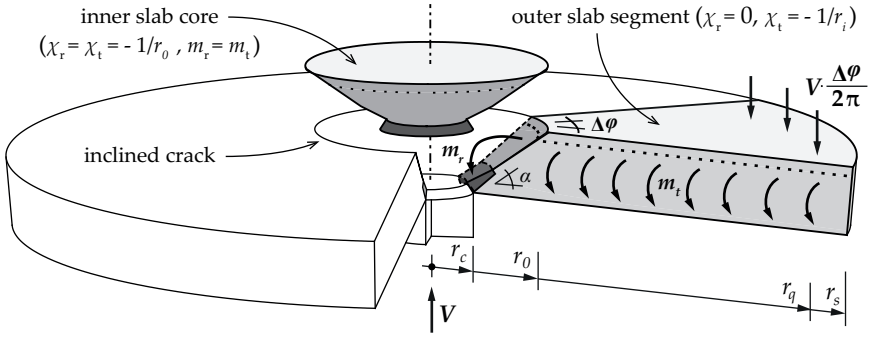

Figure 4.24 Quadrilinear model [Mut08a]: definition of the main parameters and related assumptions

The tangential moment (m_t) is calculated using a 4-linear moment-curvature law [Mut08a] with:

$$\chi_{t,i} = -\psi / r_i \geq -\psi / r_0 \tag{4.19}$$

where ψ is the slab rotation and r_0 is the distance from the centre of the slab to the point where the inclined critical shear crack (assumed angle of α = 45°) reaches the level of the flexural reinforcement, taken as $r_0 = r_c + d \cdot \tan 45°$.

According to MC 2010, the load-rotation relationship can be estimated in a simplified manner. In Level of Approximation II (recommended for a typical design of new structures), the rotation of the slab can be estimated with a relationship depending on the acting moment in the column strip as:

$$\psi = 1.5 \cdot \frac{r_s}{d} \cdot \frac{f_y}{E_s} \cdot \left(\frac{m_S}{m_R} \right)^{3/2} \tag{4.20}$$

where r_s is the radius of an isolated slab (taken as half of the side length for square specimens) or $0.22 \cdot L$ in the case of a continuous slab with regular span lengths, f_y and E_s are respectively the yield strength and modulus of elasticity of the flexural reinforcement, m_R is the moment capacity of the slab and m_S is the average acting moment in the column strip that, for interior columns in slabs with sufficiently regular geometry, can be approximated as $m_S = V/8$.

In the case of slabs with transverse reinforcement, the reinforcement contribution is accounted by adding to the concrete contribution the stresses in the elements crossed by the critical crack [Fer09]:

$$v_{R,cs,MC} = v_{R,c,MC}(\psi) + \rho_{w,MC} \cdot \sigma_{sw}(\psi) \leq k_{sys} \cdot v_{R,c,MC}(\psi) \tag{4.21}$$

where $\rho_{w,MC} = A_{sw} / (b_0 \cdot s_r)$ is the shear reinforcement ratio, and k_{sys} is a parameter that depends on the type of transverse elements describing the maximum punching resistance. In MC 2010, the recommended values of k_{sys} are 2.4 for stirrups and 2.8 for double-headed studs or 2.0 for any other details (not related to the previously mentioned ones). For specific systems, other values – potentially higher than the ones recommended– may be used after the performance was experimentally validated and quantified.

The stress in the transverse reinforcement (σ_{sw}) is calculated assuming an element placed $0.5 \cdot d$ from the column face:

$$\sigma_{sw} = \frac{E_s \cdot \psi}{6} \left(1 + \frac{\tau_{b,0}}{f_{yw}} \frac{d}{d_b} \right) \leq f_{yw} \tag{4.22}$$

where E_s is the modulus of elasticity, $\tau_{b,0}$ is an average bond stress in uncracked conditions (for deformed bars, a value of 3 MPa is recommended), f_{yw} and d_b respectively the yield strength and the bar diameter of the transverse reinforcement.

4.5.4 Comparison

The predicted influence of the amount of transverse reinforcement on the punching strength of a flat slab is presented in Figure 4.25 according to the main current code provisions. Different flexural reinforcement ratios were selected in order to represent several possible situations of practice. It has to be noted that for low to moderate amount of flexural reinforcement (ρ = 0.33 ÷ 0.75%) the ultimate load might be governed by the flexural capacity of the slab (the latter limit is not represented in the following figures).

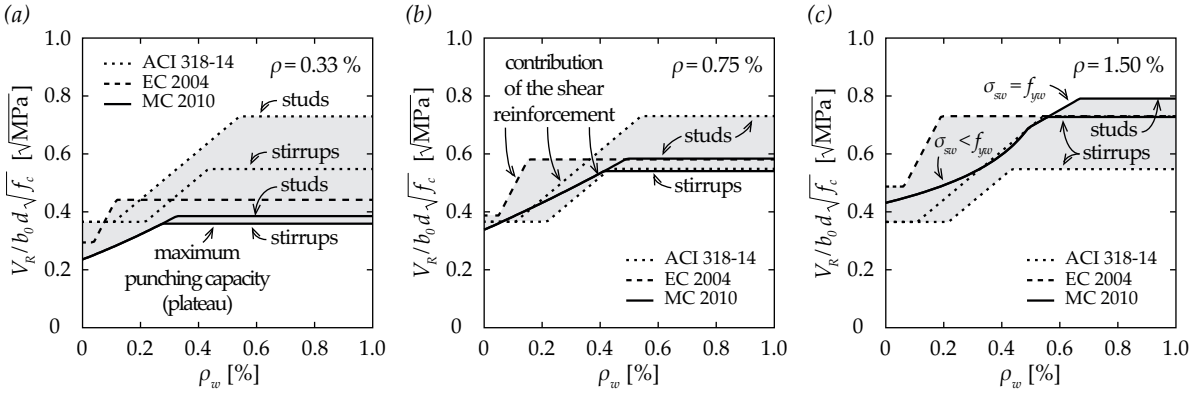

Figure 4.25 Influence of the amount of shear reinforcement (ρ_w) on the punching strength for various flexural reinforcement ratios (ρ): *(a)* low, *(b)* moderate and *(c)* large (slab span of 7.3 m; d = 210 mm; c = 260 mm; f_y = 550 MPa; f_{yw} = 450 MPa; f_c = 35 MPa; d_g = 16 mm)

Based on the CSCT, the MC 2010 [FIB13] (solid lines in Figure 4.25) distinguish three regimes depending on the amount of transverse reinforcement: failures within the shear-reinforced area associated to partial or full activation of the transverse reinforcement (see Section 4.3.2) and the maximum punching capacity (see Section 4.3.1). According to MC 2010, the latter regime is only a function of the type of transverse reinforcement considered –independently of its amount– and the differences amongst them become more significant for larger amounts of flexural reinforcement. Although the activation of the transverse element is theoretically less efficient in the latter case, experimental evidences confirm that yielding of the transverse elements can generally be achieved even for very limited rotations at failure (prestressed slender slabs or footings). Also, unlike most of the other codes, these provisions allow the determination of the deformation capacity in terms of rotation associated to the punching strength, of major importance regarding the assessment of the ductility of the structure.

In the American provisions –ACI 318-14 [ACI14], dotted lines in Figure 4.25– the reinforcing system also has an influence on the maximum achievable punching strength, with a distinction between stirrups, studs or structural steel shearheads (not presented). Also, the concrete contribution to the punching strength is considered to be higher in the case of studs compared to stirrups, leading to an earlier activation of the steel contribution. The main particularity of these recommendations is to be completely independent of the flexural reinforcement ratio.

In the European provisions –EC 2004 [CEN04], dashed lines in Figure 4.25– the punching strength used to be independent of the type of transverse reinforcement, although several investigations clearly pointed out large disparities amongst them (see for instance [Ein16a]). A recent amendment [CEN14] was introduced in this sense to allow an increase of the maximum punching capacity if the system was experimentally validated through a specific test campaign. Also, the amount of flexural reinforcement affects significantly differently the regimes related to the maximum capacity and to the activation of the transverse reinforcement, the latter being the less influenced.

In general, the provisions presented consider the same activation for all the types of transverse reinforcement, in spite of the notable differences highlighted in experimental works (see Section 4.4). This implies indirectly the strong assumption of perfect anchorage conditions, even though several observations were reported regarding anchorage limitations. In this sense, the recent and pragmatic proposition of Walkner [Wal14] is of great interest in the frame of the present research, with a distinction of the activation between stirrups and studs, being better for the latter one.

It can be concluded that a significant scatter exists between the main codes for some given conditions (grey area in Figure 4.25), mainly related to the different bases on which each of them is formulated. Also, for low shear reinforcement ratio, the limited disparities observed in the activation phase between the predictions is related to the fact that, for these conditions, the failure is associated to large rotations for which the contribution of the transverse elements is generally very close to the full capacity (yielding of the steel). For the cases presented, MC 2010 tends to be relatively conservative regarding the amount of transverse reinforcement required to achieve the punching strength in comparison to other provisions.

Although it is generally well accepted that the use of transverse reinforcement improves both the strength and the deformation capacity of the reinforced slab, experimental evidences highlighted the differences between various reinforcing systems (Figure 4.8). Aware of the potential limitations associated to the disparities of anchorage performance, additional requirements regarding the ductility at failure of the reinforced slab were recently introduced in this sense in some code provisions [FIB13, SIA13]. Although the latter proposition has the merit of providing to the designers an objective concerning the deformation capacity of the structure, significant differences between the failure modes of a reinforced slab were experimentally confirmed (Figure 4.10*(b)* and Figure 4.19*(a)*). In the context of plastic redistribution, the failure mode within the shear-reinforced area should be targeted as an objective, being the one providing the most significant ductility at failure due to the contribution of the transverse elements intercepted by the failure crack.

4.6 Synthesis

Since punching was recognized as the governing phenomenon for the design of flat slabs in the middle of the 20th century, extensive research was conducted (see Section 4.1), notably on the influence of the transverse reinforcement that appeared to be the most practical and efficient solution to enhance the structural response. The presence of transverse elements in the vicinity of the column provides locally an additional transversal stiffness to the slab and delays the opening of the internal cracks in this critical region. Both the strength and deformation capacity of the slab are usually improved, yet various disparities in the related contributions were highlighted between the reinforcing systems. The force transfer mechanisms involved in the activation of the transverse reinforcement are affected by the severe conditions –such as cracking (see Section 2.3)– developing during punching phenomenon (see Section 4.2). Amongst all, the anchorage performance has a crucial role in most of the failure modes for slabs reinforced with transverse reinforcement (see Section 4.3), by influencing the support of the first concrete strut and the transversal stiffness related to the development of internal cracks. Most of the main code provisions consider these differences in the maximum punching strength (see Section 4.5), yet the activation of the transverse elements is assumed to be similar for all types of system (although the contrary was experimentally confirmed). It has to be noted that the use of more efficient punching reinforcing systems –such as studs– is generally associated to stricter detailing recommendations (regarding the position, layout and extent of the elements around the column) compared to standard solutions such as stirrups. Limited investigations were specifically dedicated to the study of the failure within the shear-reinforced area, but the observations thoroughly selected –and systematically reworked– from literature (see Section 4.4) allowed to highlight the following interesting points:

- Experimental evidences support the fact that the development of the failure crack results either from the yielding of one of the transverse elements, or from a local failure in the compression zone between the column face and the first transverse element;

- The development of the failure crack was observed to be rather associated to the one of a splitting crack, with larger openings at the column face progressively decreasing with the interception of the further transverse elements;

- Several observations confirm that the propagation of the failure crack is performed in both radial and tangential directions, with therefore potential variations of the crack pattern and the relative steel and concrete contributions in the different axes of the slab;

- The development of a failure crack within the-shear reinforced area –intercepting one or several row of transverse elements– contributes significantly to the larger capacity of deformation at failure of the slab compared to any other punching failure mode;

- The activation of shear reinforcement is done through the interception of the transverse elements by several cracks, related to a complex combination of flexural and shear deformations;

- The activation of the transverse reinforcement is a function of the internal cracks kinematics, the location of the intersections, as well as the bond and anchorage performance of the punching system considered. Studs were experimentally recognized as more efficient with respect to other reinforcing solutions –such as stirrups– yet stricter detailing rules are applied;

- Lack of anchorage was experimentally observed during punching due to the severe conditions developing in the phenomenon –important cracking in the vicinity of the column– notably for types of transverse elements involving bond properties (bend bar details);

- The increase of force in the transverse reinforcement is ideally stable and progressive up to yielding of the material, but practically, the associated transverse stiffness can be significantly limited by external conditions with a redistributions of forces between rows leading to an earlier development of the failure crack;

- A relatively low amount of transverse reinforcement has to be provided ($\rho_w \leq 0.5\%$ for studs) in order to guarantee the development of a failure within the shear-reinforced area. For less efficient reinforcing systems (such as stirrups), this limit is expected to be even higher due to the differences in the activation of the elements;

- All the main code provisions consider both concrete and transverse steel in the prediction of the strength related to the failure within the shear-reinforced area. Only the MC 2010 –based on the CSCT– accounts for a simultaneous variation of the relative contributions in the punching phenomenon.

Although the reliability of some of the presented experimental results might be questionable –notably regarding the steel strains or crack opening– several clear tendencies arise among the investigations performed by various researchers for the failure mode of interest. Also, the fact that the majority of the aforementioned works were conducted under different test conditions –and with various types of transverse reinforcement– limited strongly the interpretations or related developments. In this sense, the information gathered in this review of literature aims at supporting the realisation of specific experimental works related on the topic, notably regarding the main aspects to be properly investigated.

A detailed study of the activation of the transverse reinforcement requires therefore systematic and simultaneous measurements of the strains in the transverse elements (even of the forces, to be more accurate), the crack openings (full and partial, to be able to make a distinction between the different cracks), and other useful data such as the vertical deflections (in order to estimate the shear deformations for instance). It might be then possible to highlight conclusions regarding the steel and concrete contributions and to confirm some of the previous phenomenological observations. Also, specific test series are required in order to improve knowledge on this failure mode, often underrated with respect to the one associated to the maximum punching strength.

Chapter 5 Experimental and Theoretical Investigations on the Activation of the Shear Reinforcement in Punching

The literature review on the punching failure mode of interest in the present research –within the shear-reinforced zone– has highlighted the limited information available for its study, and the issues related to the comparisons of the performed investigations amongst them. Since the second half of the 20th century, a significant amount of systems have been developed (see Section 4.1). It has been experimentally confirmed that the correct disposition of transverse reinforcement in the slab-column connection –intercepting the failure crack– contributed to an increase of the strength and deformation capacity of the slab (see Section 4.2). The differences in performance –associated to the quality of the anchorage of the system, its disposition and amount– directly affect most of the failure modes (see Section 4.3). Although this is generally considered in most of the punching theories and current design provisions (see Section 4.5), fundamental disparities exist in these approaches. The activation of the transverse reinforcement is a complex phenomenon due to the important number of parameters involved. It has been investigated by several researchers –rather through empirical approaches– yet no specific conclusions were generally formulated. The thorough review of the punching tests with this failure mode (see Section 4.4) aimed to contribute to this topic by discussing the main test results and related observations.

The present chapter aims to provide experimental evidences to discuss the main assumptions of the Critical Shear Crack Theory (CSCT) regarding the activation of the transverse reinforcement during punching (see Section 5.1). A series of three innovative punching tests on full-scale slab specimens was performed for this purpose (see Section 5.2). The main particularity is related to the use of an independent hydraulic system to control the activation in the first row of transverse reinforcement (systematically monitored with external load cells). Also, the detailed evaluation of the slab expansion in the main axes of the slab allowed to depict the kinematics associated to the activation of the reinforcing elements. The main test results are presented in Section 5.3 in terms of crack openings, forces in the transverse reinforcement, rotation of the slab and shear deformations. The observations highlighted are then used to review the actual theory and its main assumptions (see Section 5.4). Finally, based on the investigations performed in this research, the role of bond and anchorage conditions of the transverse reinforcement in punching is detailed in the frame of the CSCT with the implementation of a refined and extended activation model (see Section 5.5).

5.1 Main issues related to the activation of the transverse reinforcement

The presence of transverse reinforcement in a slab influences the shear force transfer mechanisms. This is particularly true for the punching failure mode within the shear-reinforced area, in which the failure crack develops through the transverse elements, involving both concrete and steel in the phenomenon. It is therefore necessary to consider the individual contribution of both components to accurately predict the related punching strength.

The definition of these contributions and their interactions are not straightforward. As a consequence, assumptions are required not only to quantify the activation of the transverse reinforcement but also to calculate the capacity of the concrete. As most of the main code provisions [ACI14, CEN04] do not consider the slab deformation in their approaches (see Section 4.5), the determination of the associated strength is often reduced to the sum of both steel and concrete components (Figure 5.1*(a)*) multiplied by contributions factors –η_s and η_c, constant values ≤ 1.0– according to their maximum respective contributions (yielding of the transverse reinforcement $V_{R,sy}$, and punching strength of the slab without shear reinforcement $V_{R,c0}$). One of the interesting aspects of Model Code 2010 (MC 2010) [FIB13] –which approach is based on the CSCT [Mut08a, Fer09]– lies in the fact that the sum is done with variable terms –possible partial activation of the transverse reinforcement for instance– depending on the effective state of deformation of the slab. It implies the acceptance of two main assumptions of the theory related to the failure criterion (Figure 5.1*(b-c)*) –never experimentally confirmed– and the simplified crack kinematics considered (Figure 5.1*(a)*).

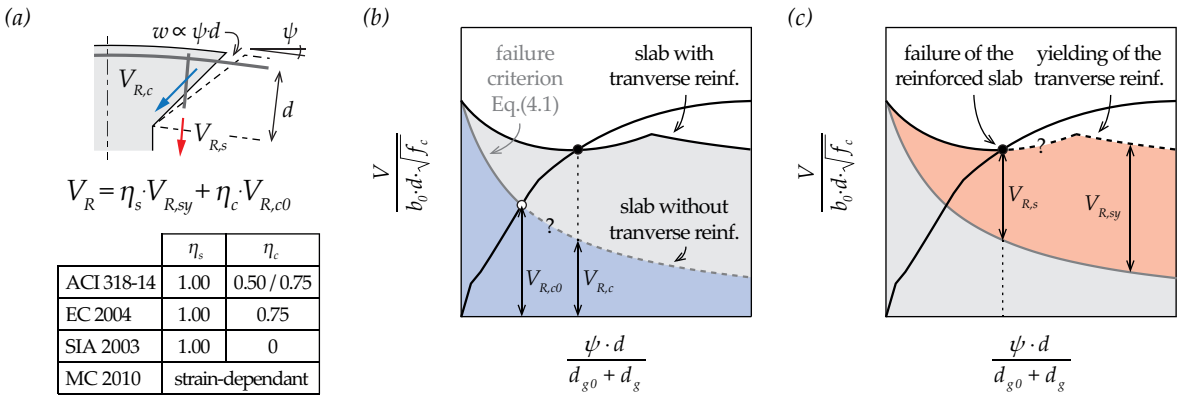

	η_s	η_c
ACI 318-14	1.00	0.50 / 0.75
EC 2004	1.00	0.75
SIA 2003	1.00	0
MC 2010	strain-dependant	

Figure 5.1 Punching failure mode within the shear-reinforced area: *(a)* disparities in the contributions factors (η) for the determination of the strength for the main code provisions; and *(b-c)* main assumptions of the CSCT (regarding concrete and steel)

The first assumption (Figure 5.1*(b)*) is related to the concrete contribution ($V_{R,c}$) that is assumed to be defined by the same failure criterion used for slabs without transverse reinforcement ($V_{Rc,0}$). This indirectly implies that the shear-carrying capacity of the theoretical concrete strut decreases (from $V_{R,c0}$ to $V_{R,c}$) for the increased rotations associated to the use of transverse elements in the slab. The second assumption (Figure 5.1*(c)*) is related to the redistribution of shear forces at failure. The systematic activation of the transverse reinforcement up to its yielding capacity ($V_{R,sy}$) –as the contribution of the concrete is potentially becoming negligible with increasing deformations ($V_{R,c} \rightarrow 0$)– must be investigated. This punching test series aims to review and discuss these two fundamental hypotheses in detail by providing experimental evidences of the aforementioned phenomena.

The original idea was related to the accurate definition of one of both contributions involved in the failure mechanism. In this sense, the definition of the steel contribution appeared as the most evident to evaluate, by using post-installed elements –locally unbonded– combined with external load cells. Although the consideration of such reinforcing system markedly limited the transverse stiffness provided in the critical zone in the vicinity of the slab-column connection, it also ensured the development of the failure mode of interest (low amount of shear reinforcement).

With respect to the test procedure, it seemed necessary to disturb the internal transfer mechanisms and observe the instauration of the new equilibrium (see Figure 5.2*(a)*) in order to study the redistribution of forces and the pertinence of the failure criteria. By acting on the opening of the critical shear crack, it is theoretically possible –according to CSCT– to control the contribution of the concrete ($V_{R,c}$) to the punching strength. A specific device was therefore designed to adjust the force in the elements of the first row of transverse reinforcement ($V_{R,s}$) independently of the load acting on the slab (V). In order to have a state of internal cracking representative of the one at failure, the main idea was to maintain at a constant value the opening of the critical shear crack (w) obtained at a load close to the failure of the reference specimen ($V_{R,c0}$). This test phase could potentially be limited by the development of other punching failure modes, not of interest in the present investigation (such as crushing of the first strut). Similarly, as the yielding of the transverse reinforcement would lead to an uncontrolled propagation of the internal cracks, steel with high yield strength was selected for the reinforcing elements expected to be critical (first row of transverse reinforcement).

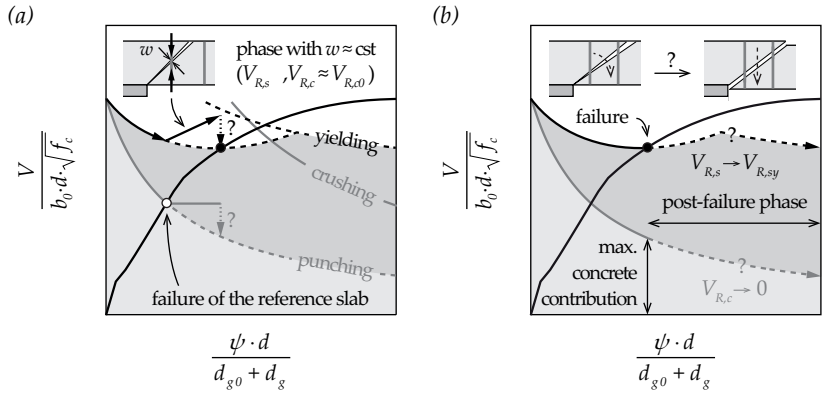

Figure 5.2 Proposed test procedures to investigate the main assumptions of the CSCT in relation with the failure mode within the shear-reinforced area for slabs with transverse reinforcement: *(a)* failure criterion for concrete contribution + redistribution of internal forces; and *(b)* maximum strength considered and internal crack development

To investigate the maximum strength associated to this failure mode –$V_{R,s}$ + $V_{R,c}$ or $V_{R,sy}$– the specimen was monolithically loaded up to failure (see Figure 5.2*(b)*), also to not influence the development of the cracks and the internal redistributions. Additionally to the aspects associated to the failure criterion, the kinematics of the cracks activating the elements of the transverse reinforcement during punching was evaluated to discuss the related main assumptions of the CSCT. The role and the interaction between shear and flexural deformations in the phenomenon of activation are notably investigated. For the latter, the second procedure presented also seems more appropriate, as the crack pattern –and the related deformations– are in this case not affected.

5.2 Experimental campaign of punching tests

The punching test series performed in this research (see Section 5.2.1) consisted of three full-scale slab specimens with the same dimensions (3000 x 3000 x 250 mm) and flexural reinforcement ratio (ρ =1.5%), similarly to previous studies performed at EPFL [Lip12b]. The investigated parameters were limited to the transverse reinforcement, which amount (ρ_w) was kept relatively low in order to ensure the development of the failure mode of interest. Headed-like systems were considered for the type of transverse reinforcement –studs or post-installed elements with external plates– in order to minimize the issues related to anchorage conditions for an optimal activation of the details. Also, to facilitate further interpretations and comparisons with existing tests, the test setup was kept identical in its properties to the one used in previous similar works (Figure 5.3).

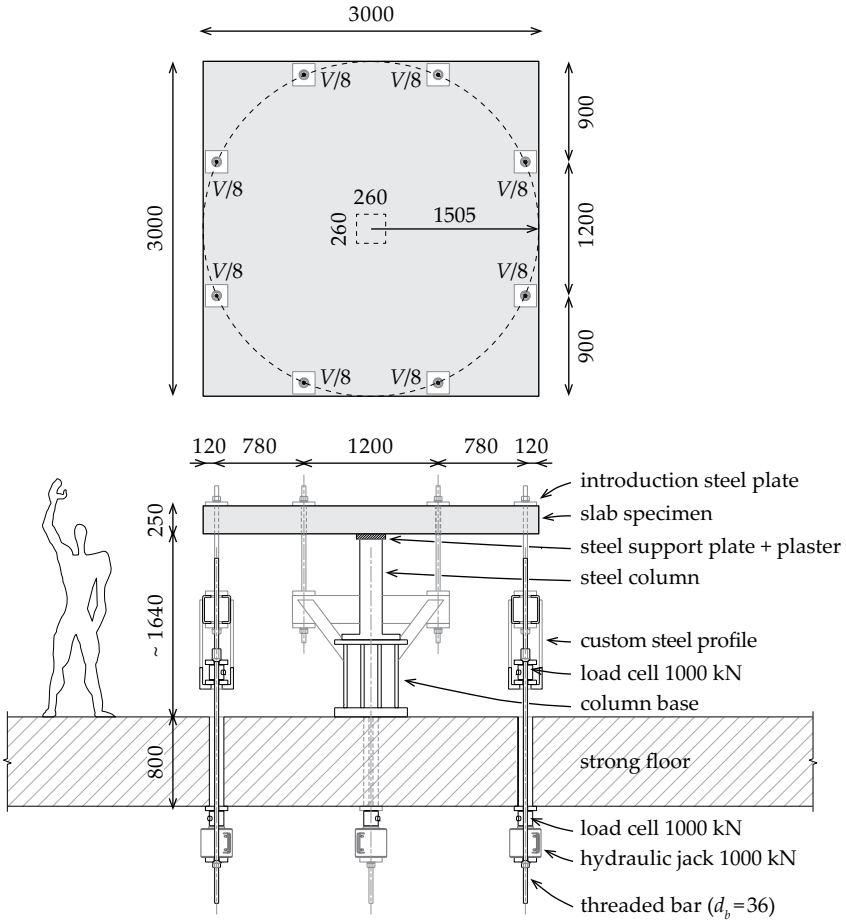

Figure 5.3 Characteristics of the test setup for the experimental campaign of punching tests on reinforced concrete slab specimens with transverse reinforcement (dimensions in [mm])

The first test –specimen *PB4* (see Section 5.2.2)– aimed at validating several aspects related to the specificities of this experimental program, such as the device for the control of the force in the transverse elements, the measurement systems or the test procedure. On that basis, improvements were then brought to specimens *PB5* and *PB6* (see Sections 5.2.3 and 5.2.4) that represent the central part of the punching test series. These investigations took place at the laboratory of the IIC of the EPFL –similarly to the campaign of pull-out tests– from November 2013 to November 2014.

5.2.1 Specimen properties, testing devices and performed measurements

The main characteristics of the reinforced slabs investigated are detailed in Figure 5.4. For all the specimens, the flexural reinforcement layout was orthogonal and parallel to the slab edges with a nominal spacing (s) between the bars of 100 mm (locally adapted to consider the presence of the transverse elements). A concrete cover of 20 mm was provided to the bars leading to an effective height of 210 mm (d). The column was square with dimensions 260 x 260 mm. The transverse reinforcement was disposed radially in 8 radii (n_r) around the column –according to the main axes of the specimen– with additional elements in-between them to prevent the development of other failure modes (disposed > 2·d). The main parameters of the slabs are summarized in Tables 5.1 and 5.2.

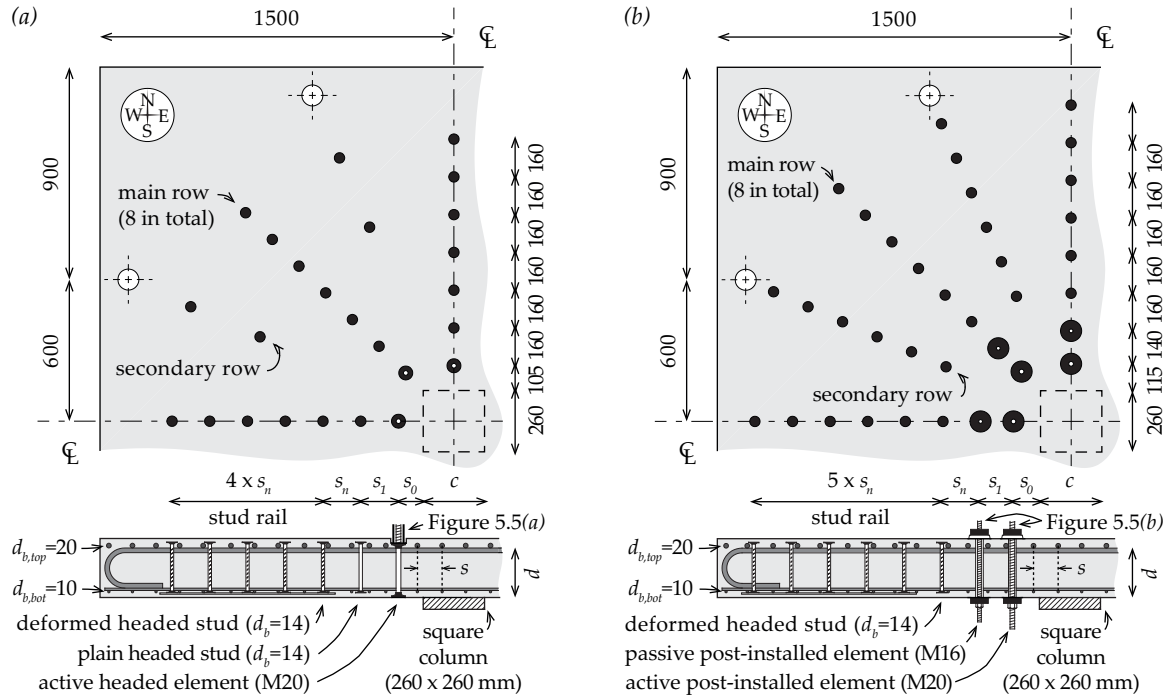

Figure 5.4 Reinforcement details of the slabs (dimensions in [mm]): *(a) PB4*; and *(b) PB5*-6

Table 5.1 Main parameters of the test specimens

Specimen	$f_{c,test}$ [MPa]	d [mm]	$d_{b,top}$ [mm]	f_y / f_t [MPa]	ρ [%]	d' [mm]	$d_{b,bot}$ [mm]	f_y / f_t [MPa]	ρ' [%]
PB4	37.5	207	20	590 / 686	1.52	45	10	579 / 619	0.38
PB5	34.2	205	20	543 / 637	1.53	36	10	533 / 609	0.38
PB6	33.3	205	20	543 / 637	1.53	34	10	533 / 609	0.38

Table 5.2 Main parameters of the transverse reinforcement

Specimen	s_0 [mm]	s_1 [mm]	s_n [mm]	n_r [-]	n_t [-]	ρ_w [%]
PB4	105	160	160	8	7	0.10 (1)
PB5	115	140	160	8	8	0.13 (1)
PB6	115	140	160	8	8	0.13 (1)

(1) computed assuming an equivalent diameter of the system

For all specimens, a normal strength concrete with a maximum aggregate size of 16 mm (d_g) was used (compressive strength determined on 160 x 320 mm cylinders). Regarding the steel, hot-rolled bars (*Topar-S*, B500C) and cold-rolled de-coiled rods (*Topar-R*, B500B) were respectively used for the top ($d_{b,top}$ = 20 mm) and bottom ($d_{b,bot}$ = 10 mm) flexural reinforcement. For the transverse reinforcement, threaded bars were generally used for the first two rows (cold-rolled M16 4.6 and hot-rolled M20 10.9, both of ductility class A) and the rest was composed of standard studs (d_b = 14 mm) made of hot-rolled bars (*BST 500*, B500B). The main properties can be found in Table 5.3.

The test procedures implied to control all the elements of the first row of transverse reinforcement simultaneously, and independently of the load acting on the slab. The disposition of hydraulic jacks –displacement controlled– associated to the use of unbonded bars allowed local adjustments of the crack opening and the related activation of the transverse reinforcement (Figure 5.5).

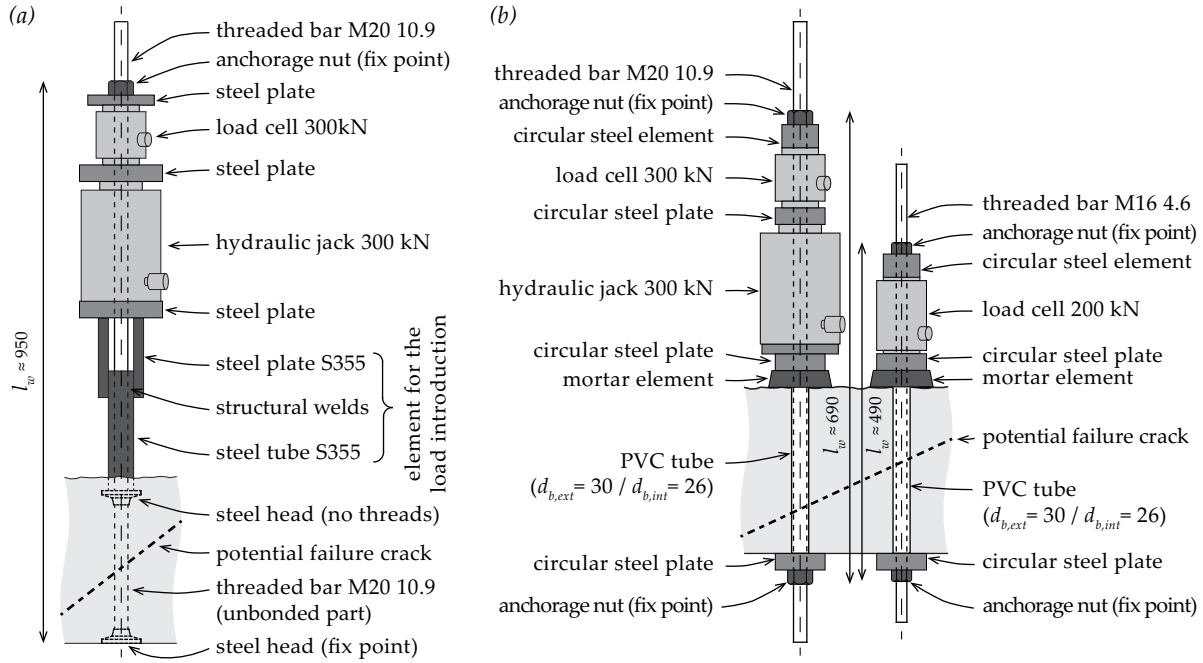

Figure 5.5 Details of the specific transverse reinforcement system considered in the punching tests (dimensions in [mm]): *(a)* 1st row of *PB4*; and *(b)* 1st and 2nd rows of *PB5*-6

Table 5.3 Main parameters of the 1st and 2nd rows of transverse reinforcement

Specimen		Type [-]	Surface [-]	d_b [mm]	l_w [mm]	E_{sw} [MPa]	f_{yw} - $f_{yw0.2}$ / f_{tw} [MPa]
PB4	1st row	M20 10.9	plain (1)	7 (3)	950	203921	1130 / 1179
PB5		M20 10.9	plain (2)	8 (3)	690	203921	1130 / 1179
PB6		M20 10.9	plain (2)	8 (3)	690	203921	1130 / 1179
PB4	2nd row	studs	plain (1)	14	210	206807	560 / 659
PB5		M16 4.6	plain (2)	12 (3)	490	207032	510 / 537
PB6		M16 4.6	plain (2)	12 (3)	490	207032	510 / 537

(1) through several plastic sheets disposed around threaded part of the bar

(2) through a PVC tube disposed prior to the casting of the specimen

(3) computed assuming an equivalent stiffness on 210 mm (length of a stud)

Also, for a specific phase of the test (vertical branch in Figure 5.2*(a)*), it was necessary to release the entire system at a given –but limited– rate in order to control the progressive opening of the crack until the failure of the specimen. This was achieved through the use of a special type of valve limiting the hydraulic stream (*Wandfluh SA*). Associated to additional electric valves, the manufactured device (Figure 5.6) allows to increase the force uniformly in the first row of transverse reinforcement –connection in parallel of the 8 elements– but also to momently interrupt the situation and to proceed to the uniform release of pressure in the system (Figure 5.7).

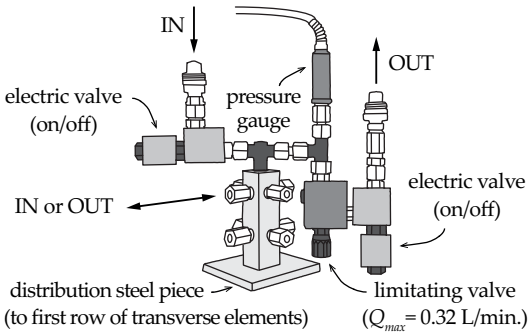

Figure 5.6 Detail of the device developed for the tests in order to centralize the hydraulic system associated to the activation of the first row of transverse reinforcement

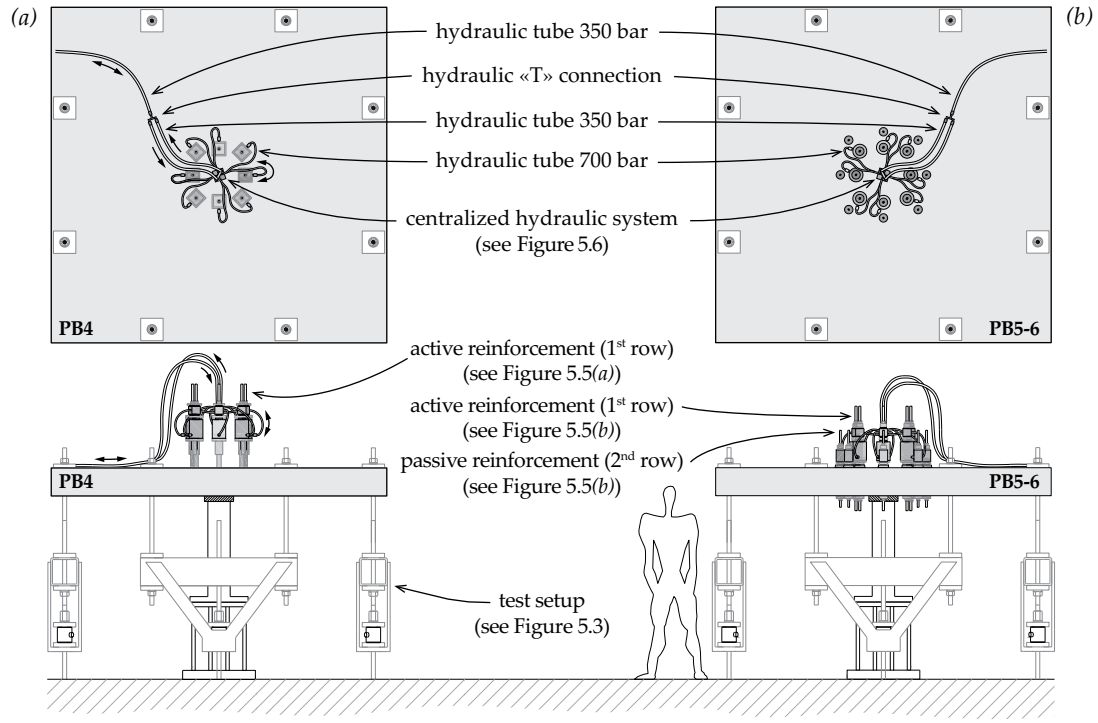

Figure 5.7 External views of the punching tests performed in the present research to investigate the activation of the transverse reinforcement: *(a) PB4*; and *(b) PB5* and *PB6*

During the development of the test, attention was given to keep the stiffness of the system as large as possible. In this sense, the stiffness of each of the individual components of the specific reinforcement (Figure 5.5) associated to the presented device (Figure 5.6) was characterized in a compression test machine. Amongst all, it is the hydraulic jack that was highlighted to be the main

source of losses in terms of stiffness, with significant disparities depending on the amount of stroke available (the shorter, the stiffer). As this appeared to be related to the type and length of the hydraulic tube used to perform the connection, high pressure tubes of the smallest dimension possible were used. The choice of 20 mm diameter threaded bars of high steel class (10.9) ensures a significant activation of the first row of transverse reinforcement without the development of plastic deformations (in order to use the same elements for all the test series). Larger diameters were not considered so as to not further weaken the concrete in the vicinity of the column and to stay representative of the dimensions that could be found in practice in similar cases.

The main improvements brought from the preliminary test (*PB4*) to the main tests (*PB5* and *PB6*) were related to the transverse reinforcement (Figure 5.8). The use of compact post-installed elements with direct introduction of the force on the surface of the slab led to a stiffer reinforcing system. Also, the disposition of a load cell in the second row –also post-installed– significantly improved the definition of the related steel contribution of the transverse reinforcement. Finally, the system was almost equivalent in stiffness to standard studs of diameter 8 mm (length: 210 mm).

Figure 5.8 Main view of the test specimens (*PB5*-6) and details of the related measurement devices (*PB4*) associated to the slab expansion (full and partial thickness variation)

Regarding the performed measurements, a specific attention was given to the accurate evaluation of the crack opening during the punching tests. Inspired from a previous work [Mül84], it was decided to use partial and full thickness variation devices (Figure 5.8) in the main axes of the slab (N, NE, E) to be able to relate them to the activation of the transverse reinforcement. In addition to this, others elements were continuously recorded during the tests such as the applied load, the slab rotations (inclinometers in the main axes and diagonal), the vertical displacements (LVDTs in the bottom surface), the surface deformations of the concrete (strain gauges), and the activation of the transverse reinforcement (load cells and strain gauges). After the test, each slab specimen was cut along the main directions to relate the internal crack development to the performed measurements.

5.2.2 Preliminary test (*PB4*)

In the frame of the study of the activation of the transverse reinforcement in the punching of slab –failure within the reinforced-area– the main idea of this test was to set up the conditions necessary for the development of a failure surface intercepting only the first row of elements (monitored with external load cells). The disposition of the elements (s_0 and s_1) was thus determined to develop a failure crack at 45° from the face of the column. The test procedure of this preliminary slab specimen (Figure 5.9) allowed to validate the measurements and testing devices. The failure was defined by the sudden activation of the transverse elements in the decreasing phase (3 in Figure 5.9).

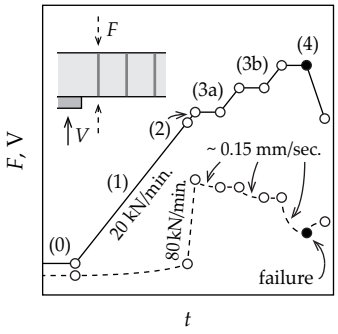

(0) initial prestressing (15 kN/transverse reinforcement)

(1) loading of the slab + passive activation of transverse elements

(2) loading of the slab + active loading of the transverse elements (phase initiated at failure load of the reference specimen ~1000 kN)

(3) maintain of load in the slab + release of the hydraulic system (acquisition rate of the main measurement devices set to 10 Hz)

(4) progressive failure of the slab (see definition of "failure" above)

Figure 5.9 Schematic representation and description of the test procedure for specimen *PB4* (solid line: load *V* in the slab, dashed line: force *F* in the 1st row of transverse reinforcement)

The specimen failed in punching with the particularity of presenting several crack patterns –associated to different failure modes– amongst the performed saw-cuts (Figure 5.10). Specific measurements –such as rotations or crack openings– indicated that the failure initiated in the weak axis (W) before propagating tangentially around the column until the opposite position (E), resulting in a progressive evolution of the failure surface inclination. Although the failure mode of interest was only observed in the strong (S-N) and diagonal (NE) axes, similar cracks were also observed in the other saw-cuts (W-E). It could finally be concluded that the active loading of the transverse reinforcement during the test –up to 85 kN/element– was not adapted and led to the development of cracks from the bottom anchorage of the first row of reinforcement (in the weak axis). This passably modified the activation of the elements complicating the related interpretation.

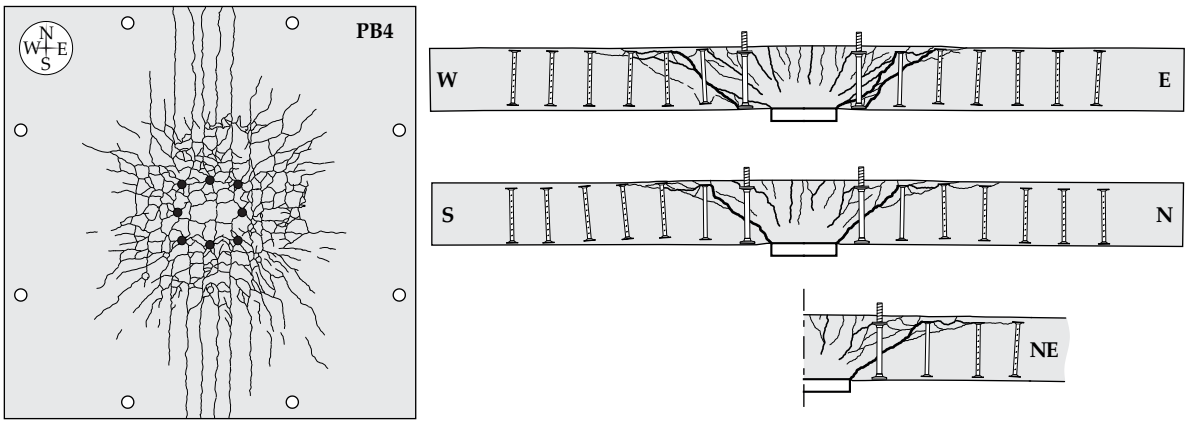

Figure 5.10 Crack pattern and saw-cuts of specimen *PB4* performed after test (W-E: weak axis, S-N: strong axis, NE: diagonal axis)

5.2.3 Test with active transverse reinforcement (*PB5*)

Although the preliminary test was satisfactory –notably regarding the measurement devices and the response of the hydraulic system related to the transverse reinforcement– several aspects required some improvements for the other specimens of the series (*PB5* and *PB6*). In this sense, and in order to avoid unexpected failure mode similar to those observed in the previous test, it was chosen to use post-installed elements (Figure 5.5*(b)*). Also, the disposition was adapted consequently, with the first row more distant from the column face and the second row closer to it. Compared to the previous version (Figure 5.5*(a)*), the use of a more compact system provided a better activation of the reinforcement both in the passive phase and at failure. A particular attention was given to the initial prestressing of the transverse elements (limited to the minimum practically possible). Finally, the test procedure (Figure 5.2*(a)*) was similar to the one of specimen *PB4* –yet considerably simplified (Figure 5.11)– to ensure more pertinent interpretations and developments.

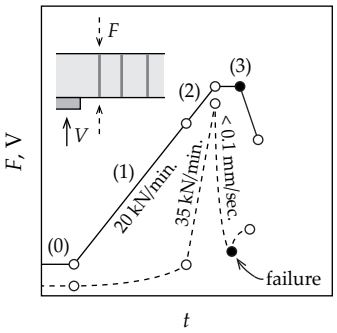

(0) initial prestressing (5 kN/transverse reinforcement)

(1) loading of the slab + passive activation of transverse elements

(2) loading of the slab + active loading of the transverse elements
(phase initiated at failure load of the reference specimen ~1000 kN)

(3) maintain of load in the slab + release of the hydraulic system
(acquisition rate of the main measurement devices set to 10 Hz)

(4) progressive failure of the slab ("failure" defined as for spec. *PB4*)

Figure 5.11 Schematic representation and description of the test procedure for specimen *PB5*
(solid line: load *V* in the slab, dashed line: force *F* in the 1st row of transverse reinforcement)

The specimen failed in punching with a very uniform crack development, contrary to the previous test. The saw-cuts confirmed the importance of the changes brought to the test specimen, notably regarding the transverse elements (up to 170 kN/element). The crack pattern was well-defined and comparable in all the axes of the slab, with a failure crack systematically intercepting at least the first two rows of transverse elements (Figure 5.12). Also, the failure surface was relatively flat, similarly to what is usually observed for slabs without transverse reinforcement [Gua05, Gui10].

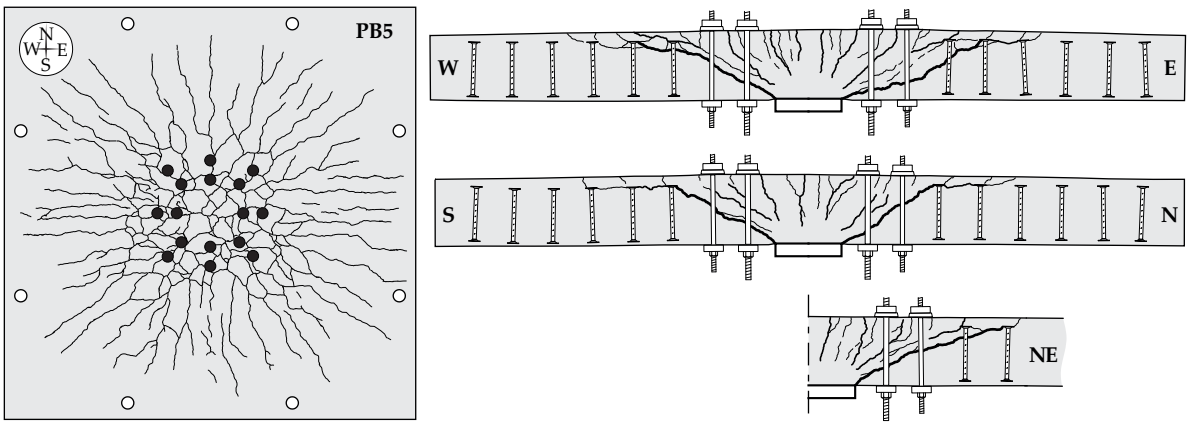

Figure 5.12 Crack pattern and saw-cuts of specimen *PB5* performed after test
(W-E: weak axis, S-N: strong axis, NE: diagonal axis)

5.2.4 Test with passive transverse reinforcement (*PB6*)

To complete the knowledge regarding the activation of the transverse elements in punching failure within the shear reinforced-area, a test was also performed with a passive state of the transverse reinforcement elements (Figure 5.2*(b)*). This is exactly the aim of specimen *PB6*, which consists in the same reinforcement layout and test configuration as specimen *PB5*. However, the test procedure was simplified (Figure 5.13), being very similar to the one of a classic punching test. The crack kinematics activating the transverse elements was particularly depicted in this test. The failure of specimen *PB6* was characterized by a significant increase of the crack openings and the force in the elements of the transverse reinforcement. Although no sudden loss of capacity was observed, a significant change of the load-rotation response could be measured and confirmed the failure of the slab specimen. In the post-failure phase, the load could be further increased and provided useful information for the related study of this specific failure mode (see Section 5.3).

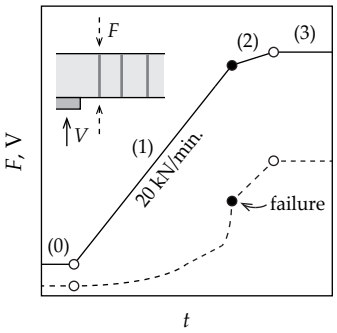

(0) limited initial prestressing (5 kN/transverse reinforcement)

(1) loading of the slab + passive activation of transverse elements

(2) failure of the slab specimen (see definition of "failure" above)
(acquisition rate of the main measurement devices set to 10 Hz)

(3) additional loading of the slab + activation (post-failure phase)
(acquisition rate of the main measurement devices set to 10 Hz)

(4) test limited by the yielding of the transverse elements (2nd row)

Figure 5.13 Schematic representation and description of the test procedure for specimen *PB6*
(solid line: load *V* in the slab, dashed line: force *F* in the 1st row of transverse reinforcement)

Specimen *PB6* failed in punching but with a consequent post-phase resulting in an extensive crack pattern on the surface of the slab (Figure 5.14), and generally larger crack openings measured. The crack pattern was similar to the one observed in the previous specimen (*PB5*), with the development of a failure crack intercepting several rows of transverse elements. The similarities highlighted between the saw-cuts of the two specimens justify the time dedicated to the preparation and definition of the test configuration and procedures.

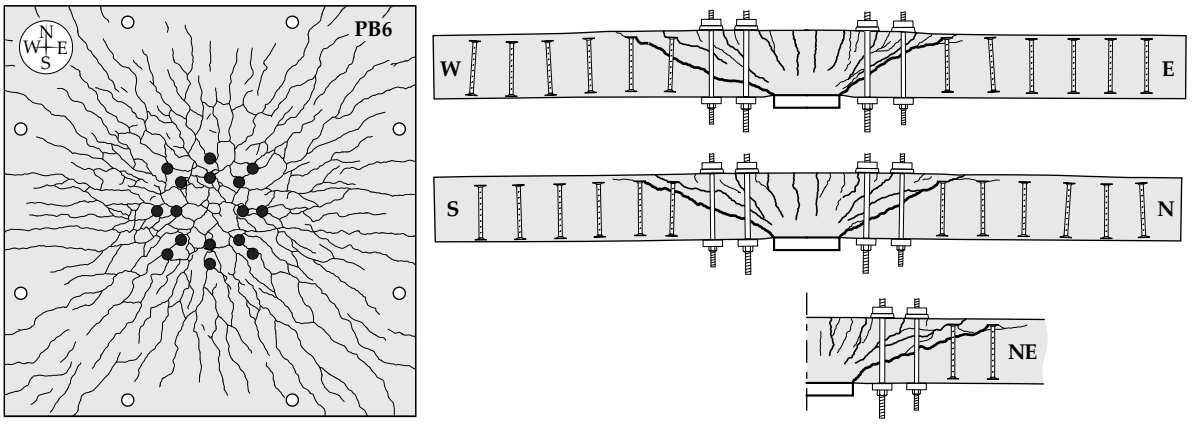

Figure 5.14 Crack pattern and saw-cuts of specimen *PB6* performed after test
(W-E: weak axis, S-N: strong axis, NE: diagonal axis)

5.3 Main results and observations

The presentation of the main results focuses on specimens *PB5* and *PB6* that constitute the central part of the experimental work on the activation of the transverse reinforcement during punching. The different approaches considered for these two tests –respectively active and passive transverse reinforcement– led to interesting observations regarding the crack openings (see Section 5.3.1), the force in the transverse elements (see Section 5.3.2), the rotation of the slab (see Section 5.3.3) and the shear deformations (see Section 5.3.4). These specific measurements are then used to discuss the main assumptions of the CSCT for the failure mode of within the shear-reinforced area (see Section 5.4). The complex test procedure considered for specimen *PB4* led to significant disparities in the crack pattern and strongly limited the related interpretations. Interest can be reasonably given to the latter test only prior to the active state of the transverse reinforcement and at failure.

In the figures related to specimen *PB5*, a distinction is made –for clarity purposes– between the measurements prior (solid line) and after (dashed line) the release of the hydraulic system controlling the first row of elements of the transverse reinforcement. Also, in this sense, the test phases involving the use of the hydraulic system (2, 3 and 4 in Figure 5.11) are highlighted with a light grey in the background as significant and sudden changes are associated to it. In the figures related to specimen *PB6*, a distinction is made for similar reasons, between the measurements prior (solid line) and after (dashed line) the failure. In all the figures, the failure of the slab specimens is systematically represented (generally through empty dots).

To enhance the interpretation of the results, the available reference slabs –without transverse reinforcement– tested under similar configurations –such as *PV1* [Fer10a] (d = 210 mm, f_c = 34.0 MPa, f_y = 709 MPa) and *PG20* [Gui10] (d = 201 mm, f_c = 51.7 MPa, f_y = 551 MPa)– are also represented in the figures. Although the mentioned slabs are passably different in terms of material properties in comparison to the performed tests –respectively higher yield strength of flexural reinforcement (*PV1*) or higher concrete compressive strength (*PG20*)– they are highlighted as important analogies were previously confirmed in other investigations for the studied failure mode (see Section 4.4).

5.3.1 Crack openings

The characterization of the failure crack kinematics is of major importance in the study of the activation of the transverse reinforcement. In this sense, the accurate and continuous measurements of the thickness variation (full and partial) led to interesting observations regarding the development of internal cracks in the slab during punching.

It has to be noted that the use of steel with high yield strength for the elements of the first row of the transverse reinforcement associated to the specific hydraulic system limited the opening of the cracks at failure. A thorough inspection of the saw-cuts was therefore necessary after the tests, in order to provide a detailed and representative description of the crack pattern for the interpretation of the results. Also, as disparities were observed amongst the axes, it was decided –for clarity purposes– to present them individually for each slab specimen.

SPECIMEN *PB4*

The complexity of the test procedure considered for specimen *PB4* required the limitation of the range of presented results for adequate interpretation. Thus, the following discussion focuses on the measurements of the crack opening performed on this slab from the beginning of the test until the active use of the hydraulic system for the transverse reinforcement (phase 2 in Figure 5.9).

For slabs with a small amount of transverse reinforcement or when systems with limited stiffness are used –the case of the present test– the development of internal cracks was previously observed to be similar to the one observed for reference slabs (see Section 4.4), with a failure resulting from the propagation of splitting crack from the column face. In both cases, the presence of a crack at 45° is observed, and specimen *PG1* [Gua05] ($d = 210$ mm, $f_c = 27.7$ MPa, $f_y = 573$ MPa) is in this sense of main interest as similar measurements –partial thickness variation– were performed for similar test conditions and material properties. The comparison of the results confirms important analogies between both specimens regarding the sequence of the internal cracking (Figure 5.15).

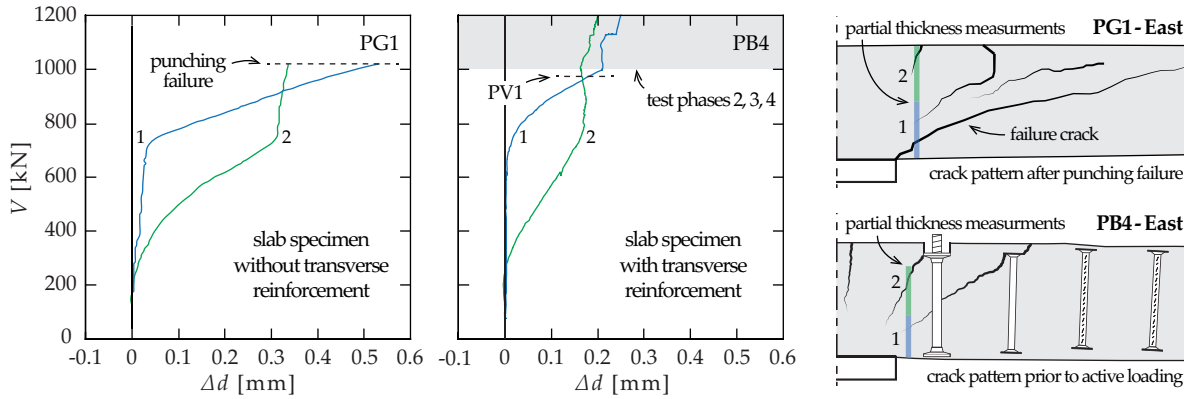

Figure 5.15 Detailed results of the partial thickness variation (Δd) compared to the acting load on the slab (V) at the column face of the weak axis for specimens *PG1* [Gua05] and *PB4*

The increase of the load acting on the slab leads to the formation of several flexural-based cracks developing from the tensile surface of the element on the inside, being progressively inclined for the transfer of the shear forces associated to bending. The load-rotation response of the slab indicates that cracking initiates at around 200 kN in the critical region for the force transfer (for similar test configuration and properties). Once formed, the opening of this crack increases almost linearly with the load until 700 kN, corresponding to 70 ÷ 80% of the failure load of the reference specimens. Then, the development of another crack –at a distance corresponding to the effective depth of the slab from the column face– leads to an internal redistribution of the deformation (1 in Figure 5.15). The opening of the previously formed crack (2 in Figure 5.15) then stays almost constant until the failure of the reference specimen (similar observations on the strong axis of the slab). From the presented results, it is evident that the presence of transverse elements in the slab limits the opening of the internal cracks –for a given load level– in comparison to a reference specimen without such reinforcement. In this sense, efficient reinforcing systems aim at better controlling the latter crack development through more performant bond and anchorage mechanisms.

SPECIMEN *PB6*

In order to consistently discuss the influence of an active state of the first row of transverse elements on the response of the slab (specimen *PB5*), it made sense to firstly detail the main results (Figure 5.16 – 5.18) for the slab with a passive state of such reinforcement (specimen *PB6*).

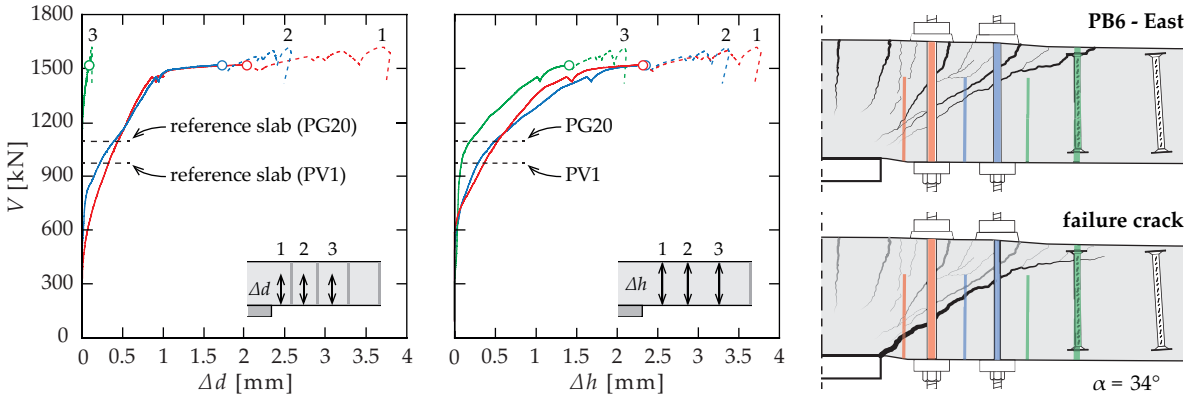

Figure 5.16 Main results associated to the weak axis of specimen *PB6* and details of the related saw-cut: partial thickness variation (*Δd*) and full thickness variation (*Δh*) compared to the acting load on the slab (*V*)

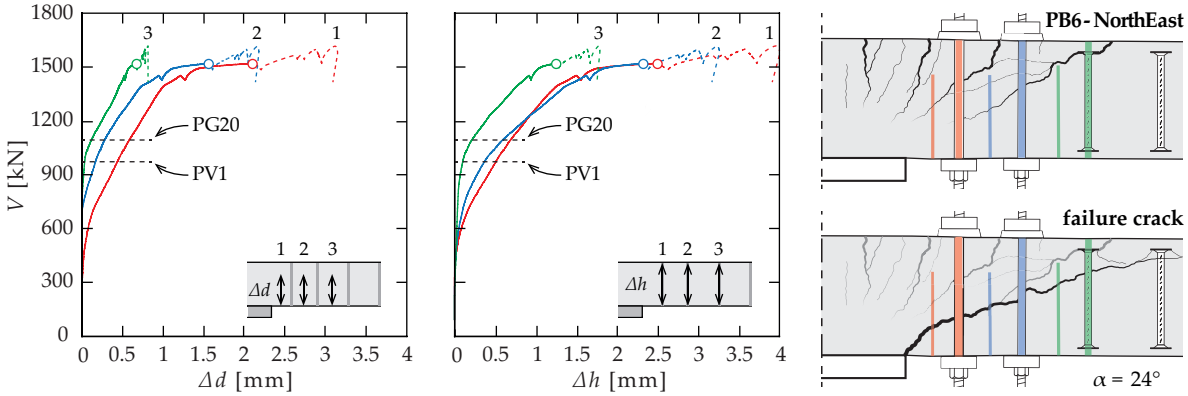

Figure 5.17 Main results associated to the diagonal axis of specimen *PB6* and details of the related saw-cut: partial thickness variation (*Δd*) and full thickness variation (*Δh*) compared to the acting load on the slab (*V*)

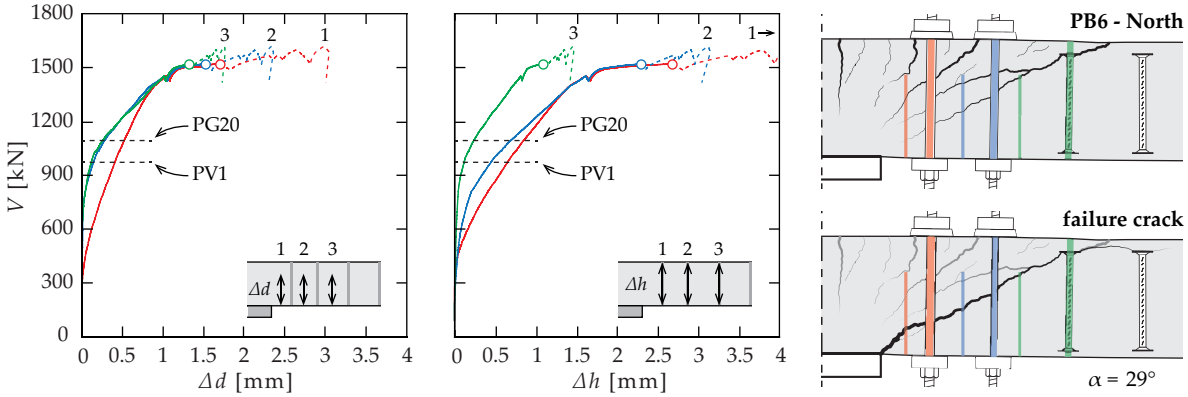

Figure 5.18 Main results associated to the strong axis of specimen *PB6* and details of the related saw-cut: partial thickness variation (*Δd*) and full thickness variation (*Δh*) compared to the acting load on the slab (*V*)

The measurements of the partial and full thickness variation –Δd and Δh– performed in the three main directions of the slab (weak, diagonal and strong axes) highlighted the fact that the internal crack development follows several successive and distinct phases. As the transverse elements of the first and second rows of reinforcement are not bonded –use of PVC tubes– the non-linearity of the curves is to be associated to the development of new cracks from the ones already formed. The cracking sequence was observed to be particularly well defined in the diagonal axis (Figure 5.17).

In the first phase of the test (up to 500 kN), the formation of cracks is not captured by any of the devices, supporting the formation of flexural cracks above the column (confirmed by other investigations on similar slab specimens [Lip12c]). Then, a progressive development of inclined flexural-based cracks takes place (up to 1400 kN) –from the centre of the slab to its periphery– intercepting and activating the transverse elements during their propagation in the specimen. It is interesting to note that, in the latter phase, the partial thickness variation measurements indicate that the development of a given crack appears to be limited by the formation of the next one (linear increase with the acting load on the slab). Finally, an internal redistribution occurs at the column face – similar to the one highlighted for specimen *PB4*– leading to the formation of the failure crack at the column face (see Figures 5.20 and 5.21) that propagates through the transverse elements.

The disparities observed in the crack pattern amongst the different axes of the slab are related to the fact that the failure initiated at the column face of the weak direction (East axis in the case of specimen *PB6*), then propagating tangentially and radially from this position. The latter is confirmed through the measured crack openings (prior, at and post- failure), rotations at failure (see Section 5.3.3) and computed shear deformations (see Section 5.3.4). As already observed for slabs without transverse reinforcement [Ein16b], this propagation from one specific position supports the fact that the failure crack does not systematically join the existing flexural ones (for instance saw-cuts at failure of the North-East, South and West axes). During its development, the failure crack tends to progressively get flatter to activate more transverse elements in order to carry the load. The performed saw-cuts highlighted that the inclination of the failure surface was systematically steeper on the side where the failure initiated (34° in East axis, see Figure 5.16) than the direct opposite one (20° in West axis, see Figure 5.19) with a gradual transition in the strong direction (29° in North axis, see Figure 5.18 and 26° in South axis, see Figure 5.19).

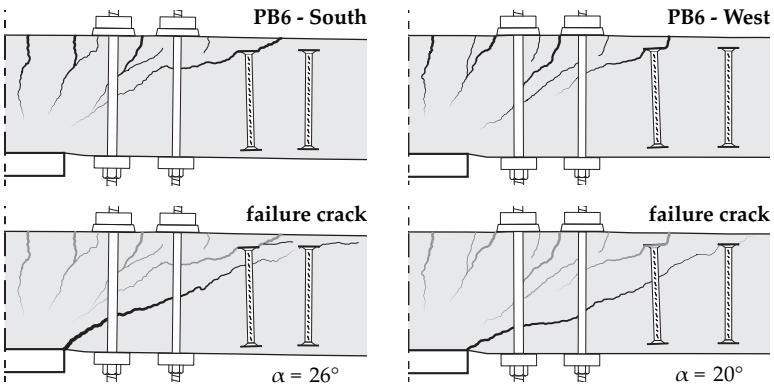

Figure 5.19 Details of the saw-cuts of the remaining main axes of specimen *PB6*

The measurements indicate that the opening of the failure crack during its propagation tends to be progressively smaller both radially (further from the column face) and tangentially (in the other axes with respect to East axis). This is supported by the markedly smaller width of the failure crack physically observed in the saw-cut of the West axis compared to the directly opposite one where the failure initiates (East axis). The difference in the activation at failure of the transverse elements of the second row in these specific axes (see Section 5.3.2) also confirmed the latter remark.

The formation of a crack at the load level corresponding to the failure load of the reference specimens *PV1* and *PG20* is also observed in the performed test (*PB6*). Due to the improved stiffness of the transverse reinforcing system, the latter was significantly better controlled (in comparison to the preliminary specimen *PB4*). At the column face, the development of one crack –or several microcracks– at a depth between 50 mm and 100 mm from the soffit of the slab (2 in Figure 5.20 and Figure 5.21) leads to the progressive failure of the specimen. The latter can be associated to a local decompression of the concrete, as indicated by the strain measurements at the slab surface ($\varepsilon_{c,r}$). This phenomenon might be related to the lateral expansion of the inclined strut in the vicinity of the column, and is supported by recent similar observations on footing specimens [Sim16].

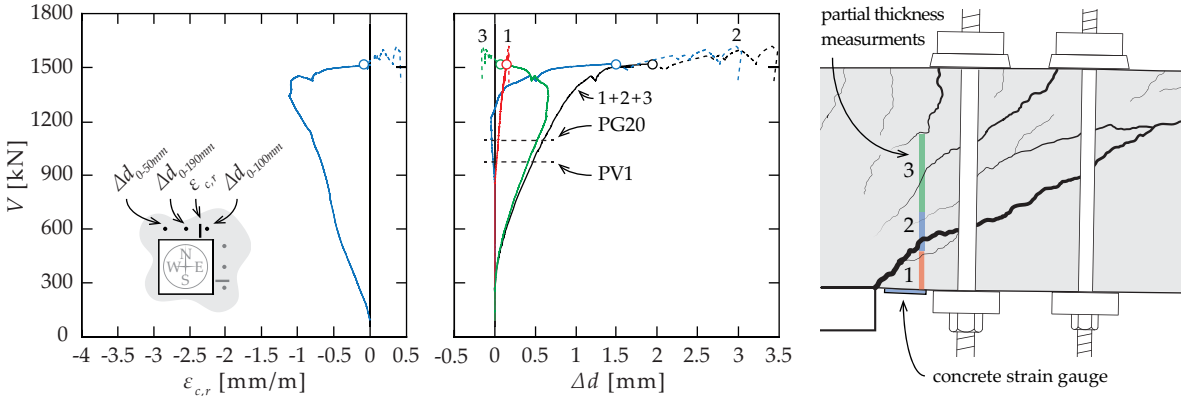

Figure 5.20 Detailed results of the radial concrete strains ($\varepsilon_{c,r}$) and the partial thickness variation (Δd) compared to the acting load on the slab (V) at the column face of the strong axis of specimen *PB6* (North)

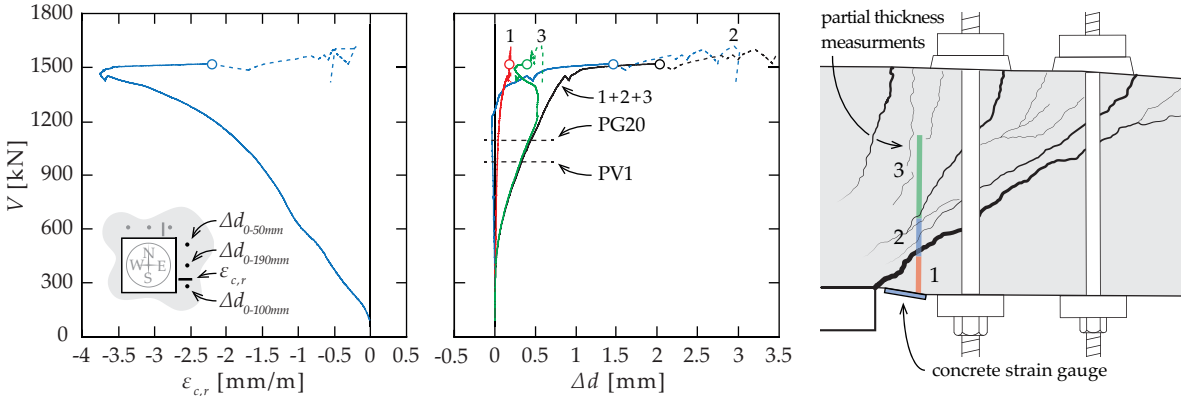

Figure 5.21 Detailed results of the radial concrete strains ($\varepsilon_{c,r}$) and the partial thickness variation (Δd) compared to the acting load on the slab (V) at the column face of the weak axis of specimen *PB6* (East)

SPECIMEN *PB5*

Prior to the active state of the transverse reinforcement and at failure, no significant differences were highlighted in the crack openings compared to specimen *PB6*. The main results confirmed a significant modification in the crack development upon use of the system (Figures 5.22 – 5.24).

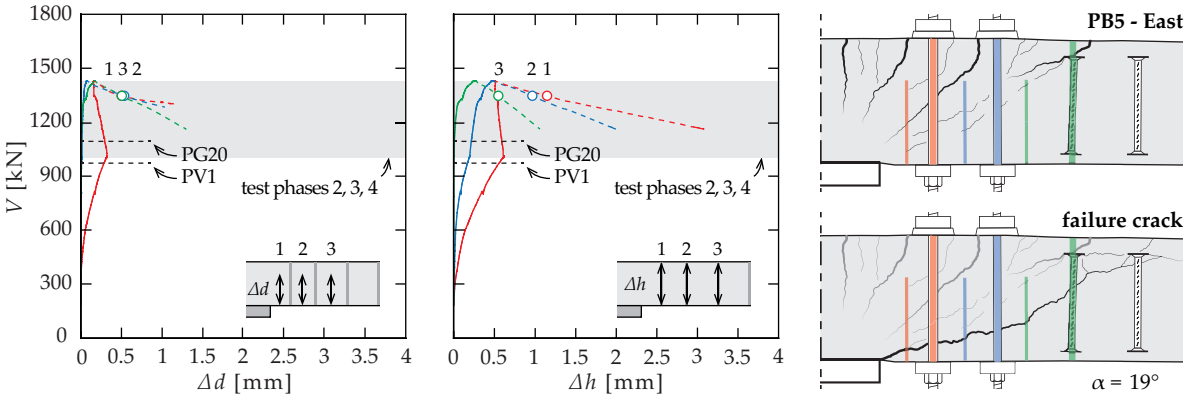

Figure 5.22 Main results associated to the weak axis of specimen *PB5* and details of the related saw-cut: partial thickness variation (*Δd*) and full thickness variation (*Δh*) compared to the acting load on the slab (*V*)

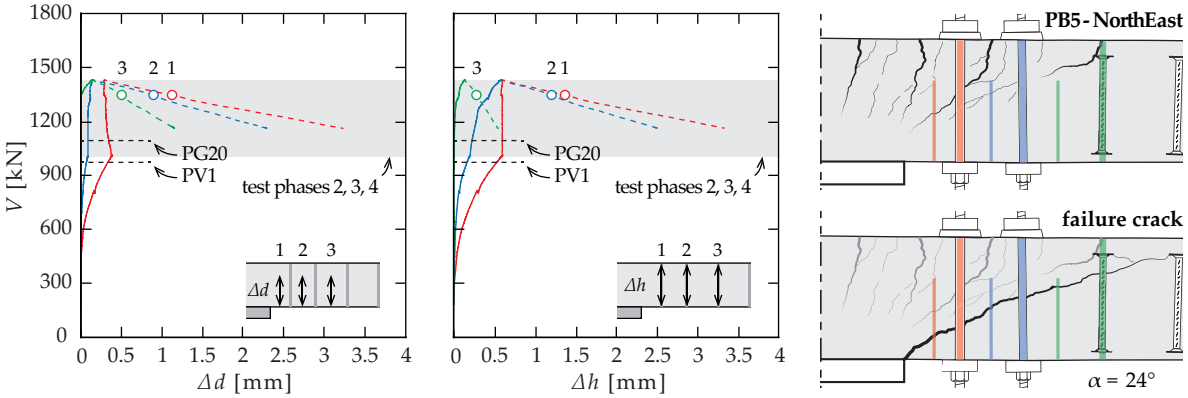

Figure 5.23 Main results associated to the diagonal axis of specimen *PB5* and details of the related saw-cut: partial thickness variation (*Δd*) and full thickness variation (*Δh*) compared to the acting load on the slab (*V*)

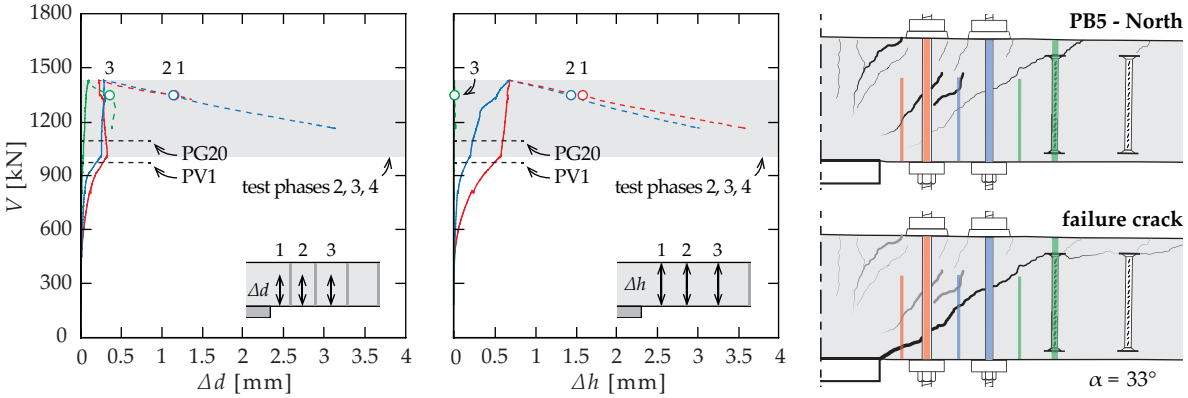

Figure 5.24 Main results associated to the strong axis of specimen *PB5* and details of the related saw-cut: partial thickness variation (*Δd*) and full thickness variation (*Δh*) compared to the acting load on the slab (*V*)

The saw-cuts suggest that the active loading did not influence the crack sequence in the slab. The measurements also confirmed that the failure initiated in the weak axis –yet in the West direction (Figure 5.25)– with similar observations regarding its propagation and development in the slab.

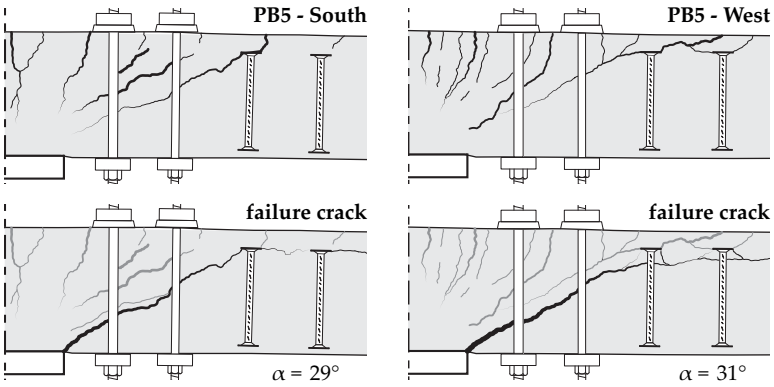

Figure 5.25 Details of the saw-cuts of the remaining main axes of specimen *PB5*

The conclusions highlighted for specimen *PB6* on the internal redistribution of deformations at failure could not be directly confirmed for specimen *PB5* due to the active loading test phase (Figures 5.26 - 5.27), but a decompression of the concrete surface could similarly be confirmed.

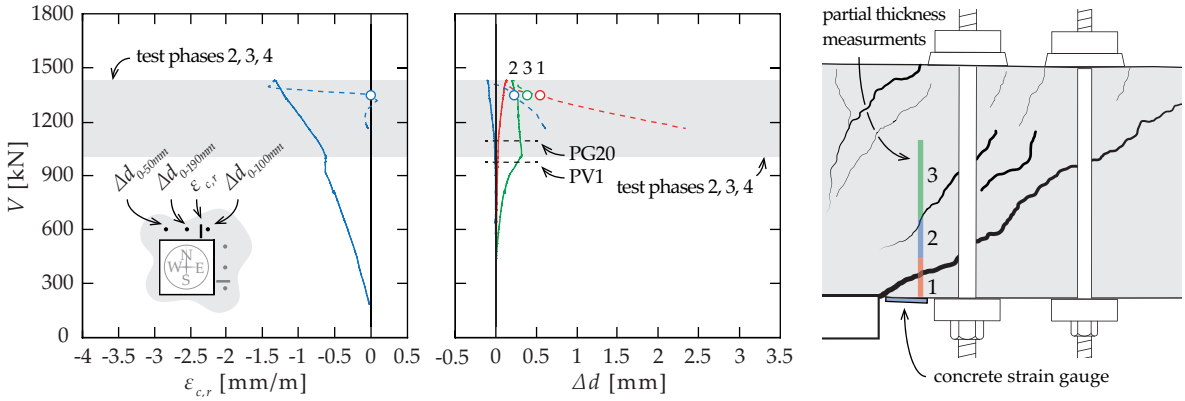

Figure 5.26 Detailed results of the partial thickness variation (Δd) compared to the acting load on the slab (V) at the column face of the strong axis of specimen *PB5* (North)

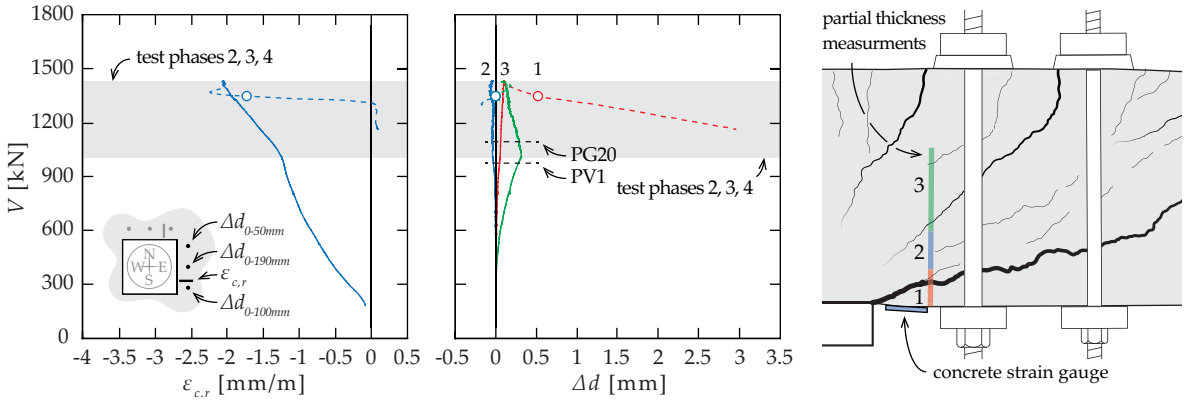

Figure 5.27 Detailed results of the partial thickness variation (Δd) compared to the acting load on the slab (V) at the column face of the weak axis of specimen *PB5* (East)

5.3.2 Force in the transverse reinforcement

The accurate definition of the force in the transverse elements is one of the main issues associated to the study of the activation of such reinforcement during punching. Together with the crack opening measurements, it allows to investigate and discuss the kinematics of the failure crack previously highlighted. Also, in the case of specimens *PB5* and *PB6*, the use of a post-installed system contributed notably to the activation of the related transverse elements as the effective length corresponded to the thickness of the slab.

The particularity of the present test series is associated to the evaluation of the activation of the transverse reinforcement through the systematic use of external load cells (first row for specimens *PB4*, *PB5* and *PB6* / second row for specimens *PB5* and *PB6*). Specific strain gauges –installed within the axis of the bar (d_b=1.5 mm) at a depth of 50 mm of the top anchorage and fixed with a special adhesive– completed the force measurements on the third row of reinforcement (only in North, North-East and East axes). The latter device presents the interest of not being sensitive to the development of cracks without also affecting the surface properties of the transverse reinforcement elements. This system gave great satisfaction compared to the external glued gauges considered for specimen *PB4* that were not stable and for which the signal was lost close to the failure load.

SPECIMEN *PB4*

Although the transverse elements of the specimen were initially provided with a consequent initial prestressing –in order to compensate the low stiffness of the system– the results highlighted a very limited passive activation of such reinforcement associated to the interception with flexural cracks (phase 1 in Figure 5.9). Also, during the active loading (phases 2 and 3 in Figure 5.9), the increase of the force was confirmed to be uniform and progressive in all the elements of the first row without significant disparities amongst them. The latter points led to the validation of the system used to locally control the activation of the transverse reinforcement. For this test, significant changes in the force were only reported during the release of the system (phase 4 in Figure 5.9), with yielding only measured in the top of the second row in the weak axis (West direction).

It is interesting to observe that, in this last phase of major interest in the present research, the decrease of the force in the first row of reinforcement is followed by a sudden reactivation of the elements (as schematically represented in Figure 5.9). The latter was associated to the internal redistribution between steel and concrete during the failure of the slab, but the limited stiffness of the system led to an insignificant increase of the force in the concerned transverse elements. An important activation was however measured in the second row of reinforcement (studs).

Finally, the complexity of the test procedure and the quality of some of the measurements made it difficult to give a detailed presentation and discussion of the results regarding the variation of force in the transverse elements. In addition to this, the lack of any information regarding the activation of the third row of reinforcement also appeared as an important limitation that motivated to mention only the main observations in the present section for the latter specimen.

SPECIMEN *PB6*

The improvements made regarding the stiffness and the anchorage conditions of the system controlling the transverse elements of the first row of reinforcement, as well as the use of external load cells also for the second row of reinforcement, led to interesting observations on the related activation. The results highlighted significant differences amongst the transverse reinforcement rows regarding the increase of force (F) both in terms of importance and distribution around the column (Figure 5.28) during loading (V). This is also confirmed by the detailed figures (Figure 5.29) representing the situation in the three main axes monitored (East, North-East and North).

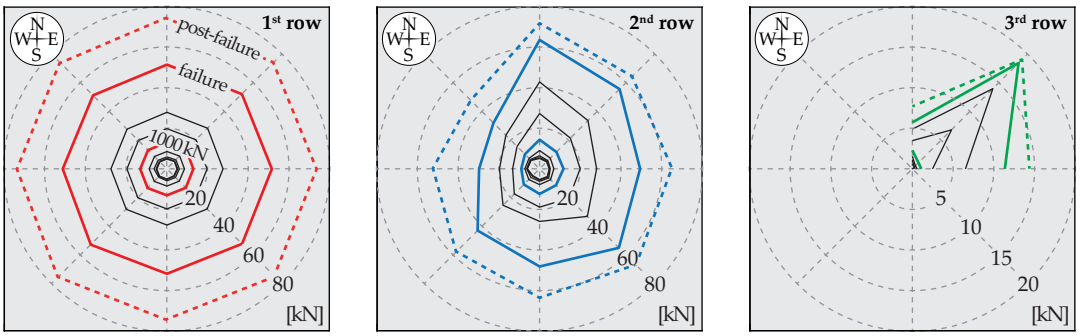

Figure 5.28 Activation of the transverse elements in specimen *PB6* for different load levels (200 kN - 400 kN - 600 kN - 800 kN - **1000 kN** - 1200 kN – 1400 kN - **failure** - **post-failure**)

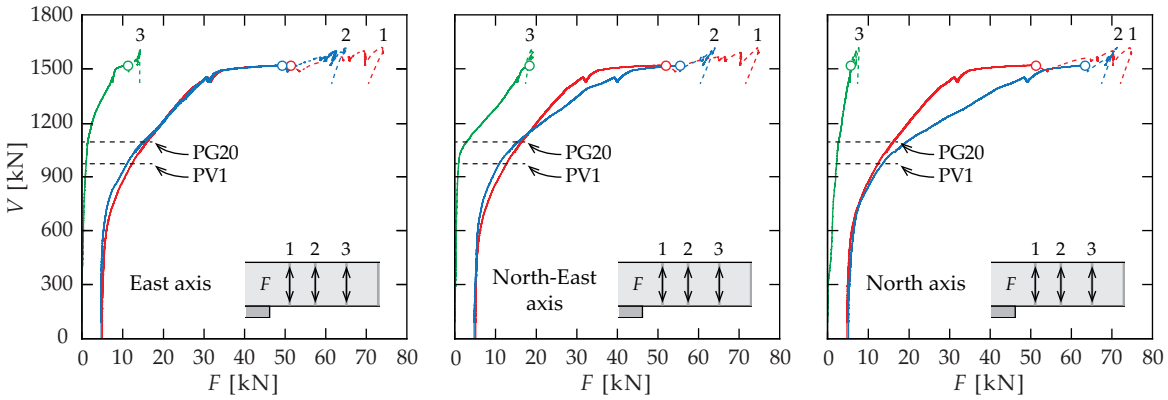

Figure 5.29 Activation of the transverse reinforcement in the main axes of specimen *PB6*: force in the transverse elements (F) compared to the acting load on the slab (V)

In the first row, similarly to what was observed in specimen *PB4*, the activation is progressive and uniform in the entire slab. It tends to accelerate markedly only at a load level close to the one corresponding to the failure of the reference slab (first colour line from the centre in Figure 5.28). Then, the increase of force is almost linear with the load before a second significant acceleration of the phenomenon at a load level corresponding to the localization of the deformation at the column face (Figures 5.20 and 5.21) until the failure of the slab (second colour line from the centre in Figure 5.28). It is interesting to observe that, where the failure seems to have initiated (East axis), the activation of both the first and second row of transverse elements is almost identical. In the post-failure phase the activation of the elements is also uniform and constant in the entire slab, without being localized in some specific directions (dashed colour line in Figure 5.28).

In the second row, disparities among the axes regarding the activation of the transverse element arise only at the failure of the reference slab. These differences progressively increase until the failure of the specimen, where in average the weak axis contributes less in the load carrying (respectively 15% and 30% less load was carried on the weak axis in comparison to the diagonal and strong axes). It is interesting to notice that the activation of the transverse element in the West axis –directly opposite from the axis where the failure initiated– appears to be the smallest of the entire row. The latter might be justified by the previously highlighted propagation of the failure crack from the East axis, resulting in progressively smaller crack opening at the same distance of the column face but in the others axes. After failure, the additional loading of the slab tends to make the activation uniform amongst the different axes of the slab. In this phase, the increase of force in the transverse reinforcement tends to be larger for the elements that were less activated at failure.

In the third row, although measurements were performed only on a quarter of the slab, the activation appears in average significantly smaller than in the two previous rows of reinforcement (change of scale in Figure 5.28). It has to be noted that due to the limited length of the stud –smaller than the thickness of the slab– the development of a crack at its position does not necessary imply an increase of the force (in the case of delamination cracks for instance). The results highlighted that most of the load in this row seems to be carried by the diagonal axis, with a minor importance of the main axes. This might be directly related to the inclination of the failure surface –observed to be particularly flat in the diagonal– therefore intercepting the stud at an adequate distance from its top anchorage to activate the bond properties of the deformed surface. Apart from the diagonal axes –that might be a particular case– the activation of the transverse elements of the third row in the main axes is expected to progressively decrease during the propagation of the failure crack from the East axis. In fact, the results in the second rows indicate that the progressive decrease of the failure crack opening during its tangential propagation might not be entirely compensated by the additional inclination of the failure surface leading to a decrease of the activation. After the failure of the specimen, observations similar to those highlighted for the second row of reinforcement can be made. The development of an additional force takes place mainly in the transverse elements that were activated the least at failure (weak and strong axes).

Generally, at failure, it appears that there is not a systematic trend regarding the activation of the transverse reinforcement. In the present test, roughly, in half of the slab the first row is more activated than the second one, in the other half the second row is more activated than the first one. The third row of transverse reinforcement is systematically less activated than the others rows. It must be remembered that the stiffness of the system was different in each row (first row < second row < third row) therefore influencing the activation of the transverse reinforcement. Thus, compared to a stiffer element, larger crack openings are necessary to develop a given force in an element with a smaller stiffness. Similar measurements –force in the transverse elements– were performed by Beutel [Beu03] on slabs reinforced with stirrups-like systems. It was observed that, in average and for the same failure mode, the elements of the first row in the weak axis contribute the least in the load carrying (20% less compared to the diagonal or strong axes).

SPECIMEN *PB5*

The results confirmed previous observations with notable disparities amongst the axes regarding the activation of the second and third rows of reinforcement (Figure 5.30). The dashed lines correspond to the load steps in the active loading phase of the transverse elements of the first row (phase 2 in Figure 5.11). The specific results in the weak, diagonal and strong axes (Figure 5.31) highlight the latter phase in details as well as the release of the system (phase 3 in Figure 5.11) –in which a similar phenomenon of reactivation of the first row, as described for specimen *PB4*, can be clearly observed– and the failure of the specimen (phase 4 in Figure 5.11).

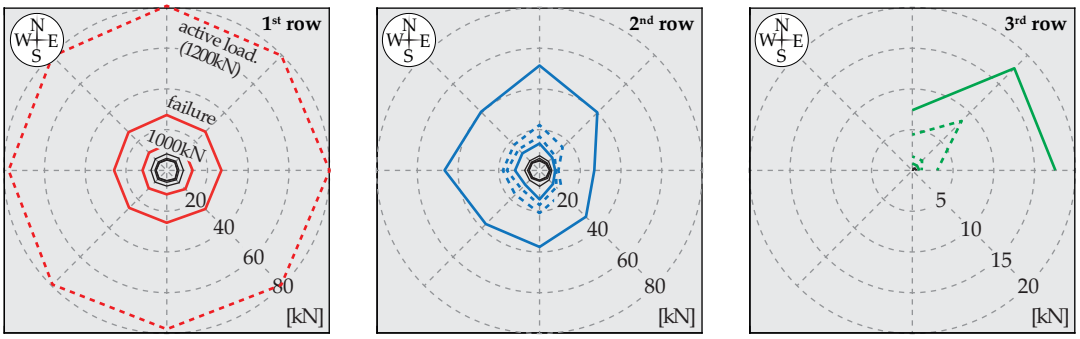

Figure 5.30 Activation of the transverse elements in specimen *PB6* for different load levels (200 kN - 400 kN - 600 kN - 800 kN - **1000 kN - 1200 kN – 1400 kN - failure**)

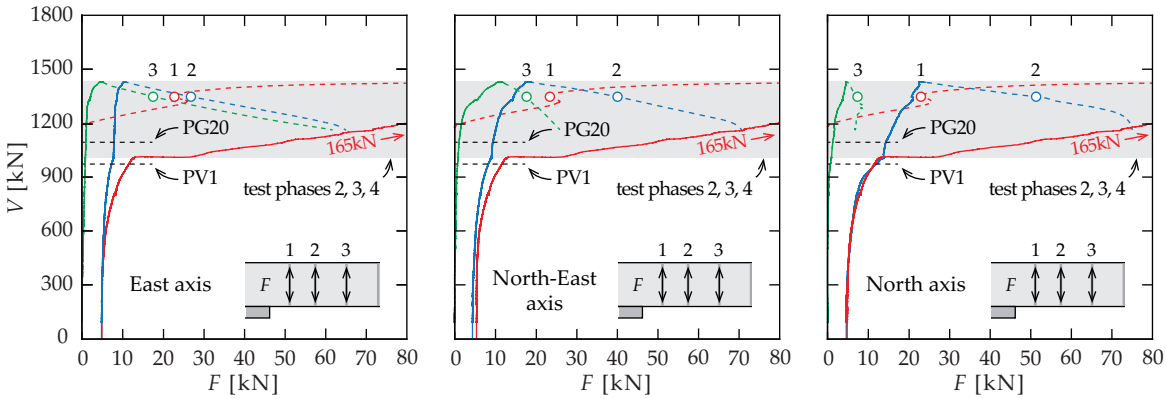

Figure 5.31 Activation of the transverse reinforcement in the main axes of specimen *PB5*: force in the transverse elements (F) compared to the acting load on the slab (V)

In the first row, the increase of force is systematically uniformly distributed amongst the axes during the passive or active loading of the row and at failure confirming the performance of the developed device. In the second row, important similarities with the previous test specimen can be highlighted. Only at a load corresponding to the failure of the reference slab do disparities arise in the activation of the transverse elements and mainly in the weak axis. The smaller force reported in the East axis at failure also supports the propagation of the failure crack from the West axis as confirmed through the measurements. At failure, the second row is systematically more activated than the first one: this is most probably related to the largest stiffness of the reinforcing system in this position. In the third row, the elements on the diagonal are still the most activated resulting from the particular crack pattern –of relatively low inclination– observed in this direction.

5.3.3 Rotations

The capacity of deformation of a slab is often associated to its rotation at the periphery of the specimen. It is indirectly related to the dissipation of energy taking place in the slab during the punching phenomenon by both the concrete and steel. Thus, some interesting remarks arise about the performed thickness variation measurements and the activation of the transverse reinforcement.

In the performed tests, the rotation was evaluated in the main axes of the slab –diagonal included– and confirmed the failure crack kinematics observed through previous measurements (notably for specimen *PB4*). Also, it allowed to depict the different phases of activation of the transverse reinforcement more, with interesting analogies between specimens *PB5* and *PB6*.

SPECIMEN *PB4*

Specimen *PB4* was characterized by the development of several failure modes, associated to some issues with the active reinforcing system used (stiffness, disposition and test procedure). It appears that the measured rotations (ψ) are particularly coherent with the variety of failures observed amongst the axes of the slab (Figure 5.32). Indeed, the crushing failure in the East axis is associated to a fundamentally different behaviour at failure –in term of rotations (1 in Figure 5.32)– compared to the others axes that all presented failures within the transverse reinforcement (2 in Figure 5.32). These disparities are balanced once the failure is well established in all the axes as a new kinematics develops in the slab mainly associated to vertical displacement (3 in Figure 5.32).

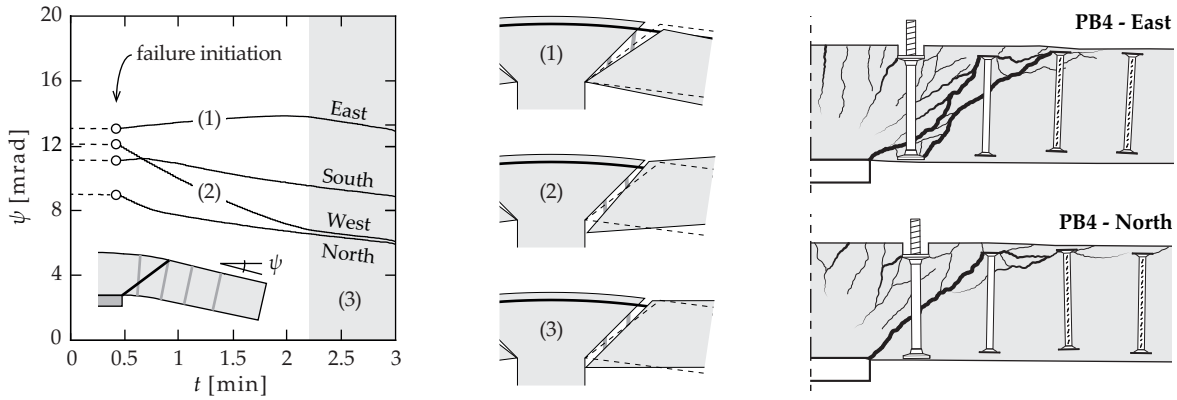

Figure 5.32 Evolution of the rotation (ψ) measured in the main axes of the specimen *PB4* close to failure (prior to unloading), related kinematics, and saw-cuts in East axis (crushing failure) and North axis (failure within the transverse reinforcement from the column face)

From the highlighted rotation sequence, it is possible to conclude –similarly to specimens *PB5* and *PB6*– that the failure potentially initiates in the weak directions of the slab (West axis in the case of specimen *PB4*, in relation to the sudden modification of the rotation observed). Propagation of the failure crack develops –almost simultaneously– in the strong direction (North and South axes) and then finally in the opposite direction (East axis). The decrease of rotation at failure can be associated to the development of a splitting crack as indicated by the measurements of the crack opening. Analogous observations were also made for slabs without transverse reinforcement [Lip12c].

SPECIMENS *PB5+PB6*

A decrease of the rotation at failure –similarly to the one highlighted for specimen *PB4*– was also observed in all the axes of specimens *PB5-PB6*, yet not of such importance. This can be explained by the fact that, in the present case, the crack openings were significantly smaller at failure due to the improved stiffness of the transverse reinforcing system and test procedure. This observation indirectly confirms the development of a splitting crack from the column face at failure, as can be clearly recognized in the presented saw-cuts of these specimens.

The use of transverse elements –locally unbonded and with very good anchorage performance– highlighted interesting observations by comparing the increase of force in the elements of the transverse reinforcement (F) and the rotation of the slab (ψ). As it was already partially discussed with respect to the measurements of the crack openings (see Section 5.3.1), several regimes can be distinguished in the activation (Figure 5.33). This is particularly obvious in the case of specimen *PB6*, for which no active loading of the transverse elements of the first row was performed during the test (compared to specimen *PB5*).

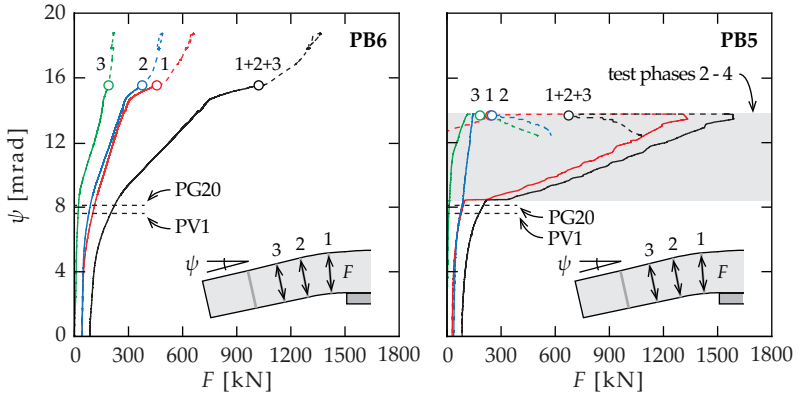

Figure 5.33 Steel contribution of the first three rows of transverse reinforcement in terms of force (F) as a function of the mean rotation (ψ) for specimens *PB5* and *PB6*

Three distinct regimes of activation can be observed during the test, with more or less well-defined transition phases in between each of them. The first one is related to an increase of the rotation without a significant activation of the transverse reinforcement, as the internal cracking mainly develops prior to the first element –above the column and in the vicinity of the column face– without any interaction. The second regime is associated to the development of flexural cracks from the column face progressively intercepting the different transverse elements in the vicinity of the column. An almost linear relation can be observed between the increase of force in the transverse reinforcement and the rotation. It is interesting to note that the transition phase between these two previously mentioned regimes progressively takes place for a rotation close to the one corresponding to the failure of the reference specimens –*PV1* and *PG20*– with the formation of some specific internal cracks. Finally, close to the failure load, the activation of the transverse reinforcement tends to increase considerably with only a limited –almost negligible– increase of the rotations. This regime is related to the development of important shear deformations at the column face –

confirmed by performed measurements (see Section 5.3.4)– therefore affecting the crack kinematics and thus contributing to the activation of the transverse elements. The transition with the flexural-based activation regime is relatively sudden in comparison to the previous one, even being generally more accentuated for the elements closest to the column face. The latter is potentially related to the formation and propagation of the failure crack from a specific position at the column face as suggested in Figure 5.21.

For the test with active transverse reinforcement –specimen *PB5*– the previous observations are less evident due to the defined test procedure that aimed at controlling the opening of the cracks associated to the flexural-based regime. Although the active loading of the elements at the end of the first transition phase did not affect the rotations –localized in other cracks– the increase of the force was sufficiently modified that the measurements of this phase could not be reasonably considered. Although fundamentally different procedures were considered for the two tests, the results are consistent (Figure 5.34). In the following, only the results prior to the active phase and at failure are presented for specimen *PB5* to be comparable with those for specimen *PB6*.

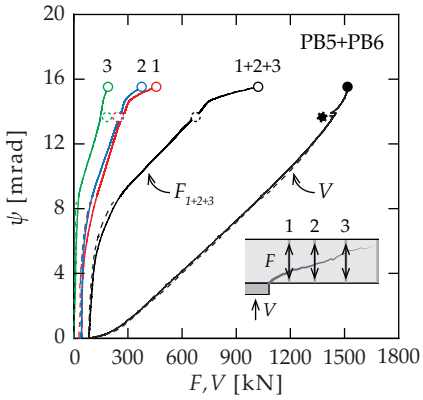

Figure 5.34 Contribution to the punching phenomenon (V) of the first three rows of transverse reinforcement in terms of force (F) as a function of the mean rotation (ψ) for specimens *PB5* (dashed lines and dashed dots) and *PB6* (solid lines and solid dots)

For a similar transverse reinforcement ratio, layout and test configuration –the case of specimens *PB5* and *PB6*– it appears that the redistribution of internal forces that takes place once the system is released leads to the achievement of an equilibrium situation (dashed dots) corresponding relatively well to the activation curves from specimen *PB6* (solid lines), yet at a lower load level. The latter implies that a certain continuity exists between the behaviour of different slabs –for given conditions– and could be of major interest in the phenomenological study of the activation in punching for this failure mode. Similar observations were also made regarding shear deformations (Figure 5.37*(b)*) as discussed in Section 5.4.1.

For slab specimens reinforced with transverse elements made of deformed bars and non-perfect anchorage (usually the case), several additional bond mechanisms are involved in the activation leading to non-linear phases. The interpretation of the steel contribution in the latter case is thereby particularly more complex than in the ideal one presented in the present section.

5.3.4 Shear deformations

The shear deformations (Δw) differ from the flexural deformations by the fact that they are independent of the rotations. In the performed tests, they were estimated with the vertical displacements in the main and diagonal axes of the slab specimens. As presented in Figure 5.35, they were computed as the difference between the displacement at point A and the extension of the secant between points B and C (similarly to previous studies on similar slabs [Lip12a, Lip12b]). As the performed saw-cuts confirmed that the penetration of the column was very limited in the tests, these assumptions can be considered sufficiently correct for the definition of the shear deformations. However, due to the excessive active loading performed on the transverse reinforcement of specimen *PB4*, the determination of the shear deformations with this formulation was not reliable (important damages were observed on the soffit of the slab after testing).

Together with the results previously highlighted –such as the crack openings and rotations– interesting observations arise for a better understanding of the activation of the transverse reinforcement, notably shortly prior to the failure when the shear deformations become significant (Figure 5.35). The loss of some sensors could unfortunately not be avoided during this test phase.

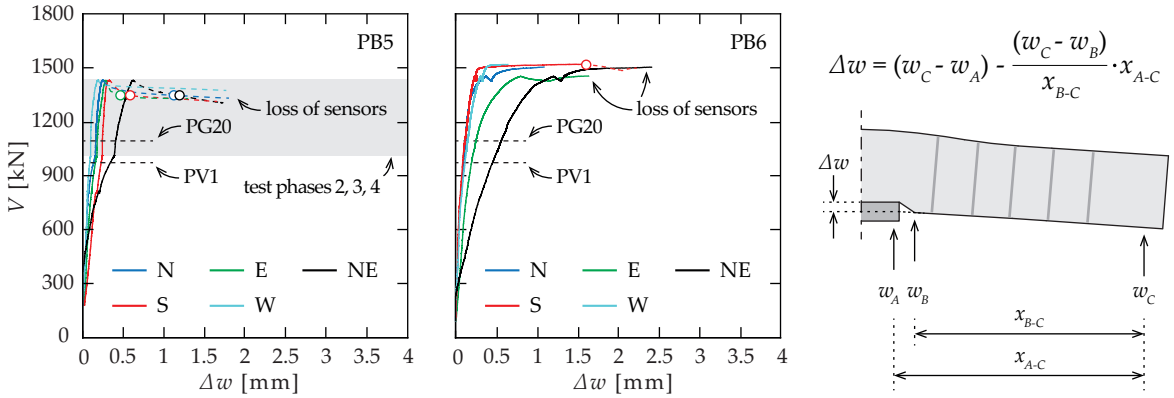

Figure 5.35 Shear deformation (Δw) function of the acting load on the slab (V) in the main axes of specimens *PB5* and *PB6* with definition of the formulation considered for computation

In both specimens –*PB5* and *PB6*– the development of the shear deformations during the loading of the slab appears more important in the diagonal axis than in the main axes, as the edges of the column induce a significant stress concentration in this specific position. Such disparities are not likely to be observed in tests with circular columns that represent an ideal case, but only limited related investigations are available [Tol88, Vaz07, Fer14].

Contrary to most of the other performed measurements presented, the development of the shear deformations do not appear to be strongly related to the failure load of the reference specimen. Also, from the presented results, the previously described failure sequence of the slab (see Section 5.3.1) can be clearly confirmed through the disparities in the initiation of the shear deformations amongst the different axes (particularly for specimen *PB6*), even though some of the vertical displacement devices were progressively lost before failure.

5.4 Discussion on the assumptions of the CSCT

The results from the punching test campaign are depicted in the frame of the CSCT [Fer09] for slabs with transverse reinforcement, which main assumptions (see Section 5.1) are reviewed in the following section on an experimental background (see Section 5.3). Major emphasis is placed on specimens *PB5* and *PB6* –which compose the central part of the present work– notably the latter one whose test procedure was the closest to a standard punching test (monotonic loading).

The discussion and developments focus on the failure kinematics (see Section 5.4.1) and the contribution of steel and concrete in the punching phenomenon (see Sections 5.4.2 and 5.4.3). These investigations aim at highlighting the main disparities between the theory and the test observations for this specific failure mode –within the shear-reinforced area– and to provide some potential improvements regarding the consideration of the latter aspects in the CSCT (see Section 5.5).

5.4.1 Kinematics

Although detailed and extensive measurements were performed regarding the opening of internal cracks, the definition of the related kinematics during the tests was not evident. The existence of two specific cracks –the critical one and the failure one, as stated by the CSCT– could be confirmed and clearly observed in the saw-cuts of the slabs (Figure 5.36). As the critical crack was observed to be rather associated to flexural deformations (in agreement with the assumptions of the CSCT), the failure crack was rather related to a splitting phenomenon (larger openings close to the column face). This was already observed by several authors on slabs both with [Ein16b] and without transverse reinforcement [Gua05, Gui10, Clé12, Ein16b]. The fact that these two cracks do not systematically join at failure indicates that they might be associated to different internal mechanisms.

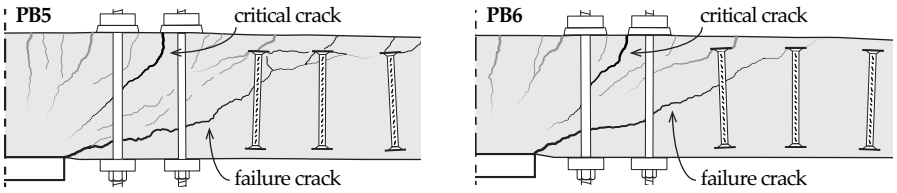

Figure 5.36 Details of the saw-cuts performed after test of specimens *PB5* and *PB6*

The CSCT claims that half of the entire flexural-based deformations of the slab ($\kappa = 0.5$) is localized in the critical shear crack (developing at 45° from the column face) at failure. Although the definition of this factor is not straightforward due to the multitude of cracks observed in the saw-cuts, the test results regarding the variation of thickness highlight that the latter is function of the load level. The internal redistribution of deformation, observed to initiate at around 80% of the failure load at the column face (Figures 5.20 and 5.21), progressively leads to similar crack openings both in the critical and failure cracks (0.35 ÷ 0.50 mm). From this level –95% of the failure load– all the additional deformations appear to be localized in the latter crack, which propagation leads to the failure of the slab specimen. It can be noted that the opening of the failure crack might be strongly related, at failure, to the shear deformations (*PB5*, East axis: $\Delta w = 0.46$ mm ≈ 0.51 mm = $\Delta d_{0\text{-}50mm}$).

The activation of the transverse reinforcement in the punching phenomenon is associated to a complex combination of flexural and shear-based deformations (see Sections 5.3.2 and 5.3.3), as also confirmed in the related state of the art (see Section 4.4). For specimen *PB6*, although the flexural cracks –amongst which the critical crack– mostly contributes to the increase of the force in the transverse elements at failure (60% for the first row, 60 ÷ 80% for the second row, 65 ÷ 95% for the third row), the development of shear deformations at the column face –in the failure crack– still provides around 30% of the total steel contribution on the punching load.

As some differences are expected for other cases, it was of interest to perform a comparison regarding the development of flexural and shear deformations in slabs reinforced with various types and amounts of headed-like systems (Figure 5.37). All the specimens are comparable in terms of concrete compressive strength (f_c = 32.3 ÷ 37.5 MPa), effective depth (d = 193 ÷ 210 mm), flexural reinforcement ratio (ρ = 1.5%) and were tested on a similar setup (Figure 5.3). The transverse elements (ρ_w = 0.1 ÷ 1.0%) were disposed radially around the column (square, c = 130 mm or 260 mm).

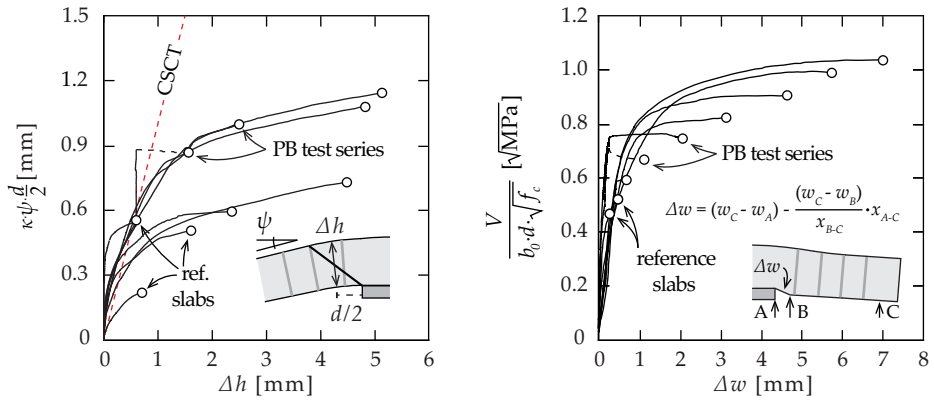

Figure 5.37 Flexural and shear deformations in slabs reinforced with headed-like systems (tests from the present research and other works performed at EPFL, notably [Lip12a])

It confirms that the previously highlighted proportions of flexural and shear deformations are expected to differ with the stiffness provided by the transverse system considered (amount, layout and anchorage performance). In Figure 5.37*(a)*, it can be noticed that the CSCT predicts reasonably at failure –through the factor κ = 0.5– the importance of the flexural deformations for the reference slabs or those reinforced with low stiffness systems (such as specimens *PB5* and *PB6*). For slabs with efficient transverse reinforcement –studs or equivalent– a larger scatter is observed between the theoretical ($\kappa \cdot \psi \cdot \frac{d}{2}$) and measured ($\Delta h$) crack openings. This is associated to the development of important shear deformations in the latter case (Figure 5.37*(b)*) not accounted in the CSCT.

Also, the flexural-based kinematics considered by the CSCT is assumed to take place simultaneously and identically in all the directions. However, the performed tests clearly confirm that the failure initiated in a specific position at the column face –in the weak axis generally– before propagating tangentially and radially around the column leading to notable differences amongst the axes. It is interesting to highlight that the elements the least activated through the flexural deformations generally appeared to be the most sensitive to the development of the shear deformations.

5.4.2 Steel contribution

The contribution of the transverse reinforcement to the punching failure load ($V_{R,s}$) is estimated by the CSCT [Fer09] with the activation model (see Appendix A) that relates the stress in the element (σ_{sw}) and the crack opening (w_b). For the performed tests, the general formulation becomes:

$$V_{R,s} = \sum_{i=1}^{n=2} \sigma_{sw,i} \cdot A_{sw,i} \tag{5.1}$$

Also, as the two first rows of transverse reinforcement intercepted by the critical crack are post-installed –no bond between the steel elements and the surrounded concrete– the formulation for plain bars is applicable, yet completed with the term related to the initial prestressing (σ_{sp}):

$$\sigma_{sw,i} = E_{sw,i} \cdot \frac{\kappa \cdot \psi \cdot h_i \cdot \cos(45)}{l_{w,i}} + \sigma_{sp,i} \leq f_{yw,i} \tag{5.2}$$

According to the CSCT, the third row of transverse elements cannot be taken into account as its distance from the column face (2.0·d) is significantly larger than the limit of 1.0·d corresponding to the 45° critical crack considered in the activation model. In fact, the performed tests confirmed that the latter elements might still contribute markedly to the failure load (see Section 5.3.2).

Notable disparities arise between the reinforcement rows when comparing the forces measured (black dots in Figure 5.38) and predicted (red dots in Figure 5.38). Although the crack kinematics is not the one highlighted in the experimental tests (see Section 5.3.1), CSCT's simplified approach still provides reasonable predictions regarding the total steel contribution (dashed lines in Figure 5.38), generally overestimated the measured one by 20 ÷ 30%. The absence of activation of the third row –according to CSCT– seems to partially compensate, in overall, the larger increase of force considered for the first and second rows in comparison to the test results.

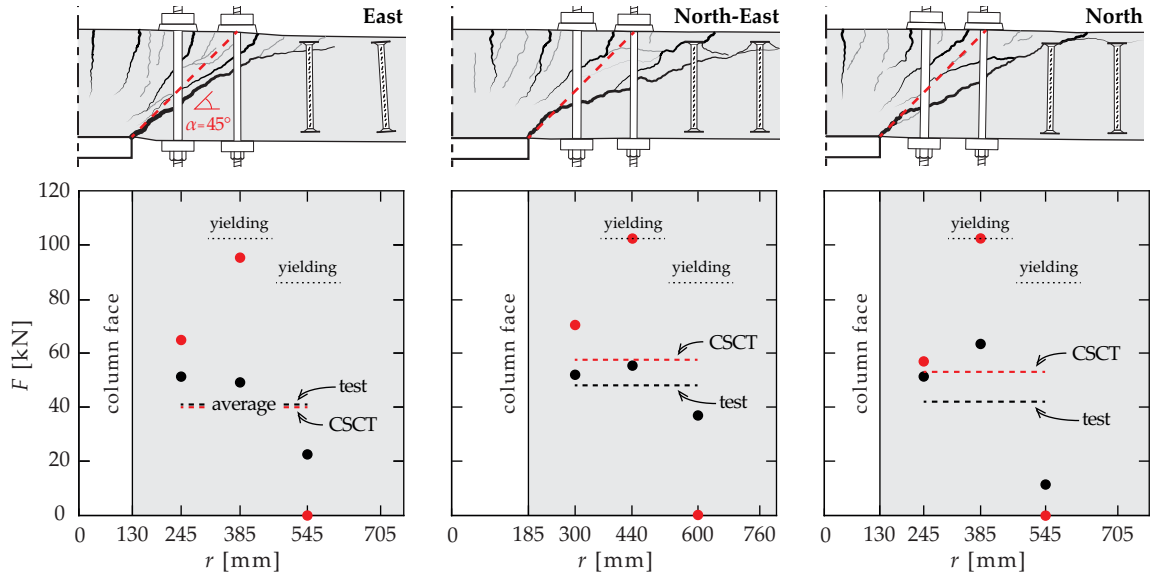

Figure 5.38 Comparison between measured (black dots) and predicted (red dots) transverse reinforcement contribution at failure in specimen *PB6* for the elements of the first three rows

It supports the fact that the activation of the transverse reinforcement is not only proportional to the rotation (as currently considered in the CSCT). The disparities between the predicted and measured forces might be related to the presence of several flexural-based cracks effectively intercepting the transverse elements, but also to the development of the failure crack from the column face (associated to shear deformations). It has to be noted that the theory and experiments would differ even more considering that a part of the force is directly transmitted to the column face through the elements of the first and second rows.

Regarding the maximal strength related to the punching failure mode within the shear-reinforced area, the activation of the shear reinforcement in the post-failure phase of specimen *PB6* provides some interesting conclusions (Figure 5.39). The additional force in the transverse elements (ΔF) was systematically more important for the closest rows with respect to the column (1 in Figure 5.39). It is interesting to highlight that, for the second row (2 in Figure 5.39), the increase of force appears to be related to the failure kinematics previously described in Section 5.3.1, with notable disparities amongst the axes. Indeed, from the East axis –where the failure initiated (Figure 5.21)– the additional load in the slab to be transmitted in this axis ($\Delta V/8$) –dashed line in Figure 5.39– is strongly correlated with the additional force (ΔF) in the second row of transverse elements. It is interesting to observe that the activation of this specific reinforcement row appears to be progressively reduced throughout the failure propagation on the other axes (with respect to the East axis).

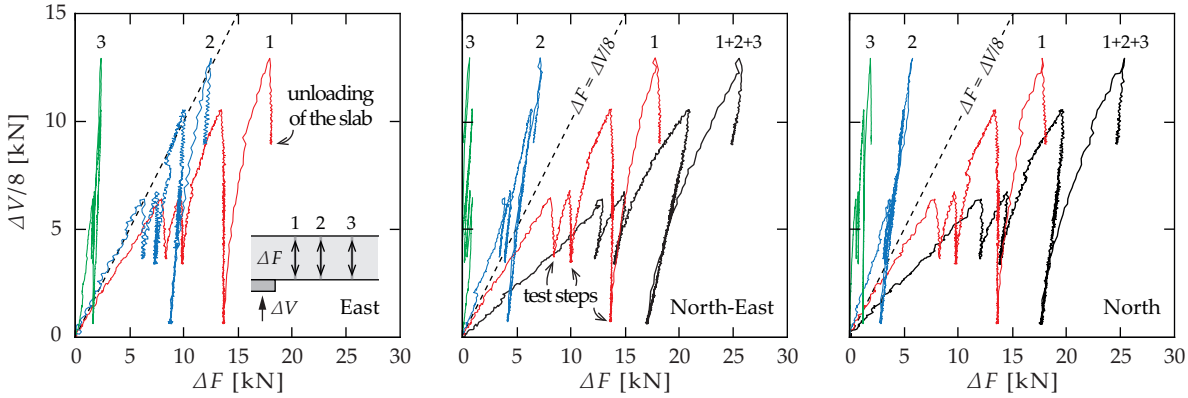

Figure 5.39 Post-punching phase for specimen *PB6* (main slab axes): additional activation of the three rows of transverse elements (ΔF) with respect to the additional load in the slab (ΔV) and assuming it uniformly distributed in the 8 rows of reinforcement (ΔV /8)

The presented results confirm that a redistribution of internal forces takes place at failure in the slab between steel and concrete. In the post-failure phase, the fact that the sum of the additional force of the transverse reinforcement in one axis (1+2+3 in Figure 5.39) is greater than the additional load introduced in this axis ($\Delta V/8$) supports that the load carried by the concrete is progressively transferred to the steel elements with increasing rotations ($V_s \rightarrow V_{sy}$ as $V_c \rightarrow 0$). The redistribution therefore allows for a further activation of the shear reinforcement after failure up to the achievement of the yielding capacity of the transverse elements or of another potential failure mode. In the case of specimen *PB6*, the test was interrupted for security reasons as soon as the development of yield stresses was measured in one transverse element (of the second row of shear reinforcement).

5.4.3 Concrete contribution

The accurate measurements of the steel contribution ($V_{R,s}$) in the test series allow to estimate the one of the concrete. Considering that the first three rows of transverse reinforcement are involved in the phenomenon, the part of the punching load (V_R) associated to concrete ($V_{R,c,exp.}$) is defined as:

$$V_{R,c,\text{exp.}} = V_R - V_{R,s1} - V_{R,s2} - V_{R,s3} \tag{5.3}$$

According to CSCT [Fer09], the concrete contribution ($V_{R,c}$) is theoretically formulated through the same expression for slabs with and without transverse reinforcement as:

$$V_{R,c} = 0.75 \cdot \frac{b_0 \cdot d \cdot \sqrt{f_c}}{1 + 15 \cdot \frac{\psi \cdot d}{16 + d_g}} \tag{5.4}$$

For specimen *PB6*, assuming a mean rotation of the slab –average value at failure between the strong and weak axes (ψ_R=15.5‰)– the estimated carrying capacity provided by the concrete is of 600 kN compared to the 495 kN obtained from the measurements (1517 kN – 457 kN – 376 kN – 189 kN). For specimen *PB5*, considering similar assumptions regarding the rotations (ψ_R = 13.5‰), the estimated carrying capacity turns to 659 kN compared to 605 kN obtained from the measurements (1347 kN – 202 kN – 313 kN – 227 kN). Generally, it can be concluded that the CSCT provides accurate predictions of the concrete contribution –confirmed to decrease with increasing rotations– through the actual formulation, both for slabs with and without transverse reinforcement (Figure 5.40). Although the presence of several cracks was observed in the performed tests on slabs, the consideration by the CSCT of a unique theoretical crack –localizing half of the deformations– provides accurate predictions at failure of the concrete contribution in punching.

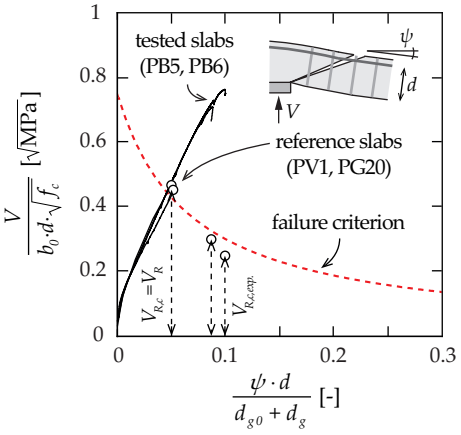

Figure 5.40 Concrete contribution in punching: theoretical predictions (dashed line) compared to experimental results (empty dots) for slabs with and without shear reinforcement

The disparities between the predictions and the experimental results might be partly related to the assumption that no transfer of shear forces is achieved between the transversal elements of the different rows. Yet, the quantification of the latter aspect is not straightforward, and, based on the performed measurements, further interpretations of this aspect could not be reasonable given.

5.5 Influence of bond and anchorage conditions in the CSCT

This section aims at a theoretical investigation of the role of bond and anchorage conditions on the activation of the transverse reinforcement in the punching phenomenon –failure mode within the shear-reinforced area– according to CSCT [Fer09]. This work concludes the present research by combining the experimental observations from the pull-out (see Chapter 3) and punching (see Chapter 5) tests campaigns. The disparities highlighted (Figure 5.41) amongst different types of reinforcing details –representative of the elements used as punching shear reinforcement– motivated the adaptation of the existing activation model of the CSCT in order to account for non-perfect development of bond and anchorage mechanisms in this specific case (see Section 5.5.1).

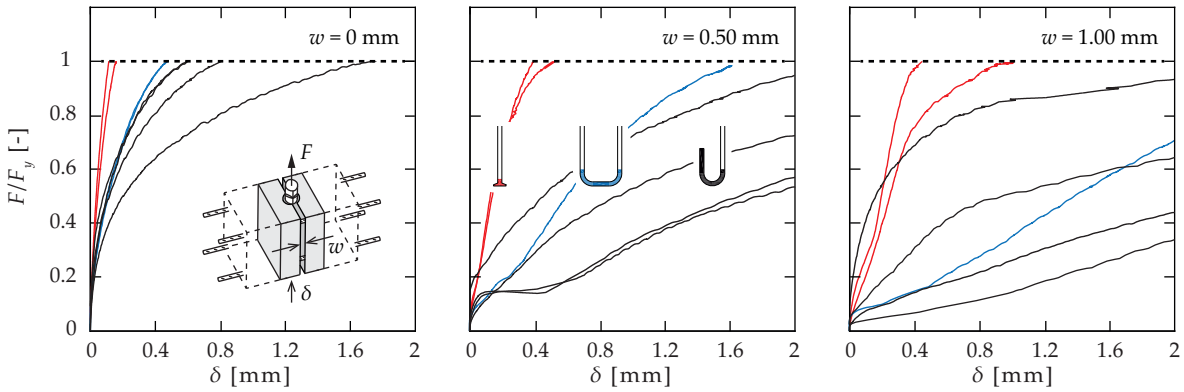

Figure 5.41 Normalized force-slip relationships of various anchorage details (headed bars, U-shaped bars and hooked bars) tested in uncracked and cracked concrete conditions (mean response, experimental scatter from tests not represented)

In the frame of this study on the activation of the transverse elements in slabs, only the initial part of the original curves –up to δ=2 mm– will be considered, as larger slip would result in a punching failure. In fact, as observed in the related literature review (see Section 4.4), the admissible crack opening prior to collapse might be dependent on the type of reinforcing system, being usually larger for elements with more efficient anchorage (larger transversal stiffness). A parametric analysis is done to appreciate the implemented modifications with respect to the CSCT (see Section 5.5.2), and the related further steps required are discussed (see Section 5.5.3).

5.5.1 Extension of the activation model

In the following, refinement proposals of the activation model of the CSCT [Fer09] are presented to account for more realistic development conditions of the transverse reinforcement (non-perfect bond and anchorage) as disparities were experimentally observed between systems [Ein16a].

Although the crack kinematics assumed in the CSCT is passably different from the one experimentally observed in the tests for the failure within the shear-reinforced area, it was previously highlighted that the model provides good predictions (see Section 5.4) with some simplifications of the phenomenon (notably, κ=0.5). In this sense, the latter point will not be changed –definition of the concrete contribution as stated by CSCT, see Eq.(5.4)– and only modifications regarding the steel contribution of the transverse elements intercepted by the critical crack will be further developed.

Bond

The consideration of a perfectly-plastic bond law is a common assumption in the analytical development related to reinforced concrete structures. It results in a linear distribution of the stresses along the embedded length of the transverse reinforcement during its activation by the opening of the critical shear crack considerably simplifying the related formulations. Yet, in the case of punching, the potential presence of cracks in the plane of the transverse elements –radial cracks associated to tangential moments (crack b1 in Figure 4.9)– can affect markedly the performance of the bond force transfer mechanisms involved in the activation of the shear reinforcement (Figure 3.15).

Assuming that a direct proportionality exists between the bond strength and the average bond stress in uncracked and cracked concrete ($f_b/f_{b0} \propto \tau_b/\tau_{b0}$), the expression proposed to quantify the decrease of bond strength of straight bars with in-plane cracks (see Section 3.3.1) can be adequately used to account for the aforementioned phenomenon (Figure 5.42*(a)*). Nevertheless, as the original equation was derived and validated for constant width cracks, it is necessary to define, for the studied case, an equivalent width of the radial crack resulting from flexural solicitations (Figure 5.42*(b)*). In this sense, it is representative to consider a mean opening ($w_{r,m}$) between the value at the tip of the crack ($w=0$) and on the tensile surface of the slab (w_r). The latter can be determined from the tangential deformations of the concrete on the top surface of the slab –at a distance $r = r_c + (r_0 - r_c)/2$ from the centre of the column– assuming plane section (reasonable in this direction) and a cracked section (compressive depth c defined according to [Mut08a]).

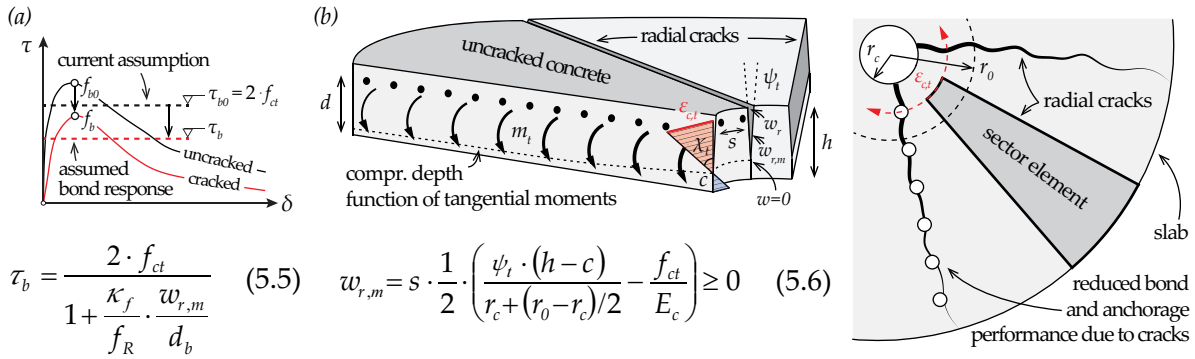

$$\tau_b = \frac{2 \cdot f_{ct}}{1 + \frac{\kappa_f}{f_R} \cdot \frac{w_{r,m}}{d_b}} \qquad (5.5)$$

$$w_{r,m} = s \cdot \frac{1}{2} \cdot \left(\frac{\psi_t \cdot (h-c)}{r_c + (r_0 - r_c)/2} - \frac{f_{ct}}{E_c} \right) \geq 0 \qquad (5.6)$$

Figure 5.42 Bond in the activation model of the CSCT: *(a)* modification proposal to account for the presence of cracks along the axis of the transverse elements; and *(b)* determination of the representative tangential opening of the radial crack to consider in the expression

In a first approach, the distance between the radial cracks in this position –multiplying the total concrete tangential strains at the surface ($\varepsilon_{c,t}$)– can be reasonably considered to correspond to the spacing of the flexural reinforcement bars (s). Although refined expressions can be found [Mut15], the latter simplification suitably reproduced recent experimental results performed at EPFL, where the opening of individual radial cracks was characterized through DIC measurements. The proposed formulations –Eq.(5.5) and Eq.(5.6)– allow to estimate, for various test configurations and specimen properties, the related reduction of the bond mechanisms in the activation of the transverse element with respect to load level in the slab (through the rotations).

Mechanical Anchorage

Based on the distribution of the transverse reinforcement and the assumed kinematics of the critical shear crack –tip at the column face with an inclination angle of 45° ($\pi/4$)– the current theory [Fer09] defines as Eq.(5.7) and Eq.(5.8) the relative displacements of the crack lips respectively parallel ($w_{b,i}$) and perpendicular ($\delta_{b,i}$) to the axis of the transverse element (Figure 5.43*(a)*). As previously discussed, the latter aspect will not benefit from any improvement as, globally, it provides correct predictions (see Sections 5.4.2 and 5.4.3) and allows to be consistent with the crack kinematics considered in the definition of the concrete contribution. Several activation regimes of the transverse elements result successively from the progressive opening of the crack associated to the increase of the slab rotation (Figure 5.43*(b)*). In practical situations, the related contribution of the transverse steel in the punching phenomenon can easily be limited –with respect to perfect activation conditions theoretically considered in the CSCT– by the development of slip at the anchorage associated to the degradation of local force transfer mechanisms (see Figure 4.23*(c)*). The latter observations emphasise the necessity of considering a more realistic response of the shear reinforcement, notably on the tensile part of the slab where the presence of cracks might markedly decrease its performance. In this sense, a tri-linear activation law (F-δ) was adopted in the following developments (Figure 5.43*(b)*) –defined with the parameters F_0, F_u, K– to represent the various disparities amongst the available and forthcoming types of punching reinforcing systems.

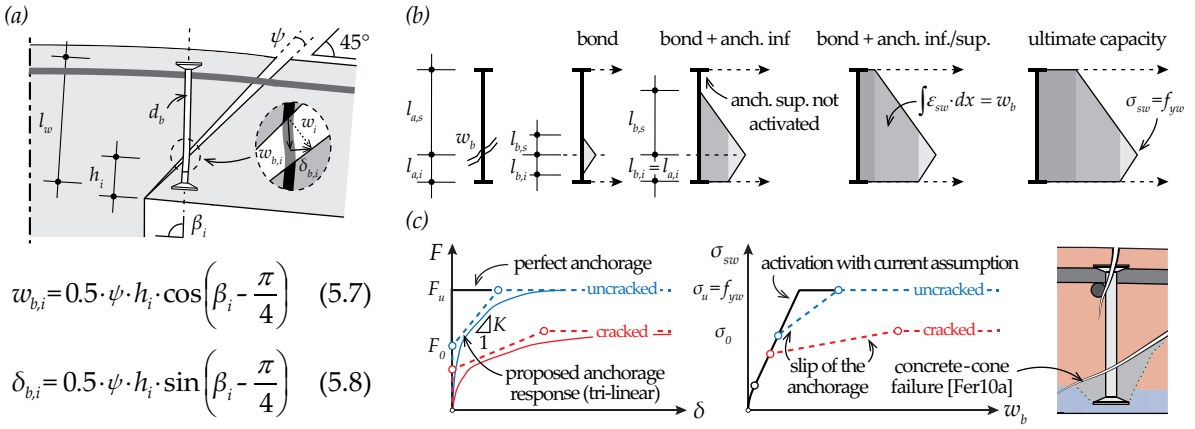

$$w_{b,i} = 0.5 \cdot \psi \cdot h_i \cdot \cos\left(\beta_i - \frac{\pi}{4}\right) \quad (5.7)$$

$$\delta_{b,i} = 0.5 \cdot \psi \cdot h_i \cdot \sin\left(\beta_i - \frac{\pi}{4}\right) \quad (5.8)$$

Figure 5.43 Anchorage in the activation model of the CSCT: *(a)* main assumptions regarding the crack opening soliciting the transverse reinforcement; *(b)* evolution of the stress distributions in a deformed transverse element; and *(c)* modification proposal to account for non-perfect activation (particularly for the anchorage situated in the tensile part of the slab)

The implementation of the modified activation model –defining the contribution of the transverse reinforcement in punching– required the determination of the new relations between the component of the crack opening in the axis of the transverse element (w_b) and its associated stress (σ_{sw}). These formulations were derived on a similar basis as in Appendix A, but to consider non-perfect bond and anchorage conditions. The top and bottom anchorages were distinguished –with the indices s and i respectively for superior and inferior– to consider differences of performance amongst them. As the developments could not be systematically rewritten in an explicit form, they are generally presented as w_b – σ_{sw} relationships (incremental approach on σ_{sw} with $\sigma_{sw} \leq f_{yw}$).

For deformed elements, the activation of the transverse reinforcement –characterized by the stress at the crack (σ_{sw})– depends on the bond and anchorage conditions. For small crack openings (w_b), the steel contribution is generally only associated to bond phenomenon (perfectly-plastic law assumed):

$$w_b = \int \varepsilon \cdot dx = \left(\frac{l_{b,i} \cdot \sigma_{sw}}{2} + \frac{l_{b,s} \cdot \sigma_{sw}}{2}\right) \cdot \frac{1}{E_{sw}} \quad \text{with} \quad l_{b,i} = l_{b,s} = \frac{\sigma_{sw} \cdot d_b}{4 \cdot \tau_b}$$

$$w_b = \left(\frac{{\sigma_{sw}}^2 \cdot d_b}{8 \cdot \tau_b} + \frac{{\sigma_{sw}}^2 \cdot d_b}{8 \cdot \tau_b}\right) \cdot \frac{1}{E_{sw}} = \left(\frac{d_b}{4 \cdot \tau_b \cdot E_s}\right) \cdot {\sigma_{sw}}^2 \qquad (5.9)$$

$$\text{conditions} \begin{cases} l_{b,s} \leq l_{a,s} \rightarrow \sigma_{sw} \leq \dfrac{4 \cdot \tau_b \cdot l_{a,s}}{d_b} \\ l_{b,i} \leq l_{a,i} \rightarrow \sigma_{sw} \leq \dfrac{4 \cdot \tau_b \cdot l_{a,i}}{d_b} \end{cases}$$

As the bottom anchorage gets activated ($0 < F_i \leq F_{0,i}$), the bond keeps on developing towards the other extremity of the element. The integration of the related strains for this regime provides:

$$w_b = \frac{\sigma_{sw} \cdot l_{b,s}}{2 \cdot E_{sw}} + \frac{\sigma_{b,i} \cdot l_{a,i}}{2 \cdot E_{sw}} + \frac{\left(\sigma_{sw} - \sigma_{b,i}\right) \cdot l_{a,i}}{E_{sw}}$$

$$\text{with} \quad \sigma_{b,i} = \frac{4 \cdot \tau_b \cdot l_{a,i}}{d_b} \quad \text{and} \quad l_{b,s} = \frac{\sigma_{sw} \cdot d_b}{4 \cdot \tau_b}$$

$$w_b = \left(\frac{d_b}{8 \cdot E_{sw} \cdot \tau_b}\right) \cdot {\sigma_{sw}}^2 + \left(\frac{l_{a,i}}{E_{sw}}\right) \cdot \sigma_{sw} - \left(\frac{2 \cdot \tau_b \cdot l_{a,i}^2}{d_b \cdot E_{sw}}\right) \qquad (5.10)$$

$$\text{conditions} \begin{cases} \left(\sigma_{sw} - \sigma_{b,i}\right) \leq \sigma_{0,i} \rightarrow \sigma_{sw} \leq \left(\sigma_{0,i} + \sigma_{b,i}\right) \\ l_{b,s} \leq l_{as} \rightarrow \sigma_{sw} \leq \dfrac{4 \cdot \tau_b \cdot l_{a,s}}{d_b} \end{cases}$$

Under some conditions ($F_i > F_{0,i}$), the bottom anchorage can potentially initiates to slip (δ_i), leading to increase markedly the crack opening and decrease the related transverse steel contribution:

$$w_b = \frac{\sigma_{sw} \cdot l_{b,s}}{2 \cdot E_{sw}} + \frac{\sigma_{bi} \cdot l_{a,i}}{2 \cdot E_{sw}} + \frac{\left(\sigma_{sw} - \sigma_{b,i}\right) \cdot l_{ai}}{E_{sw}} + \delta_i$$

$$\text{with} \quad \delta_i = \frac{\Delta\sigma_i}{K_i} \cdot \frac{\pi \cdot {d_b}^2}{4} \quad \text{and} \quad \Delta\sigma_i = \left(\sigma_{sw} - \sigma_{b,i} - \sigma_{0,i}\right)$$

$$\text{where} \ \sigma_{b,i} = \frac{4 \cdot \tau_b \cdot l_{a,i}}{d_b} \quad \text{and} \quad l_{b,s} = \frac{\sigma_{sw} \cdot d_b}{4 \cdot \tau_b} \quad \text{and} \quad \sigma_{0,i} = \frac{4 \cdot F_{0,i}}{\pi \cdot {d_b}^2}$$

$$w_b = \left(\frac{d_b}{8 \cdot E_{sw} \cdot \tau_b}\right) \cdot {\sigma_{sw}}^2 + \left(\frac{l_{a,i}}{E_{sw}} + \frac{\pi \cdot {d_b}^2}{4 \cdot K_i}\right) \cdot \sigma_{sw} - \left(\frac{2 \cdot \tau_b \cdot l_{a,i}^2}{d_b \cdot E_{sw}} + \frac{\left(\sigma_{b,i} + \sigma_{0,i}\right) \cdot \pi \cdot {d_b}^2}{4 \cdot K_i}\right) \qquad (5.11)$$

$$\text{conditions} \begin{cases} \left(\sigma_{sw} - \sigma_{b,i}\right) \geq \sigma_{0,i} \rightarrow \sigma_{sw} \geq \left(\sigma_{0,i} + \sigma_{b,i}\right) \\ l_{b,s} \leq l_{a,s} \rightarrow \sigma_{sw} \leq \dfrac{4 \cdot \tau_b \cdot l_{a,s}}{d_b} \end{cases}$$

It is also possible that, prior to the development of the latter regime, the top anchorage also gets activated ($0 < F_s \leq F_{0,s}$). The bond then provides its maximum contribution in the phenomenon, yielding to the following expression:

$$w_b = \frac{\sigma_{b,i} \cdot l_{a,i}}{2 \cdot E_{sw}} + \frac{(\sigma_{b,i} + \sigma') \cdot l_{a,s}}{2 \cdot E_{sw}} + \frac{(\sigma_{sw} - \sigma_{b,i}) \cdot l_{a,i}}{E_{sw}} + \frac{(\sigma_{sw} - \sigma' - \sigma_{b,i}) \cdot l_{a,s}}{E_{sw}} \qquad (5.12)$$

$$\text{with} \quad \sigma_{b,i} = \frac{4 \cdot \tau_b \cdot l_{a,i}}{d_b} \qquad \text{and} \quad \sigma' = \frac{(l_{a,s} - l_{a,i}) \cdot 4 \cdot \tau_b}{d_b}$$

$$\text{conditions} \begin{cases} (\sigma_{sw} - \sigma' - \sigma_{b,i}) \leq \sigma_{0,s} \rightarrow \sigma_{sw} \leq (\sigma_{0,s} + \sigma' + \sigma_{b,i}) \\ (\sigma_{sw} - \sigma_{b,i}) \leq \sigma_{0,i} \rightarrow \sigma_{sw} \leq (\sigma_{0,i} + \sigma_{b,i}) \end{cases}$$

A situation intermediate to those previously presented can also arise. Both anchorages are activated, but only the bottom one develops some slip ($F_i > F_{0,i}$):

$$w_b = \frac{\sigma_{b,i} \cdot l_{a,i}}{2 \cdot E_{sw}} + \frac{(\sigma_{b,i} + \sigma') \cdot l_{a,s}}{2 \cdot E_{sw}} + \frac{(\sigma_{sw} - \sigma_{b,i}) \cdot l_{a,i}}{E_{sw}} + \frac{(\sigma_{sw} - \sigma' - \sigma_{b,i}) \cdot l_{a,s}}{E_{sw}} + \delta_i \qquad (5.13)$$

$$\text{with} \quad \sigma_{b,i} = \frac{4 \cdot \tau_b \cdot l_{a,i}}{d_b} \quad \text{and} \quad \sigma' = \frac{(l_{a,s} - l_{a,i}) \cdot 4 \cdot \tau_b}{d_b} \quad \text{and} \quad \sigma_{0,i} = \frac{4 \cdot F_{0,i}}{\pi \cdot {d_b}^2}$$

$$\text{with} \quad \delta_i = \frac{\Delta\sigma_i}{K_i} \cdot \frac{\pi \cdot {d_b}^2}{4} \quad \text{and} \quad \Delta\sigma_i = (\sigma_{sw} - \sigma_{b,i} - \sigma_{0,i})$$

$$\text{conditions} \begin{cases} (\sigma_{sw} - \sigma' - \sigma_{b,i}) \leq \sigma_{0,s} \rightarrow \sigma_{sw} \leq (\sigma_{0,s} + \sigma' + \sigma_{b,i}) \\ (\sigma_{sw} - \sigma_{b,i}) \geq \sigma_{0,i} \rightarrow \sigma_{sw} \geq (\sigma_{0,i} + \sigma_{b,i}) \end{cases}$$

The regime that is the most fundamentally different from the one considered by the actual theory [Fer09] is related to conditions leading to the simultaneous development of slip in both anchorages ($\delta_i + \delta_s$). It is a critical phase in the activation of the transverse reinforcement in punching, as it is potentially associated to an important loss of stiffness in the behaviour and the increase of force.

$$w_b = \frac{\sigma_{b,i} \cdot l_{a,i}}{2 \cdot E_{sw}} + \frac{(\sigma_{b,i} + \sigma') \cdot l_{a,s}}{2 \cdot E_{sw}} + \frac{(\sigma_{sw} - \sigma_{b,i}) \cdot l_{a,i}}{E_{sw}} + \frac{(\sigma_{sw} - \sigma' - \sigma_{b,i}) \cdot l_{a,s}}{E_{sw}} + \delta_i + \delta_s \qquad (5.14)$$

$$\text{with} \quad \sigma_{b,i} = \frac{4 \cdot \tau_b \cdot l_{a,i}}{d_b} \quad \text{and} \quad \sigma' = \frac{(l_{a,s} - l_{a,i}) \cdot 4 \cdot \tau_b}{d_b} \quad \text{and} \quad \sigma_{0,i} = \frac{4 \cdot F_{0,i}}{\pi \cdot {d_b}^2}$$

$$\text{and with} \quad \delta_i = \frac{(\sigma_{sw} - \sigma_{b,i} - \sigma' - \sigma_{0,i}) \cdot \pi \cdot {d_b}^2}{4 \cdot K_i} \cdot \frac{K_s}{(K_i + K_s)} + \frac{\sigma' \cdot \pi \cdot {d_b}^2}{4 \cdot K_i}$$

$$\text{and with} \quad \delta_s = \frac{(\sigma_{sw} - \sigma_{b,i} - \sigma' - \sigma_{0,i}) \cdot \pi \cdot {d_b}^2}{4 \cdot K_s} \cdot \frac{K_i}{(K_i + K_s)}$$

$$\text{conditions} \begin{cases} (\sigma_{sw} - \sigma' - \sigma_{b,i}) \geq \sigma_{0,s} \rightarrow \sigma_{sw} \geq (\sigma_{0,s} + \sigma' + \sigma_{b,i}) \\ (\sigma_{sw} - \sigma_{b,i}) \geq \sigma_{0,i} \rightarrow \sigma_{sw} \geq (\sigma_{0,i} + \sigma_{b,i}) \\ \sigma_{0,i} \leq \sigma_{0,s} \end{cases}$$

Considering that the top anchorage might most likely slip prior to the bottom one, provides:

$$w_b = \frac{\sigma_{b,i} \cdot l_{a,i}}{2 \cdot E_{sw}} + \frac{(\sigma_{b,i} + \sigma') \cdot l_{a,s}}{2 \cdot E_{sw}} + \frac{(\sigma_{sw} - \sigma_{b,i}) \cdot l_{a,i}}{E_{sw}} + \frac{(\sigma_{sw} - \sigma' - \sigma_{b,i}) \cdot l_{a,s}}{E_{sw}} + \delta_s \qquad (5.15)$$

$$\text{with} \quad \sigma_{b,i} = \frac{4 \cdot \tau_b \cdot l_{a,i}}{d_b} \quad \text{and} \quad \sigma' = \frac{(l_{a,s} - l_{a,i}) \cdot 4 \cdot \tau_b}{d_b} \quad \text{and} \quad \sigma_{0,s} = \frac{4 \cdot F_{0,s}}{\pi \cdot {d_b}^2}$$

$$\text{with} \quad \delta_s = \frac{\Delta\sigma_s}{K_s} \cdot \frac{\pi \cdot {d_b}^2}{4} \quad \text{and} \quad \Delta\sigma_s = (\sigma_{sw} - \sigma_{b,i} - \sigma' - \sigma_{0,s})$$

$$\text{conditions} \quad \begin{cases} (\sigma_{sw} - \sigma' - \sigma_{b,i}) \geq \sigma_{0,s} \rightarrow \sigma_{sw} \geq (\sigma_{0,s} + \sigma' + \sigma_{b,i}) \\ (\sigma_{sw} - \sigma_{b,i}) \leq \sigma_{0,i} \rightarrow \sigma_{sw} \leq (\sigma_{0,i} + \sigma_{b,i}) \end{cases}$$

In the continuity of the previous situation, both anchorages can then also slip simultaneously –yet one anchorage might have initiated prior to the other one– thus defining:

$$w_b = \frac{\sigma_{b,i} \cdot l_{a,i}}{2 \cdot E_{sw}} + \frac{(\sigma_{b,i} + \sigma') \cdot l_{a,s}}{2 \cdot E_{sw}} + \frac{(\sigma_{sw} - \sigma_{b,i}) \cdot l_{a,i}}{E_{sw}} + \frac{(\sigma_{sw} - \sigma' - \sigma_{b,i}) \cdot l_{a,s}}{E_{sw}} + \delta_s + \delta_i \qquad (5.16)$$

$$\text{with} \quad \sigma_{b,i} = \frac{4 \cdot \tau_b \cdot l_{a,i}}{d_b} \quad \text{and} \quad \sigma' = \frac{(l_{a,s} - l_{a,i}) \cdot 4 \cdot \tau_b}{d_b} \quad \text{and} \quad \sigma_{0,s} = \frac{4 \cdot F_{0,s}}{\pi \cdot {d_b}^2}$$

$$\text{and with} \quad \delta_s = \frac{(\sigma_{sw} - \sigma_{b,i} - \sigma_{0,i}) \cdot \pi \cdot {d_b}^2}{4 \cdot K_s} \cdot \frac{K_i}{(K_s + K_i)} + \frac{(\sigma_{sw} - \sigma_{b,i} - \sigma' - \sigma_{0,s}) \cdot \pi \cdot {d_b}^2}{4 \cdot K_s}$$

$$\text{and with} \quad \delta_i = \frac{(\sigma_{sw} - \sigma_{b,i} - \sigma_{0,i}) \cdot \pi \cdot {d_b}^2}{4 \cdot K_i} \cdot \frac{K_s}{(K_s + K_i)}$$

$$\text{conditions} \quad \begin{cases} (\sigma_{sw} - \sigma' - \sigma_{b,i}) \geq \sigma_{0,s} \rightarrow \sigma_{sw} \geq (\sigma_{0,s} + \sigma' + \sigma_{b,i}) \\ (\sigma_{sw} - \sigma_{b,i}) \geq \sigma_{0,i} \rightarrow \sigma_{sw} \geq (\sigma_{0,i} + \sigma_{b,i}) \\ \sigma_{0,s} \leq (\sigma_{0,i} - \sigma') \end{cases}$$

Finally, an alternative to the latter case can also occur under some conditions related to the anchorage laws and the intersection of the crack with the transverse element, leading to the following:

$$w_b = \frac{\sigma_{b,i} \cdot l_{a,i}}{2 \cdot E_{sw}} + \frac{(\sigma_{b,i} + \sigma') \cdot l_{a,s}}{2 \cdot E_{sw}} + \frac{(\sigma_{sw} - \sigma_{b,i}) \cdot l_{a,i}}{E_{sw}} + \frac{(\sigma_{sw} - \sigma' - \sigma_{b,i}) \cdot l_{a,s}}{E_{sw}} + \delta_s + \delta_i \qquad (5.17)$$

$$\text{with} \quad \delta_s = \frac{(\sigma_{sw} - \sigma_{b,i} - \sigma' - \sigma_{0,s}) \cdot \pi \cdot {d_b}^2}{4 \cdot K_s} \cdot \frac{K_i}{(K_s + K_i)}$$

$$\text{and with} \quad \delta_i = \frac{(\sigma_{sw} - \sigma_{b,i} - \sigma' - \sigma_{0,s}) \cdot \pi \cdot {d_b}^2}{4 \cdot K_i} \cdot \frac{K_s}{(K_s + K_i)} + \frac{\left(\sigma_{0,s} - (\sigma_{0,s} - \sigma')\right) \cdot \pi \cdot {d_b}^2}{4 \cdot K_i}$$

$$\text{conditions} \quad \begin{cases} (\sigma_{sw} - \sigma' - \sigma_{b,i}) \geq \sigma_{0,s} \rightarrow \sigma_{sw} \geq (\sigma_{0,s} + \sigma' + \sigma_{b,i}) \\ (\sigma_{sw} - \sigma_{b,i}) \geq \sigma_{0,i} \rightarrow \sigma_{sw} \geq (\sigma_{0,i} + \sigma_{b,i}) \\ \sigma_{0,s} > (\sigma_{0,i} - \sigma') \end{cases}$$

5.5.2 Parametric analysis

The former expressions were derived for the most general case –different F-δ laws for the top and bottom anchorages of the transverse reinforcement– but some simplifications can reasonably be assumed regarding the activation of these elements in the punching phenomenon, with respect to the observations highlighted in the literature and from the performed experimental tests.

In this sense, the consideration by the CSCT of perfect anchorage conditions ($F_{0,i} = F_{u,i} = F_y$) in the soffit of the slab –potentially limited by a concrete-cone failure mode (Figure 5.43*(c)*) [Fer10a]– is relatively plausible (limited related investigations exist [Eli82]). This affirmation is supported by the favourable compressive state of stress developing in the vicinity of the column – together with the deformation of the slab– locally enhancing the force transfer mechanisms.

The reduction of the performance of actual reinforcing details in cracks –similar to those used in the transverse reinforcement for punching (see Section 3.2)– requires an implementation of new bond and anchorage conditions as they differ markedly from the ideal ones considered by the CSCT (Figure 5.44). The decrease of the average bond stress (τ_b/τ_{b0}) in presence of cracks is assumed to be directly related to the one of the bond strength (f_b/f_{b0}) with the proposed model (see Section 3.3.1). The reported responses of headed and U-shaped bars –representative of studs and stirrups punching systems– support that although the ultimate capacity can systematically be achieved for such anchorages ($F_{u,s} = F_y$), a progressive degradation of the initial –uncracked– stiffness (K_0) with increasing crack openings cannot be avoided ($K < K_0$). It is assumed that the top anchorage of the transverse elements begins to slip as soon as it gets activated (bi-linear law, $F_{0,s}$=0).

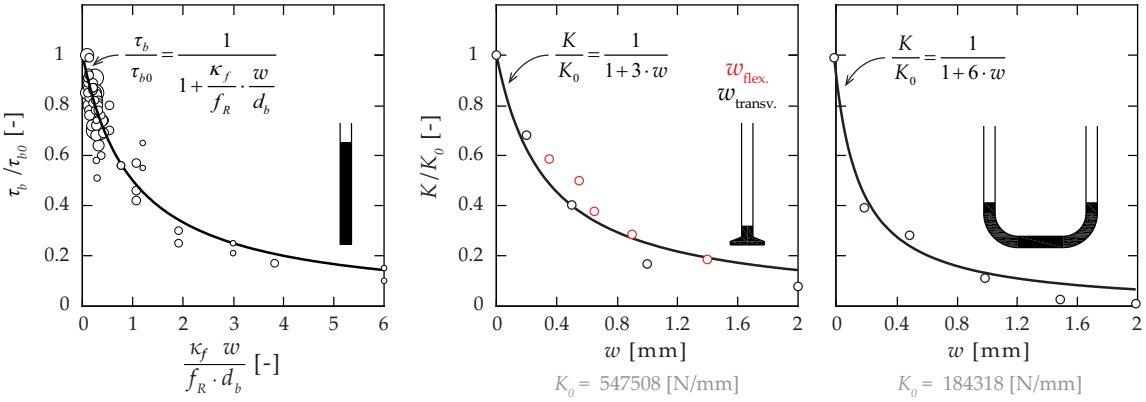

Figure 5.44 Main assumptions of the extended activation model for punching: steel contribution with the consideration of a degradation of bond and anchorage mechanisms due to the presence of cracks for straight bars, headed bars (studs) and U-shaped bars (stirrups)

In the following comparisons, the kinematics of the critical shear crack and the concrete contribution are kept as stated by the CSCT [Fer09] as the pertinence of the approach was confirmed in this investigation (Figure 5.40). The contribution of the transverse reinforcement is calculated with an element disposed on the critical perimeter (at d/2 from the column face, intercepted at its mid-height). The performance of the anchorages –affected by flexural-based cracks in the case of punching– is assumed to be reasonably well approximated, locally, by the one obtained from the experimental pull-out test campaign in transverse cracks of constant width (see Section 3.1.3).

Although a simultaneous degradation of bond and anchorage conditions should be considered, the phenomena are firstly considered independently to better appreciate their respective influences on the activation of the transverse reinforcement during punching.

For elements made of deformed steel, the development of bond on both sides of the critical shear crack governs the initial increase of the force in the reinforcing details. In presence of non-optimal development conditions –such as a crack along the axis of the bar (see Section 3.3)– the contribution of the transverse reinforcement can be distinctly delayed until the activation of the anchorage at the extremities of the element. The latter situation is particularly well highlighted in Figure 5.45, which compares the reduction of the punching strength ($V_{R,in}$) for various steel products (perfect anchorage). The decrease of the bond performance is estimated with Eq.(5.5) considering an average crack opening between the one at the level of the anchorage (w, in Figure 5.45) and at the tip of the crack. The trends will likely be even more pronounced with bars of limited surface properties – lower values of bond index f_R– in comparison to the one adopted for the parametric study (f_R=0.06, representative of the actual steel production). The role of the anchorage is also investigated for similar conditions for studs and stirrups (perfect bond) confirming the related issues (Figure 5.46).

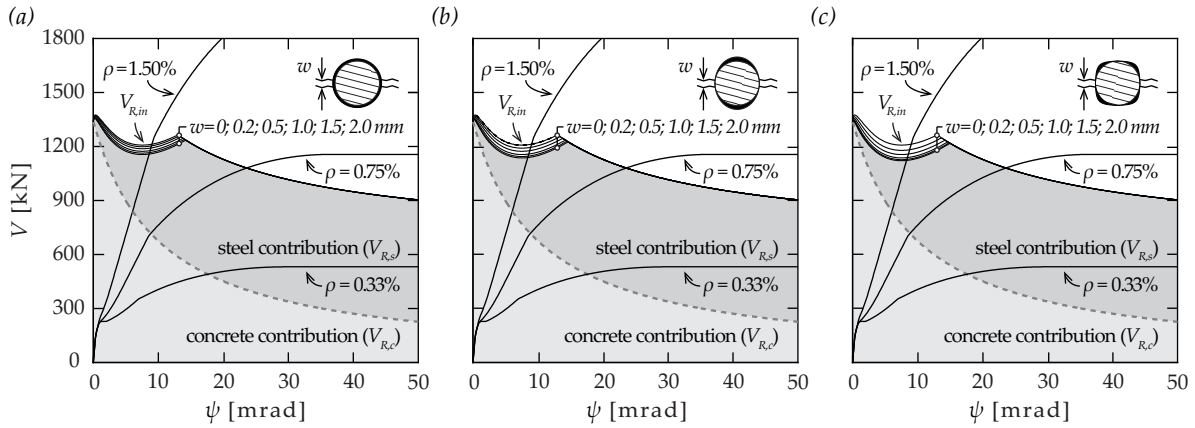

Figure 5.45 Influence of bond conditions in the activation of the transverse reinforcement in punching phenomenon (d=210 mm, f_c=30 MPa, d_g=16 mm, d_b=14 mm, f_{yw}=550 MPa): *(a)* 1-lug bars; *(b)* 2-lugs bars; and *(c)* 4-lugs bars (f_R=0.06, perfect anchorage conditions)

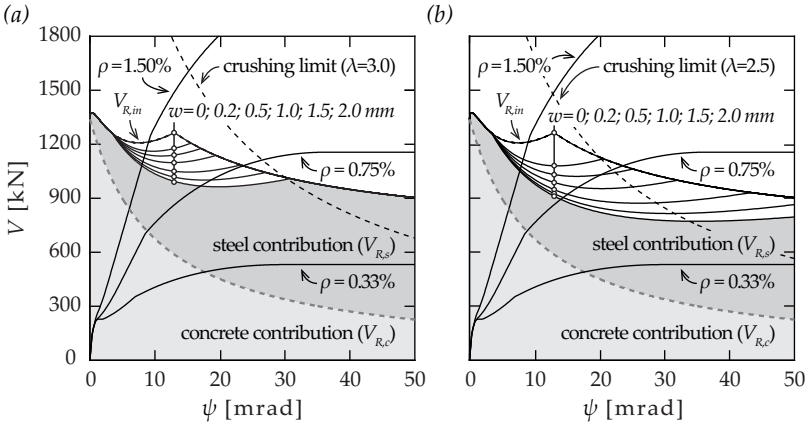

Figure 5.46 Influence of anchorage conditions in the activation of the transverse reinforcement in punching phenomenon (d=210 mm, f_c=30 MPa, d_g=16 mm, d_b=14 mm, f_{yw}=550 MPa): *(a)* studs; and *(b)* stirrups ($K_{0,studs}$ / $K_{0,stirrups}$ ≈ 3.0, perfect bond conditions)

For comparable cracking conditions –same crack width (w) at the level of the anchorage– it is suggested that, in the case of typical slender slabs, the activation of the transverse elements for punching failure within the shear-reinforced area is rather governed by the anchorage of the reinforcing system than its bond properties. The steel contribution might be so limited that crushing of the first concrete strut –in presence of large amounts of transverse reinforcement– could potentially not be achieved. This is supported by several experimental evidences in which the failure is not clearly defined in the saw-cuts, being probably related to anchorage issues (Figure 4.23). Generally, the consideration of realistic anchorage conditions (non-perfect) in the activation model (Figure 5.46) indicates that the development of the steel full capacity prior to failure –intersection between the load-rotation curve and the failure criterion– is not systematic (see Section 4.4). However, the investigations performed in the present research (see Section 5.4) confirmed that the development of shear deformations close to the ultimate load and the redistribution of internal forces at failure allow to activate the entire capacity of the transverse reinforcement intercepted by the crack (associated to larger deformation of the slab). Also, the disparities observed between the different steel products –assumed in the most critical disposition regarding cracking phenomenon– indicates that bond is not solely a determinant factor in the activation of the transverse reinforcement (Figure 5.45). The latter mechanism relies rather on the anchorage performance, for which the optimal behaviour of studs in comparison to stirrups was theoretically demonstrated. Yet, this might be fundamentally different under other configurations –such as for thick slab for instance– where the activation of the transverse elements by bond represents a more important part of the total steel contribution on the punching strength in comparison to the cases presented.

Also, it must be pointed out that the disparities between the evaluated punching reinforcing systems –studs and stirrups– might potentially be accentuated in reality, as they are usually produced from deformed steel with respectively 2 and 4-lugs (the latter ones being generally the most affected by the presence of cracks, see Section 3.4). This can be highlighted in Figure 5.47 in which the activation model combines the effect of cracks on the force transfer mechanisms by bond and anchorage. This is particularly of interest as, for large crack openings, the contribution of bond is considerably limited, and that most of the activation therefore relies on the response of the anchorage.

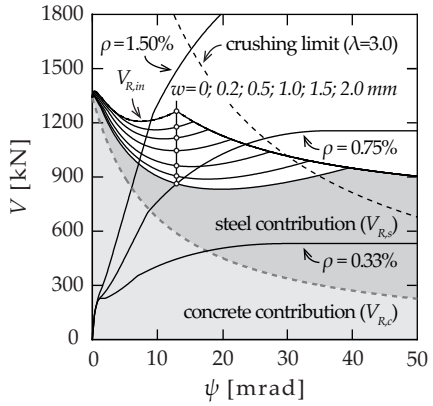

Figure 5.47 Influence of bond and anchorage conditions in the activation of the transverse reinforcement in punching (d=210 mm, f_c=30 MPa, d_g=16 mm, d_b=14 mm, f_{yw}=550 MPa): the case of standard deformed studs made of 2-lugs bars (f_R=0.06)

5.5.3 Discussion and further steps

Theoretical investigations supported by test results (see Section 3.2) and observations from literature confirmed the necessity to account for more realistic activation of the transverse elements in punching (see Section 5.4). The related developments therefore aimed at contributing on the role of bond and anchorage conditions of the transverse elements –considered as perfect by the CSCT– for the failure mode within the shear reinforced-area.

The derivation and the implementation of the formulations to account for the degradation of the force transfer in presence of cracks in the current activation model [Fer09] is certainly a first step towards the better understanding of the involved phenomena. The extended model allows to draw some interesting conclusions on the governing mechanisms –associated to bond and anchorage– controlling the activation of the transverse reinforcement. The performance of studs was observed to be better in comparison to other reinforcing systems –such as stirrups-like details– under similar conditions, confirming the higher interest given to this type of anchorage in practice.

To be consistent, a second step should necessarily be taken in the continuity of the presented developments, with respect to the critical shear crack activating the transverse elements. Indeed, the refined activation model –for which the current model is an upper bound– can only be entirely consistent with the consideration of larger crack openings or a different failure kinematics. This affirmation is supported by Figure 5.37 illustrating the fact that the actual theory –through κ-factor– tends to underestimate the effective crack width measured in tests. This is directly related to the main assumption of the CSCT –opening of the critical shear crack only associated to flexural deformations– that does not account for shear deformations although they might be significant in presence of transverse reinforcement. Improvements are required on the latter aspects in order to be closer to the experimental evidences highlighted for the studied failure mode (see Section 4.4) as well as to the results of the performed punching test series (see Section 5.3). The proposed flexural-based crack kinematics presented in Figure 5.48 appears, in this sense, as an interesting alternative, for which the concrete contribution could even be estimated with the actual failure criterion (stating that the deformations would be localized in one of the cracks at failure).

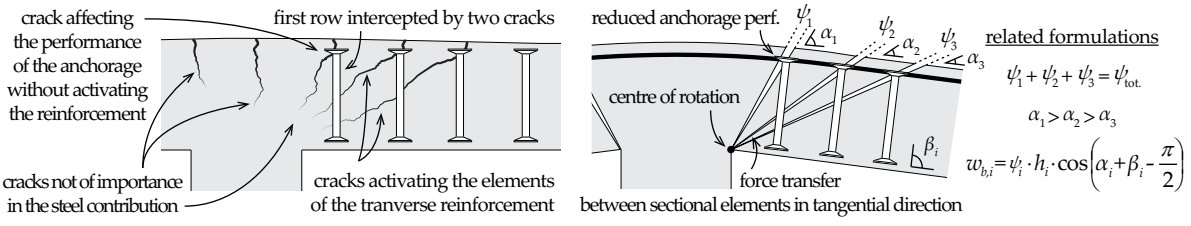

Figure 5.48 Proposed slab kinematics for the failure mode within the shear-reinforced area

The latter was motivated by the progressive development of the flexural cracks from the centre of the slab specimen to its periphery (position defined with respect to the position of the top anchorage of the transverse reinforcement). It tends to provide a larger activation of the first element (intercepted by two cracks) or equivalent for the first two rows, being more in agreement with the experimental observations presented in this thesis.

5.6 Synthesis

Although the use of transverse elements is a common and well-established solution to enhance the response of the slabs to punching, the activation of this very specific reinforcement is a complex phenomenon –still under investigation– involving both concrete and steel in the critical region close to column. This chapter contributes to the latter topic with respect to the failure mode within the shear-reinforced area (see Section 5.1) through a specific experimental campaign. Based on the limitations highlighted in the related literature review regarding the measurements performed during most of these tests, the present work aimed at the accurate definition of the force in the transverse reinforcement elements and the related crack openings (see Section 5.2). The development of a reinforcing system to control the state of the first row of transverse elements (passive/active) also constitutes an innovative aspect of the performed tests and offers interesting possibilities for further experimental investigations. The main results and observations (see Section 5.3) confirm the complexity of the force transfer mechanisms occurring in the slab, and are depicted in the frame of the CSCT (see Section 5.4) indicating that although the actual theory provides reasonable predictions, some of its aspects might be improved. The latter motivated the refinement of the existing activation model to consider non-perfect bond and anchorage conditions (see Section 5.5). For tests with low amounts of transverse reinforcement and large amount of flexural reinforcement ratio, the following points were principally highlighted in this chapter:

- The formation and development of the flexural-based cracks is progressive –from above the column to the periphery of the slab specimen– and might intercept several rows of the transverse reinforcement in the vicinity of the column;
- The position of these cracks appears to be strongly related to the position of the top anchorages of the transverse elements disposed in the slab (especially for studs-like details);
- The related steel activation is strongly associated to the slab rotation and constitutes a consequent part of the total force in the reinforcing elements at failure (usually more than 60%);
- Prior to failure, an internal redistribution of the deformations takes place, with a decompression developing at the column face (similarly to what is observed in the case of footings);
- The failure initiates at the column face in one specific location but systematically on the weak axis of the slab. The development of shear deformations in this position provides an additional activation of the transverse reinforcement (larger for the elements of the closest rows);
- The performed measurements confirm the propagation of the failure crack –radially and tangentially around the column– without systematically joining the existing ones resulting from the flexural deformations (progressive decrease of the angle of the failure crack);
- The peak contributions of the steel and concrete in the failure load are not achieved simultaneously and present some disparities amongst the axes related to the various crack patterns;

- The failure kinematics is potentially relatively different amongst the slab axes. With the propagation of the failure crack, a new kinematics associated to vertical displacement is progressively established uniformly in the slab influencing the activation of shear reinforcement;

- The current assumptions of the CSCT regarding the kinematics of the critical shear crack tend to overestimate the individual activation of the transverse elements in the slab. Yet, in overall, it provides an accurate prediction of the total steel contribution to the punching strength;

- The performed tests confirm that the failure criterion considered by the CSCT for slab without transverse reinforcement can also be reasonably used to estimate the contribution of the concrete for slabs with transverse elements (failure within the shear-reinforced area);

- For this specific case, experimental evidences highlight that the internal forces redistribution taking place at failure allow to define the related punching strength as the maximum between the capacity provided by the transverse reinforcement intercepted by the crack (at yielding) and the sum of both steel and concrete contributions (according to the CSCT);

- The latter remark is of major interest for prestressed slender slabs or footings reinforced with transverse elements –for which an extended literature is not yet available– where the rotations are relatively limited but a notable activation was generally achieved;

- The activation model of the CSCT was extended to consider more realistic bond and anchorage response, which provided promising results. To be entirely consistent with the experimental observations –larger crack openings, activation of the elements by several cracks and shear deformations– a refined failure kinematics should also be conjointly developed;

- The force transfer mechanisms associated to bond and anchorage control the activation of the transverse reinforcement, and are sensitive to the surrounding environment. The results highlight the significance of anchorage over bond conditions on the activation phenomenon. The superiority of headed studs with respect to other reinforcing systems was also confirmed.

It is evident that additional punching tests with a low to moderate amount of shear reinforcement have to be performed in order to confirm the present observations, notably with more usual reinforcement systems (studs or stirrups). The anchorage performance of such elements is also of major importance in the activation, potentially affecting the kinematics of the failure crack, contrary to the tests performed under ideal conditions (post-installed reinforcing systems).

It would also be interesting to study the cases of slabs with more reasonable –lower– amounts of flexural reinforcement, as the theoretical investigations conducted highlight the potential development of several failure modes depending on the bond and anchorage conditions of the transverse reinforcement.

Chapter 6 Conclusions and Future Research

The present research focused on the role of bond and anchorage conditions on the activation of the transverse reinforcement in the punching phenomenon of reinforced concrete flat slabs. Supported by a meticulous experimental work, the main related issues were investigated through analytical and numerical approaches. Physically-based expressions were developed to characterize the force transfer mechanisms in cracks and the main assumptions of the Critical Shear Crack Theory (CSCT) regarding the punching failure mode within the shear-reinforced area were reviewed. The activation model of the CSCT –defining the contribution of the transverse reinforcement to the punching strength– was finally extended to consider more realistic bond and anchorage conditions

In the following, the main findings of this thesis are highlighted (see Section 6.1) and some proposals for future research are put forward (see Section 6.2). For a more exhaustive synthesis, the last Section of each chapter details the main points of interest relevant to the topic covered.

6.1 Conclusions

The extensive pull-out test campaign consisted of a hundreds details arranged in beam or tie reinforced concrete specimens. It aimed at characterizing the performance in cracks of anchorage details representative of the most common types of shear reinforcement considered in slabs against punching. The main parameters evaluated were the opening, the type and the position of the crack. Size effect was also investigated through the use of two different bar diameters for each reinforcing details. The measurements of the force acting on the anchorage and of the related slip resulted in the so-called force-slip relationships describing its behaviour in the given conditions.

The investigations performed confirmed –and considerably extended– the available information from literature on the topic of the force transfer mechanisms between steel and concrete, from which the following conclusions can be drawn:

- Bond and anchorage performance were confirmed to be significantly affected by the presence of in-plane cracks, even small and controlled in their development. The actual response (force-slip relationships) is however markedly dependent on the detailing of the reinforcement:
    - Deformed straight bars and plain hooked bars are the most sensitive details, with a systematic reduction of both stiffness and strength. Such reinforcing solutions should not be solely used in structural members if the risk of cracking in the anchorage zone is not constructively avoided;

  - Deformed hooked bars also presented a progressive reduction of the stiffness with increasing crack opening, yet for limited width the yield strength could generally still be achieved. The disparities in the degradation are related to the orientation of the detail with respect to the crack and to the presence of a constructive bar passing through the bend;
  - Deformed U-shaped bars or headed bars exhibited the lowest sensitivity to cracking and could systematically be activated up to the yielding of the bar. Also, in comparison to other types of anchorage evaluated, the stiffness was in this case only merely affected.

- The formation of a concrete wedge –related to the phenomenon of bearing– was observed in some saw-cuts. Its position, geometry and size are specific to each of the evaluated details and materialize the local force transfer. The penetration of this concrete element in a formed crack seems to govern the stiffness of the anchorage response in such conditions (for large slip);

Comparisons of the few existing formulations –from code provisions and researchers– for the evaluation of the latter phenomenon for straight bars, supported the necessity to develop a more global and consistent expression (with mechanical background), notably for large values of normalized crack openings. The combination of the proposed analytical approach and the implemented numerical method offers an interesting, relevant and elegant solution to account for the presence of cracks on the bond performance for various types of steel products and situations. The following points could be highlighted from the comparisons performed:

- The influence of in-plane cracking on bond behaviour was accurately reproduced with considerations analogous to the aggregate interlock related to the surface profile –ribs or indentations– and the surrounding concrete;
- The type of surface profile –ribs or indentations– is potentially of importance in the performance of deformed details in cracks, such as straight or hooked bars for which the part of the force transfer accomplished by bond is not negligible in the overall response;
- Actual steel reinforcing products are usually composed of 1, 2, 3 or 4-lugs per section. The bars with a large number of lugs per section are the least sensitive to the orientation of the crack according to the section (exception: 1-lug section corresponding to continuously threaded bar);
- Deformed bars with indentations are the most sensitive to the presence of a crack –for a given width– in comparison to deformed bars with ribs. This appears to be mainly related to the disparities in the effective geometry of the section influencing the contact localization;
- The parameters actually considered in the definition of bond properties for reinforcing bars in concrete –bond index f_R– are solely not sufficient to characterize its performance properly in the presence of cracks as well as for various rib geometry of the reinforcement bars.

The punching test series consisted of three full-scale flat slab specimens with a low amount of transverse reinforcement and a high flexural reinforcement ratio. It aimed at improving the knowledge on the internal crack kinematic and the activation of the transverse elements for the failure mode within the shear-reinforced area. Specific measurements of the force (external load cells) and crack openings (full and partial thickness variation devices) pointed out the following observations:

- The activation of the transverse reinforcement may be divided into several phases:
    - Initially, the transverse elements are only slightly activated until the load corresponds to the failure of the reference specimen. In this phase, the concrete contributes mainly solely to the strength of the slab;
    - Then, the progressive development of several internal cracks –intercepting only one or two rows– largely contributes to the increase of the force in the transverse reinforcement. The latter phase was observed to be related to flexural deformations (function of the slab rotation);
    - Prior to failure, a redistribution of deformations at the column face leads to the sudden development of a splitting failure crack from this position –intercepting three rows or more– providing an additional contribution rather related to shear deformations (independent of the slab rotation);
    - After failure, an internal force redistribution leads to a further activation –potentially up to the yielding capacity– of the transverse elements.
- The propagation of the failure crack from a specific position at the column face –systematically in the weak axis– was confirmed in both radial and tangential directions. The inclination of the failure surface is progressively decreasing to achieve the transmission of internal forces.

The extended measurements of the activation of the transverse reinforcement –systematic in all the directions of the slab– combined to an innovative reinforcing setup allowed to track the concrete and steel contributions in the punching phenomenon. It provided the experimental information required to review the main assumptions of the CSCT for the failure mode of interest. The following conclusions were pointed out:

- The failure criteria considered originally for slabs without shear reinforcement can be adequately used to estimate the concrete contribution also for slabs with transverse elements. The part of the load carried by the concrete is confirmed to decrease for increasing slab rotations;
- The simplified flexural-based kinematics and the idealist bond and anchorage conditions considered in the activation model of the CSCT provide a reasonable approximation of the total steel contribution at failure. The individual estimation of the activation per row of transverse reinforcement at failure is not yet well captured by the current model (overestimated);

- The punching strength for the punching within the shear-reinforced area can be defined as the maximum load between the sum of the individual contributions of the concrete and the transverse reinforcement at failure, or the yielding capacity of the transverse reinforcement intercepted by the failure crack (achieved for large rotations of the slab in the post-failure phase).

Based on the review of the CSCT's main assumptions –validating the concrete contribution and crack kinematics– the present work is concluded by an extension of the current activation model. Non-perfect bond and anchorage conditions were implemented in order to highlight theoretically the influence of cracking phenomenon on the activation of the transverse reinforcement. The main points related to these developments are the following:

- The results presented suggest that, in the case of typical slender slabs, the activation of the transverse elements for punching failure within the shear-reinforced area is governed rather by the anchorage of the reinforcing system than by its bond properties;

- Under similar cracking conditions, the activation of studs in punching was observed to be systematically higher in comparison to other reinforcing systems (such as stirrups). This is directly related to the optimal force transfer performance of headed bar details in cracks highlighted in this research;

- The development of the full capacity of the transverse reinforcement prior to failure is not systematic for the failure mode of interest. The latter affirmation is partially supported by the experimental evidences from the related literature review.

6.2 Recommendations for future research

In order to contribute to the knowledge on the topic of this research, a limitation of the scope was required to ensure the achievement of the main objectives initially determined. In this sense, several related aspects –potentially of importance– would deserve some further investigations:

- Activation of various reinforcement detailing solutions in confined concrete, to characterize the response of the bottom anchorage of the transverse elements at the soffit of the slab in the vicinity of the column. Although the latter point is not critical, some systems involving bond phenomena could benefit more significantly from these favourable conditions;

- General provisions regarding the performance of anchorage types suitable in cracked concrete conditions should be proposed. Standardized test procedures and setups should be developed to characterize and compare new transverse reinforcement systems on similar bases. Also, additional studies on indented bars should be conducted, as they were clearly under-investigated in the last decades and were observed to be less efficient in severe cracking conditions;

- Additional punching tests with low amount of transverse reinforcement and moderate flexural reinforcement ratio, combined with specific measurements of the force in the transverse elements and of the crack openings in the vicinity of the column should be performed. The re-

sults aim to discuss the influence of realistic bond and anchorage conditions –associated to actual punching systems, not post-installed– on the failure kinematic and the activation of the reinforcement. As important synergies were highlighted, a reference test should be systematically considered in the test program for further interpretations;

- Activation of the shear reinforcement in the case of footings or prestressed slabs, for which the rotations at failure are particularly limited and the crack kinematics might be passably different. Attention should clearly be focused on the accurate definition of the shear deformations, contributing more significantly in this case to the increase of force in the transverse elements. It could also confirm the related maximum punching strength associated to this failure mode;

- The considerable amount of parameters involved in punching with transverse reinforcement – disposition, amount, inclination, anchorage performance– and the disparities amongst the test configurations strongly limited the related developments. In the coming years, punching numerical methods would offer an interesting alternative to experimental campaigns for the detailed study of the activation of the transverse reinforcement in punching.

In addition to these topics, some points highlighted during this research could be extended to other issues related to concrete structures. It makes sense to mention, in this concluding chapter, the potential use of some of the aforementioned developments and results for other research. The following recommendations appear, above all, to be the most interesting and the most promising:

- The pull-out tests on straight and hooked bars –made of the same steel product– pointed out interesting similarities regarding the force-slip relationships. The results make conceivable, for hooks details, a distinction of the different force transfer mechanisms involved –bond, friction and mechanical anchorage– and the development of a general method for its characterization;

- The analytical expressions developed for straight bars in in-plane cracks could be used to improve the predictions of the bond phenomenon with corrosion (usually investigated with an equivalent crack width). However, an additional roughness should be considered in the formulation proposed within this research to consider the additional roughness of the interface;

- The numerical approach proposed can be easily extended to consider intersecting cracks at the level of the bar. The evaluation of the bond performance in such severe conditions can also find potential applications in punching phenomenon (presence of radial and tangential cracks);

- Parameters related to rib geometry –such as rib inclination and orientation, lug width and spacing– should be further investigated for different bar types in order to describe, in a more consistent manner, the related bond properties with the bond index f_R;

- Finally, the extended activation model considers realistic bond and anchorage conditions – developed in the frame of this thesis for punching and steel shear reinforcement– can be used more generally to estimate the contribution of any type of element in various applications.

References

[Abr13] Abrams D. A., *Tests of Bond between Concrete and Steel*, University of Illinois Bulletin, 71, USA, 1913, 238 p.

[ACI14] ACI Committee 318, *Building Code Requirements for Structural Concrete*, ACI 318-14, American Concrete Institute, Farmington Hills, Michigan, USA, 2014, 519 p.

[Alb11] Albrecht C. and Schnell J., *Wirksamkeit örtlicher Bewehrungselemente zur Querkrafttragfähigkeit von Deckenplatten mit integrierten Leitungsführungen*, Beton- und Stahlbetonbau 106, Heft 8, Aug. 2011, pp. 522-530

[And63] Andersson J. L., *Punching of Concrete Slabs with Shear Reinforcement*, Transactions of the Royal Institute of Technology, Stockholm, Sweden, 1963

[And77] Andrä H.-P., *Ductile Slab Column Connections*, Master Thesis, Department of Civil Engineering, University of Calgary, Canada, Mar. 1977, 227 p.

[And79] Andrä H.-P., *Dübelleisten zur Verhinderung des Durchstanzens bei hochbelasteten Flachdecken*, Bautechnik, Nr. 56, H7, 1979, pp. 244-247

[And81] Andrä H.-P., *Zum Tragverahlten von Flachdecken mit Dübelleisten*, Bewehrung in Auflagerbereich, Beton- und Stahlbetonbau, Nr. 76, H3-4, 1981, pp. 53-57 (H3) and pp. 100-104 (H4)

[And92] Andreasen B. S., *Anchorage of Ribbed Reinforcing Bars*, Proceedings of the International Conference "Bond in Concrete: From Research to Practice", CEB - Riga Technical University, Riga, Latvia, 1992, pp. 1.28-1.37

[Aou13] Aoude H., Cook W. D. and Mitchell D., *Two-Way Slab Parking Structures in Canada*, Concrete International, Vol. 35, No. 12, Dec. 2013, pp. 47-54

[AST04] American Association State Highway and Transportation Officials Standard (AASHTO), *A 615/A 615M: Standard Specification for Deformed and Plain Billet-Steel Bars for Concrete Reinforcement*, ASTM, USA, 2004, 5 p.

[Bac05] Bach C., *Druckversuche mit Eisenbetonkörpern*, Mitteilungen über Forschungsarbeiten des VDI, Heft 29, Berlin, 1905, pp. 1–49

[Bac07] Bach C. and Graf O., *Versuche mit Eisenbetonbalken – Zweiter* Teil, Mitteilungen über Forschungarbeiten, Heft 45-47, 1907

[Bac11a] Bach C. and Graf O., *Versuche mit Eisenbeton-balken zur Bestimmung des Einflusses der Hakenform der Eiseneinlagen*, Deutscher Ausschuss für Eisenbeton, Heft 9, 1911

[Bac11b] Bach C. and Graf O., *Versuche mit Eisenbeton-balken zur Ermittlung der Widerstandsfähigkeit verschiedener Bewehrung gegen Schubkräfte*, Deutscher Ausschuss für Eisenbeton, Heft 10, 1911

[Bas96] Bashandy T. R., *Application Of Headed Bars in Concrete Members*, PhD Thesis, University of Texas, Austin, USA, Dec. 1996, 318 p.

[Ben89] Bensimhon J., *Étude du Comportement de Chevilles Implantées en Zone Tendue et Fissurée du Béton*, Report of the Centre Scientifique et Technique du Bâtiment, Apr. 1989

[Ber88] Bermeister K., *Stochastik in der Befestigungstechnik mit realistischen Einflussgrössen*, Dissertation, University of Innsbruck, 1988

[Ber91] Berner D. E., Gerwick B. C. and Hold G. C., *T-Headed Stirrup Bars*, Concrete International, Vol. 13, No. 5, May 1991, pp. 49-53

[Ber94] Berner D. E. and Hold G. C., *Headed Reinforcement in Disturbed Strain Regions of Concrete Members*, Concrete International, Vol. 16, No. 1, Jan. 1994, pp. 48-52

[Beu02] Beutel R. and Hegger J., *The effect of anchorage on the effectiveness of the shear reinforcement in the punching zone,* Cement and Concrete Composites, 2002, 11 p.

[Beu03] Beutel R., *Durchstanzen schubbewehrter Flachdecken im Bereich von Innenstützen,* RWTH, Aachen, Germany, 2003, 267 p.

[Bir04] Birkle G., *Punching of Flat Slabs: The Influence of Slab Thickness and Stud Layout*, PhD Thesis, University of Calgary, Calgary, Canada, 2004, 217 p.

[Bir08] Birkle G. and Dilger W. H., *Influence of Slab Thickness on Punching Shear Strength*, ACI Structural Journal, Vol. 105, No. 2, Mar. 2008, pp. 180-188

[Bos84] Bosshard M. and Menn C., *Versuche über den Einfluss der Bewehrungsanordnung auf das Tragverhalten von Rahmenecken aus Stahlbeton*, Institut für Baustatik und Konstruktion ETH Zürich, Bericht Nr. 7806-1, May 1984, 34 p.

[Bra16] Brantschen F., Faria D. M. V., Fernández Ruiz M. and Muttoni A., *Bond Behaviour of Straight, Hooked, U-Shaped and Headed Bars in Cracked Concrete*, Structural Concrete [accepted for publication, DOI: 10.1002/suco.201500199]

[Bro90a] Broms C. E., *Punching of flat plates – a question of concrete properties in biaxial compression and size effect*, ACI Structural Journal, Vol. 87, No. 3, 1990, pp. 292–304

[Bro90b] Broms C. E., *Shear Reinforcement for Deflection Ductility of Flat Plates*, ACI Structural Journal, Vol. 87, No. 6, Nov.-Dec. 1990, pp. 696-705

[Bro00] Broms C. E., *Elimination of Flat Plate Punching Failure Mode*, ACI Structural Journal, V. 97, No. 1, Jan.-Feb. 2000, pp. 94-101

[Bro05] Broms C. E., *Concrete flat slabs and footings - Design method for punching and detailing for ductility*, Department of Civil and Architectural Enginnering - Division of Structural Design and Bridges - Royal Institue of technology (KTH), 80, Stockholm, Sweden, 2005

[Bro07] Broms C. E., *Ductility of Flat Plates: Comparison of Shear Reinforcement Systems*, ACI Structural Journal, Vol. 104, No. 6, Nov. 2007, pp. 703-711

[Bro16] Broms C. E., *Tangential Strain Theory for Punching Failure of Flat Slabs*, ACI Structural Journal, Vol. 113, No. 1, Jan. 2016, pp. 95–104

[Cai92] Cairns J., *Design of Concrete Structures using Fusion Bonded Epoxy Coated Reinforcement*, Proceedings of the Institution of Civil Engineers: Structures & Buildings, Heriot-Watt University Edinburgh, Vol. 94, No. 1, Edinburgh, Scotland, 1992, pp. 93-102

[Car70] Carpenter J. E., Kaar P. H. and Hanson N. W., *Discussion of Proposed Revision of ACI 318-63: Building Code Requirements for Reinforced Concrete*, ACI Journal, Vol. 68, No. 3, Sep. 1970, pp. 696-697

[CEB82] CEB, *Bond Action and Bond Behaviour of Reinforcement*, CEB Bulletin 151, France, Paris, 1982, 153 p.

[CEB97] CEB, *Design of Fastenings in Concrete – Design Guide – Parts 1 to 3*, CEB Bulletin 233, 1997, 83 p.

[CEB98] CEB, *Ductility of Reinforced Concrete Structures*, CEB Bulletin 242, 1998, 332 p.

[CEN04] European Committee for Standardization (CEN), *Eurocode 2: Design of concrete structures – Part 1: General rules and rules for buildings*, Brussels, Belgium, 2004, 225 p.

[CEN05] European Committee for Standardization (CEN), *EN 10080:2005 – Steel for the reinforcement of concrete – Weldable reinforcing steel – General*, Brussels, Belgium, 2005, 69 p.

[CEN10] European Committee for Standardization (CEN), *EN 1992-1-1/AC:2010 Amendment for: Design of concrete structures – Part 1: General rules and rules for buildings*, Brussels, Belgium, 2010, 23 p.

[CEN14] European Committee for Standardization (CEN), *EN 1992-1-1/A1:2014 Amendment for: Design of concrete structures – Part 1: General rules and rules for buildings*, Brussels, Belgium, 2014, 4 p.

[Cha92] Chana P. S. and Desai S. B., *Design of shear reinforcement against punching*, The Structural Engineer, Vol. 70, No. 9, May 1992, pp. 159-164

[Cha93] Chana P. S., *A prefabricated shear reinforcement system for flat slabs*, Proceedings of the Institution of Civil Engineers: Structures & Buildings, Vol. 99, No. 3, UK, 1993, pp. 345-358

[Cla46] Clark A. P., *Comparative Bond Efficiency of Deformed Concrete Reinforcing Bars*, ACI Journal Proceedings, Vol. 43, No. 4, Dec. 1946, pp. 381-400

[Clé12] Clément T., *Influence de la précontrainte sur la résistance au poinçonnement de dalles en béton armé*, PhD Thesis, No. 5516, Lausanne, Switzerland, Nov. 2016, 250 p.

[Clé14] Clément T., Ramos A. P., Fernández Ruiz M. and Muttoni A., *Influence of prestressing on the punching strength of post-tensionned slabs*, Engineering Structures, Vol. 72, No. 11, Aug. 2014, pp. 56-69

[Con02] Considère A., *Spiralarmierung*, Deutsche Reichspatent, Nr. 149 944, Deutsches Reich, 1902

[Con13] Condron T. L., *Principles of Design and Results of Tests on Girderless Floor Construction of Reinforced Concrete*, ACI Journal Proceedings, Vol. 9, No. 12, USA, 1913, pp. 116-126

[Cor68] Corley W. G. and Hawkins N. M., *Shearhead Reinforcement for Slabs*, ACI Journal, No. 65-59, USA, Oct. 1968, pp. 811-824

[Daw12] Dawood N. and Marzouk H., *Cracking and Tension Stiffening of High-Strength Concrete Panels*, ACI Strctural Journal, Vol. 109, No. 1, Feb. 2012, pp. 21-30

[Des15] Desnerck P., Less J. M. and Morley C. T., *Bond behaviour of reinforcing bars in cracked concrete*, Construction and Building Materials, Vol. 94, Jul. 2015, pp. 126-136

[DeV99] DeVries R. A., Jirsa J. O. and Bashandy T., *Anchorage Capacity in Concrete of Headed Reinforcement with Shallow Embedments*, ACI Structural Journal, Vol. 96, No. 5, Sep. 1999, pp. 728-736

[Dil81] Dilger W. H. and Ghali A., *Shear Reinforcement for Concrete Slabs*, Journal of the Structural Division - ASCE, Vol. 107, USA, Dec. 1981, pp. 2403-2420

[Dil08] Dilger W. H., Discussion on [Bro07], ACI Structural Journal, Vol. 105, No. 5, Sep.-Oct. 2008, pp. 649-651

[DIN84] DIN 488-2, *Betonstahl – Betonstabstahl: Masse und Gewichte*, Deutsches Institüt für Normung, Sep. 1984

[DIN01] DIN 1045, *Tragwerke aus Beton, Stahlbeton und Spannbeton: Teil 1 Bemessung und Konstruktion*, Deutsches Institüt für Normung, Jul. 2001

[Drå86] Drågen A., *T-Headed Bars SP2: Fatigue Tests*, Report No. STF18 F86048, SINTEF, 1986

[Dra16] Drakatos I.-S., *Seismic behaviour of slab-column connections without transverse reinforcement*, PhD Thesis No. 7232, Lausanne, Switzerland, Aug. 2016, 194 p.

[Dyk88] Dyken T. and Kepp B., *Properties of T-Headed Reinforcing Bars in High Strength Concrete*, Nordic Concrete Research, No. 7, Dec. 1988, pp. 41-51

[Edd14] Eddy H. T. and Turner C. A. P., *Concrete-Steel Construction*, Heywood Mfg. Co., USA, Minneapolis, 1914, 438 p.

[Ein15] Einpaul J., Fernández Ruiz M. and Muttoni A., *Influence of moment redistribution and compressive membrane action on punching strength of flat slabs*, Engineering Structures, Vol. 86, UK, Mar. 2015, pp. 43-57

[Ein16a] Einpaul J., Brantschen F., Fernández Ruiz M. and Muttoni A., *Performance of punching shear reinforcement under gravity loading: Influence of type and detailing*, ACI Structural Journal, Vol. 113, No. 4, Jul.-Aug. 2016, pp. 827-838

[Ein16b] Einpaul, J., *Punching strength of continuous flat slabs*, PhD Thesis, No. 6928, Lausanne, Switzerland, Feb. 2016, 178 p.

[Eli82] Eligehausen R., Campi E., Bertero V. and Popov E., *Analytical model for Concrete Anchorages of Reinforcing Bars under Generalized Excitations*, Earthquake Engineering Research Center, University of California, Berkley, USA, 1982

[Eli86] Eligehausen R., Lotze D. and Sawade G., *Untersuchung zur Frage der Warscheinlichkeit, mit der Dübel in Rissen liegen*, Report No. 1/20-86/17, Institute for Building Materials, University of Stuttgart, Oct. 1989 (not published)

[Eli89] Eligehausen R. and Bozenhardt A., *Crack Widths as Measured in Actual Structures and Conclusions for Testing of Fastening Elements*, Report No. 1/42-89/9, Institute for Building Materials, University of Stuttgart, Aug. 1989 (in german)

[Eli92] Eligehausen R., *Behavior, Design and Testing of Anchors in Cracked Concrete*, ACI Journal, Special Publication, Vol. 130, Jan. 1992, pp. 123-176

[Eli06] Eligehausen R., Mallée R. and Silva J. F., *Anchorage in Concrete Construction*, Ernst & Sohn, Verlag für Architektur und technische Wissenschaften, Mar. 2006, 391 p.

[Els56] Elstner R. C. and Hognestad E., *Shearing Strength of Reinforced Concrete Slabs*, ACI Materials Journal, Vol. 53, No. 2, Detroit, USA, Jul. 1956, pp. 29-58

[Ett09] Etter S., Heinzmann D., Jäger T. and Marti P., *Versuche zum Durchstanzverhalten von Stahlbetonplatten*, Institut für Baustatik und Konstruktion, Bericht Nr. 324, Eidgenössische Technische Hochschule Zürich, Schweiz, 2009

[Fab05] Fabbrocino G., Verderame G. M. and Manfredi G., *Experimental behaviour of anchored smooth rebars in old type reinforced concrete buildings*, Engineering Structures, Vol. 27, No. 10, 2005, pp. 1575-1585

[Far14] Faria D. M. V., Einpaul J., Ramos A. P., Fernández Ruiz M. and Muttoni A., *On the efficiency of flat slabs strengthening against punching using externally bonded fibre reinforced polymers*, Construction and Building Materials, Vol. 73, Netherlands, Dec. 2014, pp. 366-377

[Fei07] Feix J. and Schustereder C., *Durchstanzen nach EN 1992-1-1 - Durchstanzversuche zur Festlegung der Nachweisgrenzen*, Bauingenieur, Vol. 82, Berlin, Germany, 2007, pp. 135-142

[Fer09] Fernández Ruiz M. and Muttoni A., *Applications of the critical shear crack theory to punching of R/C slabs with transverse reinforcement*, ACI Structural Journal, Vol. 106, No. 4, Farmington Hills, USA, Jul.-Aug. 2009, pp. 485-494

[Fer10a] Fernández Ruiz M., Muttoni A. and Kunz J., *Strengthening of flat slabs against punching shear using post-installed shear reinforcement*, ACI Structural Journal, Vol. 107, No. 4, USA, Jul.-Aug. 2010, pp. 434-442

[Fer10b] Fernández Ruiz M., Plumey S. and Muttoni A., *Interaction between Bond and Deviation Forces in Spalling Failures of Arch-Shaped Members without Transverse Reinforcement*, ACI Structural Journal, Vol. 107, No. 3, USA, May-Jun. 2010, pp. 346-354

[Fer10c] Ferreira M. P., *Punção em Lajes Lisas de Concreto Armado com Armaduras de Cisalhamento e Momentos Desbalanceados*, Tese de Doutorado em Estruturas e Construção Civil, Publicação E.TD – 007 A/10 Departamento de Engenharia Civil e Ambiental, Universidade de Brasília, Brasília, 2010, 275 p.

[Fer14] Ferreira M. P., Melo G. S., Regan P. E. and Vollum R. L., *Punching of Reinforced Concrete Flat Slabs with Double-Headed Shear Reinforcement*, ACI Stuctural Journal, Vol. 111, No. 1-6, Jan.-Dec. 2014, pp. 1-12

[Fer15] Fernández Ruiz M., Muttoni A. and Sagaseta J., *Shear strength of concrete members without transverse reinforcement: A mechanical approach to consistently account for size and strain effects*, Engineering structures, UK, May 2015, pp. 360-372

[FIB00] Fédération Internationale du Béton, *Bond of Reinforcement in Concrete*, *fib* Bulletin 10, 2000, 427 p.

[FIB11] Fédération Internationale du Béton, *Design of Anchorages in Concrete*, *fib* Bulletin 58, 2011, 280 p.

[FIB13] Fédération Internationale du Béton, *fib Model Code for Concrete Structures 2010*, Ernst & Sohn, Germany, 2013, 434 p.

[FIB14] Fédération Internationale du Béton, *Bond and anchorage in fib MC2010*, *fib* Bulletin 72, 2014, 161 p.

[Fis47] Fishburn C. C., *Strength and Slip Under Load of Bent-Bar Anchorages and Straight Embedments in Haydite Concrete*, ACI Journal, Proceedings, Vol. 19, No. 4, 1947

[Fra64] Franz G., *Versuche an Stahlbetonkröpern der Flachdecke im Stützenbereich*, Bericht über die Versuchreihe I (II) für die Deutsche Forschungsgemeinschaft, Bad Godesberg, Institut für Beton und Stahlbeton, Technische Hochschule Karlsruhe, 1964

[Fur86] Furche J. and Dieterle H., *Ausziehersuche an Kopfbolzen mit unterschiedlichen Kopfformen bei Verankerungen in ungerissenen Beton und in Parallelrissen*, Report No. 9/1-86/9, Institute for Building Materials, University of Stuttgart, Oct. 1986 (not published)

[Fur93] Furche J., *Zum Trag - und Verschiebungsverhalten von Kopfbolzen bei zentrischem Zug*, PhD Thesis, Stuttgart University, Jun. 1993

[Fyn86a] Fynboe C. and Thorenfeldt E., *T-Headed Bars SP1: Static Pullout Tests*, Report No. STF65 F86083, SINTEF, 1986

[Fyn86b] Fynboe C. and Thorenfeldt E., *T-Headed Bars SP3: Fatigue Tests – bars embedded in concrete*, Report No. STF65 F86088, SINTEF, 1986

[Fyn86c] Fynboe C. and Thorenfeldt E., *T-Headed Bars SP4: Shear Tests*, Report No. STF65 F86084, SINTEF, 1986

[Gam81] Gambarova P. G. and Karakoç C., *In tema di aderenza fra barre nervate e calcestruzzo, in presenza di fissure longitudinali da spacco*, Studi e Ricerche, edited by S. Dei Poli, Politecnico di Milano, Milan, Vol. 3, 1981, pp. 143-176

[Gam85] Gambarova P. G. and Zasso B., *Aderenza armature-calcestruzzo e fessurazione longitudinale da spacco: una sintesi di alcuni recenti risultati sperimentali*, Studi e Ricerche, edited by S. Dei Poli, Politecnico di Milano, Milan, Vol. 7, 1985, pp. 7-54

[Gam89] Gambarova P. G., Rosati G. P. and Zasso B., *Steel-to-concrete bond after concrete splitting: constitutive laws and interface deterioration*, Materials and Structures, Vol. 22, 1989, pp. 347-356

[Gam90] Gambarova P. G., Rosati G. P. and Omar Sharif S., *Aderenza armature-calcestruzzo e fessurazione longitudinale per barre di grosso diametro*, Studi e Ricerche, edited by S. Dei Poli, Politecnico di Milano, Milan, Vol. 12, 1990, pp. 45-79

[Gam93] Gambarova P.G., Rosati G. P. and Sufi G. M., *Aderenza armature-calcestruzzo e fessurazione longitudinale per barre di piccolo diametro*, Studi e Ricerche, edited by S. Dei Poli, Politecnico di Milano, Milan, Vol. 14, 1993, pp. 1-27

[Gam97] Gambarova P. G. and Rosati G. P., *Bond and splitting in bar pull-out: behavioural laws and concrete cover role*, Magazine of Concrete Research, Vol. 49, No. 179, Jun. 1997, pp. 99-110

[Ger92] Gerwick B. C., *Evaluation of Headed Stirrup Reinforcement*, Headed Reinforcement Inc. (a subsidiary of Metalock Norway), San Francisco, USA, Dec. 1992, 65 p.

[Gha92] Ghali A. and Hammill N., *Effectiveness of Shear Reinforcement in Slabs*, Concrete International, USA, Jan. 1992, pp. 60-65

[Gha05] Ghali A. and Youakim S. A., *Headed Studs in Concrete: State of the Art*, ACI Structural Journal, Vol. 102, No. 5, Sep. 2005, pp. 657-667

[Giu85] Giurani E. and Plizzari G., *Legami locali dell'aderenza in presenza di fissure di "splitting"*, Studi e Ricerche, edited by S. Dei Poli, Politecnico di Milano, Milan, Vol. 7, 1985, pp. 57-118

[Giu91] Giurani E., Plizzari G. and Schumm C., *Role of Stirrups and Residual Tensile Strength of Cracked Concrete on Bond*, Journal of Structural Engineering, ASCE, Vol. 117, No. 1, Jan. 1991, pp. 1-18

[Giu98] Giurani E. and Plizzari G., *Interrelation of Splitting and Flexural Cracks in RC Beams*, Journal of Structural Engineering, ASCE, Vol. 124, No. 9, Sep. 1998, pp. 1032-1040

[Gom99a] Gomes R. B. and Regan P. E., *Punching Resistance of RC Flat Slabs with Shear Reinforcement*, ASCE Journal of Structural Engineering, Vol. 125, No. 6, Reston, USA, Jun. 1999, pp. 684-692

[Gom99b] Gomes R. B. and Regan P. E., *Punching strength of slabs reinforced for shear with offcuts of rolled steel I-section beams*, Magazine of Concrete Research, Vol. 51, No. 2, London, UK, 1999, pp. 121-129

[Gom00] Gomes R. B. and Andrade M. A. S., *Does a Punching Shear Reinforcement Need to Embrace a Flexural Reinforcement of a Reinforced Concrete Flat Slab?*, International Workshop on Punching Shear Capacity of RC Slabs, Stockholm, Sweden, Jun. 2000, pp. 109-116

[Got71] Goto Y., *Cracks Formed in Concrete around Deformed Tension Bars*, ACI Journal, Vol. 68, No. 26, Japan, 1971, pp. 244-251

[Gra38] Graf O., *Verusche über die Widerstandsfähigkeit von allseitig aufliegenden dicken Eisenbetonplatten unter Einzellasten*, Deutsche Ausschuss für Eisenbeton, Heft 88, 1988

[Gre61] Gregory Industries, *Engineering Design Data for Nelson Concrete Anchors*, 1961, 15 p.

[Gua05] Guandalini S., *Poinçonnement symétrique de dalles en béton armé*, PhD Thesis, No. 3380, Lausanne, Switzerland, Dec. 2005, 201 p.

[Gua09] Guandalini S., Burdet O. and Muttoni A., *Punching tests of slabs with low amount of reinforcement ratios*, ACI Structural Journal, Vol. 106, No. 1, USA, Jan.-Feb. 2009, pp. 87-95

[Gui10] Guidotti R., *Poinçonnement de planchers-dalles avec colonnes superposées fortement sollicitées*, PhD Thesis, No. 4812, Lausanne, Switzerland, Sep. 2010, 226 p.

[Haj51] Hajnal-Konyi K., *Comparative Tests on Various Types of Bars as Reinforcement of Concrete Beams*, The Structural Engineer, Vol. 29, No. 5, May 1951, pp. 133-148

[Hal96] Hallgren M., *Punching Shear Capacity of Reinforced High Strength Concrete Slabs*, PhD Thesis, KTH, Stockholm, Sweden, 1996, 206 p.

[Hal99] Hallgren M., Kinnunen S. and Nylander B., *Punching shear tests on column footings*, Royal Institut of Technology, Department of Structural Engineering, Stockholm, 1999

[Haw67a] Hawkins N. M., *The Bearing Strength of Concrete: 1. Loading Through Rigid Plates Covering Part of the Full Supporting Area*, The University of Sydney, Research Report No. 54, Sydney, Australia, Mar. 1967

[Haw67b] Hawkins N. M., *The Bearing Strength of Concrete: 2. Loading Through Flexible Plates*, The University of Sydney, Research Report No. 84, Sydney, Australia, Aug. 1967

[Haw74] Hawkins N. M. and Corley W. G., *Moment Transfer to Columns in Slabs with Shearhead Reinforcement*, ACI Special Publication 42-36, Vol. 2, USA, 1974, pp. 847-879

[Heg99] Hegger J. and Beutel R., *Durchstanzen – Versuche une Bemessung*, Der Prüfingenieur, Heft 15, Oct. 1999, pp. 16-33

[Heg07] Hegger J., Häusler F. and Ricker M., *Zur maximalen Durchstanztragfähigkeit von Flachdecken*, Beton- und Stahlbetonbau, Vol. 102, No. 11, 2007, pp. 770-777

[Hei12] Heinzmann D., Etter S., Villiger S. and Jäger T., *Punching Tests on Reinforced Concrete Slabs with and without Shear Reinforcement*, ACI Structural Journal, Vol. 109, USA, Nov. 2012, pp. 787-794

[Hil83] Hillerborg A., *Analysis of a single crack*, Fracture mechanics of concrete, edited by F.H. Wittmann, Elsevier science Publishers B.V., 1983, pp. 223-249

[Hoa16] Hoang L. C. and Pop A., *Puncing capacity of reinforced concrete slabs with headed shear reinforcement*, Magazine of Concrete Research, Vol. 68, No. 3, Feb. 2016, pp. 118-126

[Hol89] Hole O. H., Lian M., Vinje L. and Thorenfeldt E., *Limte soyleforbindelser, uttrekksforsok med limforankret armering*, Betongprodukter, No. 2, 1989, pp. 49-55

[Hsu89] Hsu T., *Warscheinlichkeit, mit der Dübel in Rissen liegen*, Diploma Thesis, Institute for Building Materials, University of Stuttgart, Apr. 1989

[Hug95] Hughes B. P. and Xiao Y., *Flat slabs with fibre or link reinforcement at slab-column connections*, Proceedings of the Institution of Civil Engineers – Structures and Buildings, Vol. 110, No. 3, Aug. 1995, pp. 308-321

[Hya78] Hyatt T., *Improvement in composition floors, roofs, pavements*, United States Patent Office, US 206112 A, United States, 1878

[Idd99] Idda K., *Verbundverhalten von Betonrippenstählen bei Querzug*, PhD Thesis, Massivbau Baustofftechnologie Karlsruhe, Heft 34, 1999

[Ina12] Inacio M. G., Ramos R. P. and Faria D. M. V., *Strengthening of flat slabs with transverse reinforcement by introduction of steel bolts using different anchorage approaches*, Engineering Structures, Vol. 44, Nov. 2012, pp. 63-77

[Iso08] Iso M. and Goh M., *Evaluation of ultimate shear strength of reinforced concrete thin beams with singly arranged reinforcing bars*, Journal of Structural and Construction Engineering, Vol. 73, Issue 634, Dec. 2008, pp. 2205-2213

[ISO10] International Organization for Standardization, *ISO 15630-1:2010(E) – Steel for the reinforcement and prestressing of concrete – Test methods – Part 1: Reinforcing bars, wire rod and wire*, Geneva, Switzerland, 2010, 28 p.

[Jak94] Jakobsen B. and Rosendahl F., *The Slepiner Platform Accident*, Structural Engineering International, IABSE, Vol. 3, 1994, pp. 190-193

[Jir72] Jirsa J. O. and Marques J. L. G., *A Study of Hooked Bar Anchorages in Beam-Column Joints*, Project 77-3, Department of Civil Engineering, University of Texas, Austin, Jul. 1972, 92 p.

[Joh62] Johansen K. W., *Yield-line Theory*, Cement and Concrete Association, 1962, 181 p.

[Joh81] Johnson L. A. and Jirsa J. O., *The Influence of Short Embedment and Close Spacing on the Strength of Hooked Bar Anchorages*, PMFSEL Report No.81-2, Department of Civil Engineering-Structures Research Laboratory, University of Texas, Austin, Texas, 1981, 93 p.

[Jør14] Jørgensen H. B., *Strength of Loop Connections between Precast Concrete Elements: Part I and II*, Det. Tekniske Fakultet, Syddansk Universitet, Danemark, 2014, 423 p.

[Jør15] Jørgensen H. B. and Hoang L. C., *Strength of Loop Connections between Precast Bridge Decks Loaded in Combined Tension and Bending*, Structural Engineering International, Vol. 25, No. 1, Feb. 2015, pp. 71-80

[Kee54] Keefe R. A., *An Investigation on the Effectiveness of Diagonal Tension Reinforcement in Flat Slabs*, Massachusetts Institute of Technology, Master Thesis, Massachusetts, May 1954, 43 p.

[Kem68] Kemp E. L., Brezny F. S. and Unterspan J. A., *Effect of Rust and Scale on the Bond Characteristics of Deformed Reinforcing Bars*, Journal ACI, Vol. 65, No. 9, Sep. 1968, pp. 743-756

[Kin60] Kinnunen S. and Nylander H., *Punching of Concrete Slabs Without Shear Reinforcement*, Transactions of the Royal Institute of Technology, No. 158, Stockholm, Sweden, 1960, 112 p.

[Kin63] Kinnunen S., *Punching of Concrete Slabs with two-way Reinforcement*, Transactions of the Royal Institute of Technology, No. 198, Stockholm, Sweden, 1963, 108 p.

[Kob85] Kobarg J. and Hahn C., *Verhalten von Befestigungselementen in sich öffnenden und schliessenden Kreuzrissen*, Report No. 1/12-85/18, Institute for Building Materials, University of Stuttgart, Nov. 1985 (not published)

[Koc90] Koch R., *Flat Slab-Column-Connections with Shear Comb Reinforcement*, Otto Graf Journal, Vol. 1, 1990, pp. 125-140

[Kun11] Kunz E. and Thoma K., *Versuchbericht – UHFB Verankerung*, Hochschule Luzern, Jun. 2011, 16 p.

[Kup72] Kupfer H. and Baumann T., *Versuche zur Schubsicherung und Momentendeckung von profilierten Stahlbetonbalken*, Deutscher Ausschuss für Stahlbeton, Heft 218, 1972, 62 p.

[Lad98] Ladner M., *Durchstanzversuche an Flachdeckenausschnitten*, Untersuchungsbericht 419, Hochschule Technik+Architektur Luzern, Materialprüfstelle der Abteilung Bau, Horw, Schweiz, 1998

[Lan76] Langohr P. H., Ghali A. and Dilger W. H., *Special Shear Reinforcement for Concrete Flat Plates*, ACI Journal, Vol. 73, Detroit, USA, Mar. 1976, pp. 141-146

[Lee99] Lee S. C., Lee S. B., Teng S. and Morley C. T., *Punching shear tests on high strength concrete slabs*, Proceedings fifth international symposium on utilization of high strength/high performance concrete, Sandefjord, Norway, 1999, pp. 401-410

[Leh92] Lehmann R., *Metallspreizdübel im gerissenen Beton – Untersuchung des Tragverhaltens bei zentrischer Zugbeanspruchung und Berechnung der Gleitlasten*, Dissertation, Universität Stuttgart, 1992

[Leo65] Leonhardt F. and Walter R., *Eesctiweisste Bewehrungsmatten als Bügelbewehrung – Schubversuche an Plattenbalken und Verankerungsversuche*, Dr. Bautechnik 42J, Heft 10, Oct. 1965, pp. 3-15

[Lie87] Lieberum K.-H., *Das Tragverhalten von Beton bei extremer Teilflächenbelastung*, PhD Thesis, Technischen Hochschule Darmstadt, Germany, 1987, 127 p.

[Lin11] Lindorf C., *Bond fatigue in reinforced concrete under transverse tension*, PhD Thesis, Dec. 2011, 263 p.

[Lip12a] Lips S., *Punching of Flat Slabs with Large Amounts of Shear Reinforcement*, PhD Thesis, No. 5409, Lausanne, Switzerland, Jul. 2012, 273 p.

[Lip12b] Lips S., Fernández Ruiz M. and Muttoni A., *Experimental Investigation on Punching Strength and Deformation Capacity of Shear-Reinforced Slabs*, ACI Structural Journal, Vol. 109, USA, Nov. 2012, pp. 889-900

[Lip12c] Lips S., Fernández Ruiz M. and Muttoni A., *Durchstanzversuche an Deckenschnitten mit Durchstanzbewehrung*, Test Report, EPFL, Lausanne, Switzerland, Apr. 2012, 90 p.

[Lot87] Lotze D., *Untersuchung zur Frage der Wahrscheinlichkeit, mit der Dübel in Rissen liegen – Einfluss der Querbewehrung*, Institut für Werkstoffe im Bauwesen, Universität Stuttgart, not published, Stuttgart, Germany, 1987

[Lot92] Lotze D., *Befestigungen unter nicht vorwiegend ruhender Belastung*, Dissertation, Institut für Werkstoffe im Bauwesen, Universität Stuttgart, Stuttgart, Germany, 1992

[Lov90] Lovrovich J. and McLean D., *Punching shear behaviour of slabs with varying span depth ratios*, ACI Structural Journal, Vol. 87, No. 5, 1990, pp. 507-511

[Mac73] Mac Mackin P. J., Slutter R. G. and Fisher J. W., *Headed Steel Anchor under Combined Loading*, AISC Engineering Journal, 2nd quarter, Apr. 1973, pp. 43-52

[Mac05] Mac Gregor J. G. and Wight J. K., *Reinforced concrete: mechanics and design, fourth edition*, Prentie Hall, 2005, 1314 p.

[Mah12] Mahrenholtz C., *Seismic Bond Model for Concrete Reinforcement and the Application to Column-to-Foundation Connections*, PhD Thesis, Stuttgart University, Aug. 2012

[Mai26] Maillart R., *Zur Entwicklung der unterzuglosern Decke in der Schweiz und in Amerika*, Schweizerische Bauzeitung, Vol. 87, No. 21, Switzerland, Zürich, 1926, pp. 263-267

[Mar75] Marques J. L. G. and Jirsa J. O., *A study of hooked bar anchorages in beam-column joints*, ACI Journal Proceedings, Vol. 72, No. 5, May 1975, pp. 198-209

[Mar77] Marti P., Pralong J. and Thürlimann B., *Schubversuche an Stahlbeton-Platten*, Institut für Baustatik und Konstruktion, Nr. 7305-2, Zürich, Switzerland, Sep. 1977, 123 p.

[Mar97] Marzouk H. and Jiang D., *Experimental Investigation on Shear Enhancement Types for High-Strength Concrete Plates*, ACI Structural Journal, Vol. 94, Farmington Hills, USA, 1997, pp. 49-58

[May88] Mayer R., *Warscheinlichkeit, mit der Dübel in Rissen liegen*, Report No. 1/35-88/22, Institute for Building Materials, University of Stuttgart, Nov. 1989 (not published)

[May12] Maya Duque L. F., Fernández Ruiz M., Muttoni A. and Foster S. J., *Punching shear strength of steel fibre reinforced concrete slabs*, Engineering Structures, Vol. 40, Jul. 2012, pp. 83-94

[Men99] Menétrey P., *Punching in slabs with shear reinforcement: a tensile failure*, *fib* Symposium, Prague, Czech Republic, 1999, 6 p.

[Mic14] Micallef K., Sagaseta J., Fernández Ruiz M. and Muttoni A., *Assessing punching shear failure in reinforced concrete flat slabs subjected to localized impact loading*, International Journal of Impact Engineering, Vol. 71, Apr. 2014, pp. 17-33

[Min71] Minor J., *A Study of Bent Bar Anchorages in Concrete*, PhD Thesis, Faculty of Civil Engineering, Rice University, Houston, USA, 1971, 135 p.

[Min75] Minor J. and Jirsa J. O., *Behaviour of Bent Bar Anchorages*, ACI Journal, Vol. 72, No. 4, 1975, pp. 141-149

[Mir88] Mirza S.A., Furlong R.W., Ma J.S., *Flexural shear and ledge reinforcement in reinforced concrete inverted T-girders*, ACI Structural Journal, Vol. 85, Issue 5, Sep. 1988, pp. 509-520

[Mir10] Mirzaei Y., *Post-Punching Behavior of Reinforced Concrete Slabs*, PhD Thesis, No. 4613, Lausanne, Switzerland, May 2010, 203 p.

[Mör08] Mörsch E., *Der Eisenbetonbau, seine Theorie und Anwendung*, Stuttgart, 1908, 393 p.

[Mör12] Mörsch E., *Versuche mit Säulen und deren Berechnung*, Deutsche Bauzeitung, Nr. 14, Berlin, Germany, 1912, pp. 105-110

[Mok82] Mokhtar A. S., *Design of Stud Shear Reinforcement for Concrete Flat Plates*, Master Thesis, Department of Civil Engineering, University of Calgary, Canada, Dec. 1982, 140 p.

[Mok85] Mokhtar A. S., Ghali A. and Dilger W. H., *Stud Shear Reinforcement for Flat Concrete Plates*, ACI Journal, No. 82-60, Detroit, USA, Sep.-Oct. 1985, pp. 676-683

[Mül68] Müller H. H., *Ausziehеversuche mit Betonstahlhaken*, Forschungsarbeit, Bericht No. 80, Materialsprüfungsamt für das Bauwesen der Technishen Hochschule München, Dec. 1968, pp. 70-75

[Mül84] Müller F. X., Muttoni A. and Thürlimann B., *Durchstanzversuche an Flachdecken mit Aussparungen*, Institut für Baustatik und Konstruktion der ETH Zürich, Birkhäuser Verlag, Bericht Nr. 7305-5, Zürich, Switzerland, 1984, 118 p.

[Mus04] Musse T. H., *Punção em Lajes Cogumelo – Fibras de Aço e Armaduras de Cisalhamento*, Dissertação de Mestrado em engenharia Civil, Universidade Federal de Goiás, Goiânia, 2004

[Mut91] Muttoni A. and Schwartz J., *Behavior of Beams and Punching in Slabs without Shear Reinforcement*, IABSE Colloquium, Vol. 62, Stuttgart, Germany, 1991, pp. 703-708

[Mut97] Muttoni A., Schwartz J. and Thürlimann B., *Design of Concrete Structures with Stress Fields*, Birkhäuser Verlag, Basel, Switzerland, 1997, 143 p.

[Mut05] Muttoni A., Fürst A. and Hunkeler F., *Deckeneinsturz der Tiefgarage am Staldenacker in Gretzenbach*, Medieninformation vom 15.11.2005, Solothurn, Switzerland, 2005, 14 p.

[Mut08a] Muttoni A., *Punching shear strength of reinforced concrete slabs without transverse reinforcement*, ACI Structural Journal, Vol. 105, No. 4, 2008, pp. 440–450

[Mut08b] Muttoni A. and Fernández Ruiz M., *Shear strength of members without transverse reinforcement as function of critical shear crack width*, ACI Structural Journal, Vol. 105, No. 2, Farmington Hills, USA, Mar.-Apr. 2008, pp. 163-172

[Mut15] Muttoni A. and Fernández Ruiz M., *Structures en béton*, support de cours 5ème semestre, EPFL – ENAC – IBETON, Lausanne, 2015, 211 p.

[Myl28] Mylrea T. D., *The Carrying Capacity of Semicircular Hooks*, ACI Journal, Proceedings, Vol. 24, 1928, pp. 240-272

[Nie11] Nielsen M. P. and Hoang L. C., *Limit Analysis and Concrete Plasticity (Third Edition)*, CRC Press, Jan. 2011, 816 p.

[Nil83] Nilsson A., *Spänningstillstånd I Plattdel Utanför Skjuvarmering Vid Genomstansning*, Institutionen för byggnadsstatik, kungl. Tekniska högskolan, Vol. 140, Stockholm, Sweden, 1983, 52 p.

[Niy73] Niyogi S. K., *Bearing Strength of Concrete – Geometric Variations*, ASCE Journal of Structural Engineering, Vol. 99, No. 7, New York, USA, Jul. 1973, pp. 1471-1490

[Niy74] Niyogi S. K., *Concrete Bearing Strength – Support, Mix, Size Effect*, ASCE Journal of Structural Engineering, Vol. 100, No. 8, New York, USA, Aug. 1974, pp. 1685-1702

[Niy75] Niyogi S. K., *Bearing Strength of Reinforced Concrete Blocks*, ASCE Journal of Structural Engineering, Vol. 101, No. 5, New York, USA, May 1975, pp. 1125-1137

[NSW66] Nelson Stud Welding Company, *Concrete Anchor Tests No. 7*, Nelson Stud Project N. 802, Report No. 1966-5, 1966

[NTC08] NTC 2008, *Nuove Norme Tecniche per le Construzioni*, Feb. 2008, 439 p.

[Nyl72] Nylander H. and Sundquist H., *Genomstansning av pelarunderstödd plattbro av betong med ospänd armering*, Institutionen för byggnadsstatik, kungl. Tekniska högskolan, Vol. 104, Stockholm, Sweden, 1972, 64 p.

[OFR15] Kenel A., Stüssi U. and Ebeshner P., *Central documentation of mechanical properties of existing reinforcements*, Office Fédérale des Routes, Research project AGB 2008/007, Switzerland, 2015, 183 p.

[Oli00] Oliveira D. R., Melo G. S. and Regan P. E., *Punching Strengths of Flat Plates with Vertical or Inclined Stirrups*, ACI Structural Journal, Vol. 97, USA, May 2000, pp. 485-491

[Ørj87] Ørjaester O., *T-Headed Bars: Fatigue tests of embedded bars*, Report No. STF18 F87043, SINTEF, 1987

[Par75] Park R. and Paulay T., *Reinforced Concrete Structures*, Department of Civil Engineering, University of Canterbery, New Zealand, 1975, 783 p.

[Pet79] Petcu V., Stanculescu G. and Pancaldi U., *Punching strength predictions for two-way reinforced concrete slabs*, Académie de la République Socialiste de Roumanie, Série de Mécanique Appliquée, Vol. 24, No. 2, 1979, pp. 263-281

[Pil82] Pillai S. U., Kirk W. and Scavuzzo L., *Shear Reinforcement at Slab-Column Connection in a Reinforced Concrete Flat Plate Structure*, ACI Journal, Vol. 79, No. 4, Detroit, USA, Jan.-Feb. 1982, pp. 36-42

[Pil97] Pilakoutas K. and Li X., *Shear band: novel punching shear reinforcement for flat slabs*, Civil-Comp Proceedings, No. 46, Innovation in composite materials and structures, Edinburgh, 1997, pp. 35-45

[Pil03] Pilakoutas K. and Li X., *Alternative Shear Reinforcement for Reinforced Concrete Flat Slabs*, ASCE Journal of Structural Engineering, Vol. 129, No. 9, Reston, USA, Sep. 2003, pp. 1164-1172

[Pin77] Pinc R. L., Watkins M. D. and Jirsa J. O., *Strength of Hooked Bar Anchorages in Beam-Column Joints*, Report of Research Project 77-3, Department of Civil Engineering, University of Texas, Austin, Nov. 1977, 80 p.

[Pis00] Pisanty A., *Investigation into the performance and Bearing Capacity on Alternative Punching Reinforcement - Part II*, Isreal Institute of Technology, Ministry of Construction and Housing, Haifa, Israel, 2000, 45 p.

[Pos33] Posey C. J., *Tests of Anchorages for Reinforcing Bars*, State University of Iowa, 1933, 31 p.

[Pur05] Purainer R., *Last- und Verformungsverhalten von Stahlbetonflächentragwerken unter zweiaxialer Zugbeanspruchung*, Dissertation, Universität der Bundeswehr, München, 2005

[Pra79] Pralong J., Brändli W. and Thürlimann B., *Durchstanzersuche an Stahlbeton und Spannbetonplatten*, Birkhäuser Verlag, Institut für Baustatik und Konstruktion ETH Zürich, Nr. 7305-3, Switzerland, 1979

[Ran15] Randl N., Ricker M., Häusler F. and Steinberger S., *Erhöhung des Durchstanzwiderstands von Flachdecken durch Verbundeinbauteile aus UHPC*, Beton-und Stahlbetonbau, Vol. 110, No. 12, Dec. 2015, pp. 811-821

[Reg80a] Regan P. E., Test report obtained from private communications with the author, 1980, 118 p.

[Reg80b] Regan P. E., Test report obtained from private communications with the author, 1980, 21 p.

[Reg85] Regan P. E., *Shear Combs, Reinforcement against Punching*, The Structural Engineering, Vol. 63B, No. 4, Dec. 1985, pp. 76-84

[Reg97] Regan P. E., *Anchorage tests of M12 grade 8.8 studding with nuts as end anchorages*, Test report obtained from private communications with the author, 1997, 15 p.

[Reg00] Regan P. E., *Shear Reinforcement of Flat Slabs*, International Workshop On punching Shear Capacity of RC Flat Slabs, Royal Institute of Technology, Department of Structural Engineering, Stockholm, Jun. 2000, pp. 99-107

[Reg01] Regan P. E. and Samadian F., *Shear Reinforcement against punching in reinforced concrete flat slabs*, The Structural Engineer, London, England, May 2001, pp. 24-31

[Reg04] Regan P.E. and Kennedy Reid I.L., *Shear Strength of RC beams with defective stirrup anchorages*, Magazine of Concrete Research, Vol. 56, No. 3, Apr. 2004, pp.159-166

[Reh61] Rehm G., *Über die Grundlagen des Verbunds zwischen Stahl und Beton*, Deutscher Ausschuß für Stahlbeton (DAfStb), Heft 138, Berlin, Germany, 1961, 59 p.

[Reh68] Rehm G., Martin H. and Müller H.-H., *Ausziehversuche mit Betonstahlhaken*, Untersuchungsbericht, Nr. 1975, 1968

[Reh69] Rehm G., *Kriterien zur Beurteilung von Bewehrungsstäben mit hochwertigen Verbund*, Stahlbetonbau, Berichte aus Forschung und Praxis, Verlag Wilhelm Ernst & Sohn, Berlin, Germany, 1969, pp. 79-96

[Reh78a] Rehm G., Eligehausen R. and Neubert B., *Rationalisierung der Bewehrungstechnik im Stahlbetonbau – Vereinfachte Schubbewehrung in Balken*, Betonwerk+Fertigteil-Technik, Heft 3, 1978, pp. 147-155

[Reh78b] Rehm G., Eligehausen R. and Neubert B., Rationalisierung der Bewehrungstechnik im Stahlbetonbau, Teil 2 – Vereinfachte Schubbewehrung in Balken, Betonwerk+Fertigteil-Technik, Heft 4, 1978, pp. 222-227

[Reh79] Rehm G., Dieterle H. and Eligehausen R., *Rationalisierung der Bewehrungstechnik im Stahlbetonbau - Das Tragverhalten verschiedener Verankerungselemente in Rissen*, Institut für Werkstoffe im Bauwesen, Universität Stuttgart, Stuttgart, Germany, 1979

[Ric27] Richart F. E., *An Investigation of Web Stresses in Reinforced Concrete Beams*, University of Illinois, Bulletin No. 166, Jun. 1927

[RIL78] Réunion Internationale des Laboratoires et Experts des Matériaux, *Essais portant sur l'adhérence des armatures du béton – Essais par traction*, Recommendations RILEM / CEB / FIP – RC6, Matériaux et Constructions, Vol. 6, No. 32, 1978

[Riz11] Rizk E., Marzouk H. and Hussein A., *Punching shear of thick plates with and without shear reinforcement*, ACI Structural Journal, Vol. 108, No. 5, 2011, pp. 581-591

[Roj07] Rojek R. and Keller T., *Durchstanzversuche mit Bewehrung mit hochfestem Verbund, innovative Traganalysen und Bemessungsansätze*, Beton-und Stahlbetonbau, Vol. 102, No. 8, 2007, pp. 584-556

[Roš50] Roš M., *Die materialtechnischen Grundlagen und Probleme des Eisenbetons im Hinblick auf die zukünftige Gestaltung der Stahlbeton-Bauweise*, Eidgenössische Materialprüfungs- und Versuchsanstalt für Industrie, Bauwesen und Gewerbe, Bericht No. 162, Zürich, Switzerland, 1950

[Ros59] Rosenthal I., *Experimental Investigation of Flat Plate Floors*, ACI Journal, Proceedings, Vol. 56, Aug. 1959, pp. 153-166

[Sag11] Sagaseta J., Muttoni A., Fernández Ruiz M. and Tassinari L., *Non-axis-symmetrical punching shear around internal columns of RC slabs without transverse reinforcement*, Magazine of Concrete Research, Vol. 63, No. 6, Jun. 2011, pp. 441-457

[Sag14] Sagaseta J., Tassinari L., Fernández Ruiz M. and Muttoni A., *Punching of flat slabs supported on rectangular columns*, Engineering Structures, Vol. 77, Oct. 2014, pp. 17-33

[Sal13] Saliger R., *Schubwiderstand und Verbund in Eisenbetonbalken*, Springer-Verlag, Berlin, 1913

[Sco10] Scott W. F., *Discussion on Bond-Friction-Resistance in Reinforced Concrete*, A.S.C.E., Transactions, Vol. 73, 1910

[Scr82] Scribner C.F. and Wilhelm D.R., *Behavior of T-beams sections with varied shear reinforcement*, Journal of the American Concrete Institute, Vol. 79, Issue 2, Mar. 1982, pp. 139-146

[Sei77] Seible F., *Preassembled Shear Untis for Flat Slabs*, Master Thesis, Department of Civil Engineering, University of Calgary, Canada, Dec. 1977, 187 p.

[Sei80] Seible F., Ghali A. and Dilger W. H., *Preassembled shear reinforcing units for flat plates*, ACI Journal, Proceedings, Vol. 77, No. 1, Jan.-Feb. 1980, pp. 28-35

[She89] Shehata I. A. E. M. and Regan P. E., *Punching in R.C. Slabs*, Journal of Structural Engineering, Vol. 115, No. 7, Jul. 1989, pp. 1726–1740

[Shi08] Shima H. and Fukuju S., *Bond Stress Distribution along Bar Axis in Hook Anchorage of Deformed Reinforcing Bar*, 3rd ACF International Conference, 2008, pp. 654-660

[Sho63] Shoup T. E. and Singleton R. C., *Headed Concrete Anchors*, ACI Journal, Proceedings, Vol. 60, No. 9, Sep. 1963, pp. 1229-1235

[SIA89] Schweizerischer Ingenieur-und Architektenverein, *SIA 162/1:1989 – Betonbauten Materialprüfung*, Schweiz, Zürich, 1995, 80 p.

[SIA03] Schweizerischer Ingenieur-und Architektenverein, *SIA 262:2003 – Betonbau*, Schweiz, Zürich, 2003, 90 p.

[SIA13] Schweizerischer Ingenieur-und Architektenverein, *SIA 262:2013 – Betonbau*, Schweiz, Zürich, 2013, 102 p.

[SIA15] Schweizerischer Ingenieur-und Architektenverein, *SIA 262:2013 – Register normkonformer Betonstähle*, Schweiz, Zürich, 2015, 5 p.

[SIA16] Schweizerischer Ingenieur-und Architektenverein, *SIA 262:2013 – Register normkonformer Betonstähle*, Schweiz, Zürich, 2016, 5 p.

[Sil12] Silva R., Faria D. M. V. and Ramos A. P., *A physical approach for considering the anchorage head size influence in slabs strengthened with vertical steel bolts*, Structural Concrete, Vol. 14, No. 4, Dec. 2013, pp. 389–400

[Sim07] Simons I. N., *Verbundverhalten von eingemörtelten Bewehrungsstäben unter zyklischer Beanspruchung*, PhD Thesis, Stuttgart University, Jan. 2007

[Sim16] Simões J. T., Bujnak J., Fernández Ruiz M. and Muttoni A., *Punching shear tests on compact footings with uniform soil pressure*, Structural Concrete, Vol. 18, No. 4, 2016

[Smu18] Smulski E., *A Test of the S-M-I System of Flat-Slab Construction*, ACI Journal Proceedings, Vol. 14, No. 6, USA, 1918, pp. 206-232

[Sor79] Soretz S. and Hölzenbein H., *Influence of Rib Dimensions of Reinforcing Bars on Bond and Bendability*, ACI Journal, Vol. 76, No. 6, 1979, pp. 111-125

[Sor88] Soroushian P. and Obaseki K., Nagi M. and Rojas C., *Pullout behavior of hooked bars in exterior beam-column connections*, ACI Structural Journal, Vol. 85, No. 16, May-Jun. 1988, pp. 269-276

[Ste07] Stein T., Ghali A. and Dilger W. H., *Distinction between Punching and Flexural Failure Modes of Flat Plates*, ACI Structural Journal, Vol. 104 No. 3, USA, May-Jun. 2007, pp. 357-365

[Sti80] Stiglat K. and Steiner J., *Durchstanzen von mit Dübelleisten verstärkten Flachdecken, die auf Stahlstützen aufliegen*, Beton- und Stahlbetonbau, Nr. 75, H10, 1980, pp. 239-246

[Sto74] Stoker J. R., Boulware R. L., Crozier W. F. and Swirsky R. A., *Anchorage Devices for Large Diameter Reinforcing Bars*, Caltrans Report CA-DOT-TL-6626-1-73-30, California Department of Transportation, Sacramento, California, Sep. 1974

[Stü90] Stücki D. and Thürlimann B., *Versuche an Eckverbindungen aus Stahlbeton*, Institut für Baustatik und Konstruktion, ETHZ, Report 8701-1, Zurich, Switzerland, 1990, 68 p.

[Sun77] Sundquist H., *Betongplatta på pelare vid dynamisk engångslast. 1: Resultat av statiska fösök*, Bulletin 124, Department of Structural Mechanics and Engineering, Royal Institute of Technology, Stockholm, 1977, 70 p.

[Tas11] Tassinari L., *Poinçonnement symétrique des dalles en béton armé avec armature de poinçonnement*, PhD Thesis, No. 5030, Lausanne, Switzerland, Jun. 2011, 197 p.

[Tay16] Taylor F. W. and Thompson S. E., *A treatise on Concrete Plain and Reinforced*, John Wiley and Sons Inc., 3rd edition, USA, New York, 1916, 885 pp.

[Tep73] Tepfers R., *A theory of bond applied to overlapped tensile reinforcement splices for deformed bars*, Chalmers University, P-73:2, Division of Concrete structures, Göteborg, Sweden, 1973, 328 p.

[Tho90] Thorenfeldt E., *Limte soyleforbindelser, strekkstagforsok*, Betonprodukter, No. 2, 1990, pp. 18-22

[Tho02] Thompson M. K., Jirsa J. O., Breen J. E. and Klingner R. E., *Anchorage Behavuior of Headed Reinforcement: Literature Review*, Texas Department of Transportation, Research and Technology Implementation Office, Report No. FHWA/TX-0-1855-1, May 2002, 116 p.

[Tho06] Thompson M. K., Jirsa J. O. and Breen J. E., *Behavior and Capacity of Headed Reinforcement*, ACI Structural Journal, Vol. 103, No. 4, Jul. 2006, pp. 522-530

[Tim03] Timm M., *Durchstanzen von Bodenplatten unter rotationssymmetrischer Belastung*, Fachbereich Bauingenieurwesen der Technischen Universität Carolo-Wilhelmina zu Braunschweig, Braunschweig, Germany, 2003, 159 p.

[Tol88] Tolf P., *Plattjocklekens inverkan pa betongplattors hallfasthet vid genomstansning. Försök med cikulära plattor (in English: Influence of the Slab Thickness on the Strength of Concrete Slabs at Punching: Tests with Circular Slabs)*, No. 146, Royal Institut of Technology, Stockholm, 1988, 64 p.

[Tra01] Trautwein L. M., *Punção em lajes cogumelo de concreto armado com armadura de cisalhamento tipo « stud » interno e tipo « estribo inclinado »*, Dissertação de mestrado, Universidade de Brasília, Brasília, 2001, 168 p.

[Tra11] Trautwein L. M., Bittencourt T. N., Gomes R. B. and Bella J. C. D., *Punching Strength of Flat Slabs with Unbraced Shear Reinforcement*, ACI Structural Journal, Vol. 108, USA, Mar. 2011, pp. 197-205

[Var11] Varney J. C., Brown M. D., Bayrak O. and Poston R. W., *Effect of Stirrup Anchorage on shear Strength of Reinforced Concrete Beams*, ACI Structural Journal, Vol. 108, Jul. 2011, pp. 469-478

[Vaz07] Vaz A. P. R., *Resistência à Punção em Lajes Cogumelo de Concreto Armado: uma contribuição para definição de armadura mínima de cisalhamento*, Dissertação de mestrado, Universidade Federal de Goiás, Escola de Engenharia Civil, 2007, 136 p.

[Vaz09] Vaz A. P. R., Gomes R. B. and Shehata L. C. D., Study on Minimum Shear Reinforcement of Reinforced Concrete Flat Slabs, IBRACON Structures and Materials Journal, Vol. 2, Brazil, Mar. 2009, pp. 1-24

[Vec86] Vecchio F. J. and Collins M. P., *The modified compression-field theory for reinforced concrete elements subjected to shear*, ACI Journal, Vol. 83, No. 2, 1986, pp. 219-231

[Vie56] Viest I. M., *Investigations of Stud Shear Connectors for Composite Concrete and Steel T-Beams*, ACI Journal, Proceedings, Vol. 52, No. 8, Apr. 1956, pp. 875-892

[Voe80] Van der Voet A. F., *The Shear Strength of Slabs with Mechanically Anchored Shear Reinforcement*, Master Thesis, Department of Civil Engineering, University of Calgary, Canada, Jun. 1980, 177 p.

[Voe81] Van der Voet A. F., Dilger W. H. and Ghali A., *Concrete Flat Plates with Well-Anchored Shear Reinforcement Elements*, Canadian Journal of Civil Engineering, Vol. 9, No. 1, Canada, Mar. 1981, pp. 107-114

[Vol10] Vollum R. L., Abdel-Fattah T., Eder M. and Elghazouli A. Y., *Design of ACI type punching shear reinforcement to Eurocode 2*, Magazine of Concrete Research, Vol. 62, No. 1, 2010, pp. 3-16

[Wal81] Walraven J. C., *Fundamental analysis of aggregate interlock*, ASCE Journal of Structural Engineering, Vol. 107, No. 11, 1981, pp. 2245-2270

[Wal14] Walkner R., *Kritische Analyse des Durchstanznachweises nach EC2 und Verbesserung des Bemessungsansatzes*, PhD Thesis, Innsbruck Universität, Dez. 2014, 458 p.

[Wan69] Wantur H., *Dimensioning of Flat Slabs in the Column Region with Simultaneous Consideration of the Bending and Vertical Reinforcement*, PhD Thesis, University of Ghent, 1969, 184 p.

[Wan12] Wang X.-H. and Liu X.-L., *Analysis of RC beam with unbonded or exposed tensile steel reinforcements and defective stirrup anchorages for shear strength*, Computers and Concrete, Volume 10, Issue 1, Jun. 2012, pp. 59-78

[Wil79] Williams A., *The Bearing Capacity of Concrete Loaded Over a Limited Area*, Cement and Concrete Association, Technical Report 526, Wexham Springs, Slough, The United Kingdom, Aug. 1979

[WIP10] World Intellectual Property Organization, Muttoni A. and Fernández Ruiz M., Patent WO 2010116323 A1, *Reinforcement element for structural concrete construction*, Oct. 2010

[WIP11] World Intellectual Property Organization, Muttoni A., Lüchinger B. and Fernández Ruiz M., Patent WO 2011067027 A1, *Reinforcement device*, Jun. 2010

[WIP12] World Intellectual Property Organization, Martter R. P., Patent US 8220219 B2, *Reinforcing assembly, and reinforced concrete structures using such assembly*, Jul. 2014

[WIP14] World Intellectual Property Organization, Keller T., Patent US 8752347 B2, *Reinforcement element for absorbing forces of concrete in the area of support elements*, Jun. 2014

[WIP15] World Intellectual Property Organization, Muttoni A., Fernández Ruiz M. and Barras M., Patent EP 2851479 A2, *System for reinforcement against crushing with rods or transverse bars having anchoring heads*, Mar. 2015

[Woo01] Wood G. M., *Piper Row Car Park, Wolverhampton, Quantitiatve Study of the Causes of the Partial Collapse on 20th March 1997*, Structural Studies & Design Ltd, Surrey, England, 2001, 209 p.

[Wri97] Wright J. L. and McCabe S. L., *The Development Length and Anchorage Behavior of Headed Reinforcing Bars*, Structural Engineering and Engineering Materials, SM Report No. 44, University of Kansas Center of Research, Sep. 1997, 153 p.

[Yam92] Yamada T., Nanni A. and Endo K., *Punching Shear Resistance of Flat Slabs: Influence of Reinforcement Type and Ratio*, ACI Structural Journal, Vol. 89, No. 5, Farmington Hills, USA, Sep. 1992, pp. 555-563

[Yan12] Yang J.-M., Min K.-H. and Yoon Y.-S., *Effect of anchorage and strength of stirrups on shear behavior of high-strength concrete beams*, Structural Engineering and Mechanics, Vol. 41, Issue 3, 10 Feb. 2012, pp. 407-420

[Yit66] Yitzhaki D., *Punching Strength of Reinforced Concrete Slabs*, ACI Journal, Proceedings, Vol. 63, May 1966, pp. 527-542

Appendix A Activation of the transverse reinforcement in punching (CSCT)

This appendix presents the derivations to relate the opening of the critical shear crack and the stress σ_{sw} in the transverse reinforcement being intercepted. The original approach (discrete) will be considered, with the presence of one transverse element in the critical crack in order to simplify the formulations [Fer09]. Also, for clarity purposes, the indices i –stating for the rows of shear reinforcement– were not reported and the original notation was generally reworked to be consistent with the one of the present document.

In the following, a distinction will be done between transverse elements made of plain bars (see Section A.1) or deformed bars (see Section A.2). The case of prestressed plain reinforcing systems (post-installed) is simply obtained by adding a constant term –related to the initial prestressing value– to the formulation for plain reinforcement.

A.1 Elements made of plain bars

For plain transverse reinforcement, the bond between steel and concrete is assumed to be negligible and only the anchorages contribute to the force transfer. Perfect anchorage conditions at the extremities of the element are considered, providing a full activation of the reinforcing detail without the development of any slip. Stress and strain can therefore be reasonably assumed as constant over its entire length.

The strain (ε_{sw}) can be obtained by integrating the component of the crack width effectively acting on the transverse reinforcement (w_b) over the length between both extremities of the anchorage (l_w):

$$\varepsilon_{sw} = \frac{w_b}{l_w} \tag{A.1}$$

Consequently, assuming a linear-elastic material model for the reinforcing steel, the related stress in the element (σ_{sw}) simply becomes:

$$\sigma_{sw} = E_{sw} \cdot \frac{\kappa \cdot \psi \cdot h \cdot \cos\left(\alpha + \beta - \frac{\pi}{2}\right)}{l_w} \leq f_{yw} \tag{A.2}$$

where E_{sw} is the modulus of elasticity of the transverse reinforcement, κ is the critical shear crack opening factor (assumed 0.5), h is the vertical distance between the tip of the crack and the point where the critical shear crack crosses the transverse element, and f_{yw} its yield strength.

A.2 Elements made of deformed bars

For deformed transverse reinforcement, the bond develops on both sides of the interception of the critical shear crack with the reinforcing element, limiting considerably its opening compared to the previous case (see A.1). Also, considering a linear-elastic material model for the reinforcing steel, the difference in strain ($\Delta\varepsilon_{sw}$) per unit length (Δx) can be simply obtained as:

$$\Delta\varepsilon_{sw} = \frac{\Delta\sigma_{sw}}{E_{sw}} = \frac{4 \cdot \tau_{b,0} \cdot \Delta x}{d_b \cdot E_{sw}} \tag{A.3}$$

where $\Delta\sigma_{sw}$ is the difference in stress per unit length, related to $\tau_{b,0}$ the average bond stress (uncracked conditions) and d_b the bar diameter of the reinforcing element.

The component of the crack width effectively acting on the transverse reinforcement (w_b) corresponds to the total deformation between the two anchorages points (denoted hereafter as *a* and *b*):

$$w_b = \int_a^b \Delta\varepsilon_{sw} \cdot dx \tag{A.4}$$

In general, in the case of punching of flat slabs, the length of the reinforcing detail is generally not sufficient to allow full activation only from bond along the length of the element. Thus, the distribution of stress and strain also depends on the position of the intersection of the critical shear crack with the transverse reinforcement. Assuming that the latter is crossed at a distance l_{bi} from the lower anchorage –respectively l_{bs} from the upper one– different regimes progressively take place regarding the force transfer function of the importance of the crack opening.

A.2.1 Regime I

The development of bond on both sides of the critical shear crack initially controls the activation of the transverse reinforcing elements. Assuming a rigid perfectly-plastic bond law, the strain and stress follow a linear distribution from the position of the intersection leading to:

$$\sigma_{sw,I} = \sqrt{\frac{4 \cdot \tau_{b,0} \cdot E_{sw} \cdot w_b}{d_b}} \leq f_{yw} \tag{A.5}$$

This regime might be limited by the activation of the closest anchorage with respect to the crack intersection, leading a restriction of the use of the previous formulation (A.5) to crack widths smaller than:

$$w_b \leq w_{li,I} = \frac{4 \cdot \tau_{b,0} \cdot l_{ai}^2}{E_{sw} \cdot d_b} \tag{A.6}$$

where l_{ai} = min(l_{bi}; l_{bs}) is the shorter distance between the crack intersection and one end of the transverse reinforcement element.

The performance associated to bond phenomenon might lead to a notable contribution on the total force provided by the transverse reinforcement at failure. Yet, it was experimentally confirmed that anchorages –bends or heads– should be provided at the extremities of the transverse elements in reinforced concrete specimens to guarantee an adequate activation up to yielding.

A.2.2 Regime II

The contribution of the anchorage on the shortest side of the transverse element –with respect to the intersection with the critical shear crack– allows to further develop bond on the longest side. Using the same bond law and assumptions, the stress in the transverse reinforcement is defined as:

$$\sigma_{sw,II} = \frac{-l_{ai} + \sqrt{2 \cdot l_{ai}^2 + \frac{d_b \cdot w_b \cdot E_{sw}}{2 \cdot \tau_{b,0}}}}{\frac{d_b}{4 \cdot \tau_{b,0}}} \leq f_{yw} \tag{A.7}$$

This regime is limited by the activation of the second anchorage. The use of the previous formulation is therefore restricted to crack widths included in the following range:

$$\frac{4 \cdot \tau_{b,0} \cdot l_{ai}^2}{E_{sw} \cdot d_b} = w_{li,I} \leq w_b \leq w_{li,II} = \frac{2 \cdot \tau_{b,0}}{E_s \cdot d_b} \cdot \left[\left(l_{ai} + l_{as} \right)^2 - 2 \cdot l_{ai}^2 \right] \tag{A.8}$$

where l_{as} = max(l_{bi}; l_{bs}) is the larger distance between the crack intersection and one end of the transverse reinforcement.

Practically, this regime might be governing when the transverse element is intersected very close to one of its extremity anchorage. In the latter case, a concrete-cone breakout might develop –rather for bottom anchorages– and limit the activation of the reinforcing details [Fer10a].

A.2.3 Regime III

Once both anchorages are activated, the increase of force in the transverse reinforcement becomes linearly dependent on the crack opening up to the yielding of the steel is finally achieved:

$$\sigma_{sw,III} = \frac{E_{sw} \cdot w_b}{l_{ai} + l_{as}} + \frac{2 \cdot \tau_{b,0}}{d_b} \cdot \frac{l_{ai}^2 + l_{as}^2}{l_{ai} + l_{as}} \leq f_{yw} \tag{A.9}$$

$$w_b \geq \frac{2 \cdot \tau_{b,0}}{E_s \cdot d_b} \cdot \left[\left(l_{ai} + l_{as} \right)^2 - 2 \cdot l_{ai}^2 \right] \tag{A.10}$$

Practically, this case is determining when the effective length of the transverse element is not sufficient to perform the force transfer solely by bond. This is typically the case for thin slender slabs, where in comparison to footings, the contribution of bond in the total force provided by the transverse reinforcement to the punching strength is relatively limited.

Curriculum Vitae

NAME	**Brantschen**
FIRST NAME	**Fabio**
DATE OF BIRTH	08 July 1986
NATIONALITY	Swiss (*Zermatt*, VS) / Italian (*Villar Perosa*, TO)
E-MAIL	fabio.brantschen@gmail.com

EDUCATION

- Doctoral candidate in Civil Engineering, **Aug. 2011 – Oct. 2016**
  École Polytechnique Fédérale de Lausanne (EPFL), Lausanne, Switzerland
  Thesis "*Influence of bond and anchorage conditions of the transverse reinforcement on the punching strength of RC slabs*"
- BSc and MSc in Civil Engineering, **Sep. 2006 – Jul. 2011**
  EPFL, Lausanne, Switzerland
  weighted average grade 5.2 of 6.0 (specialization in "*Structural Engineering*")

EMPLOYMENT HISTORY

- EPFL, Lausanne, Switzerland, doctoral assistant **Aug. 2011 – Sep. 2016**
  - experience in designing and conducting large-scale tests
    punching shear of slabs with transverse reinforcement
    pull-out of anchorages in cracks on reinforced concrete ties
    investigation on the bearing pressure of bend-up bars details in beams
  - evaluation and enhancement of innovative types of punching reinforcement for several industrial partners
  - development of analytical and numerical approaches to consider the effect of cracks on bond and anchorage performance
  - improvement proposals regarding the activation of the transverse reinforcement for the punching failure within the shear-reinforced area
  - teaching assistantship for courses "*Structures*", "*Structure and Architecture*", "*Concrete Structures*", "*Advanced Concrete Structures*", "*Concrete Bridges*", "*Behaviour and Numerical Modelling of RC Members*" as well as several theoretical and practical semester/master projects

COMPUTER SKILLS

- Advanced knowledge: Microsoft Office, MATLAB, Adobe Illustrator, AutoCAD, CUBUS
- Basic knowledge: ATENA, ANSYS

LANGUAGES

- **French**: native / **German**: fluent / **Italian**: fluent / **English**: fluent / **Greek**: notion / **Russian**: beginner

PROFESSIONAL AFFILIATIONS

- Fédération Internationale du Béton *fib* / Gesellschaft für Ingenieurbaukunst

PUBLICATIONS

- Brantschen F., Faria D. M. V., Fernández Ruiz M. and Muttoni A., "*Bond behaviour of straight, hooked, U-shaped and headed bars in cracked concrete*", Structural Concrete (Accepted for publication)
- Einpaul J., Brantschen F., Fernández Ruiz M. and Muttoni A., "*Performance of punching shear reinforcement under gravity loading: influence of type and detailing*", ACI Structural Journal, Vol. 113, No. 4, Jul.-Aug. 2016, pp. 827-838